REGULATION OF TELOMERE LENGTH AND ITS MAINTENANCE IN THE ABSENCE OF TELOMERASE IN BUDDING YEAST *SACCHAROMYCES CEREVISIAE*

Thesis submitted for the degree of

Doctor of Philosophy

at the University of Leicester

by

Usha Aryal BSc

Department of Genetics

University of Leicester

June 2016

REGULATION OF TELOMERE LENGTH AND ITS MAINTENANCE IN THE ABSENCE OF TELOMERASE IN BUDDING YEAST *SACCHAROMYCES CEREVISIAE*.

Usha Aryal
Department of Genetics, University of Leicester
Thesis submitted for the degree of Doctor of Philosophy, June 2016

ABSTRACT

Telomeres are ribo-nucleoprotein structures that cap the end of linear chromosomes protecting them from nucleolytic degradation. In budding yeast *Saccharomyces cerevisiae*, telomeres are maintained by telomerase and a network of over 300 telomere length maintenance genes. Loss of telomerase leads to progressive shortening of telomeres and eventually cellular senescence. However, a few cells can undergo *RAD52* dependent recombination to elongate telomeres and become 'survivors'. Survivors can be of two major types; Type I and Type II, characterized by amplification of the sub-telomeric Y' repeats or the telomeric TG_{1-3} repeats respectively.

In this study, I have demonstrated that in addition to the genetic components, initial telomere length and the timing of senescence are essential factors that influence telomerase negative survival. Longer initial telomere lengths favour Type II survivor pathway, lead to increased efficiency of recovery from crisis and higher overall frequency of survivor formation. Furthermore, longer initial telomeres increased the proportion of Type II and Type II-like survivors in the absence of *RAD59*, a gene generally required for Type II survival. Early senescence was induced from a single critically short telomere in a telomerase negative cell population and led to higher proportion of Type II survivors. Contrary to previous assumptions, the increased proportion of Type II survivors observed was independent to the telomere length at the time of senescence.

Genetic variants that regulate telomere lengths were explored via inter-cross QTL (i-QTL) Multipool analysis using parents from two independent inbred natural populations of *S. cerevisiae*. Seven candidate genes with known telomere function were identified, with the most prominent QTLs being *EST2* and *STN1*. Five intervals containing genes with no prior association to telomere length regulation were also identified. This study demonstrated the sensitivity of the i-QTL Multipool method in determining novel genetic variants regulating telomere length even with a small sample size.

ACKNOWLEDGEMENTS

The past four years have been an extraordinary journey of learning and growing in the midst of an incredible group of people. First and foremost, I would like to extend my gratitude to Professor Ed Louis, without whom none of this would have been possible. With his continuous guidance and encouragement, I have been able to navigate through the ups and downs of research and come out all the better.

I would also like to acknowledge everyone in the Louis lab, past and present, for their support and advice in completing this work. In particular, I am very grateful to Tom Walsh for providing his bioinformatics expertise and invaluable time for the QTL study, and especially for patiently answering all my queries in the process. I would also like to thank Gemma Llargues, who I had the pleasure of working with during her Master studies, for helping me generate preliminary data for the caffeine study. Sarah Sharp, who showed me the ropes in my first year of research at Nottingham and Rob Mason for showing me the ways of Leicester. Many thanks to Sue, Aga, Yan and Dave for lending a helping hand when needed and for making work feel less like work.

I am most grateful to my Leicester family for the countless memories and good times shared in the past few years. In particular my fellow PhD students Ane, Joana, Alex, Daniel and Marcela in whom I was fortunate enough to find great friends to enjoy the experience with, and Carlo for always being ready to share a good laugh and the occasional life advice. I feel very lucky to have met you all and will miss you dearly. I am also very fortunate to have the love and support of my wonderful siblings Asish Aryal and Sabita Aryal who have time and again patiently reassured me when the stress levels were high.

Finally, I would like to dedicate this thesis to my wonderful parents, Durga Aryal and Jhabindra Aryal, for their unconditional support and belief in me. Without their guidance and sacrifice I would not be where I am today. Thank you for teaching me to dream big and for always cheering me on.

TABLE OF CONTENT

LIST OF TABLES

LIST OF FIGURES

List of Abbreviations

AIL	Advanced Inter-cross Lines
ALT	Alternative Lengthening of Telomeres
APB	ALT associated PML bodies
ARS	Autonomously Replicating Sequence
BIR	Break Induced Replication
CHEF	Clamped Homogeneous Electric Field
CST	Complex containing Cdc13, Stn1, Ten1
DDR	DNA Damage Response
DNA	Deoxy-ribonucleic acid
DSB	Double Strand Break
ECTR	Extra-chromosomal Telomeric Recombination
F1	First Filial Generation
HR	Homologous Recombination
HYG	Hygromycin
ILT	Inherited Long Telomere
i-QTL	Intercross – Quantitative Trait Loci
KAN	Kanamycin
KO	Knock-out
LB	Luria Broth
LOD	Logarithm of Odds
LYS	Lysine
MMEJ	Micro-homology Mediated End Joining
MRX	Complex containing Mre11, Rad50, Xrs2

NA	North American
NAT	Nourseothricin
NHEJ	Non-Homologous End Joining
OD	Optical Density
ORF	Open Reading Frame
PAL	Palindrome dependent mechanism
PCR	Polymerase Chain Reaction
PFGE	Pulse Field Gel Electrophoresis
PML	Promyelocytic Leukaemia
QTL	Quantitative Trait Loci
RPA	Replication Protein A
SNP	Single Nucleotide Polymorphism
SSA	Single Strand Annealing
TERRA	Telomeric-Repeat containing RNA
TLM	Telomere Length Maintenance
TRAP	Telomere repeat amplification protocol
TRD	Telomere Rapid Deletion
TRF	Terminal Restriction Fragments
URA	Uracil
t-SCE	Telomere Sister Chromatid Exchange
WA	West African
WE	Wine European
X-QTL	Extreme – Quantitative Trait Loci
YPD	Yeast extract-Peptone-Dextrose

Chapter 1 Introduction

1.1 Background to telomeres

Hermann Muller and Barbara McClintock noted in the 1930s that chromosome ends are functionally different to the rest of the chromosome (McClintock, 1939). Unlike chromosomal breaks, these end structures were protected from breakage-fusion-bridge cycles and were named telomeres. It is now known that telomeres consist of DNA-protein structures that cap the end of linear chromosomes. In 1978, Elizabeth Blackburn identified the first sequence of a telomere in ciliate *Tetrahymena* and showed it to consist of tandem repeats of TG bases (TTGGGG) at the end of the chromosomes (Blackburn and Gall, 1978). Similar repeats were soon identified in many different organisms such as *Oxytricha*, *Physarum*, yeast, and *trypanosomes* suggesting an early evolution of the structure and conservation among eukaryotic organisms with linear chromosomes (Boswell et al., 1982, Johnson, 1980, Bernards et al., 1983, Szostak and Blackburn, 1982).

1.2 Function of telomeres

Capping of linear chromosomes in eukaryotes by telomeres is crucial in providing stability to the genome and maintaining cell viability. Chromosomal capping by telomeres (nucleic TG repeats and associated proteins) is essential as it distinguishes chromosomal ends from double strand breaks (DSB). Uncapping would otherwise lead to recognition of chromosomal ends as DSB, activation of the DNA damage response (DDR), detrimental chromosomal rearrangements, end-to-end fusions and eventually cell death or senescence (Cesare and Reddel, 2008).

Furthermore, linear chromosomes are faced with the problem of end-replication in eukaryotic cells. The end-replication problem refers to inability of lagging strands to completely synthesize the terminal bases of parental DNA during replication due to lack of primer binding for 5'-3' DNA polymerase mediated extension. This results in the gradual loss of terminal chromosomal DNA sequences with each round of cell division.

Post-replication, telomere ends are also resected 5'-3' generating a 3' G-overhang. Resection coupled with end-replication leads to progressive shortening of telomeres with each round of cell division and eventually leads to loss of the protective capping at chromosomal ends (O'Sullivan and Karlseder, 2010). Upon reaching a critically short

telomere length after multiple cell divisions, the DNA damage response is activated followed by chromosomal rearrangements and cell death. Telomeres therefore protect chromosomal ends for a finite number of cell divisions before reaching a critically short length and are often considered the 'molecular clock' of ageing. The number of divisions a cell can undergo until senescence is also known as the 'Hayflick limit' of maximum cell divisions (Hayflick and Moorhead, 1961).

1.3 Telomere maintenance by telomerase

Most single celled organisms such as yeast, stem cells and germ cells maintain their telomeres using telomerase. Telomerase was first identified by Greider and Blackburn in 1985 as the enzyme 'telomere terminal transferase' shown to consist of an RNA component in addition to a protein (Greider and Blackburn, 1985). In fact, telomerase is a ribonucleoprotein complex that consists of a protein component, reverse transcriptase *TERT* (mammalian homologue of yeast *EST2*) and a RNA template *TERC* (mammalian homologue of yeast *TLC1*) that enables de novo addition of the TG repeats. The RNA template varies in size and sequence between different species. The RNA template in humans, TERC, contains an 11 bp long sequence, 5' – CUAACCCUAAC -3', complementary to the human telomeric repeat TTAGGG (Feng et al., 1995). An additional protein, dyskerin, binds to TERC stabilizing the telomerase complex in humans (Mitchell et al., 1999). Loss of telomerase results in telomere shortening and subsequently leads to various age associated diseases such as diabetes, hypertension, cardiovascular disease etc (Blasco et al., 1996, Barrett et al., 2013, Codd et al., 2013, Epel et al., 2004).

In *S. cerevisiae*, the *TLC1* gene codes for the RNA template which contains sequence 5' – CACCACACCCCACACAC – 3', complementary to yeast telomeric repeat ($(TG)_{1-6}TG_{2-3}$) or simply TG_{1-3} in short (Singer and Gottschling, 1994). In addition to *EST2* and *TLC1*, the telomerase holoenzyme consists of further regulatory protein subunits Est1 and Est3 (Hughes et al., 2000, Lundblad and Szostak, 1989). Est1 assists with the recruitment of Est2 to telomeres by interacting with single stranded telomeric binding protein Cdc13 (Evans and Lundblad, 1999). Furthermore, Est1 is also required for the association of Est2 and Est3 forming a fully functional telomerase holoenzyme (Figure 1-1A) (Osterhage et al., 2006).

1.4 Structure of the telomere in humans

In humans, the telomeric TTAGGG repeats are bound by a number of proteins forming the shelterin complex (Figure 1-1B). The double stranded telomere terminates with a 3' G overhang in the leading strand which is bound by protein 'Protection of Telomere 1' (Pot1), a telomeric protection factor (Baumann and Cech, 2001). The shelterin complex consists of the double stranded telomeric binding protein 'Telomeric repeat-binding factor 1' (Trf1) and Trf2 (Chong et al., 1995). The repressor and activator protein 1 (Rap1) interacts with Trf2 and the bridging molecule Trf1-interacting nuclear protein 2 (Tin2) binds with both Trf1 and Trf2 (Kim et al., 1999). Finally, the Pot1 and Tin2 interacting protein, Tpp1 adjoins Pot1 and Tin2 in the double and single stranded region of the telomere (O'Sullivan and Karlseder, 2010). The proteins of the shelterin complex interact transiently with many other molecules at different stages of the cell cycle that enable the establishment of a protective structure at the telomeres. The proportion of Trf1 and Trf2 proteins that are loaded onto the telomeres are essential in regulation of its length. Trf1 also plays a role in DNA remodelling and replication of the telomeres. Trf2 has a more varied role whereby it protects the telomeres by forming a loop structure (known as T-loop), prevents the activation of DDR and supresses non-homologous end joining (Stansel et al., 2001). Pot1 and Tpp1 also play a key role in telomere length regulation. Pot1 and Tpp1 compete for access to telomerase and binding of Tpp1 to telomerase results in processivity of telomeres. Therefore, increased loading of Pot1 to the 3' G overhang has an inhibitory role in telomerase binding to the telomeres (O'Sullivan and Karlseder, 2010).

1.5 Structure of telomeres in *Saccharomyces cerevisiae*

In budding yeast, *Saccharomyces cerevisiae,* telomeres consist of approximately 350 bp of $TG_{1\text{-}3}$ repeats (Shampay et al., 1984, Wang and Zakian, 1990). Adjacent to the terminal TG repeats are the sub-telomeric repeat elements which can consist of X element only or the X elements upstream of Y' repeat elements (Figure 1-4A). The sub-telomeric Y' region is highly conserved among strains of the same species and consist of zero to four tandem copies. It can be of two major sizes: 6.7 kb or 5.4 kb varying by only a number of insertions or deletions (Chan and Tye, 1983, Louis and Haber, 1992). It contains two major open reading frames (ORFs), which has very little expression during vegetative growth but much higher expression during meiosis, and an ARS (autonomously

replicating sequence) consensus sequence (Louis, 1995). The Y' region encodes a helicase protein Y-Help1 which is transcribed actively in the absence of telomerase (Yamada et al., 1998). The X elements are much more variable ranging from 0.3 to 3 kb in size. However, the X elements have a conserved 'core X' region of 473 bp that is found in all chromosomes. This core X region contains an ARS sequence along with an Abf1 binding site (Chan and Tye, 1983, Pryde et al., 1995).

1.6 Telomere binding proteins and their function

Telomere and sub-telomeres are bound by various proteins that attribute to their various functions. The X element region of the sub-telomere is richly bound by several Sir2 and Sir3 proteins conferring a silenced chromatin structure along with transcriptionally silencing the area around it (Imai et al., 2000, Pryde and Louis, 1999). The Y' repeat elements however have more open chromatin conformations where Sir2 and Sir3 are not detected, resembling the structure of euchromatin (Pryde and Louis, 1999, Zhu and Gustafsson, 2009). The double stranded telomeric region is bound by Rap1 (repressor activator protein 1), a protein that is named after its ability to regulate gene expression, not only in the telomeres but also in the rest of the genome (Gilson et al., 1993, Shore and Nasmyth, 1987). Rap1p is bound by its partners Rif1/2 and together regulate the length of the telomeres (Marcand et al., 1997). Next, the double stranded region of telomeric DNA is bound by protein yKu that consists of subunits yKu70p and yKu80p. yKu is required for DNA repair via non-homologous recombination, binds to the telomere possibly via interaction with Sir4 and localises telomeres to the sub-nuclear region (Martin et al., 1999, Laroche et al., 1998). Furthermore, yKu's ability to interact with telomerase is thought to be involved in telomerase recruitment for telomere maintenance or possibly in trafficking of telomerase to the nucleus from cytoplasm (Peterson et al., 2001, Gallardo et al., 2008). The single stranded 3' G overhang in *S. cerevisiae* is bound by proteins Cdc13, Stn1 and Ten1, together known as the CST complex that bind to the single stranded telomere ends and cap it (Figure 1-1A) (Petreaca et al., 2006).

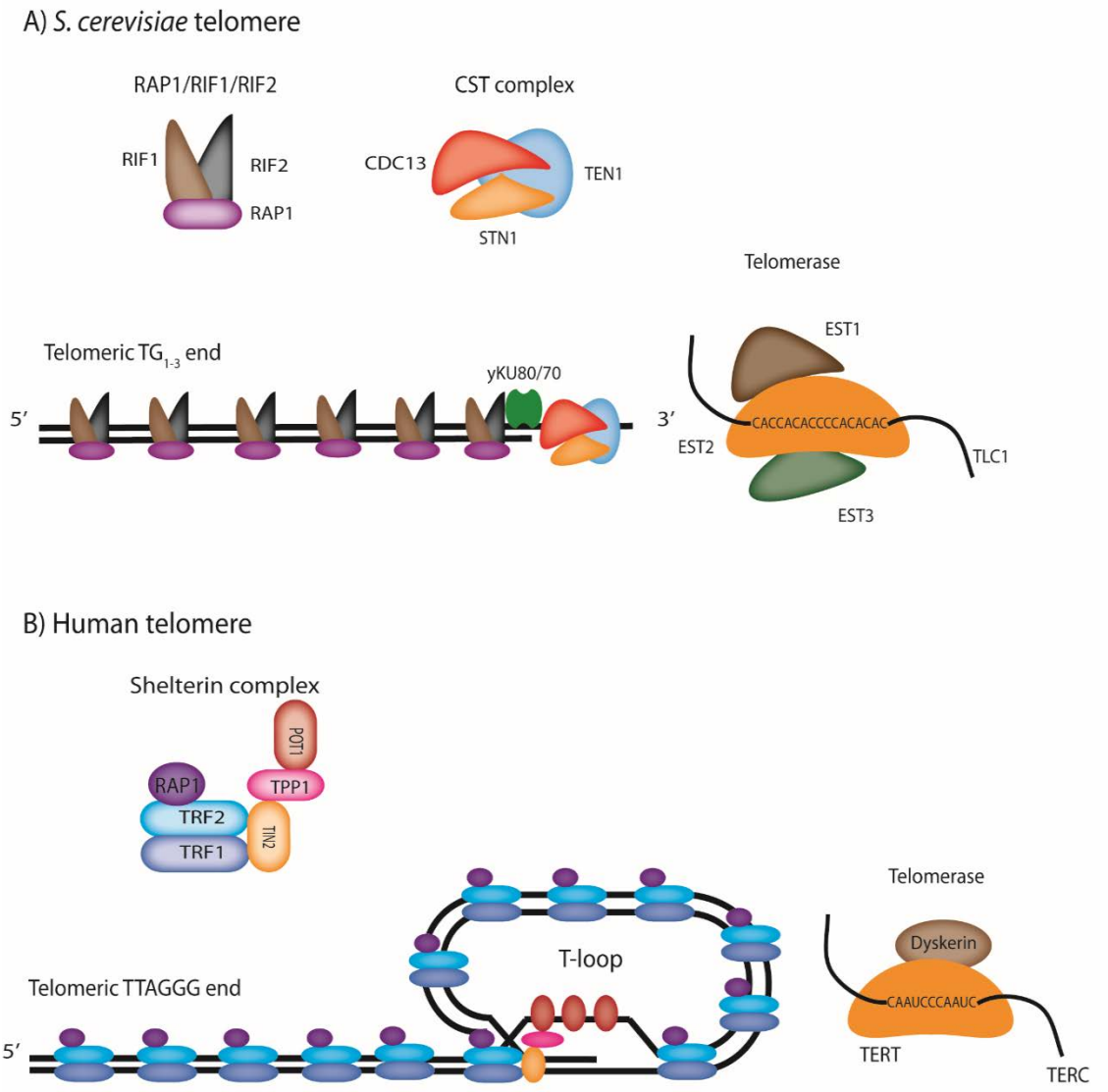

Figure 1-1: Telomere and its associated proteins in *S. cerevisiae* and humans. A) Representation of yeast telomere, its interacting proteins and telomerase. Double stranded region of the TG ends is bound by Rap1, Rif1 and Rif2 proteins whilst the single stranded region is bound by the CST complex, adapted from (Kupiec, 2014). **B)** Representation of human telomere, telomere binding proteins and telomerase. Rap1, Trf1 and Trf2 bind the double stranded region of the TG repeats whereas the single stranded 3' overhang is bound by Tin2, Tpp1 and Pot1 that enables interaction with the double stranded region forming a T-loop, adapted from (Di Domenico et al., 2014). Human telomerase consists of reverse transcriptase *TERT*, RNA template *TERC* and dyskerin.

1.7 Telomere capping proteins and telomerase recruitment

Telomere capping protects chromosomes from detrimental rearrangements arising from homologous recombination (HR) or non-homologous end joining (NHEJ) due to DDR. In *S. cerevisiae*, the CST complex forms the telomere cap. Loss of Cdc13 unit of the CST complex results in activation of DNA damage response via the Rad9 checkpoint protein and eventually cell cycle arrest, both of which are hallmarks of uncapping (Wellinger and Zakian, 2012, Weinert and Hartwell, 1993). However, Cdc13 capping is only required during S/G2 phase, suggesting the importance of capping is perhaps mainly during replication (Wellinger and Zakian, 2012). Rap1 and Rif2 also play a role in capping and preventing telomere fusions (Marcand et al., 2008). Rif2 prevents the association of Tel1, a signalling kinase, with the telomeres and the activation of MRX complex (Mre11, Rad50, Xrs2), both of which are involved in double strand break recognition and checkpoint activation (Grenon et al., 2001, Hirano et al., 2009). Another telomere capping protein is yKu which plays a more prominent role in telomere protection during G1 phase. yKu is a protein required in NHEJ, and loss of yKu during G1 phase leads to telomere resection despite a functional Cdc13 (Wellinger and Zakian, 2012, Bonetti et al., 2010, Maringele and Lydall, 2002). However, telomere resection resulting from loss of yKu is less prominent in comparison to resection that occurs due to loss of Cdc13 during S/G2 phase (Wellinger and Zakian, 2012). In mammalian cells, loss of telomere caps has been shown to result in telomere fusions via NHEJ (Smogorzewska et al., 2002). However in yeast, it was reported from a study by Liti and Louis (2003), that loss of *NEJ1*, a protein required for NHEJ, in addition to the loss of telomerase leads to the formation of higher levels of circular chromosomes. Hence, it is likely that NHEJ has a protective role at telomeres in *S. cerevisiae* that represses fusions of eroding telomeres (Liti and Louis, 2003).

In budding yeast, telomerase recruitment to the telomere end is limited to late stages of DNA replication in the S phase of the cell cycle and only at specific ends containing short telomeres (Bianchi and Shore, 2008, Bianchi and Shore, 2007). One of the key players in telomerase recruitment is Cdc13. The N-terminal domain of Cdc13 is thought to interact with Est1 subunit of telomerase along with catalytic subunit of DNA polymerase α, Pol1, helping replication of telomere (Qi and Zakian, 2000). During replication, a long 3' overhang is created which recruits Cdc13, which in turn recruits Est1. Est1 then recruits Tlc1 which in turn recruits Est2. In summary, the chain of events being, 3' overhang →

Cdc13 → Est1→ Tlc1 → Est2 (Bianchi and Shore, 2008). Furthermore, Tel1 and Mec1, DNA damage signalling kinases and orthologs of mammalian ATM and ATR respectively (which are typically recruited to short telomeres), have been shown to phosphorylate Cdc13 on several serine residues. Hence a simple model can be suggested whereby Tel1 binds selectively to short telomeres and subsequently phosphorylates Cdc13 leading to telomerase recruitment (Bianchi and Shore, 2008).

1.8 Cell cycle arrest and senescence in telomerase negative background

In *Saccharomyces cerevisiae* 3-5 bp of the TG_{1-3} repeat is lost every round of cell cycle in the absence of telomerase (Lundblad and Szostak, 1989, Shampay et al., 1984). When telomeres become critically short, they elicit a DDR followed by attempts to repair the break or a G2/M arrest such that cells can no longer divide (Sandell and Zakian, 1993, Aylon and Kupiec, 2003). In yeast, this phenomenon is termed 'senescence' . Loss of capping proteins gives access to nucleases that resect telomere ends generating single stranded DNA (ssDNA) (Garvik et al., 1995). The first molecules in action at a DSB in a chromosome are the MRX complex and nuclease Sae2 that generate 50-100 nucleotide overhang of 3' ssDNA (Mimitou and Symington, 2008). This is followed by more extensive resection by exonuclease Exo1 and helicase/nuclease Sgs1/Dna2 (Tsubouchi and Ogawa, 2000, Gravel et al., 2008, Bonetti et al., 2009, Zhu et al., 2008). In the case of telomerase positive cells, MRX is bound to telomeres but doesn't lead to extensive resection. In fact, deletion of MRX leads to extensive resection at telomere ends (Foster et al., 2006). Accumulation of ssDNA from Exo1 and Sgs1 mediated resection activates Mec1 kinase and Rad9 protein dependent DDR which in turn activates Rad53 leading to G2/M arrest (AS and Greider, 2003, Grandin et al., 2005). Rad9 is a DNA damage checkpoint protein that is activated by Mec1 and Tel1 kinases and activates Chk1 and Rad53. Activation of Chk1 and Rad53 leads to transcriptional upregulation of DNA repair genes, transcriptional repression of cyclins and stabilization of replication fork, all of which are processes associated with cell cycle arrest (Chen and Sanchez, 2004, Naiki et al., 2004, Toh and Lowndes, 2003). Tel1 preferentially binds to short telomeres via the Xrs2 subunit of the MRX complex and helps recruit telomerase. However, unlike in DDR arising from a chromosomal break, Tel1 does not elicit DDR in case of short telomeres (Figure 1-2) (Bianchi and Shore, 2007, Hector et al., 2007, Sabourin et al., 2007).

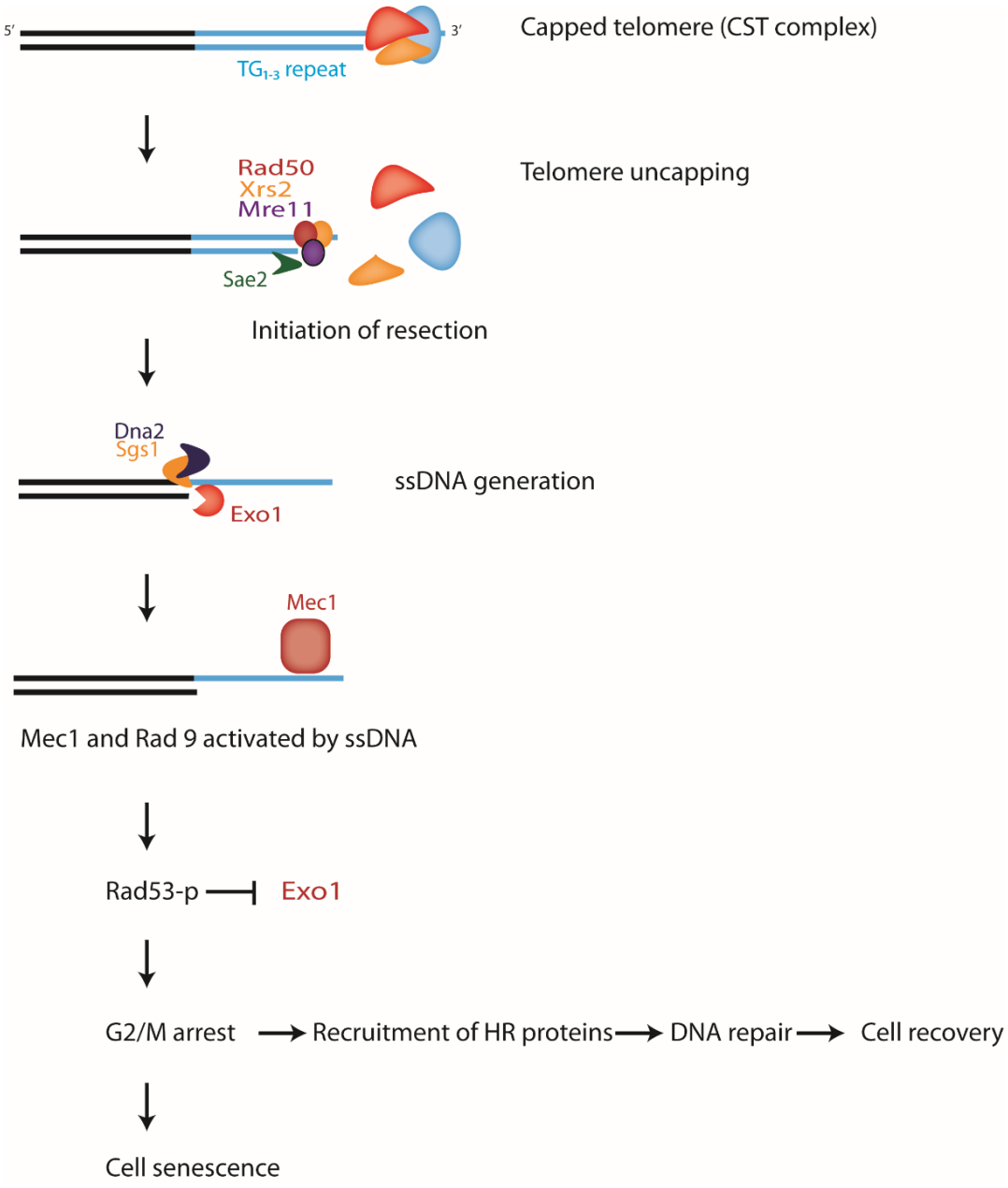

Figure 1-2: Molecular pathway upon loss of CST capping structure followed by activation of G2/M cell-cycle arrest. Loss of CST complex upon telomere shortening allows binding of the MRX complex which subsequently recruits Sae2 nuclease generating a 50-100 bp stretch of single stranded 3' overhang. Accumulation of ssDNA leads to activation of Mec1 and Rad9 dependent DNA damage response followed by Rad53 activation and G2/M arrest. Following G2/M arrest, cells can either undergo homologous recombination mediated DNA repair or undergo cellular senescence. Adapted from (Symington and Gautier, 2011).

1.9 Telomere maintenance in the absence of telomerase

In addition to loss of terminal TG_{1-3} repeats in the absence of telomerase, yeast cultures undergo a gradual decline in cell viability and growth with each round of cell division (Lundblad and Szostak, 1989, AS and Greider, 2003). The point of maximum cell death/senescence in a telomerase negative culture is termed 'crisis.' However, a few cells escape crisis and resume growth by abruptly lengthening their telomeres via an alternative mechanism (without reactivation of telomerase) and are termed 'survivors' (Figure 1-3) (Lundblad and Blackburn, 1993). In *S. cerevisiae*, survivors largely arise from *RAD52* dependent recombination. Loss of Rad52, a protein essential for strand invasion during homologous recombination, seldom permits production of survivors (Lundblad and Blackburn, 1993).

In humans, approximately 85% of tumours arising from somatic cells reactivate telomerase as a means for proliferation. This was demonstrated elegantly by Kim et al using a TRAP assay (telomere repeat amplification protocol) that synthesizes telomere extension product in vitro in the presence of telomerase and uses it as template for subsequent PCR amplification (Kim et al., 1994). However, many tumours also employ a recombination based Alternative Lengthening of Telomere (ALT) mechanism, similar to 'survivors' in yeast, in order to proliferate (Bryan et al., 1995). It has been observed, for instance, that 100% of adenocarcinomas proliferate by expressing telomerase, whereas the percentage of sarcomas proliferating by ALT is much higher, as much as 47% in the case of osteosarcomas (Henson et al., 2005, Kammori et al., 2002, Royle et al., 2008). Hence, the formation of ALT survivors is of great interest in the understanding of cancer biology.

In *S. cerevisiae*, depending on the region of the telomere amplified, telomerase negative survivors can be categorized into two major groups; Type Is containing sub-telomeric Y' amplification and the Type IIs containing TG_{1-3} repeat amplification (Teng and Zakian, 1999).

1.9.1 The Type I survivors

The Type I survivors are characterized by amplification of the Y' sub-telomeric repeat elements whilst the terminal TG_{1-3} repeats remain short at about 50-150 bp (Lundblad and Blackburn, 1993) (Figure 1-4B). Although roughly one-third chromosome ends do

not contain Y' elements, all ends eventually acquire Y' amplification after becoming a Type I survivor. This is likely due to homology mediated recombination where TG_{1-3} repeats in X-only chromosome ends use the X element of another chromosome, also containing the Y' elements, as template for elongation. Type I survivors undergo major chromosomal rearrangements which occurs prior to amplification and stabilization of the Y' sub-telomeric region (Muston, 2012). Furthermore, circular autonomously replicating Y' circles have been identified in wild-type yeast cells and in Type I survivors (Horowitz and Haber, 1985, Larrivee and Wellinger, 2006). These extrachromosomal Y' circles are thought to be the likely substrates for large Y' amplification in telomerase negative survivors.

1.9.2 Type II survivors

Type II survivors are structurally characterized by amplification of the telomeric TG_{1-3} repeat while the Y' elements remain unaltered (Figure 1-4C). The length of TG_{1-3} repeat amplification is heterogeneous across different chromosomes ranging anywhere between 2 kb to more than 12 kb (Teng and Zakian, 1999). Unlike Type I survivors, the chromosomes of Type II survivors appear to be intact and identical to that of the wild type showing no evidence of chromosomal rearrangements (Liti and Louis, 2003, Muston, 2012). In addition, Type II survivors resume a growth rate similar to that of wild-types after escaping crisis.

Type I and Type II survivors are easily distinguished in a Southern blot analysis. Terminal restriction fragments (TRFs) can be generated by digesting survivor genomes with enzyme *XhoI* that cuts into the Y' region at a unique position (Figure 1-4D). As the Y' elements are either 6.7 kb or 5.4 kb, Type I survivors have a distinct band on the blot followed by another band corresponding to the short terminal TG_{1-3} repeats. The Type II survivors on the other hand have multiple banding patterns due to the heterogeneity in the lengthening of the TG_{1-3} repeats across the different chromosomes (Figure 1-5). Although survivor types can be determined using a southern blot, it is important to note that the distinction between Type I and Type II survivors is not always straight forward. It has been shown that survivors labelled as Type I do not always show extensive Y' amplification that is characteristic of Type I survivors. Likewise, survivors labelled as Type II may sometimes arise from survivors that were previously Type I's and have

therefore retained the amplified Y' elements along with the new amplified TG_{1-3} repeats (Teng and Zakian, 1999, McEachern and Haber, 2006).

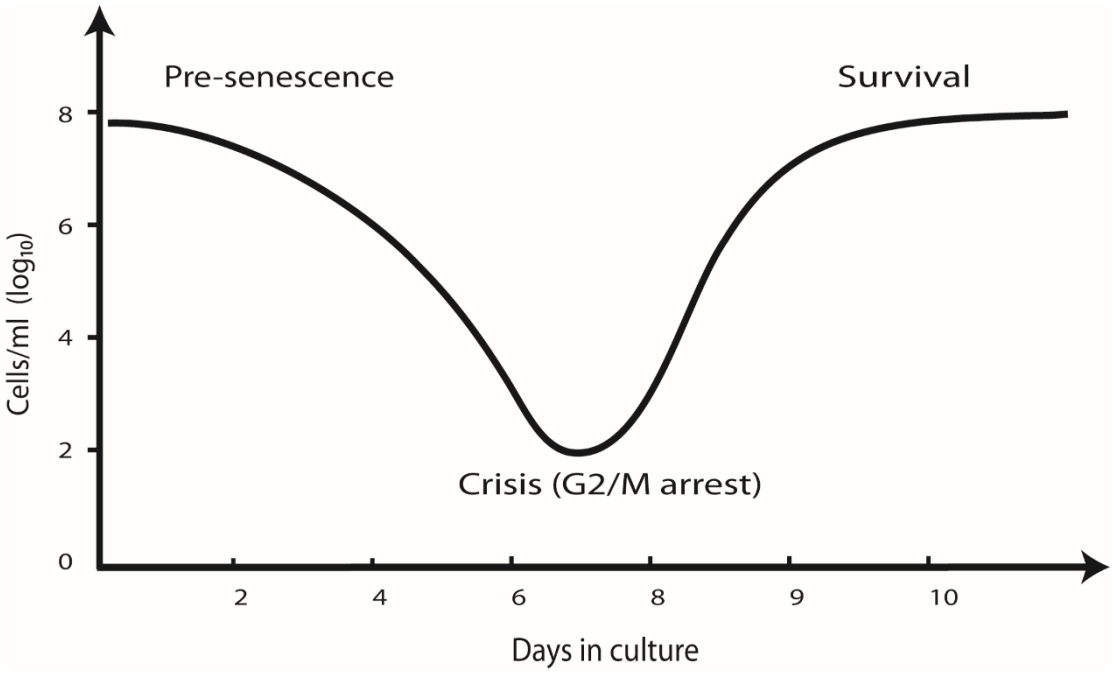

Figure 1-3: A typical growth pattern of telomerase negative cells in liquid culture. Pre-senescent cell cultures undergo gradual decline in cell viability with shortening telomeres and eventually undergo G2/M arrest after approximately 60-80 population doublings. The point of maximum decline is termed 'crisis.' After pro-longed G2/M arrest or crisis, cells eventually pick up growth by becoming survivors. Figure is a generalization of a typical telomerase negative culture and is not based on real data.

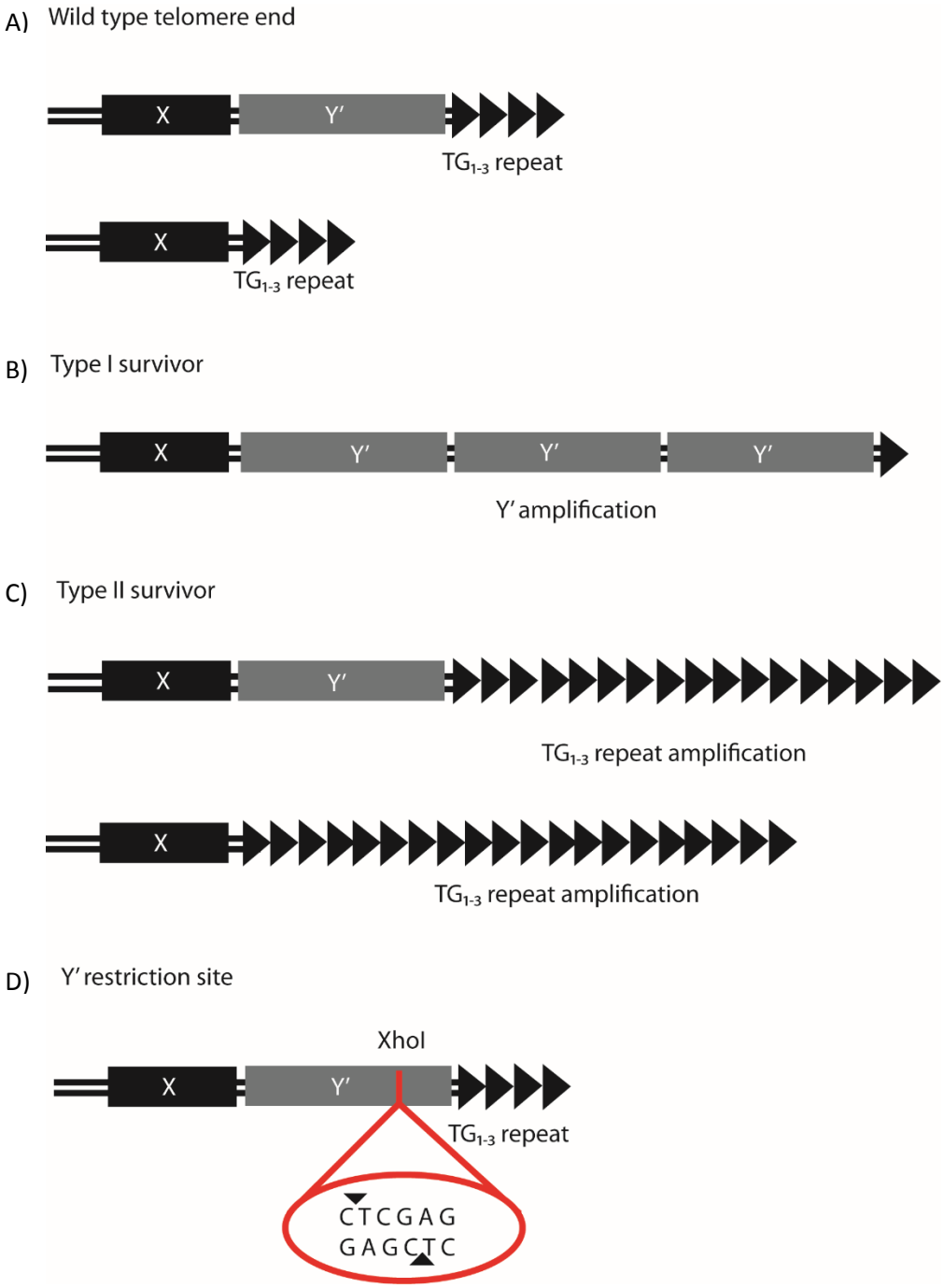

Figure 1-4: Structure of telomere and sub-telomeres in wild-type cells and telomerase negative survivors. A) Wild type telomeres consists of sub-telomeric elements (the core X element followed by Y' repeats in tandem or the core X element only) and terminal TG_{1-3} repeats. **B)** Type I survivors are characterized by amplification of Y' sub-telomeric repeat elements but terminal TG_{1-3} repeats remain short. **C)** Type II survivors are characterized by amplification of TG_{1-3} repeats. Amplification can occur in either XY or just X containing telomeres. **D)** Location of *XhoI* restriction site in the Y' repeat elements used for generating Terminal Restriction Fragments (TRFs) for survivor type analysis. Figure adapted from (Lydall, 2003)

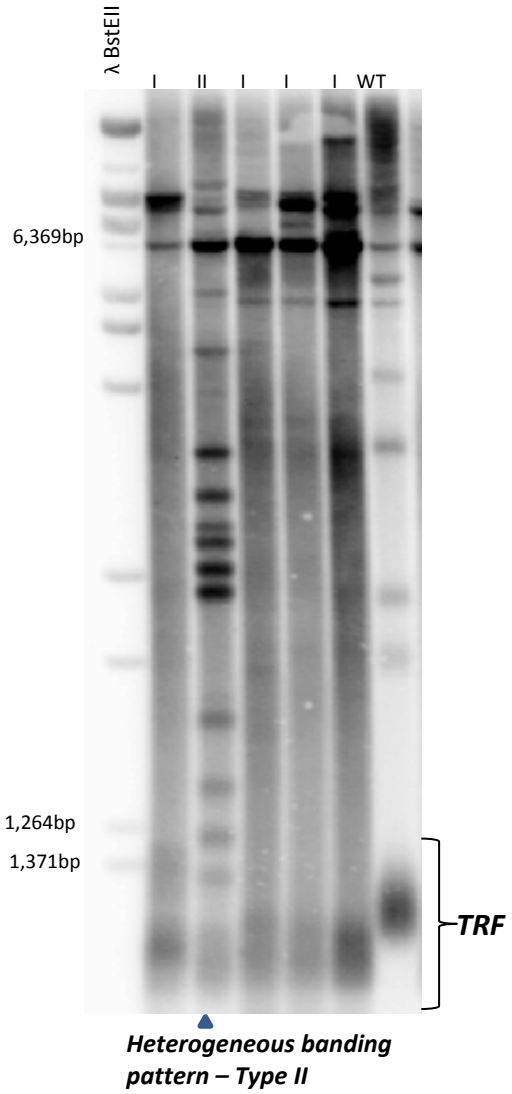

Figure 1-5: **Southern blot characterizing Terminal Restriction Fragments (TRF) pattern of survivors**. Typical pattern of Type I survivors (lane 2, 4-6), Type II survivor (lane 3), Wild-type (WT, lane7) after restriction digestion with *XhoI* along with marker DNA (lane 1). Type I survivors have short TRF fragments but a thick band around 6 kb representative of Y' amplification. Type II survivors display multiple banding pattern indicative of heterogeneous $TG_{1\text{-}3}$ amplification. Sometimes Type II survivors can contain Y' amplifications. Figure taken as example from a result blot (Appendix 7.1).

1.10 Genetics of survivor formation in *S. cerevisiae*

Telomerase negative survivors are formed when either of the components of telomerase, *EST2* or *TLC1*, is knocked out. However, the ability to generate survivors is nearly abolished in the absence of *RAD52* (Lundblad and Blackburn, 1993). *RAD52* is the central homologous recombination gene that is highly conserved in eukaryotes. Proteins that are part of the *RAD52* epistasis group are encoded by genes *RAD50, RAD51, RAD54, RAD55, RAD59, MRE11, RDH54* and *XRS2*, all of which are involved in gene conversion. It has been shown previously that triple mutants *rad50Δ rad51Δ tlc1Δ* cannot produce either the Type I or Type II survivors whereas double mutants *rad50Δ tlc1Δ* and *rad51Δ tlc1Δ* can (Le et al., 1999). This suggests *RAD50* and *RAD51* represent two distinct genetic pathways of homologous recombination for survivor formation.

Type I survivor formation is dependent on *RAD51, RAD54, RAD55* and *RAD57* genes (Wellinger and Zakian, 2012, Le et al., 1999). Rad51 binds to the 3' single stranded DNA (ssDNA) formed by resection of a DSB to promote pairing and strand exchange with a homologous duplex (Krogh and Symington, 2004). It is similar to the catalytic domain of RecA protein which also binds to ssDNA during homologous recombination. Rad52 interacts directly with Rad51 where it enables Rad51 filament assembly on ssDNA while simultaneously removing RecA (Krogh and Symington, 2004, Sugiyama and Kowalczykowski, 2002, Song and Sung, 2000). Therefore, loading of Rad51 to a DSB is dependent on Rad52. *RAD55* and *RAD57* are paralogues of *RAD51* having 20-30% sequence similarity and forms a stable heterodimer that binds to ssDNA (Krogh and Symington, 2004). The Rad55/57 heterodimer is thought to enable Rad51 nucleoprotein filament assembly and therefore mediates strand exchange during homologous recombination (Hays et al., 1995). Rad54 is the next protein part of the Rad51 pathway of homologous recombination. It is a chromatin remodelling protein that is a member of the Swi2/Snf2 family and facilitates formation of Rad51 nucleoprotein filament in the presence of RPA and stabilizes it (Krogh and Symington, 2004, Mazin et al., 2003, Wolner et al., 2003) (Figure 1-6).

Type II survivor formation is dependent on genes *RAD50, MRE11, XRS2, RAD59* and *SGS1* (Wellinger and Zakian, 2012). The proteins of the MRX complex interact to form a complex with exonuclease activity (Krogh and Symington, 2004, Trujillo et al., 2003, Trujillo and Sung, 2001). Rad59 is important in single strand annealing between

chromosomal direct repeats and is especially effective when the repeat of homology is short (Krogh and Symington, 2004, Sugawara et al., 2000). *SGS1* gene codes a helicase of the RecQ family which plays an important role in genome stability and is homologous to the human BLM and WRN helicases (Krogh and Symington, 2004, Bachrati and Hickson, 2003, Gangloff et al., 1994) (Figure 1-6). However, a study by Grandin and Charbonneau (2003) has shown that genetic requirement for Type I and Type II survivor formation is not always strict. It was shown that telomere deprotection in *cdc13-1 yku70*Δ mutant background enabled bypass of crisis exclusively via $TG_{1\text{-}3}$ amplification (Type II pathway) in both the presence and absence of telomerase. Remarkably, loss of *RAD50* or *RAD59* (otherwise Type II essential genes), did not affect the formation of Type II survivors in the *cdc13-1 yku70*Δ mutant background (Grandin and Charbonneau, 2003).

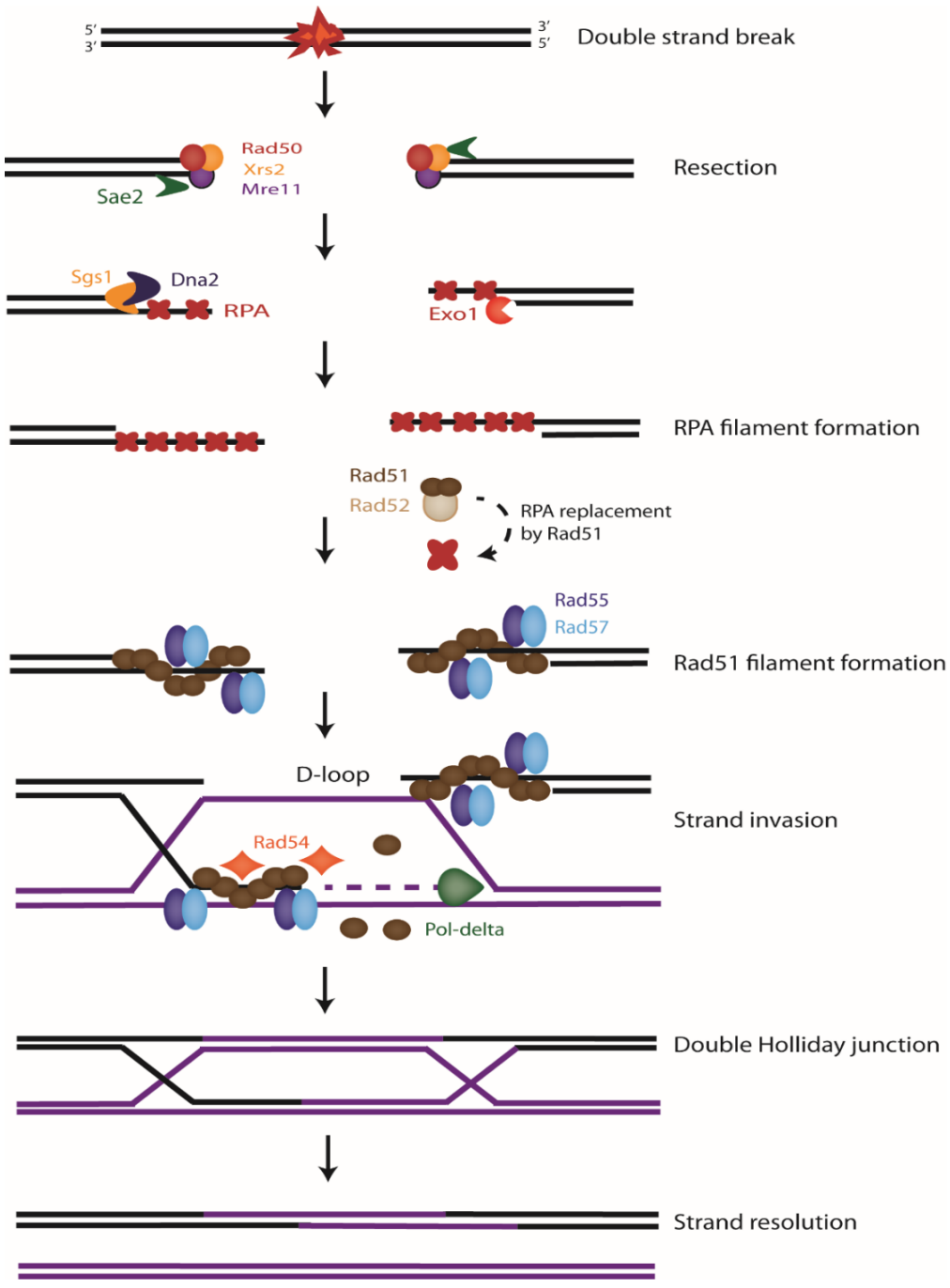

Figure 1-6: Molecular mechanism of Rad52 dependent homologous recombination pathway upon DNA damage. All the proteins known to be essential for Type I survivor formation (Rad51, Rad54, Rad55, Rad57) and for Type II survivor formation (Rad50, Mre11, Xrs2, Sgs1, Rad59) are part of the same Rad52 pathway that leads to formation of the double holiday junction followed by repair and strand resolution upon DNA damage as described in section 1.10. Adapted from (Mazon et al., 2010)

1.11 Mechanism of telomere lengthening in survivors

From the genes identified as essential for survivor generation, it is clear that alternative lengthening of telomeres is a recombination mediated process. As described earlier, all the genes for both the Type I and Type II survivor formation are part of the same homologous recombination pathway. Yet the precise mechanism of telomere elongation in the absence of telomerase is unclear. Furthermore, a simple homologous recombination mechanism is insufficient to explain the phenomenon that can lead to telomere amplification up to 20-30 times its original length. A likely mechanism that has been proposed to generate survivors via alternative telomere lengthening is recombination mediated DNA replication known as break induced replication (BIR).

1.11.1 Break Induced replication

BIR is a form of homologous recombination where a single strand of a broken DNA is used for strand invasion and replication until the end of the template chromosome (McEachern and Haber, 2006). Unlike homologous recombination resulting from DSBs within a chromosome, chromosome ends have only one broken end for finding a region of homology. Thus, standard mechanisms of gene conversion cannot repair the broken end. It is therefore thought the mechanism of telomere lengthening in ALT-like survivors to be BIR (Le et al., 1999). Furthermore, BIR is thought to have two different pathways, one that is *RAD51* dependent generating Type I survivors and other that is *RAD50* dependent generating Type II survivors, both of which are also dependent on polymerase *POL32* (Davis and Symington, 2004, Teng and Zakian, 1999).

Experiments using linearized plasmids designed to perform BIR but not gene conversion show *RAD51* to be essential for efficient repair of DSBs (Davis and Symington, 2004). The plasmid vector was modified such that one end contained short $TG_{1\text{-}3}$ tracts whilst the other end contained sequence of homology specific to a chromosomal site for strand invasion leading to BIR. The *RAD51* dependent BIR pathway was responsible for 95% of repair activities and also required *RAD54*, *RAD55* and *RAD57* (Davis and Symington, 2004). Loss of *RAD50* and *RAD59* slightly reduced the frequency of BIR repair however it was not as significant a reduction as in the absence of *RAD51*. In addition, Y' recombinations were shown to be reduced in the absence of *RAD51*.

The *RAD51* independent pathway of BIR requires *RAD50, RAD59, RDH4* and seems to be coupled to the single strand annealing pathway (SSA) (Ira and Haber, 2002). Furthermore, whilst the *RAD51* dependent pathway of gene conversion requires longer regions of homology for strand invasion (100 bp), the *RAD51* independent pathway can proceed with homology as little as 33 bp. In fact, the presence of *RAD51* was shown to impair BIR from short regions of homology. This fits in line with *RAD51* being required for Type I survivor pathway as Y's can provide a larger region of homology for strand invasion. Likewise, amplification of TG_{1-3} for Type II survivors potentially arises from short region of homology in a *RAD51* independent BIR (Ira and Haber, 2002).

1.11.2 Model for telomere amplification

Several models of telomere amplification have been proposed based on BIR. The data for these models have mostly been derived from work in *Kluyveromyces lactis*, a close relative of *S. cerevisiae*. A study by McEachern in *K.lactis* used a system of tagging telomere repeats by creating a mutation in *TER1* (RNA template of telomerase) such that a *Blc1* restriction site was added every 25 bp (McEachern et al., 2002). In post-senescence survivors arising from the *ter1* mutant, telomere amplification was found to consist of 50-150 bp mixture of basal TG repeats and repeats containing *Blc1* in tandem. The same pattern was found in almost all ends of a single survivor clone however different survivors had different patterns of repeat. This suggested a small fragment of the same TG repeat was used to generate the large amplification seen in survivors. A likely mechanism proposed by the authors was the generation of rare small circular telomeres (t-circles) at the time of senescence from a single end via intra-telomeric recombination. The t-circle is then used as template to enable rapid TG amplifications using rolling circle synthesis at an end with critically short telomere. The amplified end is then thought to act as template for inter-telomeric BIR to amplify TG repeats at other ends (Figure 1-7). How the telomere end primes to a t-circle has not been fully elucidated but a possible mechanism is 3' strand invasion and annealing to t-circle. Telomere circles consisting of Y' repeats have in fact been found in *S. cerevisiae* and TG repeats circles have been found in *K. lactis* (Groff-Vindman et al., 2005, Horowitz and Haber, 1985) although direct

evidence of TG amplification from such t-circles has not yet been reported in *S. cerevisiae*.

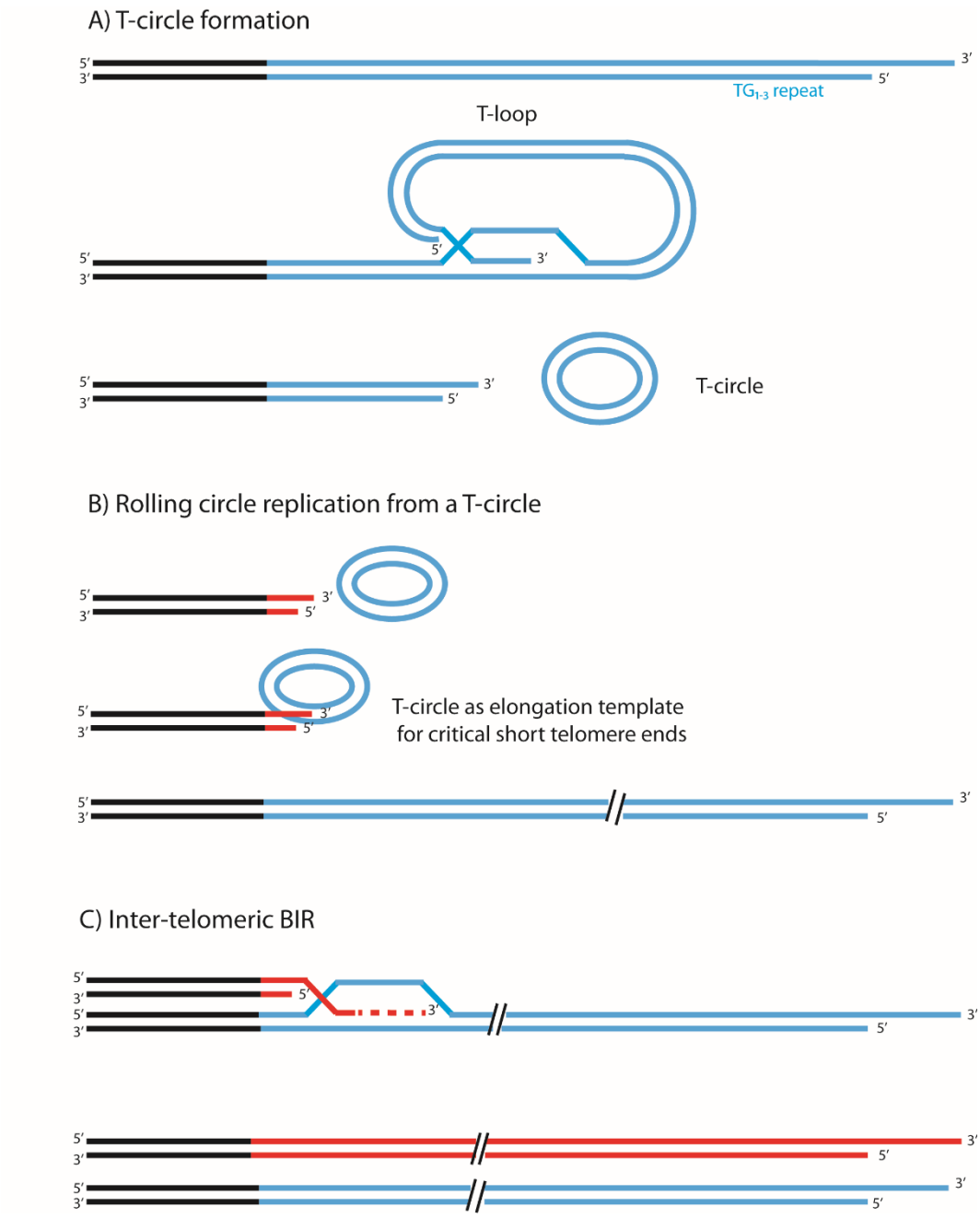

Figure 1-7: Repair by break induced replication (BIR) mechanism at critically short telomere ends. BIR can potentially lead to telomere amplification in telomerase negative *S. cerevisiae* survivors. **A)** Long telomere ends are thought to fold-back forming T-loops and undergo intra-telomeric recombination generating T- circles. **B)** Rolling-circle replication is mediated through the T-circles that act as substrate for TG_{1-3} amplification of critically short telomere ends. **C)** Alternative inter-telomeric recombination whereby short telomere ends use sister chromatids with longer telomere ends as substrate for amplification. Adapted from (McEachern and Haber, 2006)

1.12 Alternative survivor types in *S. cerevisiae*

Apart from the more frequent Type I and Type II survivors that are generated in the absence of telomerase, there are other rare survivor types that have been described in previous studies. Because of the rarity of these survivor types, they are not the main focus in this study.

1.12.1 PAL survivors

Unlike the conventional recombination dependent Type I and Type II survivors, PAL (Palindrome dependent mechanism) survivors can be formed in the absence of *RAD52* in a telomerase negative background when the gene *EXO1* is also knocked out (Maringele and Lydall, 2004). *EXO1* is a 5' – 3' exonuclease that leads to rapid resection of the terminus when telomeres become short and uncapped, leading to accumulation of 3' single-stranded DNA, induction of cell cycle arrest and eventually senescence or survivor formation (Tran et al., 2002). In the absence of *EXO1*, it is thought that cells no longer accumulate ssDNA responsible for cell arrest and thereby allow progression of the cell cycle. Hence, in PAL survivors, much of the telomere and sub-telomere are lost due to continued cell cycle progression along with gross chromosomal changes (Maringele and Lydall, 2004).

The PAL survivors are called such because they generate large palindromes at termini of a chromosome which effectively solves the end-replication problem and prevents deletion of essential genes. Palindromes are suggested to form after several rounds of cell division when the 3' overhang during replication at the terminus happens to be at a site containing inverted repeats which can loop back forming a hairpin structure (Maringele and Lydall, 2004). The fold-back hairpin then acts as primer to allow break induced replication (BIR) without loss of further sequences in one daughter cell but not the other. Or likewise, inverted repeats can allow the formation of di-centric chromosomes that are identical on either side of the palindrome. If latter is the case then chromosomes will break during metaphase such that further sequence loss during replication is compensated by gene duplication in one daughter cell but can also lead to loss of essential genes in the other daughter cell followed by cell death. PAL survivor formation has increased efficiency when other exonucleases such as *MRE11* are also mutated (Maringele and Lydall, 2004).

1.12.2 Inherited long-telomere survivors

Inherited long-telomere (ILT) survivors are phenotypically similar to Type II survivors but are formed in the absence of *RAD52* and telomerase given the cells have abnormally long initial telomere length (Grandin and Charbonneau, 2009). Unlike Type II survivors, ILT survivors can be formed in the absence of *RAD59* and *RAD52* suggesting a homologous recombination independent pathway for ILT survivor formation and consequently ruling out BIR as a likely mechanism. Furthermore, ILT survivors do not require Dnl4, Yku70, or Nej1 suggesting non-homologous end joining (NHEJ) is not a likely mechanism either. Single strand annealing (SSA) was likewise ruled out as RPA which is required for SSA was dispensable for ILT survivor formation. However, ILT survivor formation does require the *MRE11, RAD50, ELG1* and *RAD1* genes which are involved in micro-homology mediated end joining (MMEJ). Furthermore, *stn1* mutants, which are known to be involved in telomere rapid deletion (TRD) in *K. lactis*, had increased efficiency of recombination in telomerase negative and *rad52*Δ background (Iyer et al., 2005). Hence, a proposed mechanism of the ILT pathway is telomere rapid deletion (TRD) in the presence of long telomeres generating telomere circles (t-cricles) which then acts as template for MMEJ followed by telomere lengthening. Lastly, despite producing survivors, ILT is a less stable form of survivor pathway as it has slower growth compared to the Type I and Type II survivor pathways (Grandin and Charbonneau, 2009).

1.13 ALT in mammalian cancer cells

In telomerase negative human cancer cells, alternative lengthening of telomeres (ALT) can lead to amplification ranging from 3 kb to 50 kb (Bryan et al., 1995, Murnane et al., 1994, Opitz et al., 2001, Grobelny et al., 2000). Human germ cells have mean telomere lengths of approximately15 kb which can shorten to 5-8 kb at senescence (Allshire et al., 1989, Delange et al., 1990, Martens et al., 2000). Unlike in yeast, a characteristic of ALT in humans is the presence of ALT-associated PML bodies (APB's). PML (promyelocytic leukaemia) tumour suppressor protein is found in the nuclear matrix and is involved in regulation of a wide variety of function via sequestration and post-translation modification of proteins (Bernardi and Pandolfi, 2007). APBs are different to PML nuclear bodies (PNB's) as they contain telomere DNA and telomere associated proteins, TRF1 and TRF2 (Telomere repeat binding factor) (Yeager et al., 1999). Furthermore, mammalian ALTs contain extra-chromosomal telomere DNA in the form of double

stranded telomere circles (t-circles) or partially single stranded c-circles (Cesare and Griffith, 2004, Henson et al., 2002).

t-circles: Extrachromosomal t-circles are thought to arise from recombination mediated resolution of t-loop structure and trimming of the telomere ends in ALT cells (Wang et al., 2004). T-loops are fold-back structures formed at telomeres when the single stranded G-rich end, approximately 150 bp in length, invades the upstream double stranded region in cis. Although high levels of t-circles are characteristic of ALT cells, they have also been shown to be present in telomerase positive cells as a by-product of trimming of long telomeres (Pickett et al., 2009). The formation of t-circles is prevented in the presence of the shelterin protein TRF2, and recombination proteins NBS1 (Nijmegen breakage syndrome 1) and XRCC3 (X-ray repair cross-complementing 3), suggesting t-circles arise when telomeres become unstable after shortening (Compton et al., 2007, Wang et al., 2004). Hence, the presence of t-circles is not unique to ALT cells but rather it is the increased abundance of t-circles that characterizes the ALT phenotype.

c-circles: Unlike t-circles, c-circles are single stranded self-priming telomeric C-rich circles, more specific to ALT cells. The precise mechanism in the origin of c-circles is not yet fully understood but is thought to be via partial degradation of the G-rich strand of a t-circle (Henson et al., 2009). Like c-circles, g-circles (contains G-rich strand) are also present in ALT cells but are 100-fold less abundant compared to c-circles. Specificity of c-circles to ALT cells is being developed to use as assays for detection of tumours via a blood test (Henson et al., 2009).

1.14 Recombination in mammalian ALT

Like in yeast, rapid telomere elongation and truncation in mammalian ALT is widely considered a recombination based mechanism. There are two major models in mammalian ALTs: The ‘unequal t-SCE’ (telomere sister chromatid exchange model) and the ‘homologous recombination-dependent DNA replication model’

Unequal t-SCE: This model comes from observation of increased t-SCE in ALT cells compared to telomerase positive cells. The model suggests unequal sister chromatid exchange at telomeres such that one daughter cell inherits the long telomeres at all ends leading to increased proliferation of that cell population whereas the other daughter cell inherits all the short telomere ends (Bailey et al., 2004, Muntoni and Reddel, 2005,

Blagoev and Goodwin, 2008). However, there is no evidence suggesting segregation of telomeres based on length and the model remains largely hypothetical.

Homologous recombination-dependent DNA replication model: This model suggests elongation of telomere length via invasion of the double stranded region of one telomere by the 3' ssDNA of another telomere or the same telomere, followed by replication via Pol32 (Inter-telomeric replication, Figure 1-8A). Key evidence for this model comes from experiment where one tagged telomere end was found in multiple other ends in an ALT positive cell (Dunham et al., 2000). Another possibility is telomeres can copy themselves via the T-loop structure (Henson et al., 2002, Muntoni et al., 2009). In normal cells, T-loops are prevented from replicating by the protein Pot1 in mammals (Baumann and Cech, 2001). However, in the absence of Pot1 in critically short telomeres, it is likely that replication occurs in the T-loop resulting in telomere elongation (Henson et al., 2002). However, replication from a T-loop is unlikely to be a continuous process as it requires lagging strand synthesis after each round of replication to provide template for second T-loop formation. Another possible mechanism is rolling circle replication through the extra-chromosomal t-circles or c-circles whereby 3' ssDNA of a telomere undergoes branch migration and uses an extra-chromosomal T-circle (which consists of TG repeats) as template for indefinite replication (Henson et al., 2002) (Figure 1-8). In support of replication from telomere circles, c-circles have been demonstrated to be excellent template for rolling circle mechanism of telomere elongation in-vitro (Henson et al., 2009). Finally, a fourth possible method is replication and telomere elongation via strand invasion of a linear extra-chromosomal telomeric fragment (ECTR).

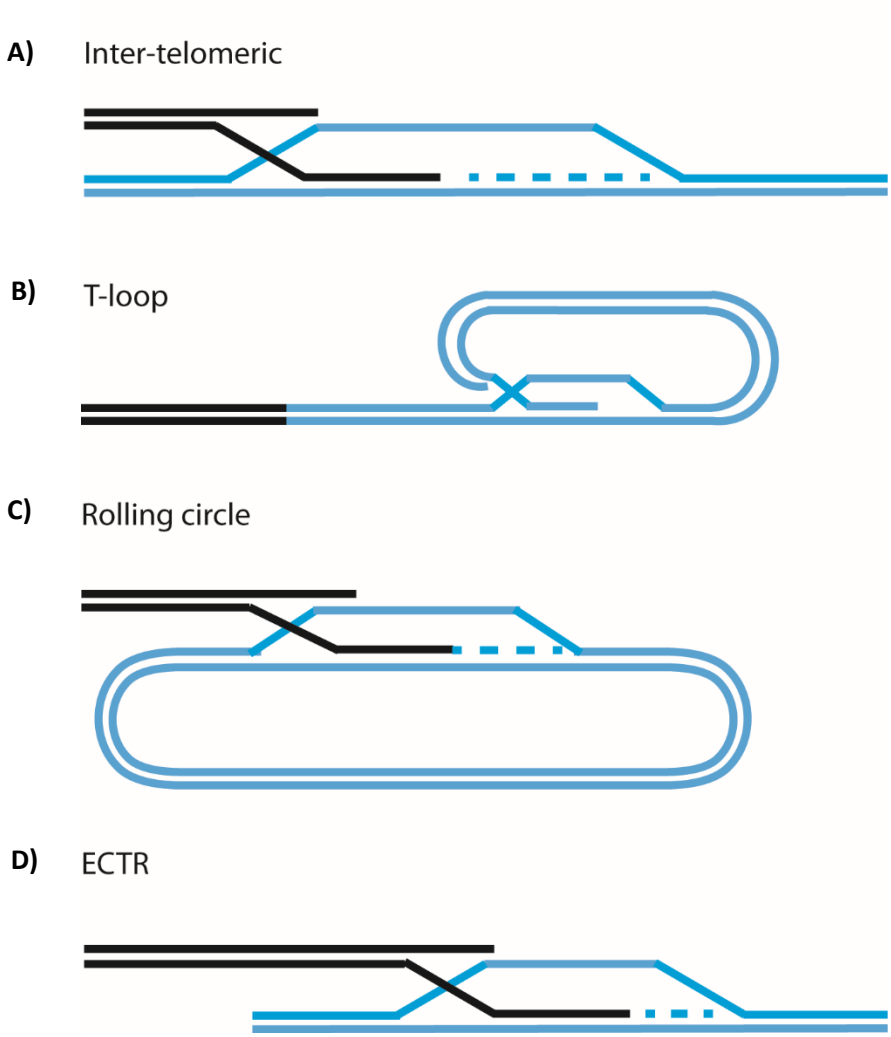

Figure 1-8: Potential recombination based mechanisms of telomere repeat amplification in mammalian ALT+ cells. **A)** Inter-telomeric recombination where a critically short telomere end invades a sister telomere end and undergoes Pol32 mediated replication. **B)** Single stranded region of a short telomere invades a distal region of its own telomere via regions of homology forming a cis loop followed by rolling circle replication. **C)** Rolling circle replication from an extra-chromosomal t-circle. **D)** Replication via strand invasion of a linear extra-chromosomal telomeric fragment. Adapted from (Henson et al., 2002).

1.15 Telomere length homeostasis in *S. cerevisiae*

S. cerevisiae has an average telomere length of 350 bp and is maintained under a strict genetic regulation. Telomere length homeostasis arises from a balance in factors that lead to telomere shortening such as end-replication and factors that lead to telomere lengthening such as telomerase. In addition to end-replication, telomere shortening arises from the action of nucleases that resect ends of leading strand during replication generating 3' overhangs. In the case of *S. cerevisiae* cells with extremely long telomeres, telomere rapid deletion (TRD) can also take place via intra-chromatid homologous recombination mechanism to maintain average length (Bucholc et al., 2001, Li and Lustig, 1996). Loss of Rad50 and Mre11 has shown to inhibit TRD in *S. cerevisiae* whereas loss of Rad52 leads to diminished rate of TRD. TRD is also observed in *K. lactis* and has been evidenced to generate extra-chromosomal telomeric DNA circles whilst shortening telomeres (Bechard et al., 2011).

Unlike telomere shortening, telomere lengthening in the presence of telomerase doesn't occur at all ends during replication. Telomeres with the shorter TG tracts tend to be preferentially chosen by telomerase for elongation (Teixeira et al., 2004). This was shown in a study where telomerase mediated extension of a tagged short telomere was sequenced after a single round of cell cycle. Out of 25 individual CHRVR telomere ends that were sequenced, only 9 showed evidence of added TG repeats suggesting not all ends are extended during cell division. Furthermore, it was noted that the ends which do get extended also contained the least number of TG repeats. The extent of elongation was shown to be dependent on the initial TG repeat length.

Telomere length regulation is orchestrated by a number of different proteins that either recruits telomerase or nucleases. Rap1 is one of the central regulators that bind to the TG tract at an average of one Rap1 molecule per 18 bp of $TG_{1\text{-}3}$ repeats (Gilson et al., 1993). A study by Wotton and Shore demonstrated that loss of Rap1 or the Rap1 interacting factors (Rif1 and Rif2) led to dramatic increase in telomere length (Wotton and Shore, 1997). Likewise, overexpression of Rif1/2 led to a decrease in telomere length. It was later shown that Rap1 along with Rif1 and Rif2 perform a counting mechanism where the length of the telomere is directly proportional to the number of Rap1 proteins bound to the TG tract (Levy and Blackburn, 2004). This mechanism arises from the inhibitory effect of Rap1 binding in Tel1 mediated telomerase recruitment for elongation (Hirano

et al., 2009). For instance, as telomeres shorten, the number of Rap1 bound to the TG tract decreases, allowing access for Tel1 mediated telomerase recruitment and subsequent elongation.

Tel1 is also a crucial protein in telomere length regulation (Hector et al., 2007). Absence of Tel1 not only causes telomere shortening but also reduces the association of Est1 and Est2 proteins to telomere ends suggesting a Tel1 association to short telomeres and telomerase recruitment (Goudsouzian et al., 2006). Indeed, ChIP measurements of protein levels at short and long telomere ends, showed increased levels of Tel1, Est1, Est2 and Cdc13 at the short telomeres (Bianchi and Shore, 2007, Sabourin et al., 2007). Furthermore, Tel1 is thought to be recruited to short telomeres by Xrs2 of the MRX complex (Sabourin et al., 2007). A possible explanation for the MRX-Tel1 interaction at short telomeres might be the decreased levels of Rif2 which is otherwise inhibitory (Marcand et al., 2008). Support for Tel1 recruitment also comes from study showing Rif2 blocking association of Tel1 at longer TG tracts by competing for Xrs2 binding (Hirano et al., 2009). Another negative regulator of telomerase and thereby telomere elongation is a 5'-3' helicase Pif1. In the absence of Pif1, the level of Est1 increases at telomeres along with increased association of both Est1 and Est2 at the TG ends (Boule and Zakian, 2006).

In addition to the genetic control, telomere length homeostasis can be highly influenced by environmental stimuli. A study by Romano et al, measured perturbations in telomere length after exposure to environmental stress factors for 100-400 generations (Romano et al., 2013). Stress factors such as acetic acid and alcohols such as ethanol, methanol and isopropanol were shown to increase telomere length whereas others such as caffeine, heat and low levels of hydroxyurea were shown to decrease telomere length. Another model for telomere length regulation proposed recently, known as the 'replication-fork' model, suggests that telomerase is carried along the replication fork and eventually deposited at the end of the telomere for it to be elongated (Greider, 2016). However, the longer the telomere, greater the number of proteins to pass through for the replication fork with telomerase and thereby increasing the chances of dissociation. This model fits with the finding that shorter telomeres are preferentially elongated by telomerase (Bianchi and Shore, 2007).

1.16 Telomeric-Repeat containing RNA (TERRA)

Recent studies on telomere silencing and heterochromatic structure has revealed that telomeres are often transcribed producing non-coding **Te**lomeric-**R**epeat containing **R**N**A** (TERRA) that plays an important role in telomere length regulation (Azzalin et al., 2007, Iglesias et al., 2011, Luke et al., 2008). TERRA has been found in various eukaryotic species from budding yeast to plants. In *S. cerevisae*, TERRA consists of sub-telomeric X, Y' sequences and TG repeats. They are transcribed by RNA polymerase II, polyadenylated and range from 100-150 bp in length. The level of TERRA within a cell is regulated by RNA exonuclease *RAT1* which degrades the telomere transcripts (Luke et al., 2008, Rosonina et al., 2006).

One function of TERRA is thought to be in telomere length regulation and cellular senescence. It was shown that deletion of *RAT1* leads to increased levels of TERRA which in turn leads to shortening of telomeres and early cellular senescence (Maicher et al., 2012). This effect was reversed by increasing the level of RNase H suggesting that TERRA directly binds to the TG tract (Luke et al., 2008). On the other hand, in a different study by Balk et al, telomerase was knocked out in conjunction with knock-out of *RNH1* (codes for RNase H) which led to telomere elongation and increased number of population doubling (Balk et al., 2013). More interestingly, the binding of TERRA to telomeres also led to increased recombination events in pre-senescent cells prior to survivor generation. TERRA mediated HR recombination in the absence of *RNH1* was shown to act in cis to enable lengthening of telomeres. However, in the absence of *RAD52* and thereby HR, the TERRA-telomere hybrid was shown to shorten telomeres instead (Balk et al., 2013). Similar results were also produced by Tai-Yuan Yu et al who also demonstrated TERRA mediated telomere elongation to delay cellular senescence (Yu et al., 2014). Hence, the role of TERRA is quite dynamic in telomere function.

A study by Iglesias et al has shown that TERRA is negatively regulated by *RAP1* at the level of transcription and degradation suggesting an association of telomere length with TERRA levels (Iglesias et al., 2011). However, over elongation of telomere lengths using Cdc13-Est2 fusion protein (increases access of telomerase to TG ends) did not lead to increased levels of TERRA suggesting the length of the telomeres is not essential in determining TERRA levels. Furthermore, increased levels of TERRA are also associated

with increased Type II survivor formation in addition to premature senescence (Yu et al., 2014). The study suggested the increased proportion of Type II survivors to be the consequence of increased DNA-RNA hybrid formed at telomeres with the TERRA transcripts enabling efficient HR.

1.17 Role of initial telomere length in Type II survivor formation

Past research has vastly covered the genetic and molecular mechanisms of telomerase negative survivor formation. More recently it has been suggested that initial telomere length is pivotal in determining the type of survivor formed in *S. cerevisiae* in addition to the genetic requirements. In a study conducted by LeBel et al, *RAD52* is knocked-out in addition to telomerase in *S. cerevisiae* strains W303 and S288c prior to survivor formation. While W303 produced no survivors in the absence of *RAD52*, the strain S288c was surprisingly able to produce very rare Type II survivors (LeBel et al., 2009). The authors concluded this to be a result of inherent differences in initial telomere length between the two strains with W303 having relatively shorter telomeres than S288c. In fact, elongating the telomeres in W303 prior to survivor establishment by knocking-out Rif2 was able to generate Type II survivors at low frequency in a *POL32* independent manner (LeBel et al., 2009). This suggests initial telomere length to play a significant role in survivor formation with longer telomeres favouring Type II survivor formation. In another study by Chang et al, it has been observed that long telomeres in telomerase negative cells are preferentially elongated and are more proficient in bypassing senescence by becoming Type II survivors (Chang et al., 2011). Furthermore, previous work in the Louis lab has examined the proportion of survivor types generated from various *S. cerevisiae* isolates (European, North American, Sake, West African, Y55 and S288c) that possess varying initial telomere lengths. The study showed a positive correlation between increasing telomere length with the proportion of Type II survivors generated (Liti et al., 2009a, Muston, 2012) (Figure 1-9). Taken together, these data make a strong case for the importance of initial telomere length in determining the survivor type pathway taken by a telomerase negative cell.

A)

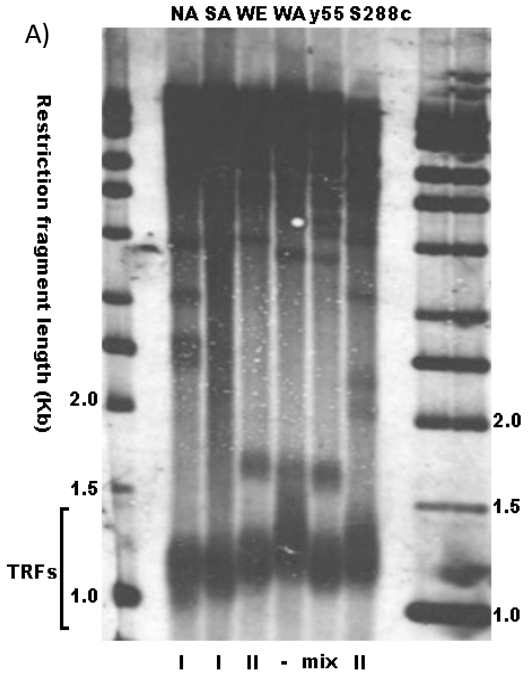

B)

Isolate	Tel. Length	Survivor type (%)	
		I	II
NA	Shortest	100	0
S		74	26
Y55		56	44
WE		8	92
S288c		8	92
WA	Longest	0	100

TRF – Terminal Restriction Fragment with *XhoI*

Figure 1-9: Association of initial telomere length with survivor type proportions in wild isolates of *S. cerevisiae* (Muston, 2012). A) Increasing telomere length in various *S.cerevisiae* isolates corresponds to increase in Type II survivor formation. Various *S. cerevisiae* isolates, North American (NA), Sake (S), Y55, Wine European (WE), S288c and West African (WA), were analysed for their telomere TRF using Southern blots. TRF in Southern blot shows relative differences in telomere length between the isolates. **B)** Telomerase was knocked out in each of the isolates and survivor proportions were analysed. The date shows a positive correlation between telomere length and Type II survivor formation (i.e. isolates with longer telomeres produce higher proportion of Type II survivors).

1.18 Telomere length as a complex trait

Complex traits are phenotypes that are affected by multiple genes with varying degrees of influence on the trait itself. Such traits regulated by multiple genes and gene-interactions can produce large diversity within populations of any organism with regard to physiology, morphology, resistance to disease or other environmental stress factors (Mackay et al., 2009). Likewise telomere length is regulated by more than 300 genes and gene interactions known as telomere length maintenance (TLM) genes making it a complex trait. TLM genes have mostly been identified via knock-out or knock-down studies in laboratory strains of yeast (Askree et al., 2004). Furthermore, majority of these TLM genes are non-essential identified via knock-out screening for telomere length in haploid cells. However, a large gap still remains in understanding the effect of essential genes and the wider gene interactions in maintaining telomere length equilibrium.

Loss of essential genes produces inviable cells making it difficult to study their function. Ungar et al conducted a study to identify essential TLM genes using strains containing hypomorphic alleles of genes of interest (Ungar et al., 2009). They identified 87 essential genes involved in telomere length from a total of 1033 in *S. cerevisiae*. However, it is likely that not all hypomorphic mutants have reduced phenotype essential for identifying their TLM function leading to exclusion of a vast number of candidates.

An alternative method employed by Liti et al is the use of Quantitative Trait Loci (QTL) analysis in F1 progenies arising from a cross of diverse parents with varying telomere lengths (Liti et al., 2009b). In this study, two divergent parental strains of *S. paradoxus* (CBS and YPS) with varying telomere lengths were mated generating 84 F1 progeny with a continuum of telomere lengths. Subsequent linkage analysis identified *YKU80* and *TLC1* as major QTLs in determining telomere length. Furthermore, the study was able to identify negative epistatic interaction between *YKU80* of CBS strain with the *YKU70* of YPS strain that led to very short telomeres. This study demonstrates that telomere length can in fact be studied as a complex trait and enable identification of novel variants (essential or non-essential) and gene interactions involved in telomere length homeostasis.

1.19 The X-QTL and i-QTL methods of quantitatively studying complex traits

Complex traits, such as telomere length, are not only affected by genes that have a direct effect on the phenotype but also consist of gene-gene interactions and gene-environment interactions with varying degree of input to the phenotype. One method of statistically identifying genes regulating a complex trait is Quantitative Trait Loci (QTL) analysis. Presence of natural variations such as single nucleotide polymorphisms (SNPs) underpin QTL analysis that help identify genes affecting complex traits. QTL mapping uses phenotypic and genetic marker information (such as SNPs) and employs maximum-likelihood linkage analysis to estimate the most probable loci responsible for the trait of interest at every point in the genome (Lander and Schork, 1994).

QTL mapping works under the fundamental principle that the marker locus or SNPs and the trait under investigation do not segregate independently and are therefore at linkage. Linkage of the marker to the trait can be statistically quantified by measuring the likelihood of the marker interval being associated to a QTL against the likelihood of association by chance using a Logarithm of Odds (LOD) score. A LOD score greater than 3 generally indicates presence of a statistically significant QTL (Kearsey, 1998). However, there are certain challenges associated with classical QTL mapping such as limited marker availability and the presence of large linkage blocks resulting in low resolution mapping i.e. numerous genes present within the marker interval. Furthermore, to have greater statistical power requires very large sample sizes which can be laborious and costly.

Complex trait analysis using QTL methods was first carried out in *S. cerevisiae* by the Davis group (Steinmetz et al., 2002). They crossed a laboratory strain S288c with another strain found in the lungs of an AIDs patient to examine the genetic architecture of high temperature growth. This demonstrated yeast to be a great model for dissecting complex traits, however, mapping studies in model organisms, such as yeast, typically detect only a fraction of the loci underlying heritable traits, implying that they lack sufficient marker pool and statistical power. Separate work by Kruglyak group and Louis group have developed more advanced methods for high resolution mapping known as X-QTLs (extreme QTL mapping) (Ehrenreich et al., 2010) and intercross-QTL (i-QTLs) (Liti and

Louis, 2012, Parts et al., 2011) respectively that addresses the challenges of classical QTL analysis.

The X-QTL method uses the standard two-hybrid model where variations in large number of F1 segregants are used for mapping. Using two different parents broadens the marker pool increasing resolution of QTL analysis. The three core principles of X-QTL analysis is firstly to generate a very large pool of F1 segregants ($>10^7$) with underlying variances in phenotype and genotype. Secondly, segregants showing extreme phenotypes for trait of interest are selected which increases the sensitivity of the study. Lastly, pooled allele frequencies are quantitatively measured by sequencing across the genome of control segregants and those selected for extreme-phenotype for mapping (Ehrenreich et al., 2010). Pooling segregants with extreme phenotypes from a large population increases the sensitivity of QTL mapping (picks up multiple causal loci) while also being cost effective.

Another method for fine mapping of QTLs is the generation of advanced inter-cross lines (AILs) where parental strains are subjected to 12 rounds of mating before producing large pool of segregants (Figure 1-10) (Parts et al., 2011). This method known as i-QTL can provide much better resolution in terms of mapping as it allows breakage of large linkage blocks via multiple rounds of meiotic shuffling of the genome and requires smaller sample size of segregants than the X-QTL method. Any variant in strong linkage with the trait of interest will be within a small region containing the likely target gene or even identified down to the single gene itself. In other words, mapping is more precise as the candidate gene pool will be smaller and close-by loci that are often missed due to co-inheritance will have greater likelihood of being detected. i-QTL method, can also be done using four parental strain backgrounds which are similarly subjected to 12 rounds of mating. The benefit of the four-way cross is the addition of more variants in the gene pool and increased ability of identifying gene interactions.

The process of QTL mapping in yeast has been advanced by the availability of whole genome sequences such as the S288c reference genome along with whole genome sequences of different parental strains that enable efficient bio-informatic analysis. Previous experiments have demonstrated (i-QTL) to be a successful approach in identifying genes associated with complex traits such as heat resistance (Parts et al.,

2011). In the study, Parts et al subjected cell populations to 12 rounds of selections and identified 21 gene intervals with significant changes associated with heat resistance, 9 of which contained two or fewer genes.

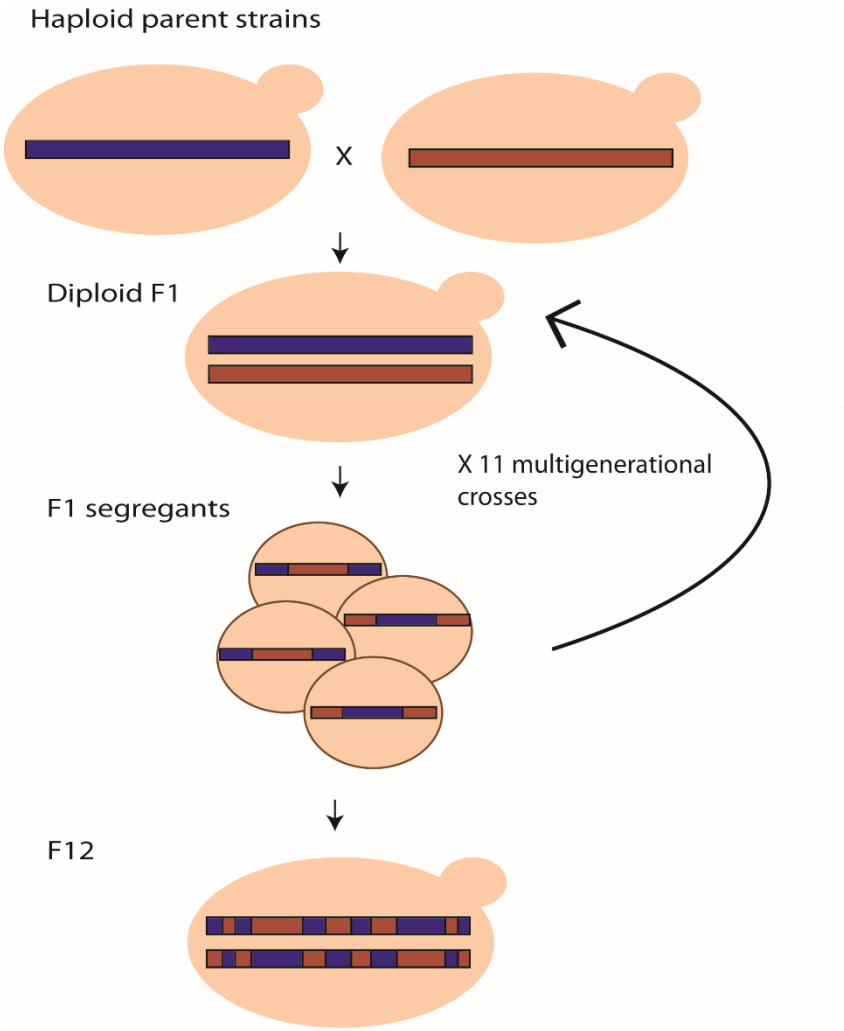

Figure 1-10: Process of multi-generational cross of two haploid parental strains for subsequent i-QTL analysis. Two independent parents with diverged backgrounds found in natural populations are subjected to 12 rounds of mating to generate advanced inter-cross lines (AIL). Subsequent F12 progenies generated from the cross are expected to result in significant shuffling of their genomes and consequently display wide variation in the phenotype of interest. Presence of natural variations in the parental strains and thorough genome shuffling is key to i-QTL method that enables high resolution mapping for causal genes.

1.20 Aims of this study:

Given the recent findings highlighting the importance of initial telomere length in determining telomerase negative survivor pathway, the main focus of this study is to investigate changes in survivor proportions and growth characteristics upon perturbations in initial telomere length and to gain a better understanding of inherent genetic differences that regulate telomere length via QTL analysis.

The first objective is to establish whether an increase or decrease in initial telomere length achieved via exposure to environmental stress factors, will correspond to a similar increase or decrease in the proportion of Type II survivor formation in three different laboratory strains of *S. cerevisiae* (Chapter 3). Next, based on the findings of LeBel et al, the requirement of *RAD52* epistasis group is further investigated upon alterations in initial telomere length i.e. are Type II essential genes such as *RAD59*, *SGS1*, *MRE11* and *SAE2* still required for Type II survivor generation after artificial telomere lengthening? Another question to be addressed is whether telomere lengthening at a single chromosome end is sufficient to shift survivor formation towards Type II.

The second objective is to understand the role of timing of senescence in relation to survivor type proportions (Chapter 4). It has been suggested in a study by Chang et al that longer telomeres at the time of senescence leads to higher proportions of Type II survivors (Chang et al., 2011). This will be addressed by examining survivor type proportions arising from a strain containing a construct that is able to induce early senescence from a single short telomere end while the remaining ends are relatively long. Furthermore, early senescence will be induced in conjunction with short telomere to examine whether the effect is dependent on telomere length.

The final objective is to study telomere length as a complex trait and identify genetic variances responsible for telomere length regulation. Two inbred and isolated populations of *S. cerevisiae* will be used to generate F12 advanced inter-cross lines to identify variants responsible for telomere length regulation using the i-QTL method along with the bio-informatic tool ‘Mulitpool’ (described in Chapter 5).

Chapter 2 Materials and Methods

2.1 DNA extractions

2.1.1 Yeast genomic DNA extraction

Yeast genomic DNA was extracted using 'E.N.Z.A® Yeast Genomic DNA isolation' kit supplied by Omega Bio-Tek. A single colony of yeast was inoculated in 5 ml of growth media in a 30 ml sterilin tube and cultured overnight at 30^{o}C in a shaking incubator (220 rpm). After overnight growth, cells were pelleted by centrifugation (Heraeus Multifuge 3SR+, Thermoscientific) at 4500 g for 5 minutes. The E.N.Z.A® yeast genomic DNA isolation protocol employed a combination of enzymatic and glass bead mediated breakdown of cell wall followed by cell lysis to extract DNA. The extract was incubated with RNase A to remove RNA. The system combined the reversible nucleic acid binding properties of HiBind® matrix to bind genomic DNA, followed by multiple high salt ethanol/propanol washes to remove impurities such as proteins and RNA. Finally, DNA was eluted in 50 µl of elution buffer and collected in 1.5 ml eppendorf tubes.

2.1.2 Bacterial plasmid extraction

Bacterial plasmid DNA was extracted as per the E.N.Z.A® plasmid DNA mini I kit protocol supplied by Omega Bio-Tek (Product number: D6942). *E.coli* containing plasmids of interest were taken out from -80^{o}C freezer and streaked into singles on LB/Ampicillin plates (Luria Broth) and incubated overnight at 37^{o}C. Next day, a single colony of *E.coli* was inoculated in 3 ml of liquid LB media containing 3 µl of 100 mg/ml ampicillin in a 15 ml loosely capped falcon tube and grown for 16-18 hours in a 37^{o}C shaking incubator. When the culture had become saturated, the cells were harvested by centrifugation in a multifuge and the supernatant was removed. The cells were transferred to a 1.5 ml eppendorf tube for plasmid extraction as per the E.N.Z.A® plasmid DNA mini I kit protocol. In brief, the protocol lysed the bacterial cells enzymatically and cleared the lysates via centrifugation. The supernatant containing the DNA was transferred to HiBind® mini Column for a simple bind-wash-elute procedure. The column contained a unique silica membrane that can bind between 40-70 µg of DNA in the presence of high concentration of chaotropic salt and allowed elution using a low-salt buffer in small volumes.

2.1.3 Quantification of double stranded DNA

Yeast genomic DNA and plasmid DNA concentrations extracted using E.N.Z.A® yeast genomic DNA isolation kit and E.N.Z.A® plasmid DNA mini I kit respectively were quantified using an IMPLEM nanophotometer. A microliter of the DNA sample was loaded onto the nanophotometer and exposed to a range of wavelength in the UV spectrum. The resulting optical density (OD) at 260 nm, the wavelength at which DNA absorbs light (Glasel, 1995), was used to calculate DNA concentration of the samples. The A_{260}/A_{230} ratios were noted as a measure of purity of the DNA samples against protein contaminants. A ratio within the range of 1.8 to 2 indicated good purity.

2.2 Sporulation and dissection

Diploid cells were sporulated in potassium acetate media (KAc) containing reduced amounts of nitrogen and glucose. Sporulation is a survival mechanism for when cells are deprived of essential nutrients for growth such as nitrogen and carbon sources and undergo meiosis. In addition, potassium acetate metabolism has been known to increase sporulation efficiency by promoting synthesis of proteins essential for sporulation itself (Esposito et al., 1969, Freese et al., 1982). A single colony of a diploid strain was initially patched on YPD media (Yeast extract-Peptone-Dextrose) and incubated overnight at 30^{o}C. After overnight incubation, cells were replica plated on to KAc media and incubated at 23^{o}C for 5-10 days. Once tetrads were formed (timing of which varied depending on the strain), they were scraped from KAc plates and added to 95 µl of dissection buffer (1 M sorbitol, 10 mM EDTA, 10 µM sodium-phosphate buffer pH 7.2). 5 µl of 10 mg/ml zymolase (1Unit zymolase per 100 µl reaction, supplied by Seikagaku) was added to the mix to break down the polysaccharide ascus wall of the tetrad containing the four spores (Kitamura et al., 1971). The digest was terminated after 15 minutes incubation at 37^{o}C by adding 400 µl of cold dissection buffer. Zymolase treated tetrads were transferred to YPD plates and spores from each tetrad were carefully re-located on the agar plate (dissected) using a dissection microscope (Zeiss Axioskop 40 Tetrad). Spores were grown for two days in 30^{o}C incubator until distinct colonies were produced.

2.3 Gene knock-out

2.3.1 Primer design for PCR based site specific gene disruption

Primers for gene deletions using selectable markers were designed to enable site specific recombination at the target loci. 65 bp forward and reverse primers were created such that the first 45 bp of the primers (5' end) were homologous to the sequences of the target gene and the last 20 bp (3' end) specific to either kanamycin (KAN), Hygromycin (HYG) or Nourseothricin (NAT) drug cassette plasmids. The drug cassette was then amplified via PCR and flanked on each 5' end by a 45 bp of homology to the target gene mediating homologous recombination based gene deletion upon transformation (Figure 2-1).

2.3.2 Lithium acetate transformation for gene knock-out

A single colony was inoculated in 5 ml of YPD and incubated overnight at 30^{o}C shaking incubator. Next day, the overnight culture (at stationary phase) was diluted 1/10 in 5 ml of fresh YPD and incubated at 30^{o}C for further 4 hours such that cells were once again growing in the log phase. An optical density measurement was taken of the culture at 600 nm wavelength (OD_{600}) before transformation using a spectrophotometer (HeλIOS У, Spectronic Unicam). Once the cells were at a density of around 10^7 cells/ml (indicating growth at the log phase), they were harvested by centrifugation at 3000 g for 5 minutes and washed in 1ml of sterile water. The cells were then resuspended in 1 ml of 100 mM LiAc and pelleted at maximum speed for 15 s. The supernatant was discarded and 240 µl of 50% PEG (polyethylglycene), 36 µl of 1 M LiAC (lithium acetate), 40 µl of 2 mg/ml single stranded salmon sperm DNA (denatured for 10 min in 100^{o}C) and 0.5-1 µg of transformation specific DNA sequence were added to the cells in sequential order to a final volume of 360 µl made up with sterile distilled water. The mixture was vortexed at maximum speed resuspending the cells and incubated at 30^{o}C for 30 minutes followed by heat-shock at 42^{o}C for 30 minutes. The cells were pelleted at 6000 rpm for 15 s in a table top centrifuge and supernatant was removed before re-suspension in 1ml of water. 200 µl of resulting cell suspension was plated on selective medium and incubated at 30^{o}C for 2-3 days. For transformation of DNA containing a drug resistance cassette (Kanamycin, Hygromycin or Nourseothricin), cells were resuspended in YPD media for 2-4 hours at 30^{o}C shaking incubator prior to plating on selective media. Transformants were obtained on selective media after 3 days of

incubation at 30°C and the efficiency of transformation varied depending on the strain background. Successful transformants were further verified via diagnostic PCR (Figure 2-1).

2.3.3 Diagnostic PCR mix

Diagnostic PCR was used to verify correct insertion of a construct or gene knockout after transformation. A single large colony was suspended in 20 µl of 0.02 M NaOH for 5 minutes at room temperature and lysed by vortexing at maximum speed. The cell suspension was centrifuged briefly at maximum speed to separate insoluble cell debris from the supernatant. The supernatant contained the DNA and was used as template for PCR. A total volume of 20 µl was used for PCR reaction which contained 11.4 µl of DNase/RNase free PCR water, 0.8 µl of 5 mM dNTPs, 0.6 µl of 50 mM Mg^{2+}, 2 µl of 10X NH_4 containing buffer, 1 µl of 10 µM forward primer, 1 µl of 10 µM reverse primer, 2 µl of 10X Rediload buffer, 1 µl of supernatant from NaOH treated cells containing template DNA and 0.2 µl of Biotaq polymerase (10,000 U/ml). Primers were designed such that the forward primer bound to sequences upstream of expected site of transformation and the reverse primer bound within the construct that was transformed (Figure 2-1). The PCR programme was as follows:

Stage	Temperature (°C)	Time (seconds)	
Initial denaturation	94	120	
Denaturation	94	30	Repeat cycle 29X
Annealing	52	30	
Extension	72	90	
Finish	72	300	
Store	15	∞	

2.3.4 Gel electrophoresis

Electrophoresis to check size of PCR fragments was run in 0.9% agarose gel (supplied by SeaKem) made in 0.5X TBE (1.09% Trizma base, 0.55% (w/v) Boric acid, 0.093% (w/v) EDTA with distilled water). 1 µl of EtBr was added per 100 ml to the agar. Samples were loaded and run at 80-100 V for 40 minutes to an hour.

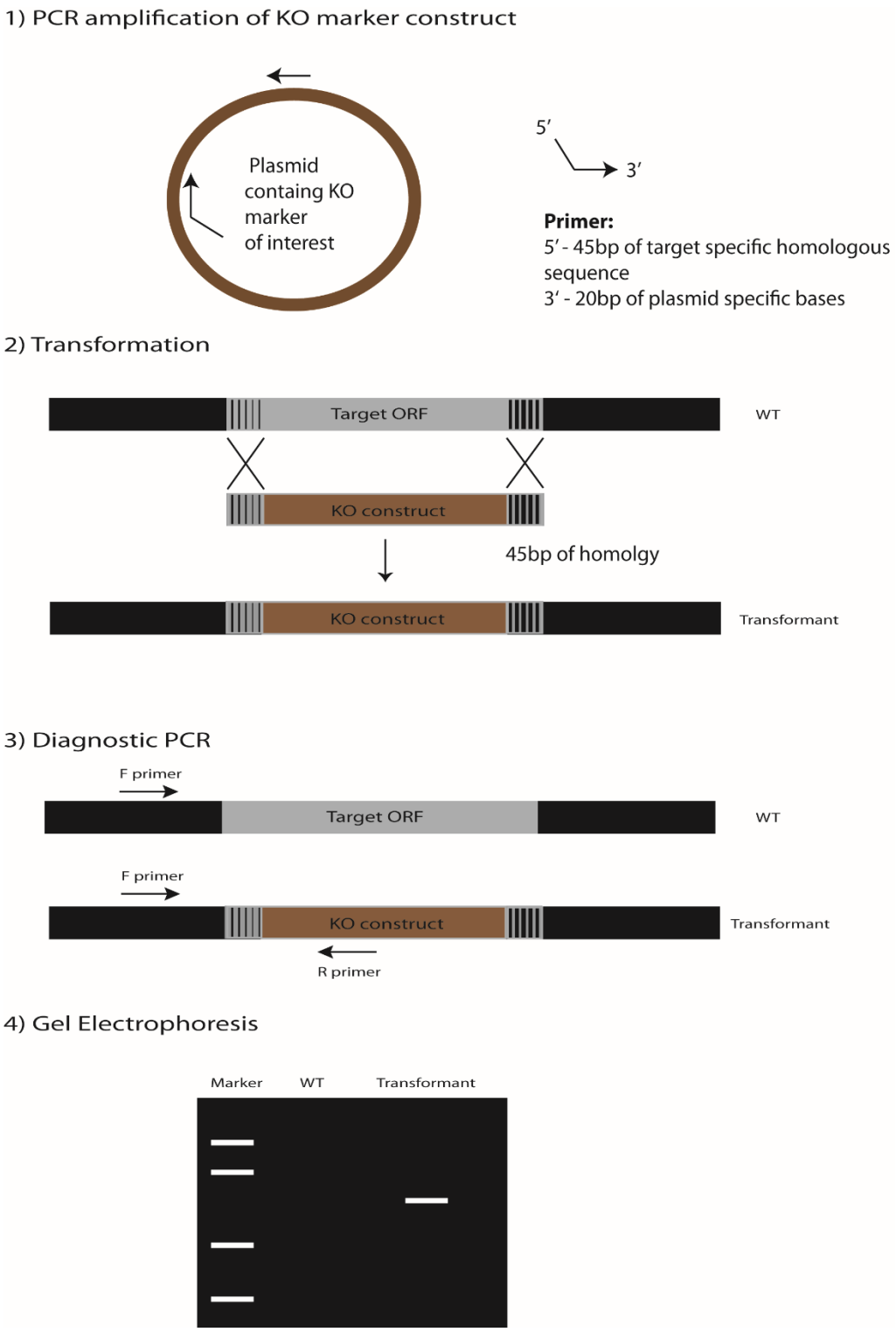

Figure 2-1: Steps involved in site specific gene-knock using a selective marker in *S. cerevisiae*. 1) Initially, a knock-out (KO) construct is amplified via PCR using 65 bp primers containing regions of homology with the target gene. **2)** The knock-out construct is transformed using the LiAc protocol. **3)** Successful transformants are further verified using diagnostic PCR using reverse primer specific to the transformed construct and forward primer in an upstream region of the target gene. **4)** The diagnostic PCR products are subjected to gel electrophoresis where only the transformant is able to produce a band but not the wild-type.

2.4 PCR methods

2.4.1 PCR mix for standard sequence amplification (size <4 kb)

Standard sequence amplification (size <4 kb) was carried out from either clean genomic DNA preps or plasmid DNA preps (described section 2.1.1 and 2.1.2) such that they were suitable for use in downstream experiments such as transformation. A 50 µl reaction was set up consisting of 5 µl of 10X NH_4 containing buffer (16 mM), 1.5 µl of 50 mM Mg^{2+} buffer, 4 µl of 5 mM dNTP's, 1 µl template DNA (2-4 ng), 2.5 µl of 10 µM forward primer, 2.5 µl of 10 µM reverse primer, 0.5 µl of Biotaq polymerase (10,000 U/ml – supplied by Bioline Ltd) and 33 µl of nuclease free water.

2.4.2 Long template PCR mix (size >4 kb)

Long template PCR (product size >4 kb) was carried out using commercially available Expand Long Template PCR system (supplied by Roche) containing Taq polymerase and Tgo polymerase with 3' – 5' exonuclease 'proofreading' activity. A 50 µl reaction was set up consisting of 1.75 µl of 10 mM dNTP mix, 1 µl of template DNA (2 ng), 5 µl of Buffer 2 (27.5 mM $MgCl_2$), 1.5 µl of 10 µM forward primer, 1.5 µl of 10 µM reverse primer, 0.75 µl of Taq and Tgo polymerase enzyme mix and 38.5 µl of nuclease free water.

2.4.3 PCR programmes

PCR was carried out using a Peltier Thermal Cycler (DNA engine, DYAD) with constant lid control at 100^{o}C. For standard product amplification (size <4 kb), the following program was used:

Stage	Temperature (^{o}C)	Time (seconds)	
Initial denaturation	94	120	
Denaturation	94	30	Repeat cycle 29X
Annealing	52-55	30	
Extension	72	60s per kb	
Finish	72	300	
Store	15	∞	

For long template PCR consisting of sizes > 4 kb, the following programme was used:

Stage	Temperature (°C)	Time (seconds)	
Initial denaturation	94	120	
Denaturation	94	10	Repeat cycle 9X
Annealing	55	30	
Extension	68	360	
Denaturation	94	15	Repeat cycle 19X
Annealing	55	30	
Extension	68	360 + 20 per cycle	
Final	68	420	
Store	15	∞	

2.5 Telomerase negative survivor assays

2.5.1 Ethanol and caffeine pre-treatments

Diploid *S. cerevisiae* cells, heterozygous for telomerase switch (*EST2/est2::URA3*, described in chapter 3) were subjected to growth under ethanol or caffeine stress in order to modulate initial telomere lengths. For telomere lengthening under ethanol stress, a single colony of the desired strain background was inoculated in 5 ml YPD consisting of 5-7% ethanol and grown overnight at 30°C shaking incubator. The next day, the cell cultures were diluted 1/50 (volume) in fresh 5-7% 5 ml YPD media and were similarly diluted for 8 consecutive days (>50 generations of cell doubling). For telomere shortening under caffeine stress, a single colony was likewise inoculated in 5 ml of 4 mM - 12 mM caffeine containing YPD media and grown overnight at 30°C shaking incubator. The next day, cells were diluted 1/50 in fresh 4 mM – 12 mM caffeinated 5 ml YPD media and similarly diluted for 10 consecutive days (approximately 100 generations of cell doubling). After day 8 and day 10 of growth under ethanol stress and caffeine stress respectively, the cells were pelleted and resuspended in 1 ml of sterile water. 100 µl of resulting cell suspension was directly plated on KAc media for sporulation and the remaining cells were used for DNA extraction to measure Terminal Restriction Fragments (TRFs).

2.5.2 Liquid culture propagation

Telomerase negative haploid cells were propagated in liquid media to generate survivor growth curves and asses parameters such as the timing of crisis in days, population doubling until crisis and efficiency of recovery from crisis. First, heterozygous telomerase switch diploids *(EST2/est2::URA3)* were sporulated for 5 days followed by tetrad dissection on YPD plates. The plates were incubated for two days at 30^{o}C until the segregants had grown into small colonies. These segregants were replica plated on URA drop-out plates and grown overnight at 30^{o}C. Segregants growing on URA drop-out plates were selected as telomerase negative haploids (*est2::URA3)* and inoculated in 5 ml of liquid URA drop-out media in a 30ml sterilin tube. Every 24 hours, cell densities were measured using a spectrophotometer (HeλIOS У, Spectronic Unicam) at a wavelength of 600 nm (OD_{600} 1 ~10^7 cells/ml) and approximately 1.5X10^5 cells/ml were transferred to fresh URA drop-out liquid media to a total volume of 5 ml for 10-15 consecutive days generating a growth curve. Cell cultures for liquid culture assays were grown in 30^{o}C shaking incubators (220 rpm).

2.5.3 Plate propagation assay

The plate propagation assay was carried out to determine the proportion of survivor types generated in the strain of interest. Telomerase negative cells grown in liquid culture favour higher representation of Type II survivors as they are more stable and grow faster compared to Type I survivors. To avoid such growth bias, telomerase negative cells were propagated on agar plates which enabled a fairer measurement of survivor type proportions. Telomerase negative (*est2::URA3*) haploid segregants from different strain backgrounds were generated as described in the section above (2.5.2) and were propagated on URA drop-out plates until survivors were produced. A single colony was transferred to a fresh plate every 3 days for a total of 6-8 re-streaks (approximately 20-25 generation per streak) until survivors were formed. Cells were grown in 30^{o}C incubators. After the final re-streak, a single colony from each of the starting 20-40 segregants were inoculated in individual 5 ml cultures and grown for 2 days prior to DNA extraction and TRF analysis. The 2 day growth prior to extraction was due to slower growth rate of survivors requiring more time for cultures to reach saturation.

2.5.4 Spot assay

Spot assays of pre-senescent telomerase negative cells were carried out to qualitatively determine the frequency of survivor formation in various strain backgrounds. Telomerase negative haploids were propagated in liquid URA drop-out media and serially diluted every 24 hour as described in section 2.5.2 leading to telomere erosion. When the pre-senescent culture attained low cell densities ranging between $1X10^6$-$5X10^6$ cells/ml after 24hr of growth, they were considered to be in the pre-crisis stage and ready to be plated for spot assays. A total of 10^7 cells were carefully measured using a spectrophotometer from the culture and pelleted in a microfuge (4500 g, 5 min). The cell pellet was resuspended in 50 µl of water and transferred to a 96 well plate. The cells were then serially diluted six times by a factor of 10 in 50 µl volumes. 5 µl volume of cells from each dilution (ranging from 10^6 cells to 10 cells) was plated as circular spots on appropriate media and grown for 3 days at 30^{o}C and 4 days at room temperature before taking picture of cell growth.

2.6 Statistical analysis

To determine the significance of change in proportion of survivor types, a 2X2 two tailed Fisher's Exact test was performed. Fisher's Exact test was used due to the small sample size in some cells of the 2X2 table (despite large enough sample size in total) arising from uneven distribution of survivor types in most strain backgrounds.

	*c*ontrol	test	Total rows
Type I survivor count	a	b	a+b
Type II survivor count	d	c	d+c
Total column	a+d	b+c	a+b+c+d = n

$$p = \frac{(a+b)!\,(d+c)!\,(a+d)!\,(b+c)!}{a!\,b!\,c!\,d!\,n!}$$

In order for the change in survivor proportions to be significant at a 5% threshold (less than 5% chance the change is occurring at random) and to reject the null hypothesis that the observed data was occurring by chance, the p value from the Fishers exact calculation had to be less than 0.05.

Likewise, to determine the statistical significance of change in population doubling until crisis and the peaks of crisis between control and test groups, a pairwise two tailed student's T-test was carried out. For change to be significant at a 5% threshold and to reject the null hypothesis of no change, the p value had to be less than 0.05.

2.7 Southern blot for Terminal Restriction Fragment (TRF) analysis

2.7.1 Endonuclease digestion of genomic DNA for generating TRF

Approximately 700 ng of quantified genomic DNA is restriction digested with enzyme *XhoI* in a 25 µl reaction volume in order to generate TRF's. 0.5 µl of restriction enzyme *XhoI* (10,000 U/ml) is added to 2.5 µl of CutSmart buffer (supplied by NEB), 2.5 µl of 10X Rediload loading dye and 1 µl of RNaseA (10mg/ml). Appropriately measured volume of aqueous DNA consisting of 700 ng is added to the mix and made to a total reaction volume of 25 µl with DNase free distilled water. The reaction mixture is incubated at 37^{o}C for 2 hours for the digest to complete.

2.7.2 Electrophoresis for Southern blot

300 ml of long 0.9% agarose gel containing 2 µl/100 ml of 10 mg/ml ethidium bromide solution was prepared using 0.5X TBE buffer to run DNA samples for southern blot. 700 ng of sample DNA were run in the 0.9% gel for 16 hrs at 50V in a tank also containing 0.5X TBE buffer. 10 µl of marker DNA containing 375 ng of *BstEII* digested lamda DNA (size ranging from 8,454 bp to 720 bp) or 200 ng of φ X174 *HaeIII* digest marker (size ranging from 1,353 bp to 72 bp) diluted in 1X loading dye was run in the gel alongside samples to assess the size of the bands generated.

2.7.3 Capillary transfer of DNA from gel to nylon membrane

DNA from agarose gel was transferred to nylon membrane overnight through capillary transfer using 20X SSC solution. The DNA was initially denatured by treating the agarose gel with 200 ml of alkaline denaturing buffer for 30 min in a shaker. This was followed by 2X 15 minute treatment of the gel with 200 ml of neutralising solution each

time. A tray containing 800 ml of 20X SSC was set up with a glass plate mounted on top. A 3MM Whatmann paper was soaked in 20X SSC and placed on top of the glass tray such that each end of the paper was dipped in the 20X SSC solution within the tray. The agarose treated with denaturing buffer and neutralizing buffer was mounted on top of the 3MM Whatmann paper. A nylon membrane covering the surface of the gel was cut and soaked in water followed by 4X SSC and placed on top of the gel. Any bubbles formed were carefully rolled out. Three more pieces of 3MM Whatmann paper were similarly soaked in water followed by 4X SSC and placed on top of the nylon membrane one by one rolling out the bubbles each time. Next, 10 cm thick stack of paper towels were placed on top, followed by another glass plate and a heavy weight mounted on top. This set up was left overnight for capillary transfer to occur from the 20X SSC solution up to the paper towels moving the DNA onto the nylon membrane in the process (Southern, 1975, Reed and Mann, 1985). Next day, the transferred DNA was cross-linked to the membrane by exposure to UV light (120,000 µJ/cm^2).

2.7.4 Radioactive probe labelling for TRF detection

Plasmid pRED571 was used to create a probe that binds specifically to TG_{1-3}repeats enabling detection of TRF fragments in a southern blot. Likewise, plasmid pRED513 containing *URA3* specific sequence was used as probe to verify transformation of the *URA3* marked telomere at CHRXIL. Probe specific to *BstEI*I digested lambda DNA and probe specific to φ DNA was also created to detect the size markers. 35 ng of pRED571 plasmid or pRED513 plasmid and 20 ng of *BstEII* digested lambda DNA or φ DNA was diluted with water in separate tubes in a total volume of 20 µl each. The DNA was denatured by incubating samples in 95ºC heat block for 5 minutes followed by rapid cooling on ice for 5 minutes. Condensation was collected by centrifuging the tubes at 10,000 g for 30 seconds. 1µl of Klenow polymerase (10,000 U/ml), 1 µl of BSA (100X), 1 µl of oligo labelling buffer (OLB) and 2.5 µl of radioactive ^{32}P tagged α-CTP were added to each tubes. The mix was incubated at 37ºC for 1 hr 30 min allowing klenow polymerase to mediate synthesis of nascent oligonucleotides which incorporated the radioactive ^{32}P tagged α-CTP. Free nucleotides not incorporated into the synthesis of the probe were removed by diluting the mix in 400 µl of elution buffer (10 mM Tris-HCL pH7.5, 1 mM EDTA, 0.1% SDS) and passing it through a sephadex column. First flow from the column produced a radiation free elute. Second flow through the sephadex column with 400 µl of elution buffer resulted in elution of clean

probe. The probe was then denatured into single strands by heating at 95ºC for 10 minutes followed by rapid cooling on ice for another 10 minutes.

2.7.5 Hybridisation and development of southern blot

The DNA bound nylon membrane was initially pre-hybridized with 30 ml of Church-Gilbert buffer (0.5 M Na_2HPO_4/NaH_2PO_4 pH7.4, 7% SDS, 1 mM EDTA, 1% BSA) for 2 hours in a cylindrical glass tube placed within a circular rotor in a 65ºC oven. After pre-hybridisation, the radio-actively labelled probe (described above) was added to the glass tube and left to hybridise overnight in the 65ºC oven. Next day, the membrane was washed four times with 30 ml of wash buffer (3X SSC/0.1% SDS) at 65ºC in the hyb-tubes, removing the unbound probe. The membrane was then wrapped in cling film, placed in a phosphor screen cassette and exposed overnight. After 24 hours, the signals in the phosphor screen were detected using Typhoon phosphor screen scanner.

2.7.6 Characterising survivor types via TRF analysis

Survivors were classified into either Type I, Type II or Type II-like survivors upon examination of XhoI restriction digested TRFs in Southern blots. Whilst Type I survivors display TRF pattern specific to amplification of Y' sub-telomeric repeat elements with short terminal TG_{1-3} ends, Type II survivors display multiple heterogeneous amplification of TG_{1-3} ends (Figure 1-5). However, not all TRF patterns are straight forward to characterize as some Type II survivors also contain Y' amplification. Hence in this study, any survivor with heterogeneous amplification of TG_{1-3} repeats of multiple ends was classed as Type II regardless of Y' repeat amplification. Furthermore, if survivors displayed amplification of TG_{1-3} repeats between two to four ends, they were described as Type II-like survivors but classed within Type II survivors. All other survivors were classed at Type I survivors.

2.7.7 Estimating TRF size using Image J and MS Excel

Size of TRFs observed in a Southern blot was quantified using Image J and MS Excel. Image J was used to measure the distance travelled by the marker from the well in the blot and that of the TRF bands. As TRFs are heterogeneous in length, they produce a band with a range of size. Hence, the distance measured was of the median of the TRF band. Size of the marker and its respective distance from the well was used to generate

a polynomial curve in MS Excel. Equation of the polynomial curve was subsequently used to estimate the size of the TRF.

2.8 Pulse field gel electrophoresis (PFGE)

Pulse field gel electrophoresis allows separation of large chromosomes by periodically alternating the electric field applied to the gel in two different directions at a desired angle. Although the electric voltage passes at an angle from two directions, the net movement of the DNA will still be in a forward direction.

2.8.1 Preparation of DNA plugs

Cells were grown in 5 ml culture overnight in a 30ºC shaking incubator and harvested the next day by centrifugation (4500 g, 5 min) removing the supernatant. Cells were initially washed with 1 ml of 50 mM cold EDTA in an eppendorf tube and resuspended in 200 µl of 50 mM EDTA. 100 µl of solution 1, consisting of SCE (1 M sorbitol, 0.1 M sodium citrate, 0.05 M EDTA pH 5.8), 25 µl/ml β-mercaptoethanol and 3 mg/ml zymolase 20T was added to the cells followed by 0.5 ml of warm 1% low melting point agarose (Seaplaque®) made in 0.125 M EDTA. 100 µl of the mixture consisting of the cells, solution 1 and agarose was loaded into a plug mold and left to set on ice for 1 hour, creating rectangular agarose plugs containing the cells. When plugs had set, they were transferred into a new eppendorf tube containing 0.5 ml of solution 2 (0.45 M EDTA / 0.1 M Tris, 5 µl/ml β-mercaptoethanol) and incubated at 37ºC overnight. Next day, solution 2 was removed from the tubes containing the plug and replaced with 0.5 ml of solution 3 (1% Sarkosyl / 0.4 M EDTA, 1 mg/ml proteinase K, 0.1 mg/ml RNAse) and incubated at 37ºC overnight. The plugs were then rinsed with 0.5 ml of cold EDTA and overlay with 0.5 ml of 0.45M EDTA / 0.1 M Tris. A third of the plug was then loaded on to wells in a 1% ultra-pure grade agarose gel (Bio-rad) prepared in 0.5X TBE and run for 24 hrs with alternating currents for PFGE in a tank also containing 0.5X TBE buffer at 14ºC.

2.8.2 Program for PFGE run for intact chromosomal DNA

Chromosomes ranging from 0.2 mb to 1.2 mb in size were separated with PFGE using the program below in a clamped homogeneous electric field (CHEF) electrophoresis machine (CHEF-DRIII system).

Stage	Initial switching time (seconds)	Final switching time (seconds)	V/cm	Angle(^{o})	Run time (hours)
1	60	60	6	120	15
2	90	90	6	120	9

2.9 Two parent multi-generational cross for i-QTL analysis

2.9.1 Cloning and plasmid transformation

A unique 35 bp palindromic tag containing a *SpeI* restriction site was added to the pFEP24 plasmid (containing *URA3* marker, core X and terminal TG_{1-3} sequences) and transformed into commercial JM109 vector cells. The tag was inserted via long-template PCR (described above 2.4.2 and 2.4.3) of the circular pFEP24 plasmid using primers that contained the tag as a 5' overhang in addition to the sequences specific to the site of insertion. The entire plasmid was amplified by PCR producing a linear DNA with the *SpeI* containing tag flanking both ends. 1 µg of amplified DNA was digested with 1 µl of enzymes *DpnI* and *SpeI* each for 90 minutes at 37^{o}C in a 50 µl reaction with 1X NEB buffer 4. The reaction was subsequently heat inactivated at 80^{o}C for 20 minutes and cleaned to remove buffers using the E.N.Z.A PCR clean kit. Approximately 100 ng of resulting DNA was ligated using 1 µl of T4 ligase and 2 µl of 10X T4 ligase buffer in a 20 µl reaction made up with nuclease free water and incubated at 16^{o}C overnight for re-circularization. The final ligated circular plasmid was then ready for transformation into commercially available competent JM109 *E.coli* cells. 50 µl of JM109 cells were thawed in ice for 5 minutes in an eppendorf tube. 5 µl of ligated plasmid DNA (25 ng) was added to the cells and gently flicked before being heat shocked at 42^{o}C for 50 seconds. The cells were immediately transferred to ice for 2 minutes after the heat shock. 950 µl of SOC medium was added and the cells were left

to incubate at 37ºC for 90 minutes. Approximately 200 µl of the culture was plated on LB/Amp media and incubated overnight at 37ºC. Successful transformants produced viable colonies after overnight incubation.

2.9.2 Multi-generational crossing

Inbreed wild type parental strains North American (NA) and Wine European (WE) were subjected to 12 generations of mating and sporulation in order to shuffle the genome during meiosis. Haploid NA (MAT α, *lys2::URA3, ura3::KanMX*) and WE (MAT a, *ura3::KanMX,* NAT-*speI* tagged CHRXIL) were mated on YPD plate by mixing the cells of two strains together. The cells were incubated overnight at 30ºC and replica plated on minimal media (without any amino acids) the next day. This enabled selection for NA X WE diploids that were now able to complement the others auxotrophies. The NA X WE diploids (UOS1) were again replica plated from minimal plates (MIN) to KAc plates and sporulated for 5 days at 23ºC allowing meiosis to occur.

Approximately $10^7 – 10^8$ of sporulated cells were collected and suspended in 0.5 ml of sterile water in an eppendorf tube. 0.5 ml of diethyl ether (supplied by Fisher) was added to the cells and vortexed for 10 minutes to kill any non-sporulated cells. The cells were then centrifuged at maximum speed for 2 minutes and supernatant removed. They were resuspended and washed in water 2 times to remove traces of diethyl ether. The cells were then pelleted and resuspended in 900 µl of dissection buffer (1 M sorbitol, 10 mM EDTA, 10 µM sodium-phosphate buffer pH 7.2) and 100 µl of 10 mg/ml zymolase and incubated at 37ºC for 30 minutes. After incubation, the cells were vortexed at maximum speed for 2 minutes to separate the spores from the ascus wall. The spores were then pelleted and resuspended in 200 µl of dissection buffer before plating on NAT media. They were evenly spread across the plate using glass beads and incubated overnight at 30ºC for random mating to occur again. The cells were then replica plated on MIN plates and grown overnight at 30ºC to select for diploids. The next day, cells were again replica plated on KAc media and incubated for 5 days at 23ºC leading to sporulation. The procedure was repeated 11 more times allowing shuffling of the genome and thereby creating variation in F12 progenies.

2.10 Bioinformatics analysis script: Geno2Pheno

Sequenced reads produced using the Illumina MiSeq platform were assembled using an internal script 'Geno2Pheno' written by Matthew Blades and Tom Walsh. The Geno2Pheno script contained two major components. First, it aligned the sequenced FASTQ files to the *S. cerevisiae* reference genome S288c using program BWA 0.7.17 (Li and Durbin, 2009). Here, it was set to output all alignments with the reference genome and mark shorter hits as secondary alignment. Reads were then locally realigned using program GATK3.4-0 (McKenna et al., 2010), filtering out any reads without stored bases, and recalibrate base quality scores using variants identified by Bergström (Bergstrom et al., 2014) as a reference set of known variant sites. Duplications were marked for deletion with Picard 1.93

Second aspect of Geno2Pheno was pooled variant calling and QTL scan. Variants were identified in pooled samples using FreeBayes with standard filters with ploidy set to 20 (as it contained genome from 20 segregants), minimum alternative allele fraction set to 0.05 and minimum alternative allele count set to 1. A custom script was used to calculate allele frequencies in each pool such that each allele in a diallelic variant was assigned to one of the founder strains. Non-diallelic variants were removed. The allele frequencies were then input to Multipool created by Edwards and Gifford (Edwards and Gifford, 2012) in contrast mode with pool size set to 20.

2.11 Strain backgrounds

2.11.1 Y55 derivatives

No.	Strain Name	Genotype Description	Notes
1	3465	*MAT α/a; ho/ho; ura3/ura3; TRP1/trp1, leu2/leu2*	
2	3466	*MAT α/a; ho/ho; ura3/ura3; TRP1/trp1, leu2/leu2; EST2/est2::URA3*	
3	3466.1	3466 + *SAE2/sae2::KanMX*	

4	3466.2	3466 + *SGS1/sgs1::KanMX*	
5	3466.3	3466 + R*AD59/rad59::KanMX*	
6	3466.4	3466 + *MRE11/mre11::KanMX*	
7	2369	*MATα; ura2-1; tyr1-1*	Mating type tester
8	2370	*MATa; ura2-1; tyr1-1*	Mating type tester

2.11.2 W303 derivatives

No.	Strain Name	Genotype Description
1	YAB0	*MATa; ho/ho; ade2-1; can1-100; his3-11; leu2-3; trp1-1; ura3*
2	YAB1	*MATα; ho/ho; ade2-1; can1-100; his3-11; leu2-3; trp1-1; ura3*
3	YAB610	YAB0 + *lys2::hphMX3; LEU2::pPgalCre-Li*
4	YUD610	YAB610 (MATa) X YAB1 (MATα)
5	YUD610.1	YUD610 + *EST2/est2::URA3*
7	YAB892	YAB610 + *adh4::TELox33*
8	YUD892	YAB892 (MATa) X YAB1 (MATα)
9	YUD892.1	YUD892 + *EST2/est2::URA3*
10	T131	YAB610 + *adh4::TELox131*
11	YUD131	YAB131 (MATa) X YAB1 (MATα)
12	YUD131.1	YUD131 + *EST2/est2::URA3*

2.11.3 S288c derivatives

No.	Strain Name	Genotype Description

1	M206	*MATα; leu2; lys2; ura3-52*
2	M205	*MATa; leu2; lys2; ura3-52*
3	SUA01	M205 X M206
4	SUA02	SUA01 + *EST2/est2::URA3*

2.11.4 Clean lineage strains obtained from the wild population

No.	Strain Name	Genotype Description	Geographic region
1	OS3	*Mat a; ho::HYG; ura3::KanMX*	(Wine European)
2	OS3.11	OS3 + *telCHRXIL::URA3-speI*)	(Wine European)
3	OS3.12	OS3.11 (*telCHRXIL::NatMX-speI*)	(Wine European)
4	OS104	*Mat α; ho::Hyg; ura3::KanMX*	(North American)
5	OS104.23	OS104 + *lys2::URA3*	(North American)
6	UOS1	OS3.12 X OS104.23	(Wine European X North American)

2.12 Plasmid backgrounds

No.	Name	Description
1	pRED713 (pFG2)	Telomerase switch plasmid, derived from pGEM7ZF(+) with *URA3* at *BamHI* site and *EST2* fragment at the *XhoI* site
2	pS30 (pRED231)	Plasmid containing Kanamycin resistance gene (KanMX), derived from pFA with KanMX cloned into *PmeI* site. Also known as pFA6-kanMX4
3	pRED459	Plasmid containing the Nourseothricin (NAT) resistance gene. Also known as pAG25.
3	pRED467	Y' element and telomeric TG_{1-3} repeats probe cloned into *SalI* site of plasmid pGEM3ZF (+). Also known as pEL30.
4	pRED571	TRF probe derived from pUC19 vector with TG_{1-3} repeats inserted
5	pFEP24	Plasmid containing 200 bp of homology to Telomere XIL

		followed by *URA* marker, Core X sequence and TG_{1-3} repeats.
6	pUA01	pFEP24 with 35 bp of *SpeI* containing tag inserted upstream of the TG_{1-3} repeats

2.13 Primers

Name	Sequence (5' - 3')	Description
K2	GTTTCATTTGATGCTCGATGAG	Diagnostic reverse primer specific to Kanamycin (KANMX)
H2	GAGATTCTTCGCCCTCCGAG	Diagnostic reverse primer specific to Hygromycin (HYGMX)
H3	ACAGCGGTCATTGACTGGAG	Diagnostic forward primer specific to Hygromycin (HYGMX)
N2	ACAGTCACATCATGCCCCTG	Diagnostic reverse specific to Nourseothricin (NATMX)
N3	GAATCGGACGACGAATCGGA	Diagnostic forward primer specific to Nourseothricin (NATMX)
s8	CCTCTAGGTTCCTTTGTTACTTCT	Diagnostic reverse primer for *EST2* knock-out. Binding specific to *URA3* gene in *est2::URA3*
329	GGACTTGTCGCATTTGAGTAG	Diagnostic forward primer that anneals to upstream region flanking the *EST2* gene.
UA5	TGGAGTCATT GGCTAGAGGA AAGGAAAAAA TACAGATTAT TGTTGCGTACGCTGCAGGTCGAC	Forward primer for amplification of *sgs1::KANMX*
UA6	AAGAGGTAAA GAAGCTAAAA AAGTGCCCAA AAAGAATGCT TGGCGATCGATGAATTCGAGCTC	Reverse primer for amplification of *sgs1::KANMX*

	G	
UA7	TGCGAACGAAACTGAATGAGT	Diagnostic reverse primer specific to sequences downstream of *SGS1*
UA8	TCGGCTGCCAGGATTTGTTT	Diagnostic forward primer specific to sequences upstream of *SGS1*
UA9	TTACGTAGAG GAGAAGAGCA TATTTCAGGA TAAACAGACA AAATACGTACGCTGCAGGTCGAC	Forward primer for amplification of *rad59::KANMX*
UA10	GATACCTGTT CCGTTCGCAT CAAATACAAA TGCCACTTAT TTTGTATCGATGAATTCGAGCTCG	Reverse primer for amplification of *rad59::KANMX*
UA11	TTTCACCCAGTCACCTGCAA	Diagnostic reverse primer specific to sequences downstream of *RAD59*
UA12	ACAGTTTGGCAAGGGCAGAT	Diagnostic forward primer specific to sequences upstream of *RAD59*
UA29	AAACATGGGCACGCAGATTC	Forward primer binding upstream of *MRE11* for amplification of *mre11::HYGMX*
UA30	CAGTTAACGCTTGCTTCCGT	Reverse primer binding downstream of *MRE11* for amplification of *mre11::HYGMX*
UA44	CTTCCCTGAACCGTTTTGCG	Diagnostic forward primer specific to sequences upstream of *MRE11*
UA45	TGTGGGGAGTGTAACAGCAC	Diagnostic reverse primer specific to sequences downstream of *MRE11*
UA31	TTCCATCCATGCTGTAAGCCATTA GGTGTTTGTATGTGAGCGTACGCT GCAGGTCGAC	Forward primer for amplification of *sae2::KANMX*
UA32	TTTCCCATATGCCAACGAGGAAA	Reverse primer for amplification

	AAAGCCCTTTCAACCATATCGAT GAATTCGAGCTCG	of *sae2::KANMX*
UA33	ACGATGCGGAAGGATGTGTT	Diagnostic forward primer specific to sequences upstream of *SAE2*
UA34	CGTCGTTCCCGTGGTAGAAA	Diagnostic reverse primer specific to sequences downstream of *SAE2*
UA19	CTCTCAGAGTGTGGACTCACTAGT CCATAACAAGGGAGACAGGTTGA TCAGGGTTGGA	Forward primer for insertion of *SpeI* tag at pFEP24 plasmid
UA20	CCCTTGTTATGGACTAGTGAGTCC ACACTCTGAGAGCCAAACCTACC CTCACATTACCC	Reverse primer for insertion of *SpeI* tag at pFEP24 plasmid
UA21	GAACTTTTACGTTAATGACGTCAT GGTGGTATAGATACGCCGTACGC TGCAGGTCGAC	Forward primer for replacement of *URA* marker with NATMX in CHRXIL of OS3.11 strain
UA22	TAATACATAAACACACTCAATTA CGTCGACAGATCCGAGCATCGAT GAATTCGAGCTCG	Reverse primer for replacement of *URA* marker with NATMX in CHRXIL of OS3.11 strain
UA15	ATGACTAACGAAAAGGTCTGGAT AGAGAAGTTGGATAATC GCTGTGGTTTCAGGGTCCAT	Forward primer for amplifying *lys2::URA3* knock out product
UA16	AGCAACTAGACTTATTTGCGCTTG AGTTAGTTCTATACTT ATTACGACCGAGATTCCCGG	Reverse primer for amplifying *lys2::URA3* knock out product
UA17	TTGGCTACTTCAAGCTGGGG	Diagnostic forward primer specific to sequences upstream of *LYS2* of the *lys2::URA3* knock out
UA18	AGCATCCCTTCCCTTTGCAA	Diagnostic reverse primer specific to sequences internal to the *URA* gene of the *lys2::URA3* knock out

2.14 Media

All media were sterilized prior to use by autoclaving at 115ºC for 20 minutes at 15 psi. For solid media, agar was added at quantities specified. For liquid media, all the components mentioned below were added apart from the agar.

YPD per 100 ml (non- selective media)

1 g yeast extract

2 g bacto-peptone

2 g dextrose (D-glucose)

1 ml of 0.5% adenine solution made up with 0.05 M HCL

2 g Bacto agar

pH 6.5

URA drop-out per 100 ml

0.675 g Yeast Nitrogen Base (YNB) without amino acids

2 g dextrose (D-glucose)

0.1 g URA drop-out powder

0.625 ml 1% Leucine

0.3 ml 1% Lysine

2 g Bacto agar

pH 6.5

LYS drop-out per 100 ml

0.675g Yeast Nitrogen Base (YNB) without amino acids

2g dextrose (D-glucose)

0.1g LYS drop-out powder

0.625ml 1% Leucine

2g Bacto agar

pH 6.5

URA/LYS drop-out per 100 ml

0.675 g Yeast Nitrogen Base (YNB) without amino acids

2 g dextrose (D-glucose)

0.1 g URA/LYS drop-out powder

0.625 ml 1% Leucine

2 g Bacto agar

pH 6.5

KANAMYCIN (G418/400) per 100 ml

1 g yeast extract

2 g bacto-peptone

2 g dextrose (D-glucose)

1 ml of 0.5% adenine solution made up with 0.05 M HCL

2 g Bacto agar

pH 6.5

Post autoclave: 0.04 g of G418 drug added after media had cooled down below 60^{o}C

HYGROMYCIN per 100 ml

1 g yeast extract

2 g bacto-peptone

2 g dextrose (D-glucose)

1 ml of 0.5% adenine solution made up with 0.05 M HCL

2 g Bacto agar

pH 6.5

Post autoclave: 30 mg of Hygromycin drug added after media had cooled down below 60^{o}C

NAT (nourseothricin) per 100 ml

1 g yeast extract

2 g bacto-peptone

2 g dextrose (D-glucose)

1 ml of 0.5% adenine solution made up with 0.05 M HCL

2 g Bacto agar

pH 6.5

Post autoclave: 10 mg of Nourseothricin drug added after media had cooled down below 60^{o}C

KAC per 100 ml

0.22 g yeast extract

0.05 g dextrose (D-glucose)

2 g potassium acetate (KAc)

0.087 g complete drop-out powder (no missing amino acids)

2 g Bacto agar

pH 6.5

LB amp per 100 ml

0.5 g yeast extract

1 g typtone

0.5 g sodium chloride

Post autoclave: 0.01 g ampicillin was added after media had cooled down below 60^{o}C

SOC per 100 ml

2 g Bacto Tryptone

0.5 g Bacto Yeast Extract

0.2 ml 5M NaCl.

0.25 ml 1 M KCl.

1 ml of 1 M MgCl2

1 ml of 1 M MgSO4

2 ml of 1 M glucose

GALACTOSE per 100 ml

1 g yeast extract

2 g bacto-peptone

1 ml of 0.5% adenine solution made up with 0.05 M HCL

2 g Bacto agar

pH 6.5

Post autoclave: 2 g of galactose was added after media had cooled down below 60^{o}C

MINIMAL per 100 ml

0.675 g Yeast Nitrogen Base (YNB) without amino acids

2 g dextrose (D-glucose)

2 g Bacto agar

pH 6.5

Amino acid drop-out powder mix

A complete drop-out powder mix (COM powder) was made by adding a combination of different amino acids and nucleic acids which are the most common auxotrophies found within laboratory yeast strains. To create drop-out media for selection of strains expressing a specific amino acid or nucleic acid, the appropriate amino/nucleic acid was removed from the drop-out powder mix. For example, to create URA drop-out powder, all the 11 amino acids except URA was added to the drop-out powder.

Amino acid/nucleic acid	Amount (mg)
Adenine	800
Argenine	800
Aspartic acid	4000
Histidine	800
Leucine	800
Lysine	1200
Methionine	800
Phenylalanine	2000
Threonine	8000
Tryptophan	800
Tyrosine	1200
Uracil	800

2.15 Reagents

All solutions were made to the desired volume using distilled water.

Denaturing buffer per 100 ml

5.84 g Sodium chloride

2 g Sodium hydroxide

Neutralizing buffer per 100 ml

6.06 g Trizma base

17.5 g Sodium chloride

3.3 ml 1M hydrochloric acid

20X SSC per 100 ml

17.6 g sodium chloride

8.82 g Tri-sodium Citrate

pH 7

5X TBE per 100 ml

5.45 g Trizma base

5 ml 1 M sodium citrate

6 ml 0.5 M EDTA

10X TE buffer per 100 ml

10 ml 1 M Tris-HCL

2 ml 0.5M EDTA

Autoclaved at 115^{o}C for 20minutes at 15 psi

Dissection buffer per 100 ml

50 ml 1 M Sorbitol

2 ml 0.5 M EDTA

1 ml of 1 mM sodium phosphate buffer pH 7.2

Church Gilbert buffer per 100 ml

5.11 g disodium phosphate

2.18 g sodium dihydrogen phosphate

7 g SDS

0.2 ml of 0.5 M EDTA (pH 8)

1 g BSA

SCE for PFGE plug preparation per 100 ml

50 ml of 2 M Sorbitol

10 ml of 1 M sodium citrate

12 ml of 0.5 M EDTA

Filter sterilized

5X OLB (Oligo Labelling Buffer) per 100 µl

20 µl Solution A (1.25 M Tris HCL pH 8.0, 0.125 M $MgCl_2$, 0.5 mM dATP, 0.5 mM dGTP, 0.5 mM dTTP, 257 mM 2-Mercaptoethanol in distilled water)

50 µl Solution B (2 M Hepes pH 6.6)

30 µl Solution C (100 µM Hexamer primers - mixture of single-stranded random hexanucleotides with 5'- and 3'-hydroxyl ends)

Chapter 3 The role of initial telomere length in recombination-based telomere maintenance of telomerase negative *S. cerevisiae*.

3.1 Introduction

In the last two decades, a vast amount of research has made a major leap in understanding the genetics behind telomerase negative survivor formation in yeast and mammals. In budding yeast *S. cerevisiae*, telomerase negative alternative lengthening of telomeres is largely a *RAD52* dependent recombination mechanism that is further sub-divided into the Type I and Type II pathways (Le et al., 1999). Although pre-senescent cells have genetically equal probabilities of producing either survivor types in an otherwise wild-type state, it is often the case that some strains tend to favour one survivor pathway over another resulting in different proportion of survivor types being generated (Muston 2012). In addition to the genetic requirements for survival type, several recent studies have indicated initial telomere length to be an important factor in determining the proportion of survivor types formed (Chang et al., 2011, LeBel et al., 2009). In fact, the study by LeBel et al suggests, when initial telomere length is sufficiently long, survivors can arise even in the absence of the *RAD52* gene (LeBel et al., 2009). Hence, the role of initial telomere length in determining survivor types is investigated in *S. cerevisiae* in this chapter.

In order to examine the importance of initial telomere length in survivor type formation, ethanol and caffeine have been used as environmental stress factors in this study to perturb telomere length. Stress induced telomere length perturbation was a precursor to the subsequent study of alteration in survivor type proportions. Ethanol mediates non-conventional stress response via the Rap1/Rif1 pathway that ultimately leads to telomere elongation (Romano et al., 2013). Rap1 has a wide range of functions throughout the cell and is also an essential regulator of telomere length that binds to the double stranded telomeric TG_{1-3} repeats (Hardy et al., 1992, Marcand et al., 1997). The study by Romano et al has revealed that ethanol dissociates the binding of Rap1 with the telomeric TG_{1-3} repeats allowing telomerase to elongate the telomere ends. Caffeine also acts via the Rap1/Rif1 pathway but unlike ethanol it leads to telomere shortening rather than lengthening. This is because in addition to the Rap1/Rif1 pathway, caffeine also inhibits the Tel1/Mec1 kinases which are essential in regulating DNA damage signalling at the telomeres and in the recruitment of exonucleases for repair activities (Romano et al.,

2013). Hence, it is worth noting that both ethanol and caffeine are able to regulate telomere length via the Rap1/Rif1 proteins albeit having an opposite effect.

After alteration of initial telomere length using environmental stress factors, its downstream consequences in the timing of senescence, efficiency of recovery from crisis and survivor type proportions were examined. The effect of telomere lengthening and shortening were examined in three different lab strains of *S. cerevisiae*, S288c, Y55 and W303, that are known to have varying initial telomere lengths with S288c having comparatively longer telomeres than W303 in their wild-type states (LeBel et al., 2009). In fact it is known from previous work in the Louis lab that S228c gives rise to mostly Type II survivors and Y55 gives rise to approximately equal proportions of both survivor types which could be down to the initial telomere length (Muston 2012). It is therefore of interest whether these proportions can be altered with manipulations of the initial telomere length using environmental stress factors.

The role of genes generally required for Type II survival was further investigated after bulk telomere elongation with regard to its presumed requirement for Type II survivor formation. The study by LeBel et al was carried out in the S288c strain known to have relatively longer telomeres in the wild-type state which was then able to produce Type II survivors even in the absence of *RAD52* (LeBel et al., 2009). However, in this study the effect of telomere lengthening in the absence of genes thought to be required for Type II survival was investigated in the Y55 strain that has no previous evidence of generating stable Type II survivors at wild-type telomere lengths in the absence of the Type II genes. Diploid heterozygous double knock-outs for telomerase and a Type II gene *SAE2, SGS1, RAD59* or *MRE11* were subjected to ethanol mediated artificial telomere lengthening. Survival type was then determined in these genetic backgrounds to see if the genes thought to be essential for Type II survival were still in fact essential for Type II survival after artificial elongation of telomeres.

Taken together, this study aims to shed light into the non-genetic factors responsible for telomere length maintenance in the absence of telomerase.

3.2 Telomerase disruption in yeast strains using a reversible switch construct

A reversible *EST2* knock-out construct was designed on plasmid pRED713 and transformed into three different laboratory strains W303 (YUD610), Y55 (3465) and S288c (SUA01) in order to generate heterozygous telomerase negative diploids. Plasmid pRED713 consists of a *URA3* maker and a 384 bp internal fragment of the *EST2* gene that contains a unique *SpeI* restriction site. Digestion of pRED713 with *SpeI* produced linear DNA that contained approximately 200 bp of the *EST2* sequence on either side of the *URA3* marker. Upon transformation, successful knock-outs for the *EST2* gene (*est2::URA3*) were selected by growth on URA drop-out plates. The resulting telomerase negative heterozygous strains were labelled YUD610.1 (W303), 3466 (Y55), SUA02 (S288c). The *EST2* knock-out is reversible post transformation as the fragments of *EST2* gene flanking the *URA3* marker of the linear transformant DNA forms direct repeats which can undergo spontaneous recombination, restoring the *EST2* gene and deleting the intervening sequences. Although the construct is fairly stable, spontaneous recombination can restore the *EST2* function and remove the *URA3* marker in the process (Figure 3-1) and so selection for *URA3* is maintained until reversion is desired. Revertants can be selected for by plating cells containing the telomerase switch on 5-FOA (5-Fluoroorotic Acid) media which is toxic for cells expressing *URA3*.

Successful transformants were further verified by diagnostic PCR (primer pair 329 + S8) to ascertain insertion of the knock-out construct in the correct locus within the genome (Figure 3-2). Primer 329 binds 826 bp downstream of the *EST2* start site whereas primer S8 binds within the *URA3* gene itself producing a band of approximately 1.6 kb upon PCR. Alongside check PCR of transformants, negative controls were made using DNA of the respective strains prior to transformation. After running the PCR products on a gel, it was observed that transformants did in fact produce bands of expected size, 1.6 kb, whereas no bands were seen for negative controls that lacked the *est2::URA3* switch.

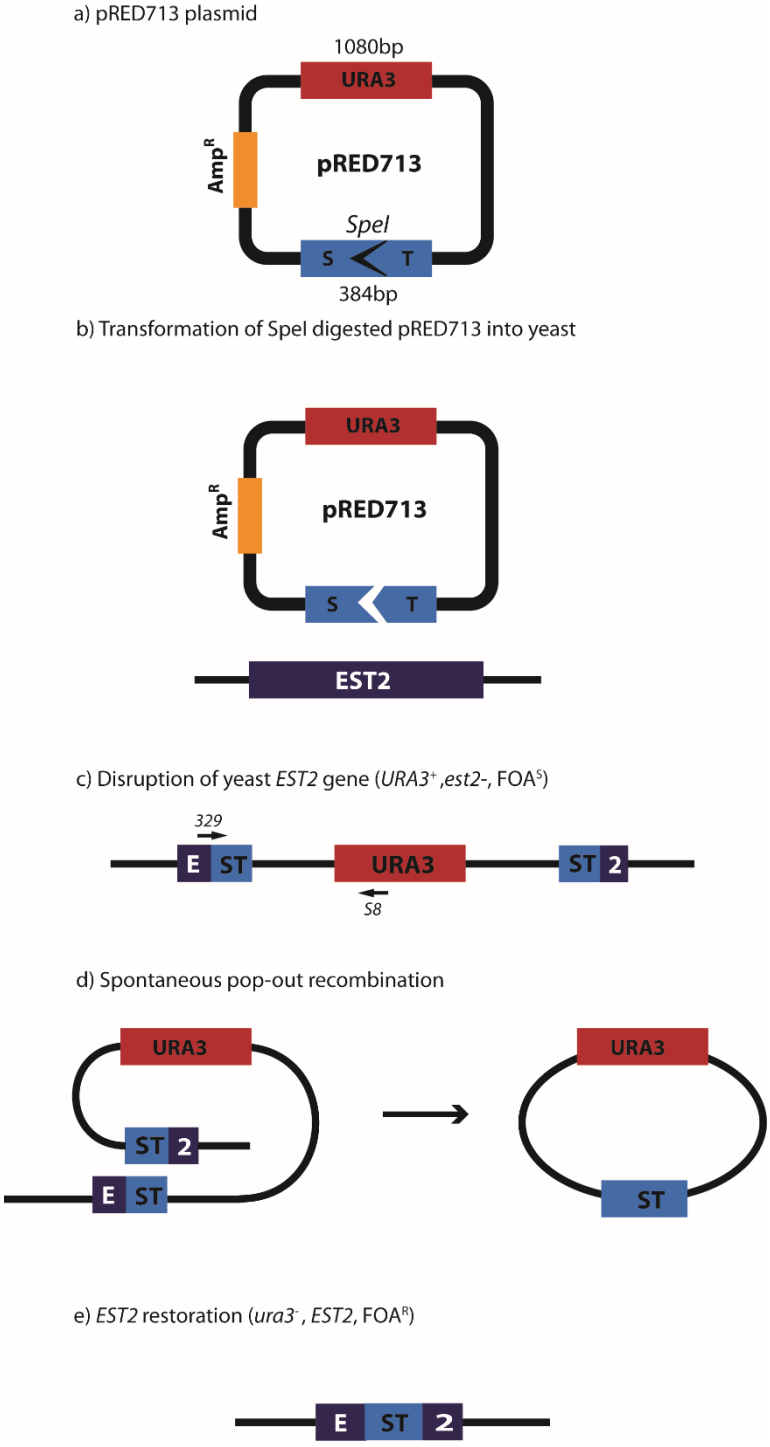

Figure 3-1: **The design and transformation of the telomerase switch (*est2::URA3*) plasmid in *S. cerevisiae*. a)** Structure and **b)** transformation of the pRED713 plasmid into a *S. cerevisiae* strain leading to **c)** disruption of the *EST2* gene in the form of a reversible switch using the *URA3* marker making it sensitive to drug 5-FOA in the process. The site for primer annealing is indicated by arrows within the *est2::URA3* construct. **d)** Spontaneous recombination arising from the availability of direct repeats can lead to the *URA3* marker popping out and **e)** restoration of the *EST2* gene and gain of 5-FOA resistance as *URA3* is lost.

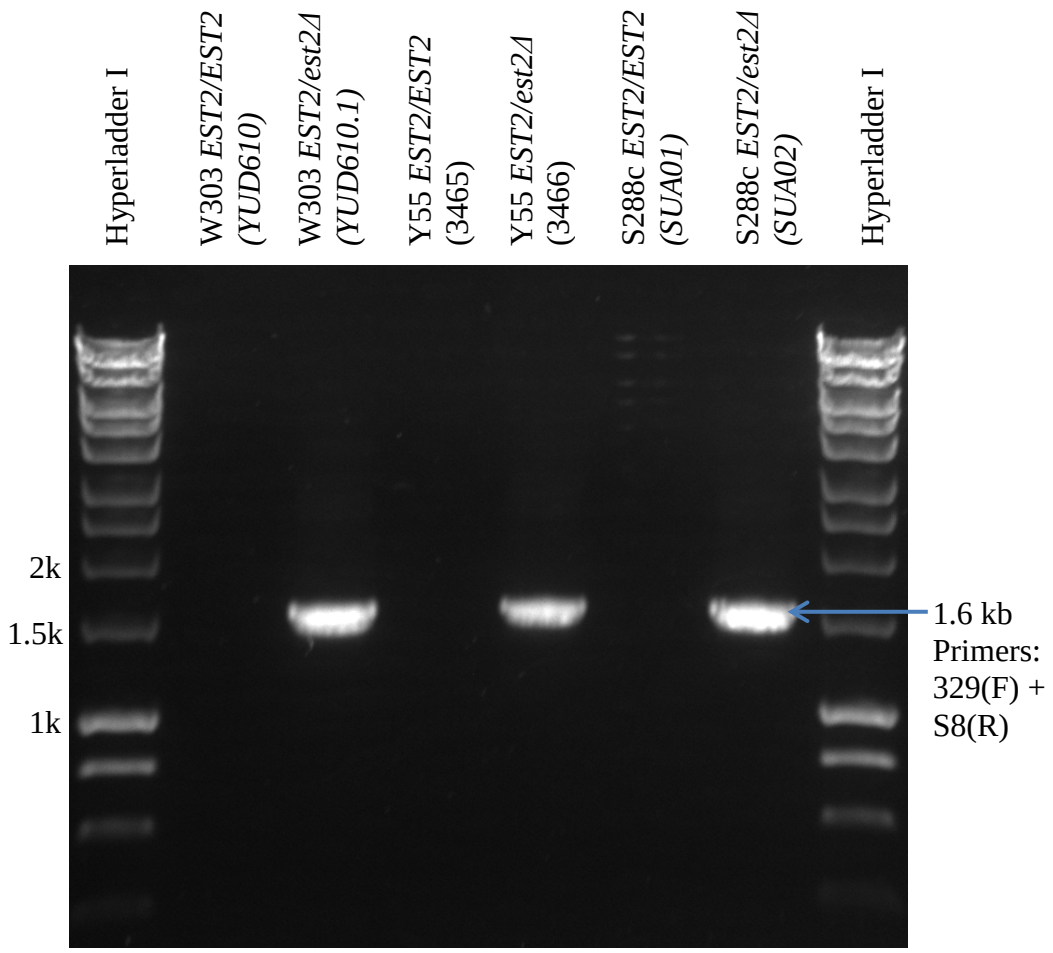

Figure 3-2: Diagnostic PCR confirming the insertion of telomerase switch in strains W303, Y55 and S288c. PCR product of *est2::URA3* transformant colonies and their respective negative controls were run on 0.9% agarose gel. Primer pairs 329 (F) and S8 (R) were used for all PCRs. Lane 1 and 8 contain Hyperladder I ranging from 10 kbp to 200 bp. Lane 2, 4, 6 contain negative controls (w/o the *est2::URA3* switch) of strains W303 (YUD610), Y55 (3465) and S288c (SUA01) respectively and do not produce any bands as expected. Lane 3, 5, 7 contain *est2::URA3* transformants of strains W303 (YUD610.1), Y55 (3466) and S288c (SUA02) respectively and produce a PCR product size of approximately 1.6 kb as expected.

3.3 Manipulation of telomere length in laboratory strains W303, Y55 and S288c using environmental stress factors

Initial telomere lengths in three different *S. cerevisiae* strains, W303, Y55 and S288c were manipulated via growth under exposure to ethanol or caffeine stress. For artificial telomere lengthening, W303 (YUD610.1) diploid heterozygous for the telomerase switch were subjected to 5% ethanol stress in YPD whereas diploids, Y55 (3466) and S288c (SUA02), also heterozygous for the telomerase switch were subjected to 7% ethanol stress in 5 ml YPD cultures. The cell cultures were diluted 1/50 every 24 hours onto fresh ethanol containing YPD media for >50 generations (8 days). After over 50 generations of growth under ethanol stress, DNA was extracted from the cells in order to examine the telomere length by generating *XhoI* digested Terminal Restriction Fragments (TRFs) (Lundblad and Blackburn, 1993) (Figure 3-3A). Alongside, an aliquot of the ethanol pre-treated diploids heterozygous for telomerase switch from all three strain backgrounds were plated on KAc media for sporulation. The variation in percentage of ethanol stress between the strains was due to relatively low tolerance and diminished growth capacity of the W303 strain at a higher concentration of 7% ethanol. A 5% ethanol exposure nonetheless resulted in slight telomere elongation in the W303 cell population as evidenced from measurements of the TRFs (Figure 3-3B). However, the telomere lengthening was much more prominent in the S288c cell population (+180 bp) compared to Y55 (+61 bp) or W303 (+63 bp) cell populations after ethanol treatment. This may be due to the existence of genetic differences and subsequent variation in response to ethanol stress between the different strains.

For artificial telomere shortening, the W303 diploid cell population was subjected to 4 mM caffeine stress in 5 ml YPD culture. The Y55 and S288c cell populations, were subjected to 12 mM caffeine stress. The cells were cultured for >100 generation with 1/50 dilutions every 24 hours onto fresh caffeine containing media for 10 days. As with ethanol pre-treatment, after 100 generations of cell culture under caffeine stress, DNA was extracted in order to measure *XhoI* specific TRF lengths. Alongside, an aliquot of cells were sporulated in KAc media to generate telomerase negative haploids for downstream studies. Due to inviability of W303 cell population at caffeine concentration of 12 mM, it was grown at a lower concentration of 4 mM. Similar to growth under ethanol stress, there was evidence of some telomere shortening after caffeine treatment in the W303

background (-59 bp). However, the shortening was more prominent in the Y55 cell population (-144 bp) compared to W303 or S288c (-88 bp) (Figure 3-3B).

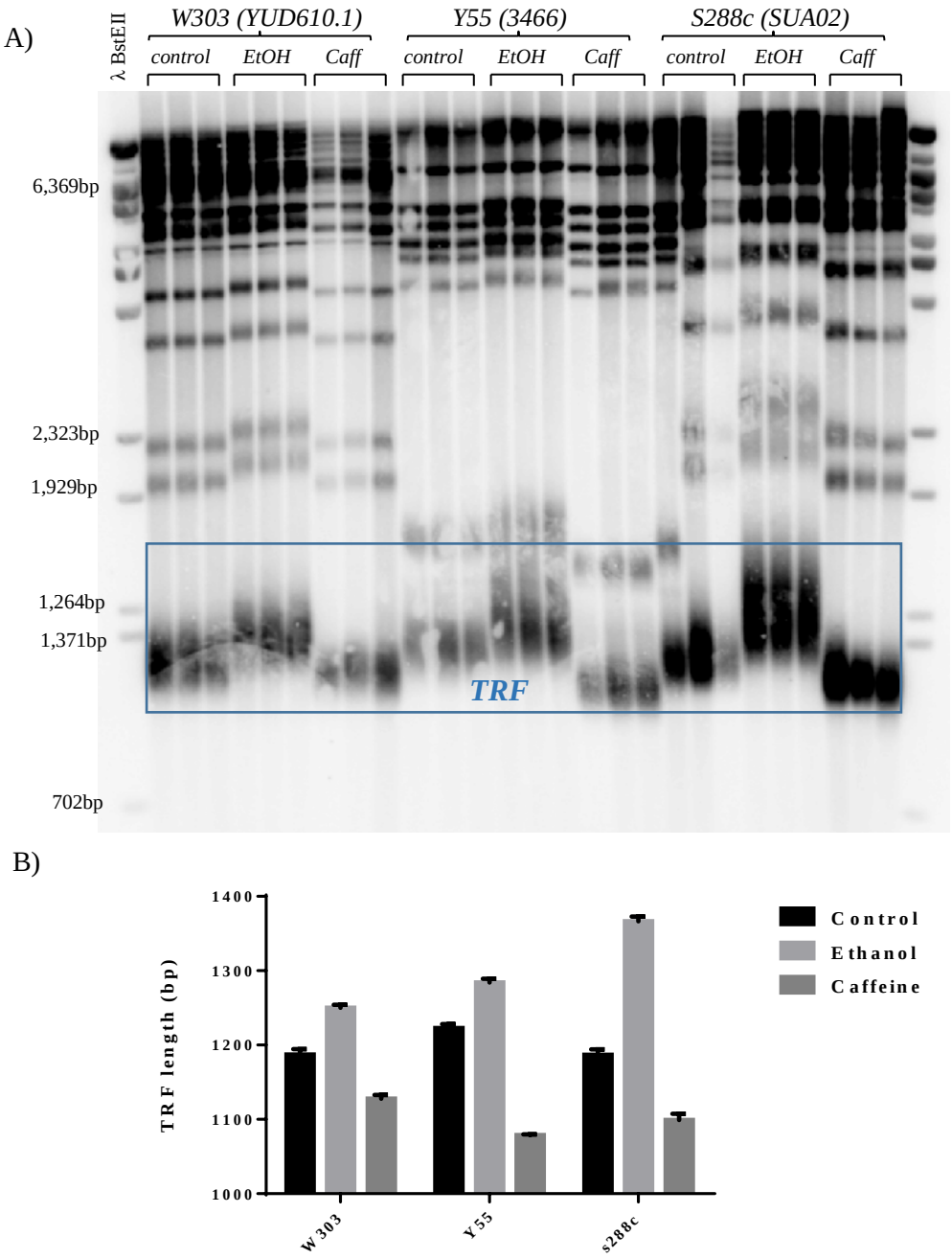

Figure 3-3: Alteration of initial telomere lengths after EtOH or caffeine treatment. **A)** Southern blot (probed with pRED571 specific to TG_{1-3} repeats) showing TRFs of strains W303, Y55 and S228c after growth under standard conditions, under 5-7% ethanol (EtOH) stress and under 4 mM-12 mM caffeine (caff) stress in three independent diploid replicates. **B)** Graph showing measurements of TRFs (n=3, ±SEM) obtained using ImageJ. There is an increase in telomere length in all three strain backgrounds after ethanol treatment and likewise a decrease in telomere lengths after caffeine treatments compared to control.

3.4 Delay in senescence in telomerase negative cells after elongation of telomeres and vice-versa after shortening of telomeres

Following growth under ethanol and caffeine stress conditions described in section 3.3, heterozygous telomerase negative diploids of strains W303 (YUD610.1) and Y55 (3466) were sporulated in KAc media for 5 days. Strain S288c (SUA02) was sporulated for 10 days due to poor sporulation efficiency. Resulting tetrads were dissected on YPD plates and subsequently replica-plated on URA drop-out plates to select for telomerase negative haploid segregants. 4-12 telomerase negative haploid segregants from each strain background per condition were propagated in liquid media until recovery from crisis. The average survivor growth curves generated is displayed in Figure 3-4.

Survivor growth curves of telomerase negative haploid strains W303, Y55 and S288c all show a delay in senescence after pre-treatment with ethanol and early senescence after pre-treatment with caffeine. This correlates with the elongation and shortening of initial telomere lengths induced from pre-treatment to ethanol and caffeine respectively. The change in the timing of senescence was quantified by measuring the total population doublings until senescence/peak of crisis of each growth curve (population doublings calculated based on OD measurements). Strains W303, Y55 and S288c had a change in population doubling of approximately +26, +29 and +89 number of doublings respectively after ethanol pre-treatment compared to their untreated counterparts (Figure 3-5A). Likewise, all three strains had a change in population doubling of approximately –23, -37 and -24 number of doublings respectively after caffeine pre-treatment (Figure 3-5A). The change in the number of doublings resulting from manipulation of initial telomere lengths was significantly different when compared to that of control in all backgrounds ($p<0.001$) (Figure 3-5A). Furthermore, in strain Y55, the change in the timing of cellular senescence in response to caffeine induced telomere shortening was sharper compared to its response to ethanol induced telomere lengthening. This was found to be opposite for strain S288c which responded much better to ethanol mediated telomere lengthening than caffeine mediated telomere shortening (Figure 3-5A). This variation in timing of senescence was in correlation with the initial telomere lengths (Figure 3-3).

Another parameter examined was the efficiency of recovery from crisis after telomere lengthening or shortening in all three strains compared to their wild-type counterparts with unaltered telomeres. This was done quantitatively by comparing mean cell densities

of each growth curve at their peak of crisis (Figure 3-5B). The deeper the peak of crisis, the less efficient the process of escape from G2/M arrest or survivor formation. In strain W303, although there was a delay in senescence after telomere lengthening, there was no significant increase in efficiency of recovery from crisis ($p=0.74$) (Figure 3-5B). This could have been due to the fact that telomere lengthening itself wasn't very prominent after ethanol pre-treatment to start off with. However, in strains Y55 and S288c, there was a significant increase in efficiency of recovery from crisis after ethanol induced telomere elongation ($p=0.0035$ and $p=0.00023$ respectively) (Figure 3-5B). Similarly, there was a significantly sharp decline in the efficiency of recovery from crisis in all three strains, W303, Y55 and S288c when telomeres were shortened after caffeine pre-treatment ($p=0.0014$, $p=0.0025$ and $p=0.00071$ respectively) (Figure 3-5B). This suggests that longer telomeres enable effective recovery from crisis and vice-versa.

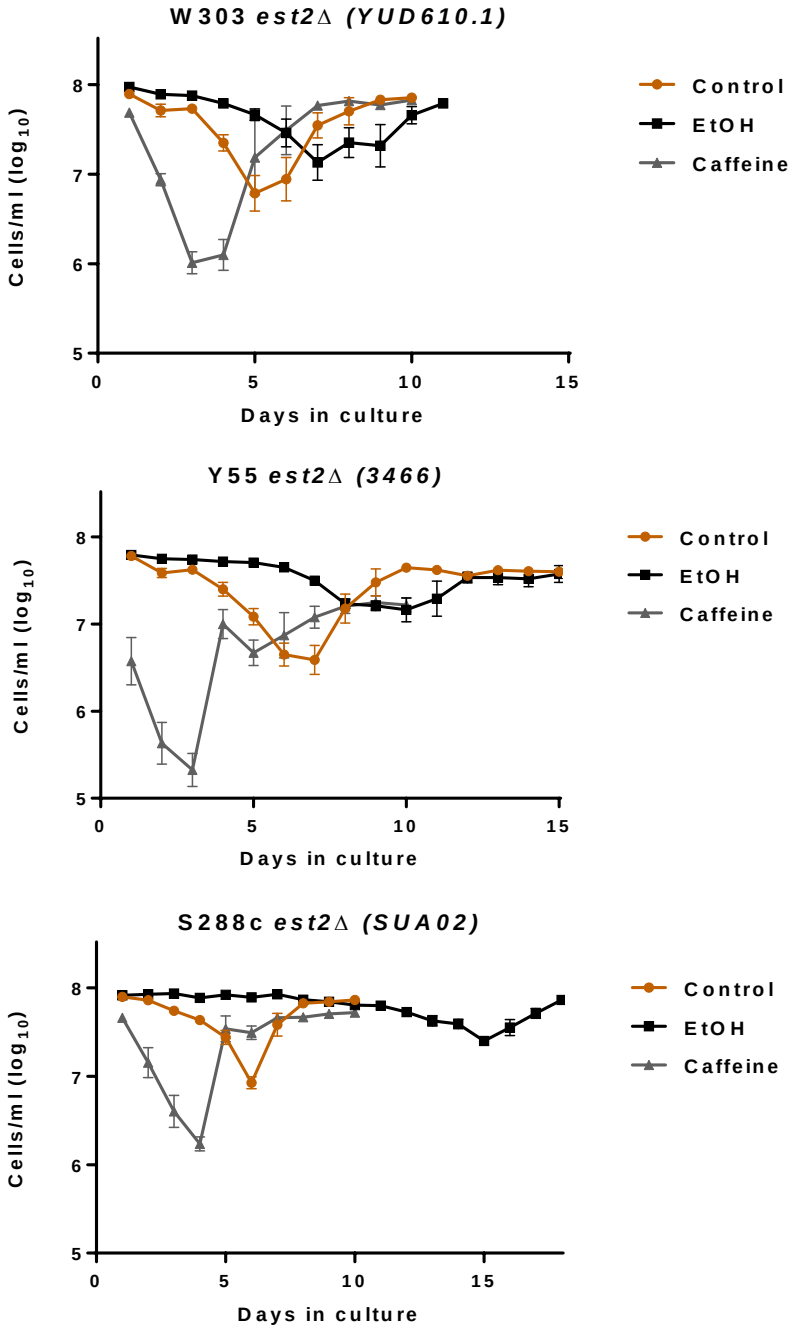

Figure 3-4: Growth curves of senescing telomerase negative cultures after pre-treatment with EtOH or caffeine. Average growth curves of telomere negative haploids (n= 4-12, ±SEM) over the course of 10-18 days in strains W303, Y55 and S288c propagated under standard conditions, after 5-7% ethanol pre-treatment (whilst in diploid state), after 4-12 mM caffeine pre-treatment (whilst in diploid state) or no pre-treatment (control). Cultures were diluted and measurements of cell density were taken every 24 hr until cells entered crisis (troughs of the growth curves) and eventually picked up growth by becoming survivors. Whilst all cultures undergo senescence followed by recovery, those pre-treated with caffeine have deep troughs indicating prolonged senescence and those pre-treated with ethanol have shallower troughs indicating faster recovery from senescence.

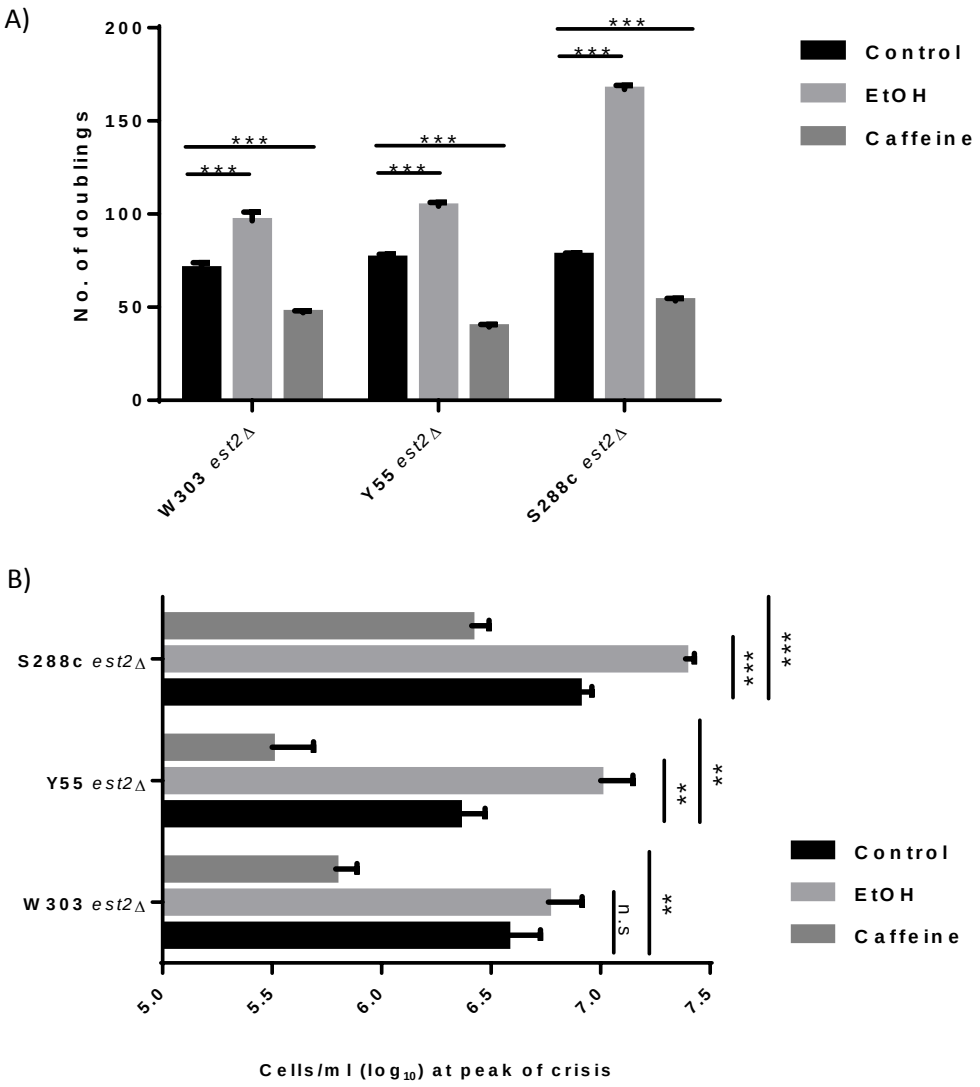

Figure 3-5: Changes in number of population doubling and efficiency of recovery from crisis in accordance with telomere lengthening or shortening. A) Average population doublings of telomerase negative haploids (n= 4-12, ±SEM) in strains W303 (YUD610.1), Y55 (3466) and S288c (SUA02) propagated under standard conditions, after 5-7% ethanol pre-treatment (whilst in diploid state), after 4-12 mM caffeine pre-treatment (whilst in diploid state) or no pre-treatment (control). Number of population doublings was estimated by converting the relevant OD measurements into approximate cell counts and adding the number of doublings each day until the peak of crisis for each growth curve. There is a significant increase in the number of population doubling compared to control after ethanol pre-treatments in all three stain backgrounds ($p<0.001$) and likewise a significant decrease in the number of population doublings after caffeine pre-treatment ($p<0.001$). **B)** Graph showing cell densities at peak of crisis (n= 4-12, ±SEM). Cell densities at peaks of crisis is used as a measure to estimate the ability of cell cultures to recover from crisis are significantly lower after caffeine pre-treatment in all three strain backgrounds. On the other hand, cell densities at peak of crisis after ethanol pre-treatment is significantly higher in the S288c background and Y55 but is not significantly higher in strain W303. (* $p<0.05$, ** $p<0.01$, *** $p<0.001$)

3.5 Downstream consequences of telomere length perturbation: shorter telomeres generate fewer Type II survivors.

It was observed in the previous section that telomere length is essential in determining the timing of senescence and that longer initial telomere length enables efficient recovery from crisis and vice-versa. It is also known that Type II survivors grow more robustly in liquid cultures compared to Type I survivors that have slower and fluctuating growth rates, most likely owing to the short terminal $TG_{1\text{-}3}$ tracts (Teng and Zakian, 1999). It can then be hypothesized the increased efficiency of recovery from crisis after telomere elongation could be a result of high frequency generation of comparatively robust Type II survivors. Therefore, I next examined the proportion of survivor types generated in telomerase negative haploids of each of the three strains W303 (YUD610.1), Y55 (3466) and S288c (SUA02) after ethanol and caffeine pre-treatments using the plate propagation survivor assay as carried out in several previous studies (Huang et al., 2001, Liti and Louis, 2003).

For examining the effect of telomere lengthening on the proportion of survivor type formation, only strains W303 and Y55 were used. W303 with wild-type telomere lengths produced approximately 7% Type II survivors whereas Y55 with wild-type telomere length produced 43% Type II survivors (Table 3-1, Appendix 7.1, 7.3). An increase in the proportion of Type II survivors was expected with longer initial telomere length; therefore strain S288c was not used for this aspect of the study as more than 78% of its survivors were already Type II under wild-type telomere lengths (Table 3-1, Appendix 7.5). Hence, the consequence of further telomere elongation on survivor type proportions would be hard to discern quantitatively in the S288c strain with a standard sample size. However, after telomere elongation in strains W303 and Y55, there was no significant change in the proportion of Type II survivors generated (0% and 38% in W303 and Y55 respectively) (Table 3-1, Appendix 7.1-7.3). This was possibly due to the fact that W303 and Y55 responded poorly to telomere elongation with ethanol stress leading to only minor increase in length.

As ethanol mediated telomere lengthening did not produce a significant change in survivor type proportions, the effect of telomere shortening on survivor proportions was examined in strains Y55 and S288c. Strain W303 was not used for this study as it already produced a very low proportion of Type II survivors with wild-type telomere length making the effects of further telomere shortening hard to discern. There was a significant

decrease in the proportion of Type II survivors after telomere shortening in the Y55 strain from approximately 43% to 12% (p=0.02) (Table 3-1, Appendix 7.3-7.4). Likewise, there was also a significant decrease in the proportion of Type II survivors after telomere shortening in the S288c strain from 78% to 52% (p=0.0376) (Table 3-1, Appendix 7.5-7.6).

Hence, it can be concluded that initial telomere length does in fact alter the proportion of survivor types generated with longer initial telomeres favouring the Type II pathway and shorter initial telomeres favouring the Type I pathway (Figure 3-6). Although no change in survivor proportion was observed for the W303 and Y55 strain after ethanol pre-treatment, the result remains inconclusive as telomere lengthening itself was very minor and possibly not significant enough to cause a shift in survivor proportions.

Strain (*est2Δ)*		N	Type I	Type II	Type I (%)	Type II (%)	Fishers Exact p value (vs control)
W303 (YUD610.1)	Control	41	38	3	93	7	
	5% EtOH	30	30	0	100	0	0.2575
Y55 (3466)	Control	21	12	9	57	43	
	7% EtOH	29	18	11	62	38	0.7759
	12mM caff	33	29	4	88	12	0.02*
S288c (SUA02)	Control	41	9	32	22	78	
	12mM caff	29	14	15	48	52	0.0376*

Table 3-1: Changes in survivor type proportions after alteration of initial telomere lengths. Total sample size and the proportion of each survivor types generated (rounded to whole numbers) in three different *S. cerevisiae* strains (W303, Y55 and S288c) when propagated under standard conditions, after 5-7% ethanol pre-treatment (EtOH - whilst in diploid state), after 4-12mM caffeine treatment (caff - whilst in diploid state) or no pre-treatment (control). Initial telomere lengths displayed in Figure 3-3B. Survivor types were characterised using Southern blot analysis of *XhoI* digested TRFs as described in Methods 2.7.6 (Southern blots in Appendix 7.1 – 7.6). A 2X2 two-tailed Fishers exact test was used to calculate the p-value and determine statistical significance of changes in survivor type proportions compared to control. Groups with $p<0.05$ were considered to be significantly different from their respective controls and marked with an asterisk.

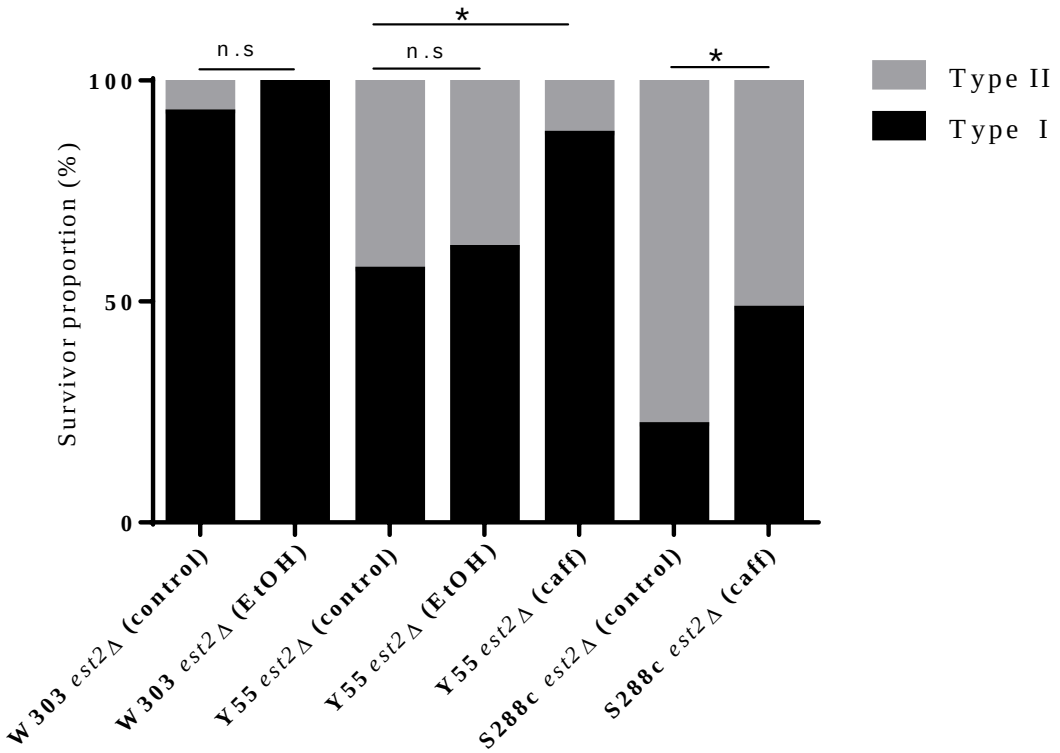

Figure 3-6: Changes in survivor type proportions after alteration of initial telomere lengths. Bars represent survivor type proportions (Type I and Type II) in percentage obtained in three different *S. cerevisiae* strains propagated under standard conditions, after 5-7% ethanol pre-treatment (EtOH - whilst in diploid state), after 4-12mM caffeine treatment (caff - whilst in diploid state) or no pre-treatment (control) as per data in Table 3-1. (*$p<0.05$) (Southern blots in Appendix 7.1 – 7.6)

3.6 Telomere elongation in telomerase negative double knock-outs with gene generally required for Type II survival.

We have seen an increase in the efficiency of recovery from crisis and a higher proportion of Type II survivors when telomerase negative cells have longer initial telomere lengths. The question addressed here is whether knocking out genes generally thought to be required for Type II survival (*SAE2*, *SGS1*, *RAD59* and *MRE11*) will negate the observed increase in recovery from crisis after artificial telomere elongation.

This study was carried out in the Y55 background due to its ability to produce both survivor types in roughly equal proportions under standard conditions. Hence any changes in survivor proportions under variable conditions could be easily observed in either direction. *SAE2*, *SGS1*, *RAD59* and *MRE11* were knocked out using either the kanamycin or hygromycin drug cassette in diploids heterozygous for the telomerase switch (3466) generating double heterozygous strains 3466.1 (*EST2/est2Δ; SAE2/sae2Δ)*, 3466.2 *(EST2/est2Δ;SGS1/sgs1Δ)*, 3466.3 *(EST2/est2Δ;RAD59/rad59Δ)* and 3466.4 *(EST2/est2Δ;MRE11/mre11Δ*). Diagnostic PCR was carried out subsequently verifying the gene knock-outs were in fact in the correct loci (Figure 3-7).

As described in section 3.3, all four double heterozygotes (3466.1, 3466.2, 3466.3 and 3466.4) were subjected to 7% ethanol stress for >50 generations (8 days) in order to elongate telomeres. Their TRFs when grown under standard conditions were analysed alongside their TRFs after growth under ethanol stress via Southern blot analysis (Figure 3-8A). Loss of a single copy of the gene required for Type II survival led to a decrease in the initial telomere length under standard conditions in the double heterozygotes 3466.1, 3466.2, 3466.3 and 3466.4 (-30 bp, -69 bp, -38 bp and -53 bp respectively) compared to the single heterozygote for telomerase knock-out (3466). This effect can be attributed to haplo-insufficiency in diploids upon loss of a single copy of the gene. However, telomere length was rescued after ethanol mediated telomere elongation in all four double heterozygotes in comparison to their un-treated counterparts and even lengthened beyond that of the wild-type 3466 (Figure 3-8B).

It is also worth noting that the different genotypes responded variably to ethanol mediated telomere lengthening compared to their untreated counterparts in the diploid background. For instance, heterozygous strains containing *SAE2* and *RAD59* knock-outs responded well to ethanol induced telomere lengthening (+143 bp and +128 bp respectively)

whereas heterozygous strains containing *MRE11* and *SGS1* knock-outs had a marginally reduced response (+95 bp and +107 bp respectively) comparatively.

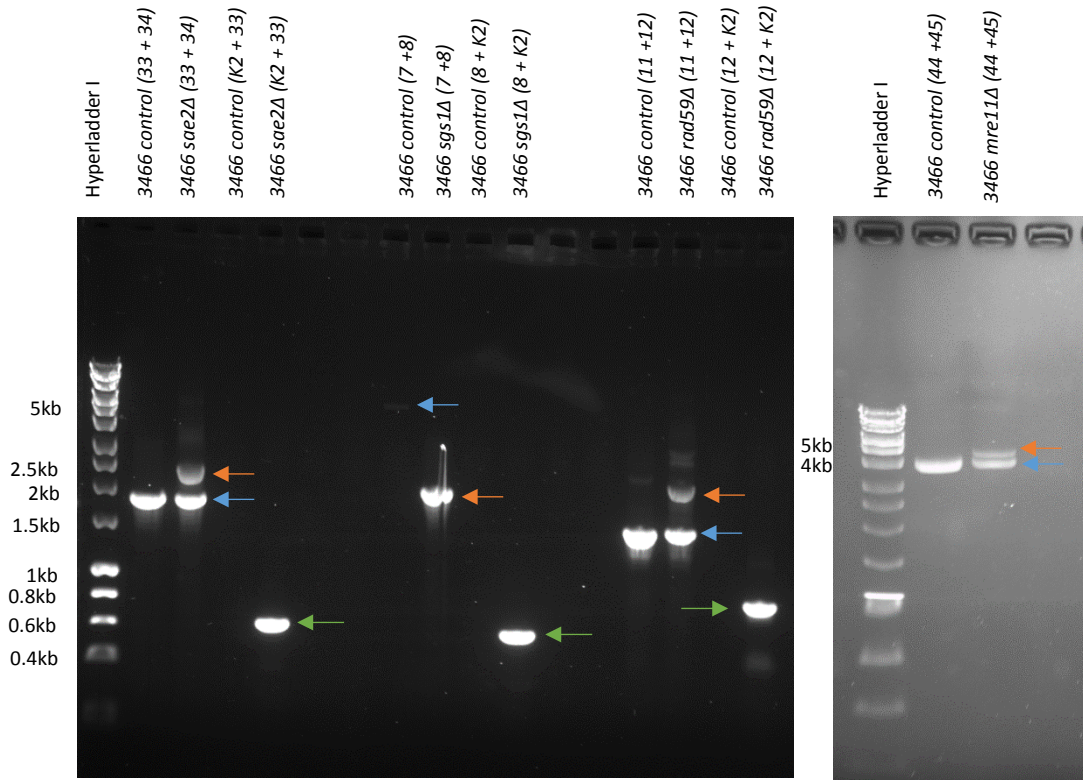

Figure 3-7: Diagnostic PCR for confirmation of knock-out of genes *SAE2, SGS1, RAD59 and MRE11* in strain Y55 (3466). The blue arrow points to the expected band size of wild-type genes whereas the red arrow points to band corresponding to the knock-out version. The green arrow points to bands produced using the reverse K2 primer specific to the kanamycin knock-out marker and a forward primer specific to the upstream sequences of the gene of interest. No bands are produced with the K2 primer in control samples. Altogether, the diagnostic PCR confirms successful knock-out of the relevant genes. (The primer pairs used are labelled within brackets)

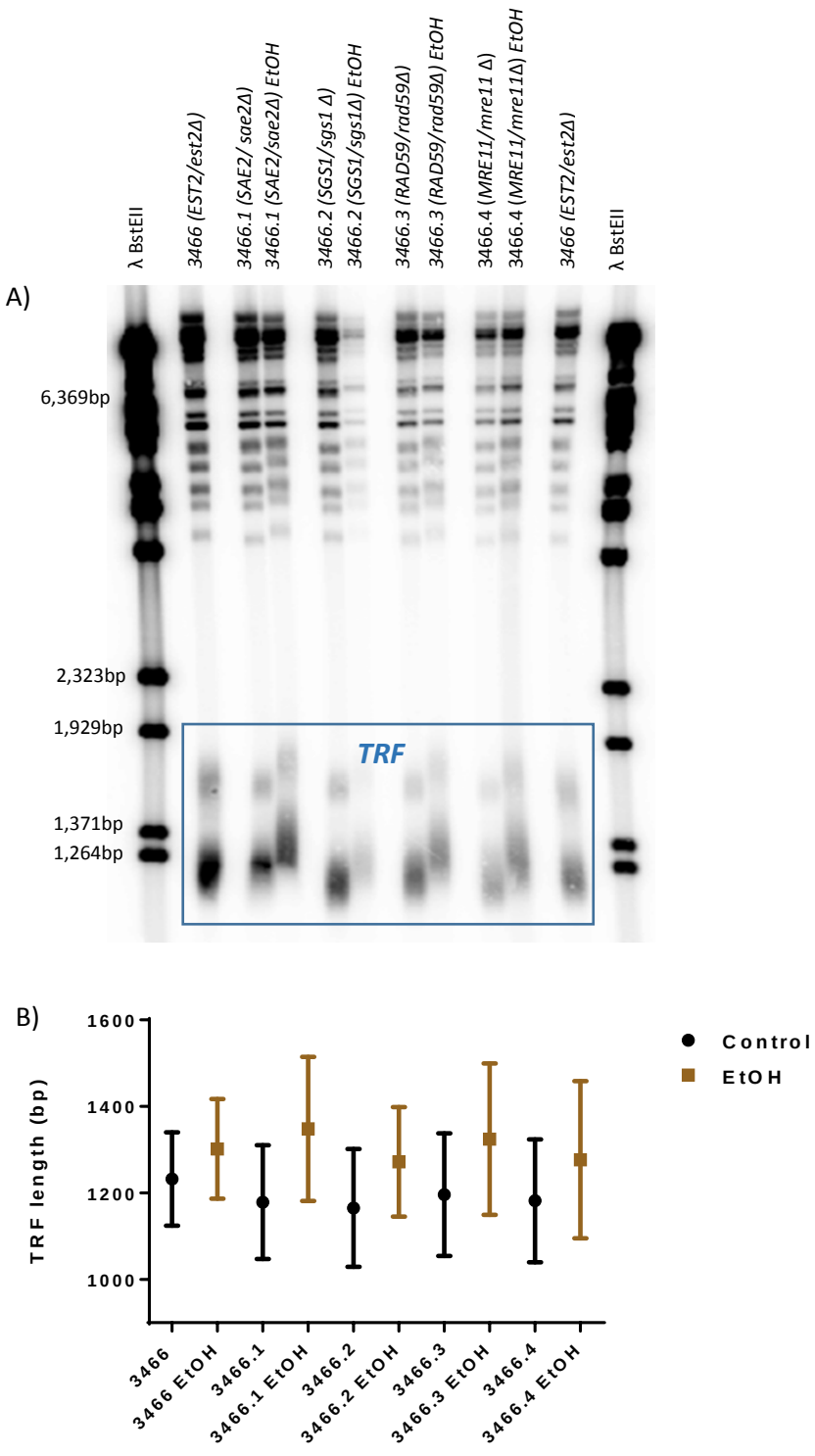

Figure 3-8: TRF length analysis of diploids heterozygous knock-out for telomerase and a Type II gene. A) Southern blot displaying *XhoI* digested TRFs (probed with TG_{1-3} specific pRED571) of Y55 diploids double heterozygous knock-out for telomerase and genes *SAE2*, *SGS1*, *RAD59* or *MRE11*, before and after ethanol treatment. Cultures were treated with 7% EtOH for >50 generations to allow telomere lengthening. Loss of a Type II gene in all double heterozygous knock-outs leads to telomere shortening however, the telomeres are elongated after growth in ethanol. **B)** Graph displaying measurement of TRFs (median and spread from the median) using ImageJ analysis.

3.7 Increased frequency of survivor formation subsequent to telomere lengthening despite the absence Type II survival pathway genes.

Haploid double-knockouts *est2Δ sae2Δ, est2Δ sgs1Δ, est2Δ rad59Δ* and *est2Δ mre11Δ* were generated from each of the four heterozygous diploid parents (3466.1, 3466.2, 3466.3 and 3466.4 respectively) pre-treated with 7% ethanol and their respective untreated controls. The double knock-outs were selected by growth on both URA drop-out plates (*EST2* knock-out marker) and on either KAN or HYG plates (Type II gene knock-out marker), ensuring correct genotype for downstream studies.

9-12 segregants, per condition (standard and ethanol pre-treated) per genotype *est2Δ sae2Δ, est2Δ sgs1Δ, est2Δ rad59Δ* and *est2Δ mre11Δ,* were propagated in liquid media to generate survivor growth curves (Figure 3-9 and Figure 3-10). *est2Δ sgs1Δ* segregants that had grown under standard conditions (without ethanol pre-treatment) underwent significant early senescence compared to *est2Δ* control (-9 population doublings, p=0.0021) (Figure 3-11A). This correlated with the observation that *est2Δ sgs1Δ* segregants had relatively shorter initial telomere lengths compared to *est2Δ* segregants (Figure 3-8). However, the opposite was true for *est2Δ sae2Δ* segregants grown under standard conditions as they underwent delayed senescence despite having slightly shorter telomeres (+9 population doublings, p=0.004) (Figure 3-11A). There was no significant change in population doubling of *est2Δ mre11Δ* or *est2Δ rad59Δ* segregants grown under standard conditions compared to *est2Δ* control. This suggests differences in the timing of senescence can be attributed to the genetic background in addition to the initial telomere lengths. Furthermore, loss of genes generally required for Type II survival led to a steep decline in the efficiency of recovery from crisis in all four double knock-out backgrounds (p= 0.052358, p= 0.000556, p= 0.000105 and p=0.05472 for *est2Δ sae2Δ*, *est2Δ sgs1Δ*, *est2Δ rad59Δ* and *est2Δ mre11Δ* respectively compared to 3466) (Figure 3-11B). This could be attributed to their inability to produce stable Type II survivors.

All of the four double knock-outs pre-treated with ethanol underwent significant delay in senescence compared to their untreated counterparts (+42, +27, +45 and +29 population doublings for *est2Δ sae2Δ*, *est2Δ sgs1Δ*, *est2Δ rad59Δ* and *est2Δ mre11Δ* respectively) (Figure 3-11A). More interestingly, they also had a significant increase in efficiency of recovery from crisis after telomere elongation (measured by cell densities at the peak of crisis) despite lacking a gene generally required for Type II survival (Figure 3-11B). In addition, the efficiency of recovery from crisis after telomere elongation in *est2Δ sae2Δ*

and *est2Δ rad59Δ* double knock-outs were much more prominent (p=5.97E-06 and p=4.88E-07 respectively) than in the *est2Δ sgs1Δ* and *est2Δ mre11Δ* double knock-outs (p=9.70731E-05, p=5.52E-04 respectively). This suggested that while telomere lengthening increased the efficiency of recovery from crisis, the extent of recovery was, to some degree, still dependent on the genetic background.

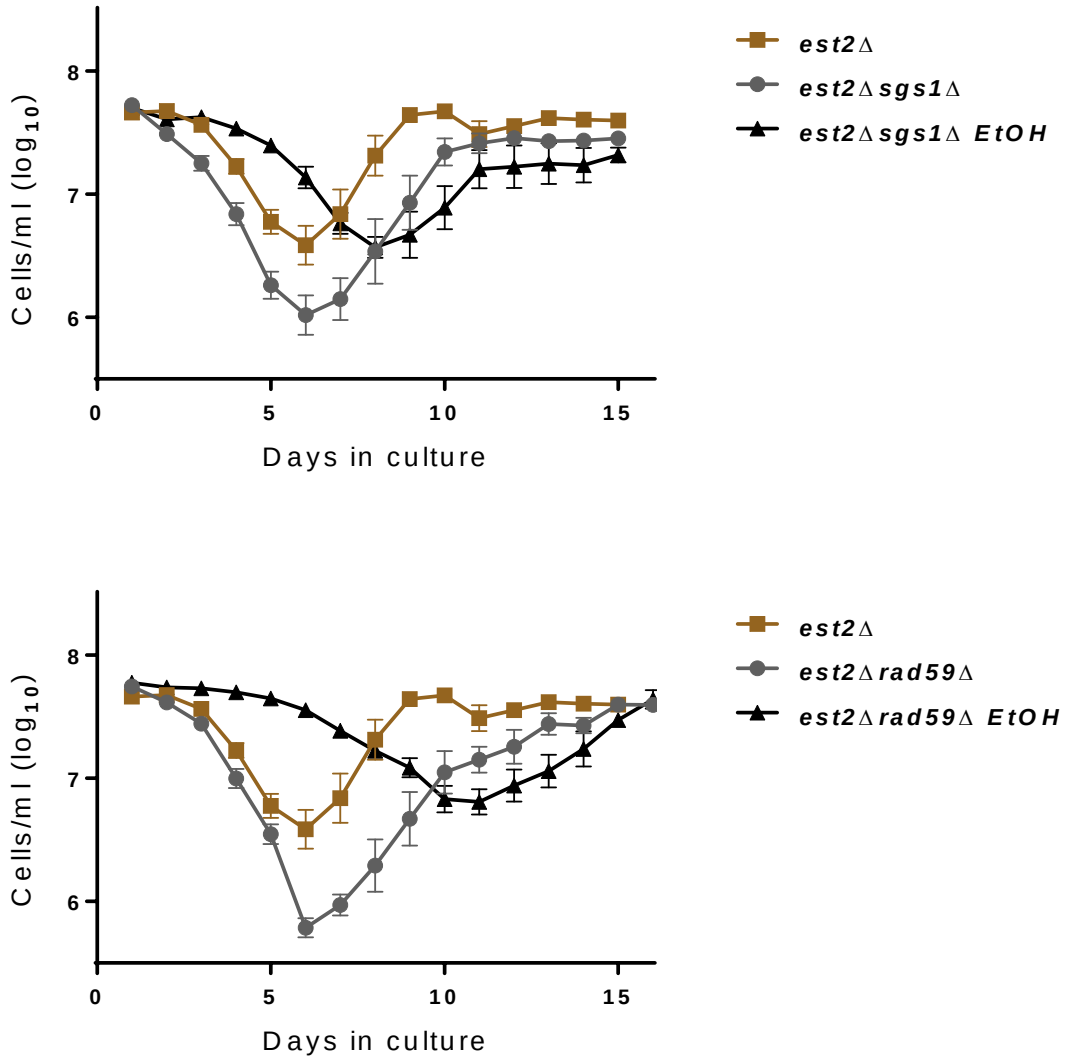

Figure 3-9: Growth curves of senescing *est2Δ sgs1Δ* and *est2Δ rad59Δ* double knock-out cultures. Graph showing average growth curves of 9-12 independent replicates (±SEM) of telomerase negative haploid double knock-outs propagated under standard conditions after 7% ethanol pre-treatment (whilst in the diploid state) or after no pre-treatment. Knock-outs were created in the Y55 strain background and were propagated for 15-16 days with dilutions every 24 hrs. When cells are pre-treated with ethanol, their timing of senescence is delayed and the nadir of growth is shallower.

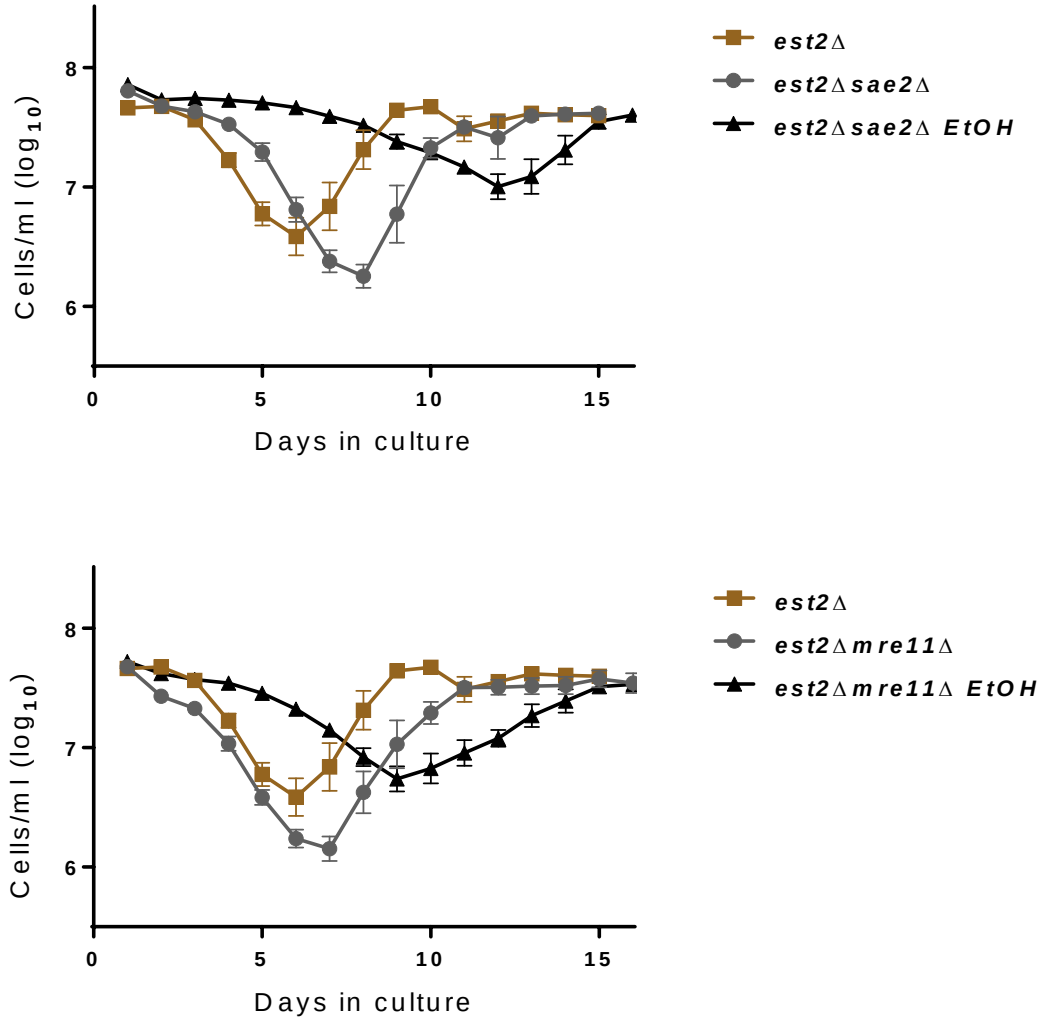

Figure 3-10: Growth curves of senescing *est2Δ sae2Δ* and *est2Δ mre11Δ* double knock-out cultures. Graph showing average growth curves of 9-12 independent replicates (±SEM) of telomerase negative haploid double knock-outs propagated under standard conditions after 7% ethanol pre-treatment (whilst in the diploid state) or after no pre-treatment. Knock-outs were created in the Y55 strain background and **were** propagated for 15-16 days with dilutions every 24 hrs. When cells are pre-treated with ethanol, their timing of senescence is delayed and the nadir of growth is shallower.

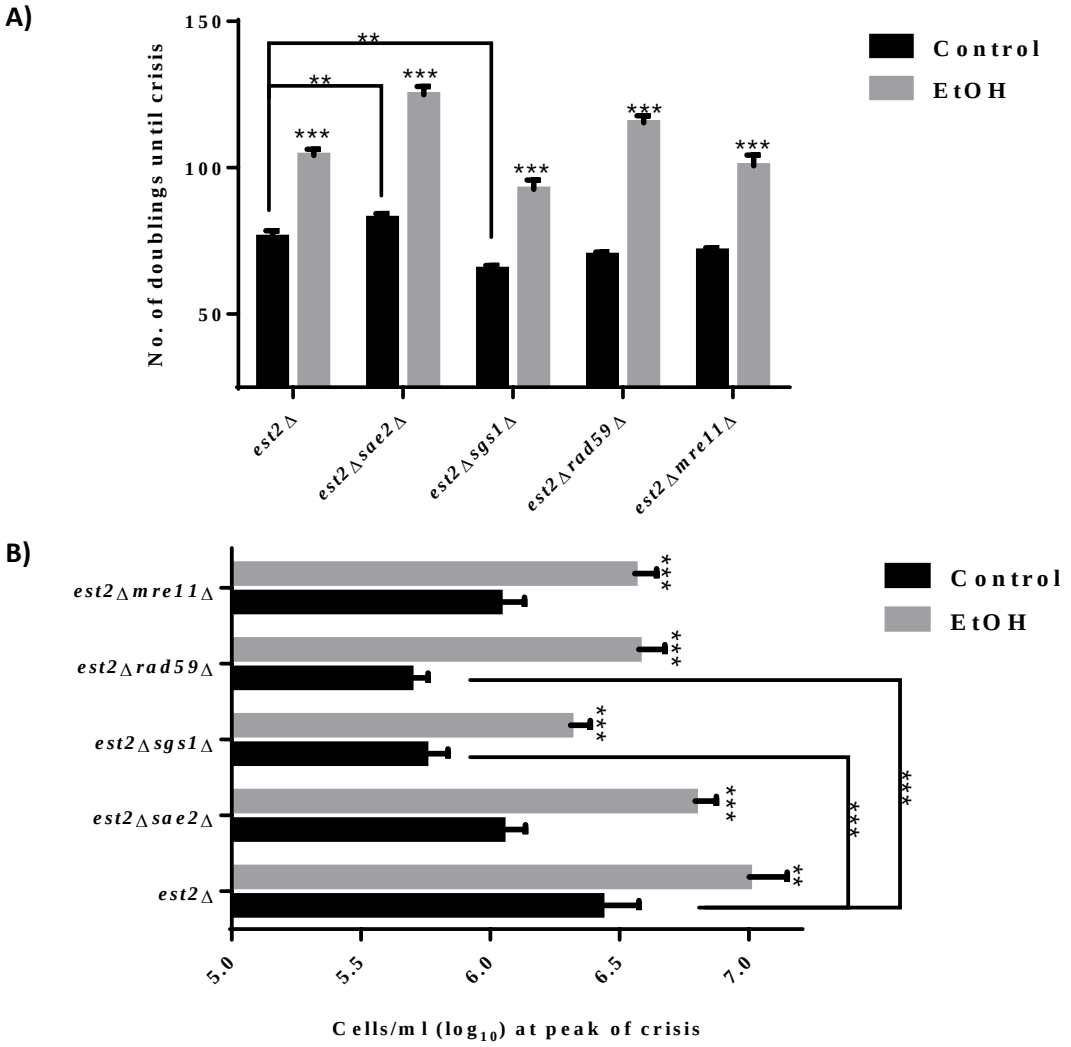

Figure 3-11: Changes in number of population doubling and efficiency of recovery from crisis in telomerase negative double knock-outs with a Type II survival gene. A) Graph showing average population doublings of telomerase negative haploid double knock-outs with Type II genes (n= 7-12, ±SEM) when propagated under standard conditions after 7% ethanol pre-treatment (EtOH- whilst in the diploid state) or after no pre-treatment (control). Number of population doublings was estimated by converting the relevant OD measurements into approximate cell counts and adding the number of doublings each day until the peak of crisis for each growth curve. There is a significant increase in population doubling after ethanol pre-treatment compared to control in all five genotypic backgrounds *est2Δ, est2Δ sae2Δ, est2Δ sgs1Δ, est2Δ rad59Δ* and *est2Δ mre11Δ* ($p<0.001$). **B)** Graph showing cell densities at peak of crisis (n= 7-12, ±SEM). Cell densities at peak of crisis is used as a measure to estimate the ability of cell cultures to recover from crisis and is significantly higher in all genotypic backgrounds after ethanol induced telomere lengthening. (* $p<0.05$, ** $p<0.01$, *** $p<0.001$)

3.8 Spot assay for qualitative assessment of survivor growth and frequency

The growth curves in Figure 3-9 and Figure 3-10 suggest longer telomeres facilitate efficient recovery from crisis (or G2/M arrest), potentially even in the absence of the Type II survivor pathway. One explanation is that longer telomeres lead to an increase in overall number of survivors produced irrespective of the survivor types and thereby explain the efficient recovery from crisis observed in the growth curve assay. In order to test whether longer telomeres generate higher overall frequency of survivors, spot assay experiments were conducted. 5-8 haploid replicates, pre-treated with 7% ethanol, of genotypes *est2Δ sae2Δ, est2Δ sgs1Δ, est2Δ rad59Δ* and *est2Δ mre11Δ* and their respective un-treated controls, were propagated in liquid cultures and harvested at a fixed time-point in the pre-senescent stage of growth (Methods 2.5.4). The harvested pre-senescent cells were spotted in URA drop-out plates at a concentration ranging from 10^6 cells to 10 cells with consecutive 10 fold dilutions. The spotted pre-senescent cells were allowed to grow on plates for three days at 30^{o}C and a further four days at room temperature providing sufficient time for survivor generation prior to imaging. It was expected that cells with longer telomeres would display better growth with more survivor colonies in the spot assay.

Pre-senescent haploids with elongated telomere lengths (via ethanol pre-treatment) displayed an increase in cell density in the spot assay when compared to untreated controls in all four genotypes. This is particularly evident when comparing spot 3 (highlighted in red in Figure 3-12) of ethanol pre-treated cells and their respective untreated controls in the spot assay. This increase in cell density could be a result of an increase in the frequency of survivors generated after ethanol pre-treatment. Likewise, it could also be attributed to increased stability of the survivors as a consequence of telomere lengthening. While there is an observable increase in the frequency of survivors, particularly in the case of *est2Δ rad59Δ* and *est2Δ mre11Δ* cell populations (as per the number of survivor colonies observed in spot 4), it can also be said that colonies are generally bigger in size after telomere elongation despite being grown under exact same conditions for the same number of days. It is also worth noting that pre-senescent cells were harvested when the growth culture reached cell densities below $7.5x10^6$ cells after 24 hrs of growth. In the case of *est2Δ sae2Δ* haploids that were ethanol pre-treated, 3/8 cultures never reached such low densities (as they had efficient recovery from crisis) making the spot assay biased towards cultures with less efficient growth.

Hence, while it is difficult to quantify the exact frequency of survivor generation as they arise from a senescing population with variable growth rates, it is nonetheless discernible qualitatively from the spot assay that telomere elongation enhances growth along with a noticeable increase in the frequency of survivors formed.

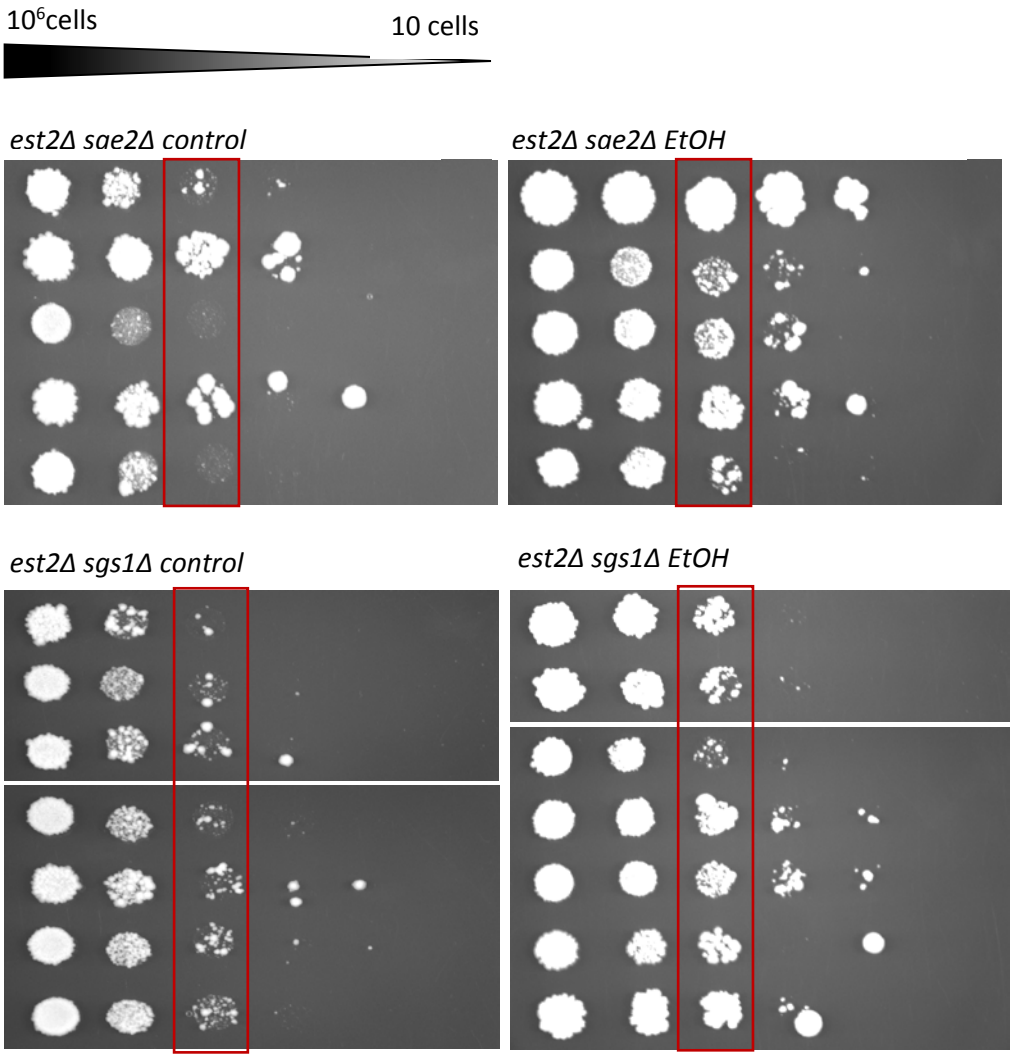

Figure 3-12

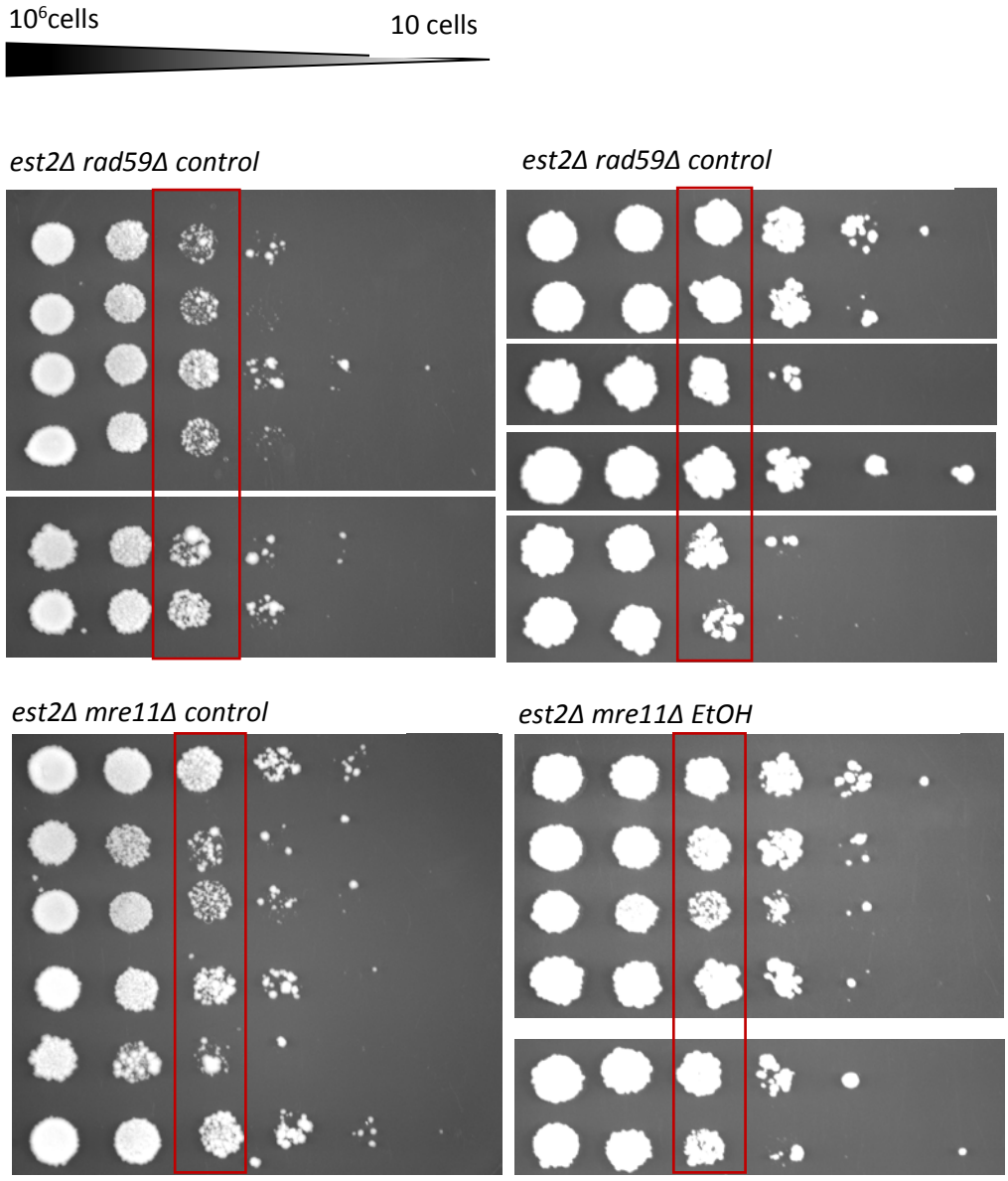

Figure 3-12: Spot assay of pre-senescent haploids *est2Δ sae2Δ*, *est2Δ sgs1Δ*, *est2Δ rad59Δ* and *est2Δ mre11Δ* after ethanol pre-treatment in comparison with untreated controls. Pre-senescent cells from 5-7 independent replicates of each genotype were plated at concentrations ranging from 10^6 cells to 10 cells with 10 fold dilutions in a total of 6 spots. Growth of individual cultures varied leading to differences in the time of spotting and thereby staggering of images from replicates in figure above. Upon plating cells were grown for three days at 30ºC and a further four days at room temperature (Method 2.5.4). It can be observed that in all four backgrounds, ethanol pre-treatment (7%) leads to increased frequency of survivors compared to their respective un-treated controls (based on cell density in individual spots). This is particularly clear when comparing spot 3 (highlighted in red) of all backgrounds where the cell density is qualitatively much higher after ethanol pre-treatment compared to control.

3.9 Increase in generation of Type II and Type II-like survivors in *est2Δ rad59Δ* cells after telomere elongation

From previous experiments, it can be said that longer telomeres enable efficient recovery from crisis and result in an increase in the frequency of survivors formed despite lacking genes generally required for Type II survival. This suggests the function of longer initial telomere length in the escape of G2/M arrest may not be limited to just the Type II survivor pathway. Nonetheless, a possible alternative hypothesis was in fact the generation of Type II survivors, despite the lack of genes generally required for Type II survival, when the initial telomere lengths were sufficiently long. Hence, ethanol pre-treated haploid progenies *est2Δ sae2Δ*, *est2Δ sgs1Δ*, *est2Δ rad59Δ* and *est2Δ mre11Δ*, were subjected to plate propagation assay and changes in the proportion of survivor types were analysed in comparison with their respective untreated controls (Table 3-2, Figure 3-13).

For control *est2Δ sae2Δ* haploids, 1 in 19 survivors was a Type II survivor, which is significantly lower than that generated by control *est2Δ* knock-out (38% Type II, n= 21, p=0.0089) (Table 3-2). After ethanol pre-treatment, the proportion of *est2Δ sae2Δ* Type II survivors increased to 11% (4/36 Type II) however was not found to be statistically significant compared to untreated control (p=0.6449) (Table 3-2). Haploids of genotype *est2Δ sgs1Δ* did not produce any Type II survivors in control conditions and after telomere elongation (n=14 and n=33 respectively) (Table 3-2). In both cases here, it can be suggested that *SAE2* and *SGS1* are essential in Type II survivor formation regardless of initial telomere lengths or that ethanol induced telomere lengthening was not significant enough to cause a shift towards Type II survivor formation.

In the case of *est2Δ rad59Δ* double knock-outs with unaltered telomere lengths, 9% of the survivor types (n=35) were Type II or Type II-like (presence of a few heterogeneous bands indicative of $TG_{1\text{-}3}$ repeat amplification rather than high number of multiple bands typical of a classic Type II survivor, Appendix 7.9-7.10) (Table 3-2). Remarkably, after telomere elongation a significantly higher proportion of Type II and Type II-like survivors (29%, n=41, p=0.0408) were observed (Table 3-2). Although, *RAD59* is generally thought to be a Type II essential gene, it is likely that some Type II survivors can arise transiently in the absence of *RAD59* and the gene is only essential for the stability and maintenance of these survivors long term. In order to verify this, three

replicates of *est2Δ rad59Δ* cultures were grown in liquid media for 15-20 days and their DNA was extracted for TRF analysis. It is known that in liquid culture, stable and fast growing survivors out-compete the growth of slow growing survivors. Hence, if stable Type II survivors were generated they would eventually take over the culture but if Type II survivor formation was transient and unstable, they would eventually disappear from the culture. As expected, there was very little indication of stable Type II survivor in the *est2Δ rad59Δ* background with wild-type telomere length (control) as one out of the three cultures displayed a Type II-like banding pattern (Figure 3-14). However, there was no indication of Type II banding pattern in *est2Δ rad59Δ* survivors after telomere elongation suggesting the Type II survivors observed in the plate propagation were in fact transient (Figure 3-14). Altogether, it can be concluded that although *RAD59* is generally a gene, required for Type II survival, its loss in the presence of longer telomeres does favour an increase in the generation of Type II survivors and promotes efficient recovery from crisis but does not support long term maintenance. Furthermore, this data highlights the difference between the processes of survivor generation and survivor maintenance.

Finally, survivor proportions were analysed in the *est2Δ mre11Δ* cell population after ethanol pre-treatment compared to controls. In both cases, 8/20 survivors were Type II or Type II-like showing that telomere lengthening had no effect in changing survivor proportions in this background (Table 3-2, Appendix 7.11). The Type II-like survivors generated were once again transient and unstable, eventually out-competed by Type I survivors or converted into Type I survivors in the absence of *MRE11* evidenced by TRF analysis after prolonged growth in liquid culture (Figure 3-14) and as described previously (Le et al., 1999)

Y55 strains	N	Type I	Type II	Type I (%)	Type II (%)	Fishers Exact p value (vs control)
est2Δ control	21	12	9	57	43	
est2Δ EtOH	29	18	11	62	38	0.7759
est2Δ sae2Δ control	20	19	1	95	5	
est2Δ sae2Δ EtOH	36	32	4	89	11	0.6449
est2Δ sgs1Δ control	14	14	0	100	0	
est2Δ sgs1Δ EtOH	33	33	0	100	0	1
est2Δ rad59Δ control	35	32	3	91	9	
est2Δ rad59Δ EtOH	41	29	12	71	29	0.0408*
est2Δ mre11Δ control	20	12	8	60	40	
est2Δ mre11Δ EtOH	20	12	8	60	40	1

Table 3-2: Changes in survivor type proportions after alteration of initial telomere length in telomerase negative double knock-outs with a Type II survival gene. Total sample size and the proportion of survivor types generated (rounded to whole number) in four different haploid backgrounds that lack telomerase and a Type II gene. Individual segregants were propagated under standard conditions after 7% ethanol pre-treatment (EtOH- whilst in the diploid state) or after no pre-treatment (control). Survivor types were characterised using Southern blot analysis of *XhoI* digested TRFs as described in Methods 2.7.6 (Southern blots in Appendix 7.1-7.3, 7.7 – 7.11). A 2X2 two-tailed Fishers exact test was used to analyse the changes in survivor proportions compared to control and calculate the p-value. Groups with $p<0.05$ is considered to be significantly different from their respective controls and marked with an asterisk.

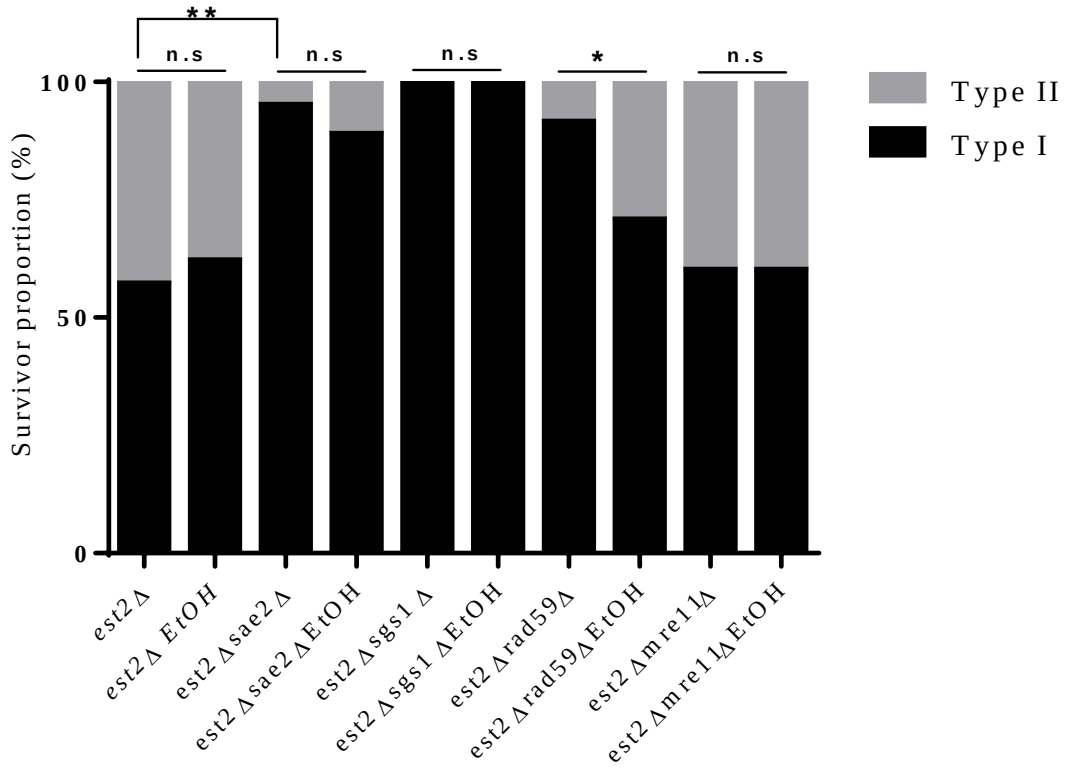

Figure 3-13: Changes in survivor type proportions after alteration of initial telomere length in telomerase negative double knock-outs with a Type II survival gene. Bars represent survivor type proportions (Type I and Type II) in percentage in four different haploid backgrounds lacking telomerase and a Type II gene as per data in Table 3-2. Individual segregants were propagated under standard conditions after 7% ethanol pre-treatment (EtOH- whilst in the diploid state) or after no pre-treatment (control). (*$p<0.05$, **$p<0.01$) (Southern blots in Appendix 7.1-7.3, 7.7 – 7.11)

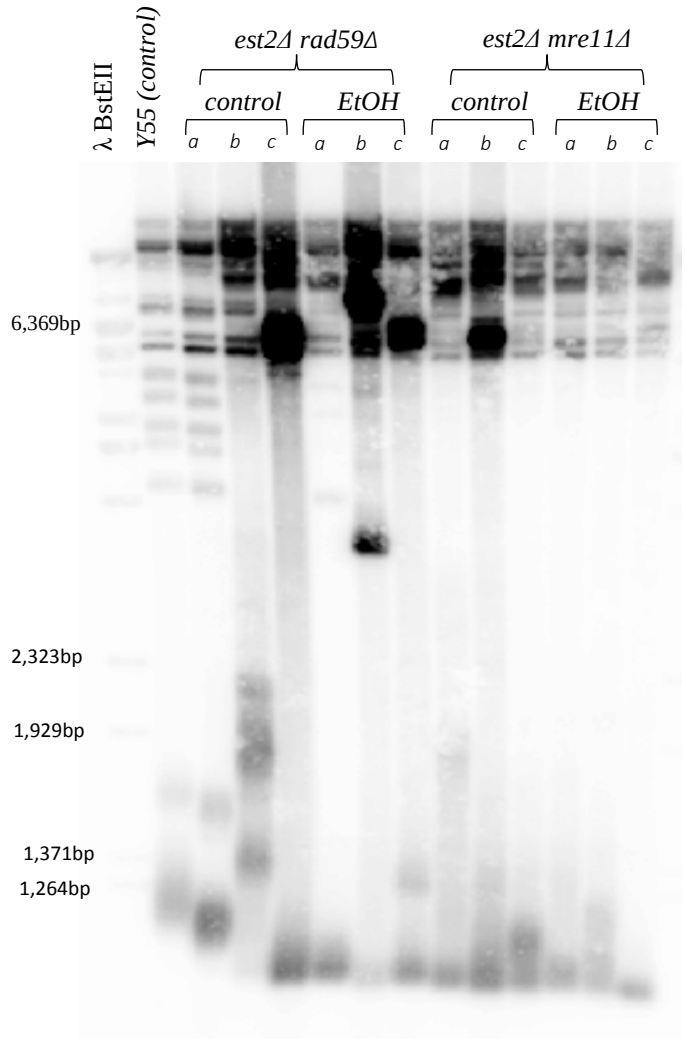

Figure 3-14: Southern blot examining survival type of telomerase negative double knock-outs *est2Δ rad59Δ* and *est2Δ mre11Δ* in long term liquid cultures. TRFs of haploid telomerase negative survivors were examined in strains *est2Δ rad59Δ* and *est2Δ mre11Δ* that started with either wild-type initial telomere lengths (control) or artificially elongated initial telomere lengths (EtOH). Cultures were propagated in liquid media for 15 and 20 days with 24hr dilutions prior to DNA extraction and TRF analysis to examine the dominant survivor type present in each background. TRFs were analysed via Southern blot analysis (probed with $TG_{1\text{-}3}$ specific pRED571). Out of the three control replicates of *est2Δ rad59Δ* cultures, replicate 'a' is excluded from the study as it is in the pre-senescent stage with telomeres still shortening. Replicate 'b' displays three Type II-like bands in contrast to a classic Type II survivor with multiple bands, and replicate 'c' is a Type I survivor. After telomere elongation all three replicates in the liquid culture above are Type I survivors. This is in contrast to the Type II survivors seen in *est2Δ rad59Δ* population in the plate-propagation assay (Appendix 7.9-7.10). Likewise, all replicates of *est2Δ mre11Δ* cultures, three with wild-type telomere lengths (control) and three with ethanol elongated telomere lengths (EtOH), have become Type I survivors.

3.10 Discussion

In this study, I examined the relationship between initial telomere length and its role in telomerase negative survivor formation. Further to the studies conducted by LeBel et al (2009) and Chang et al (2011), I was able to manipulate telomere length in both directions using environmental stress factors to study the consequences of telomere length alteration in survivor type formation.

Initial telomere lengths were altered in three different laboratory strains of *S. cerevisiae*, W303, Y55 and S288c. While all three strains responded to ethanol mediated telomere lengthening or caffeine mediated telomere shortening, there was a large variation in the degree of response depending on the strain background. Strain S288c responded the most to ethanol mediated telomere lengthening whilst strain Y55 responded the most to caffeine mediated telomere shortening. Strain W303 responded the least to both telomere lengthening and shortening. Remarkably, telomere lengthening was associated with significant increase in efficiency of recovery from crisis in strains Y55 and S288c after measurements of their cell density at peak of crisis. This was however not true in strain W303 with the discrepancy most likely reflecting the rather small response to ethanol induced telomere lengthening at the start. Likewise, telomere shortening led to significant decrease in efficiency of recovery from crisis in all three strain backgrounds.

Faster recovery from crisis with long telomeres and vice-versa from short telomeres suggested a possible mechanism of increased Type II recombination in the presence of long telomeres generating more Type II survivors. It has been previously found that Type II survivors grow faster compared to Type I survivors (Teng and Zakian, 1999), making the speculation a plausible hypothesis. Upon examining the proportion of survivor types generated, it was found that telomere elongation did not produce higher proportions of Type II survivors in strains Y55 and W303. However, the lack of shift in survivor proportions in Y55 and W303 is likely to be due to its low response to ethanol mediated telomere lengthening at the start. In contrast, it was found that telomere shortening significantly reduced the proportion of Type II survivors in strains Y55 and in S288c where bulk telomere shortening was very prominent. Together, these data strongly argue for the case of longer initial telomere lengths to effectively facilitate the Type II survivor pathway leading to faster recovery from crisis. Similarly, short telomeres can be argued to be unfavourable in initiating the Type II pathway, thereby resulting in inefficient recovery from crisis. This finding is in line with the work of Chang et al where it was

demonstrated that knock-out of *RIF1/RIF2* genes led to a drastic increase in initial telomere length followed by higher proportions of Type II survivors in a telomerase negative background (Chang et al., 2011). A likely mechanism for increased proportion of Type II survivors with longer telomeres is the availability of longer $TG_{1\text{-}3}$ repeats as substrate for either shorter telomeres to elongate their telomeres prior to becoming Type II survivors or a direct Type II break induced recombination that can potentially commit the cell towards the Type II survivor pathway at G2/M arrest.

Although ethanol pre-treatment leads to telomere elongation and subsequently enables more efficient recovery from crisis, it can be argued that telomere length at the time of senescence is not much different when compared to untreated cells as the timing of senescence is delayed in proportion to telomere elongation. This, can be justified by taking into account the study by Khadaroo et al which demonstrates that the DNA damage response starts much earlier at an eroded telomere than the onset of senescence and recruits Cdc13, replication protein A, DNA damage checkpoint proteins and DNA repair protein Rad52 into a single focus at the nuclear periphery (Khadaroo et al., 2009). These foci containing *RAD52* were observed as early as 20-40 generations after the loss of telomerase. Therefore it is likely that an increased recovery rate from crisis and an increased overall frequency of survivor formation with longer telomeres observed in this study is due to early onset of the DNA damage response while the telomeres are amply long to promote efficient telomere-telomere recombination.

In addition, ethanol mediated telomere lengthening is heterogeneous at varying ends and it is known that a single short telomere is sufficient to induce cell arrest (Abdallah et al., 2009). Hence the drastic increase in the efficiency of recovery from crisis in ethanol pre-treated population could be a result of cell arrest induced from a few short telomeres, where the shorter telomeres can undergo recombination with the longer telomeres, in what maybe a precursor to becoming a survivor. In fact, a study by Fu et al has found shorter telomeres to undergo recombination with the longer sister chromatids prior to becoming survivors and is discussed in more detail later on (Fu et al., 2014). Alternatively, it is also possible that longer telomeres lead to increased formation of t-circles via processes such as TRD (telomere rapid deletion) (Bechard et al., 2011) which could then act as substrate for Type II recombination (discussed more in the next chapter). Although t-circles have been observed in Type II survivors in *S. cerevisiae* using 2D gel assays (Larrivee and Wellinger, 2006), there is no report of increased t-circles in strains

with longer telomeres, which could partly be due to technical challenges in identifying them (Cesare et al., 2008).

In the 2009 study by LeBel et al (LeBel et al., 2009), Type II survivors were shown to arise even in the absence of *RAD52* given the cells had long initial telomere lengths. It has been established above that longer telomeres generate more Type II survivors and can recover more efficiently from crisis. So next, I explored whether the requirement of genes generally required for Type II survival (*SAE2, SGS1, RAD59* and *MRE11)* in telomerase negative backgrounds were still strictly essential for Type II survivor generation when the initial telomere lengths were artificially elongated. From this study, it was observed that loss of *SGS1* leads to complete loss of Type II survivor generation whereas loss of *RAD59* and *MRE11* can lead to formation of a few transient Type II and Type II-like survivors which are unstable and eventually lost in long term liquid cultures. Loss of *SAE2* significantly reduces the proportion of Type II survivors generated. More interestingly, it was seen that telomere elongation did not lead to a significant increase in the proportion of Type II survivors in backgrounds *est2Δsae2Δ*, *est2Δsgs1Δ* and *est2Δmre11Δ* despite the liquid culture assay showing significant increase in efficiency of recovery from crisis. This suggests, that while long telomeres facilitate Type II recombination more efficiently giving rise to higher proportions of Type II survivors, it must to some extent also enhance Type I recombination to boost recovery from crisis when the Type II pathway is not available.

The spot assay experiment further confirmed that longer telomeres can produce higher frequency of survivors with better growth. It was recently demonstrated via live cell imaging assay from Xu et al, that telomerase negative cells can undergo two different routes to senescence. The first route leads to abrupt and irreversible senescence whereas the second leads to multiple stochastic cell arrests followed by repair before eventually becoming survivors or senescing (Xu et al., 2015). Furthermore, the cells were also pre-treated with ethanol leading to telomere elongation which also led to an increase in the proportion of cells undergoing multiple cell arrests followed by an increase in overall proportion of cells becoming survivors. Although the study does not examine the proportion of survivor types produced after telomere lengthening, it is clear that telomere elongation enables higher frequency of survivor generation in line with my findings above. However, this increase in survivor frequency, once again, is not dependent on just the Type II survivor pathway.

Remarkably, telomere elongation in the *est2Δrad59Δ* background did in fact generate a significantly higher proportion of Type II and Type II-like survivors. However, these Type II survivors once again seemed to exist transiently as they were not stable enough to be detected in long term liquid culture assays. This gives insight into the potential decision-making process of a cell in selecting a survivor pathway during crisis where although long telomeres might be sufficient to initially commit the cell towards the Type II pathway, it would eventually require the necessary Type II genes in maintaining the long-term stability of those survivors. In addition, it can also be argued that while *SGS1* is essential early on in the formation of Type II survivors (as the loss of the gene showed no indication of Type II or Type II-like survivors), *RAD59* and *MRE11* are likely to be more crucial in the latter stages of the process once the telomere amplification has begun.

One of the earliest steps in alternative telomere amplification of telomerase negative yeast was proposed more than 20 years ago by Lundblad and Blackburn to be acquisition of mini Y' sub-telomeric elements by the short terminal TG_{1-3} repeats. These mini Y' elements are remainders of the Y' repeat elements after large deletions and were found to hybridize to the heterogeneous bands containing large amplifications of TG_{1-3} repeats produced by Type II survivors (Lundblad and Blackburn, 1993). However, the mechanistic details of how the initial rearrangements ensued were not fully known. Recently, a study by Churikov et al (Churikov et al., 2014) conducted in the W303 strain demonstrated that *RAD59* facilitated the acquisition of Y' telomeres at short telomere ends in line with the observations made by Lundblad et al (Lundblad and Blackburn, 1993). More interestingly, the *RAD59* dependent acquisition of Y' elements was found to be independent of the *RAD51* pathway of Type I survivor formation and delayed the onset of senescence in preparation for telomere maintenance by HR (Churikov et al., 2014). In addition, it was shown that shorter telomeres acquire Y' faster than longer telomeres. Hence, it can be suggested that the increase in Type II and Type II-like survivors observed in *RAD59* deleted cells with longer telomere lengths could be due to inefficient acquisition of Y' elements. It is also worth noting, the Y55 strain used in this study has low copy number of Y' elements (14 copies) compared to other strains such as S288c (26-30 copy number) (Louis and Haber, 1990) and possibly W303, which may to some extent also favour the cells opting for the Type II pathway.

Furthermore, lack of Y' mediated delay in senescence is likely to cause a cell at arrest to adapt via other means such as Type II recombination using the available long TG_{1-3}

repeats. The requirement of *RAD59* in Type II survivor formation has been well studied previously with its loss predominantly producing Type I survivors (Chen et al., 2001, Le et al., 1999, Teng and Zakian, 1999). Taking into light the study from Churikov et al, it can be suggested that whilst *RAD59* is essential for Y' acquisition at early stages of survivor formation, its role later on is largely involved in maintenance of Type II survivors. This, in line with my findings above suggests that loss of *RAD59* while impairs the ability to maintain Type II survivors long term, possibly due to significant reduction in intra-chromosomal recombination (Bai and Symington, 1996), can nonetheless generate more Type II survivors when provided with longer TG template at an earlier stage, possibly as an alternative means for fast recovery from cell arrest or to cause a delay in the onset of senescence.

In this study, we have observed higher proportion of Type II survivors and an increase in the efficiency of recovery from crisis when cells have longer initial telomere lengths. Studies, contrary to the above findings, have shown instances where shorter telomeres are preferentially elongated leading to Type II survivor formation. In a study by Teng et al, it was suggested that Type II survivor formation is an abrupt one-step process that occurs in a cell population with short telomeres within a window of approximately 10 cell cycles and at reproducible time points (Teng et al., 2000). Furthermore, it is suggested in the study that the likely donors or templates for such lengthening to be $TG_{1\text{-}3}$ circles via rolling circle replication. However, this study examines short telomeres in a cell population with eroding telomeres and doesn't provide insight into the exact mechanism leading to telomere amplification. As mentioned earlier, it is now known that a single short telomere is sufficient to induce cell arrest (Abdallah et al., 2009). Likewise, in a cell population with eroding telomeres, it is possible that whilst a single short telomere initiates cell arrest leading to recruitment of recombination proteins, other ends with relatively longer telomeres might likewise engage in recombination favouring the Type II survivor pathway (possibly via clustering of telomeres in one foci (Khadaroo et al., 2009)). This is further explored in the next chapter.

Another study by Fu et al examined telomere elongation at individual ends in telomerase negative cells and demonstrated that only short telomere ends, less than 100 bp, are elongated by recombination events (Fu et al., 2014). It was shown that not all telomere ends are elongated at once and the short telomeres that are elongated do not extend more than the length of the remaining telomere ends. This suggests an intermediate

recombination step for cells nearing crisis where sister chromatids with longer telomere lengths act as substrate for elongation of shorter telomeres prior to the massive lengthening that is characteristic of Type II survivors. Furthermore, the authors propose the low frequency of survivors obtained from a population could be due to insufficient recombination activity occurring within cells when majority of the telomeres are already short. Hence, it can be argued that whilst short telomeres may get elongated first, it is the presence of longer telomeres in other sister chromatids that boosts recombination resulting in an increase of survivor frequency and potentially in the proportion of Type II survivors as observed from my data.

My study highlights the role of initial telomere length in determining the efficiency of recovery from crisis. I have shown that longer telomeres not only increase the efficiency of recovery from crisis but also promotes the formation of Type II survivors in an otherwise wild-type background. More interestingly, my data suggests that longer telomeres not only promote the formation of Type II survivors but promotes the overall frequency of survivor formation including Type I survivors when genes generally required for the Type II survival pathway are absent. Hence in addition to suggestions from previous literature whereby longer telomeres are thought to promote just the Type II survivor pathway, I conclude longer telomeres promote the formation of both Type I and Type II survivors.

Chapter 4 Investigating the timing of cell senescence as a factor influencing telomerase negative survival pathway

4.1 Introduction

It was established in the previous chapter that in budding yeast *Saccharomyces cerevisiae*, initial telomere length influences the type of recombinant survivor produced as well as the dynamics of senescence. Senescence in telomerase negative cultures refers to the nadir of cell growth when majority of the cells are in a state of non-dividing cell arrest. Longer initial telomere length leads to higher proportions of Type II survivors (similar to mammalian ALT survivors) whereas shorter initial telomeres leads to higher proportions of Type I survivors.

Another aspect of survivor formation is the timing of senescence. The study by Chang et al showed knocking out genes *RIF1* and *RIF2* elongates telomeres in a telomerase positive background which then leads to early cell arrest and senescence upon growth in a telomerase negative background along with an increase in the proportion of Type II survivors formed (Chang et al., 2011). The study suggests this to be the consequence of longer initial telomere lengths in conjunction with early cell senescence leading to more efficient Type II recombination.

Rif1 and Rif2 (Rap1 interacting factor) are crucial telomere length regulation proteins that associate directly with Rap1 (Hardy et al., 1992, Wotton and Shore, 1997). Rap1 is a repressor/activator protein that binds to telomeric TG_{1-3} repeats along with serving as a transcriptional activator across 300 genomic loci (Lieb et al., 2001, Shore and Nasmyth, 1987). Rap1 together with Rif1/2 plays an important function of capping telomere ends in conjunction with the CST complex. In addition, they regulate the length of telomeric TG_{1-3} repeats by opposing the action of telomerase in a manner proportional to the amount of Rap1 molecules bound at the end (Marcand et al., 1997). In *S. cerevisiae*, approximately 15-20 Rap1 molecules bind to the TG_{1-3} repeats. As telomeres get shorter, the number of Rap1 molecules bound is reduced, allowing telomerase to elongate the ends and maintain wild type length. In telomerase positive yeast cells, mutating Rap1 or knocking out Rif1/2 protein, such that it can no longer interact with the TG_{1-3} repeats, leads to unregulated telomere elongation.

In this chapter, I used an alternative method to investigate the effect of early senescence in the formation of Type II survivors in a cell population. In this method, the number of Rap1 protein and consequently the number of Rif1/Rif2 proteins bound at a single telomere end was negatively altered (without mutating or knocking out the genes themselves) by using a telomere truncation construct. This ensured that a wide range of functions dependent on the Rif1, Rif2 and Rap1 proteins within the cell remained constant whilst enabling the investigation of early senescence from a truncated telomere on survivor type formation. The inducible short telomere construct, TELox33, was designed by the Bianchi et al in W303 derivative strain YAB892 to induce early senescence whilst the remaining telomere ends were maintained at a wild-type length (Bianchi and Shore, 2007a, Bianchi and Shore, 2007b). It was found in the previous chapter that longer initial telomere length leads to higher proportion of Type II survivors. The question asked here is whether early senescence induced from a single critically short telomere in a telomerase negative background can lead to an increase in the proportion of Type II survivor formed.

Furthermore, the initial telomere lengths at other chromosome ends of the cell can be artificially altered in addition to having a truncated telomere using the TELox33 construct. This can subsequently enable a study that can distinguish the role between the timing of senescence and initial telomere length with regard to survivor type formation. Assuming early cell arrest from a single short telomere leads to increased recombination with the relatively longer telomeres in other chromosomes and eventually higher proportion of Type II survivors as suggested by Chang et al (2011), it is likely that even longer initial telomeres could potentially augment that effect. Therefore, the strain with the TELox33 construct at a single chromosome end was subjected to bulk telomere lengthening using 5% ethanol pre-treatment. The aim was to enable telomere elongation at all chromosomal ends whilst also maintaining a single short telomere via the TELox33 construct and examine the effects of early cell arrest in the presence of artificially elongated telomere ends. Likewise, the strain with the TELox33 construct were also subjected to bulk telomere shortening using 4 mM caffeine pre-treatment in order to examine the effects of early cell arrest in the presence of extremely short telomeres and its subsequent consequence on survivor type formation. The diagram below displays the hypothesis with regard to telomere length, timing of cell arrest and proportion of Type II survivors generated (Figure 4-1). In

short, it can be hypothesized that the longer the telomeres and earlier the senescence, the higher the chances of becoming a Type II survivor.

Another query addressed in this chapter is whether a single long telomere is sufficient to push survivor formation towards Type II. Unlike bulk telomere lengthening where telomeres at all chromosome ends are elongated, here a single telomere end was targeted for elongation using an inducible construct TELox131. Assuming critically short telomeres in a pre-senescent cell uses longer sister telomeres as template for recombination in producing higher proportions of Type II survivors, this experiment examines whether a single long telomere is sufficient for observing similar results.

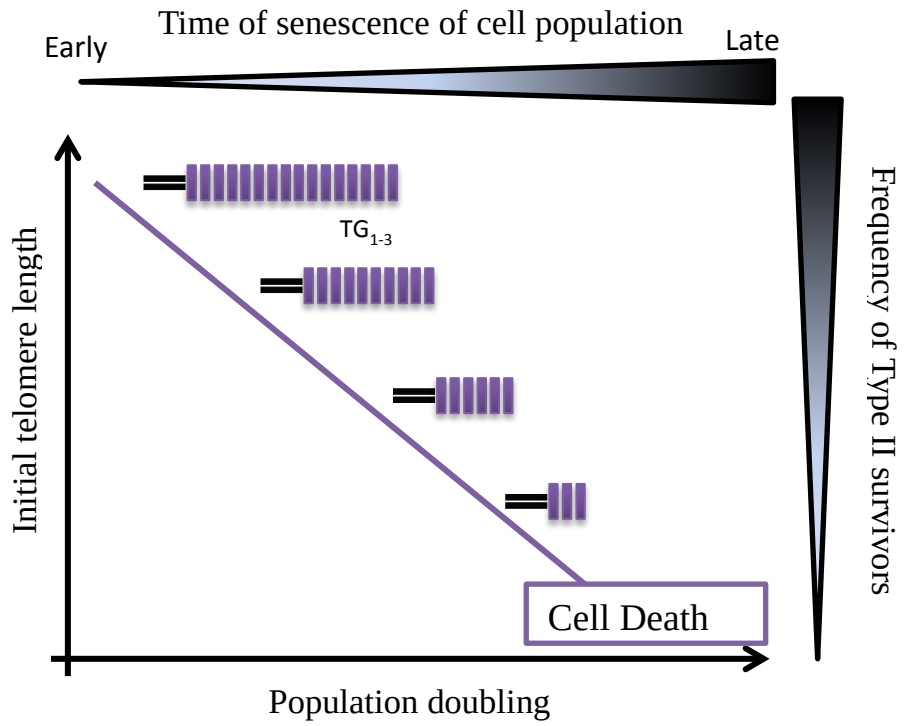

Figure 4-1: Hypothesis linking telomere length and time of senescence to the frequency of Type II survivors formed. It was previously seen that longer telomeres lead to increased proportion of Type II survivors (Chapter 3). Here I hypothesize that early senescence in the presence of relatively longer telomeres might provide a better substrate for break-induced recombination that leads to TG_{1-3} amplification characteristic of Type II survivors. Hence according to the hypothesis, the longer the initial telomere lengths and the earlier the timing of senescence, the greater the chances of pre-senescent cells (undergoing gradual telomere erosion) opting for Type II survival pathway and ultimately higher frequency of Type II survivors within a cell population.

4.2 Design and verification of the YAB892 construct

YAB892 cells containing the TELox33 construct was designed by the Bianchi group in order to generate a single short telomere at chromosome VIIL in a haploid W303 strain background (Bianchi and Shore, 2007a, Bianchi and Shore, 2007b) and was used in this study to induce early cell arrest and senescence in a cell population. The construct TELox33 consists of a lysine marker upstream of Rap1 binding sites and is flanked by loxP sites on either side. Downstream of the Rap1 binding site of the TELox33 construct is a stretch of 50 bp of TG_{1-3} repeats inserted at the *BamHI* restriction site. The construct TELox33 was then inserted at an *MluI* restriction site of the *ADH4* locus of chromosome VIIL resulting in the replacement of sub-telomeric core X. Rap1, a key regulator of telomere length, prevents telomerase from associating and elongating the terminal TG_{1-3} repeats of the construct and essentially renders them short at approximately 160 bp (Bianchi and Shore, 2007a). The strain further contains a Pgal-Cre plasmid integrated at *leu2 (leu2::pPgal-Cre)* such that Cre recombinase is expressed from the *GAL* promoter in the presence of galactose. Cre recombinase leads to recombination in the LoxP sites resulting in the removal of the Rap1 binding site and the lysine marker of the construct, which should then allow access to telomerase for elongation of the TG_{1-3} repeats (Figure 4-2A).

In order to verify that the construct does in fact produce a single short telomere, DNA was extracted from three replicates of YAB892 cells propagated independently on either LYS drop-out media or GAL (galactose) media for approximately 100 generations and subjected to a five way digest with restriction enzymes *AluI, BamHI, MseI, HaeIII* and *HinfI* to generate terminal restriction fragments (TRFs). TRFs of the YAB892 cells, with the construct intact (CI, propagated on LYS drop-out media) and with the Rap1 binding sites of the construct flipped at LoxP sites (CF, propagated on GAL media) were compared with those of control YAB0 cells (not containing the construct) by performing a Southern blot using TG_{1-3} specific probe pRED571. The blot showed a new short TRF of approximately 140 bp present in the YAB892 strain which was not present in control YAB0 strain (Figure 4-2B). This provided evidence that a very short single telomere was generated via the construct in strain YAB892 which is not present in control strain YAB0. Surprisingly, removal of the Rap1 binding sites of the construct in YAB892 cells by growing them on galactose media still generated the band corresponding to a single short telomere when it was expected to re-

lengthen. This suggests that telomere shortening at CHRVIIL might be influenced, not just by the Rap1 binding sites, but also by the sub-telomeric region which was removed whilst building the construct. Nevertheless, a single short telomere was generated for the purposes of this study. A diploid strain W303ST (YUD892.1 with single short telomere), heterozygous for the telomerase switch (*EST2/est2::URA3)* was subsequently created by mating YAB892 with YAB0 and transforming the resultant diploid with the *est2::URA3* switch plasmid described in chapter 3.

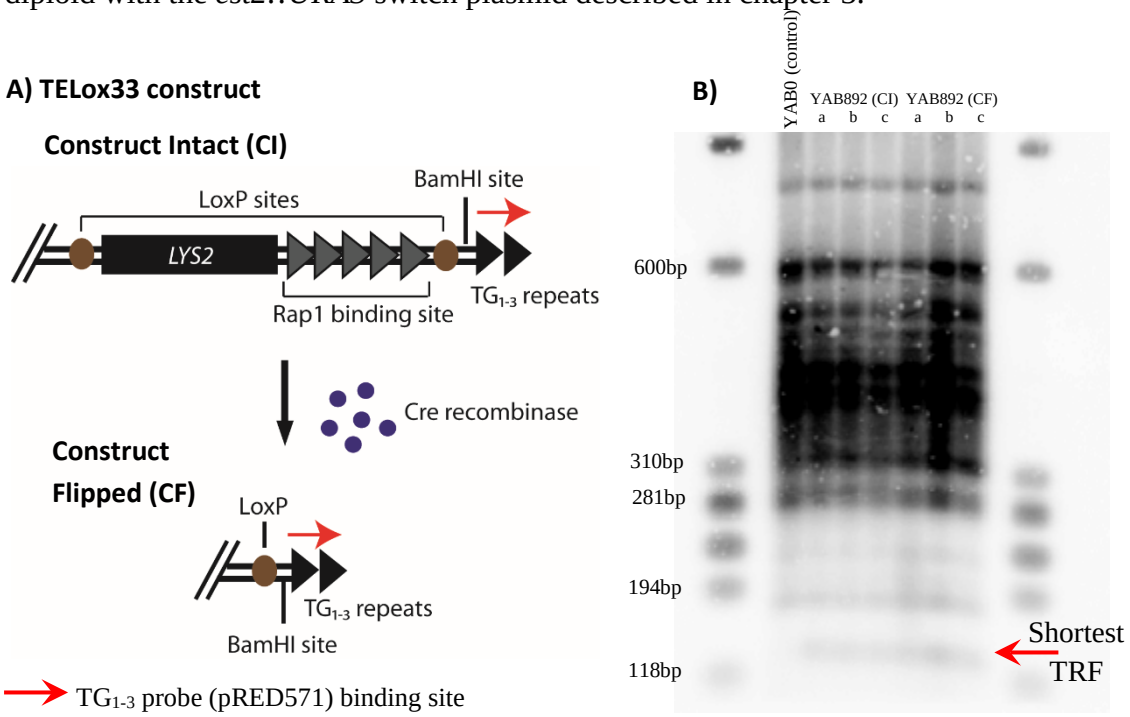

Figure 4-2: Structure of the TELox33 construct and verification of single short telomere generation. A) Diagram showing the structure of the short telomere construct TELox33 in telomerase positive haploid cells YAB892 and corresponding diploids W303ST (YUD892.1) heterozygous for telomerase switch. The construct, consisting of a lysine (*LYS2*) marker and a stretch of Rap1 binding site flanked by LoxP sites, is inserted in the restriction site *MluI* of the *ADH4* locus at CHRVIIL. Immediately downstream of the construct and the second LoxP site is a short stretch of 50 bp of $TG_{1\text{-}3}$ repeats (construct intact – CI). Upon expression of the Cre recombinase from the GAL promoter, the region between the LoxP sites including the *LYS2* marker and Rap1 binding site is excised resulting in a short $TG_{1\text{-}3}$ end (construct flipped – CF). **B)** Southern blot showing terminal restriction fragments (TRF) after a five way restriction digest of control strain YAB0 (no construct) and strain YAB892 (containing TELox33 construct) with restriction enzymes *AluI, BamHI, MseI, HaeIII and HinfI*. A very short terminal fragment of approximately 140 bp is generated in three independent replicates of strain YAB892 when the TELox33 construct is intact (CI) or when it is flipped (CF) but not in control strain YAB0 (without the TELox33 construct). The red arrow highlights the region where the $TG_{1\text{-}3}$ probe binds in diagram **A** and the resulting short telomere from the TELox33construct in figure **B**.

4.3 A single short telomere leads to early senescence in the W303ST cell population

Telomerase negative (*est2::URA3*) haploid W303ST (YUD892.1) cells containing the TELox33 construct and haploid W303 (YUD610.1) control (without the construct), were propagated in URA drop-out culture for 10 days (approximately 100 generations) to generate survivor growth curves and measure the timing of senescence. Three to seven replicates per genotype and condition were cultured in 30^{o}C and diluted to 10^5 cells/ml every 24 hours for 8-11 days. Haploid W303ST cell cultures when propagated with the TEL0x33 construct intact or flipped at loxP sites entered early senescence compared to W303 control. W303ST cells reached the peak of crisis at days 2-3 on average compared to day 6 of control population (Figure 4-3). Furthermore, the peak of crisis in W303ST cells was much deeper compared to control W303 cells (Figure 4-4B). This was likely to be an effect of synchronized cell arrest arising from the short telomere construct. Next, population doublings until the peak of crisis was calculated. W303ST cells had a significantly ($p<0.05$) lower average number of population doublings of 49 compared to that of W303 control which had approximately 72 rounds of population doublings (Figure 4-4A). The significantly lower number of population doublings were indicative of early senescence in W303ST cell population arising from the single short telomere.

Growth curves were also generated of telomerase negative haploid W303ST and W303 cell populations that were either pre-treated with 5% ethanol for >50 generations or pre-treated with 4 mM caffeine for >100 generations. Ethanol pre-treatment led to a small increase in telomere length in both diploid W303 and W303ST cell populations compared to untreated controls (+Δ63 bp and +Δ30 bp respectively) (Figure 4-4C&D). Telomere lengthening delayed the onset of senescence by approximately 26 population doublings in strain W303 compared to its untreated counterpart. The timing of senescence was also delayed in the W303ST strain after telomere elongation by 29 population doublings when the construct was flipped at LoxP sites and by 33 population doublings when the construct was intact despite containing the construct to induce early senescence (Figure 4-4A). Nonetheless, the average population doubling for ethanol pre-treated W303ST (76 population doublings with construct flipped at loxP sites) was still significantly lower ($p=0.0374$) than the ethanol pre-treated W303 control (96 population doubling) demonstrating that a single short telomere still induces relatively

early senescence despite ethanol induced bulk telomere lengthening (Figure 4-4A). Furthermore, the peaks of crisis for ethanol pre-treated W303ST cells was not significantly different than that of ethanol pre-treated W303 cells nor as deep compared to untreated W303ST controls (Figure 4-4B). This indicated the presence of heterogeneity in telomere lengths after bulk telomere lengthening of the W303ST cells.

Telomeres were shortened in diploid W303 and W303ST strains (heterozygous for telomerase switch) by approximately 63 bp and a 100 bp respectively after 4 mM caffeine pre-treatment (Figure 4-4C&D). As mentioned in chapter 3, bulk telomere shortening led to a significantly (p=4.53E-05) accelerated senescence in W303 cells with approximately –Δ23 population doublings compared to its untreated counterparts. Likewise, caffeine pre-treated W303ST cells with the TELox33 construct had significantly reduced number of population doublings compared to caffeine pre-treated W303 cells (-Δ7 population doubling, p=0.007 when the TELox33 construct is flipped at loxP sites and p=0.012 when the construct is intact). Furthermore, caffeine pre-treated W303ST cells with the TELox33 construct intact had a more severe crisis compared to caffeine pre-treated W303 cells (p=0.033) (Figure 4-4B). For example, one culture out of seven replicates of caffeine pre-treated W303ST stayed at crisis for 5 days without any growth prior to generating a survivor. Cells in two other replicates failed to recover and become survivors at all. The average growth curves of the five viable replicates out of seven are displayed in Figure 4-3C. Likewise, caffeine pre-treated W303ST cells with the TELox33 construct flipped at LoxP sites also had a more severe crisis compared to caffeine pre-treated W303 cells but the difference was not statistically significant (p=0.072). Altogether, the data indicate extreme telomere shortening in combination with early senescence of the cell population leads to decreased efficiency of recovery from crisis and survivor generation.

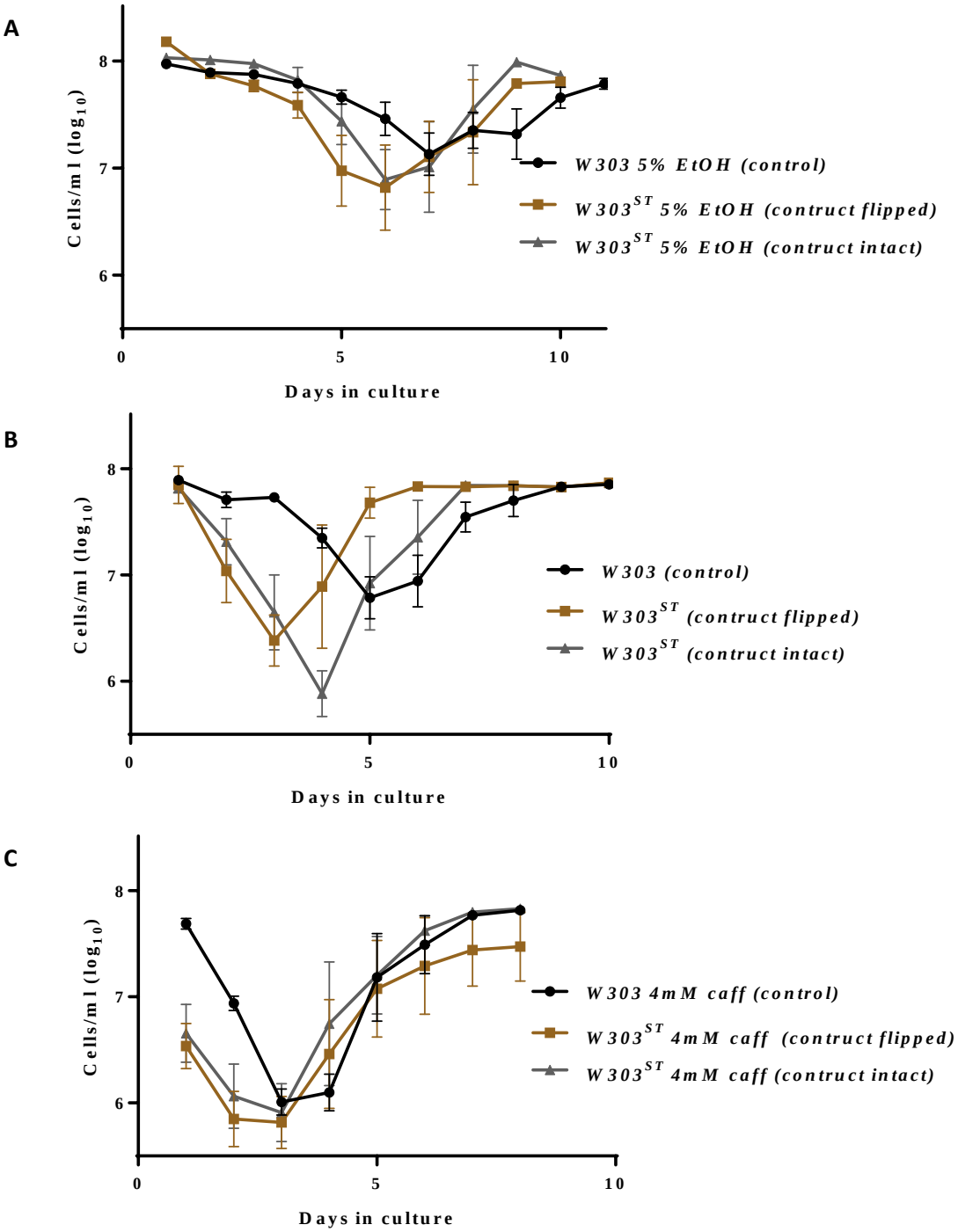

Figure 4-3: Growth curves of senescing telomerase negative haploids W303 and W303ST after pre-treatment with EtOH or caffeine. Average growth curves (n=3-7, ±SEM) of telomerase negative haploid strains W303 (YUD610.1) control and W303ST (YUD892.1) containing short telomere construct TELox33 (both when the construct is flipped – CF, and when the construct in intact - CI) were generated when propagated in liquid medium under standard conditions **A)** after no pre-treatment (control) **B)** after >50 generation of 5% EtOH pre-treatment in diploid state and **C)** after 100 generation of 4 mM caffeine pre-treatment in the diploid state. Cultures were propagated for 8-11 days in which period they underwent senescence followed by recovery via survivor formation.

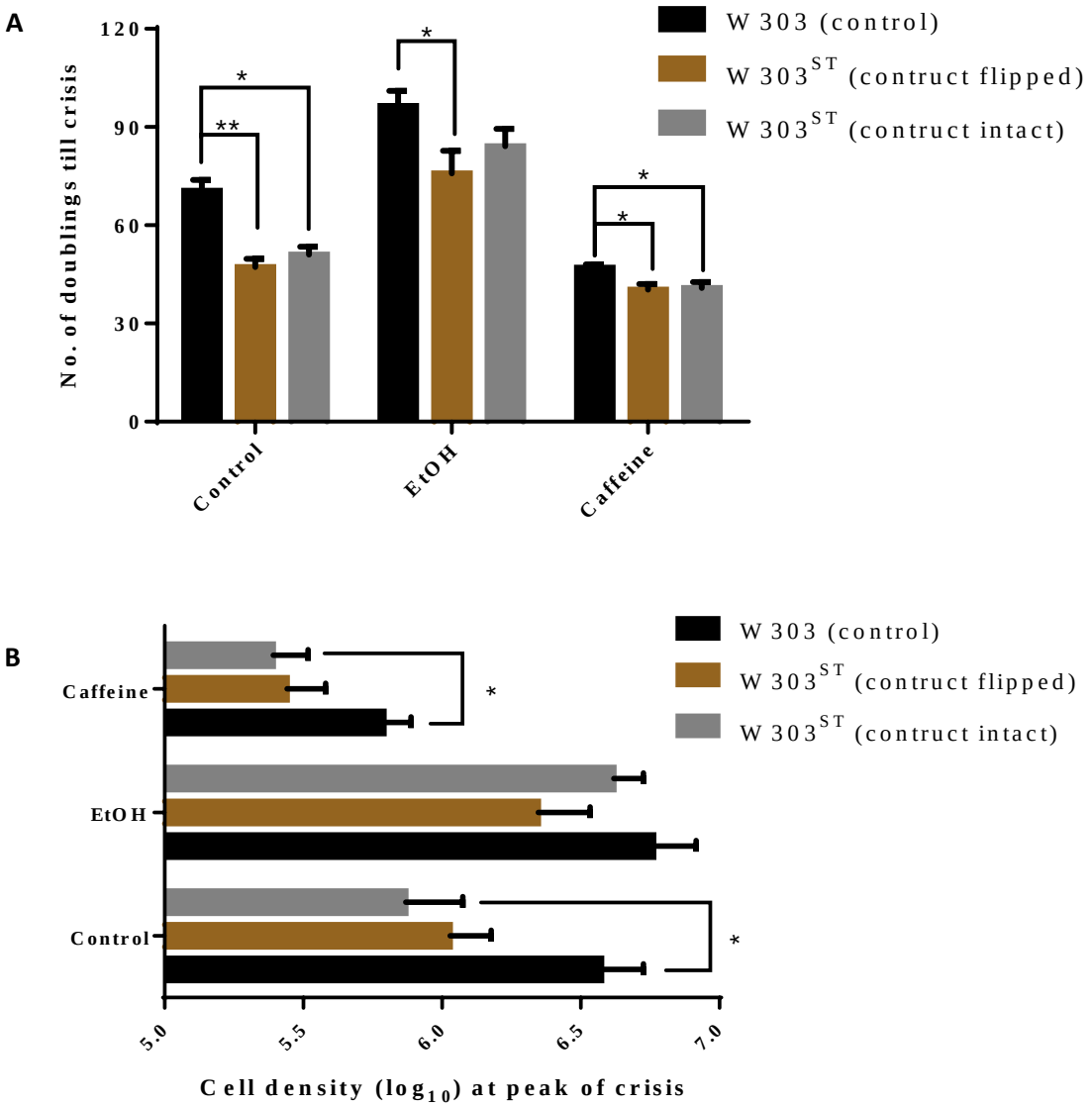
A
120
90
60
30
0
No. of doublings till crisis
*
**
*
*
*
Control
EtOH
Caffeine
W 303 (control)
W 303ST (contruct flipped)
W 303ST (contruct intact)
B
Caffeine
EtOH
Control
*
*
5.0
5.5
6.0
6.5
7.0
Cell density (log10) at peak of crisis
W 303 (control)
W 303ST (contruct flipped)
W 303ST (contruct intact)

Figure 4-4:

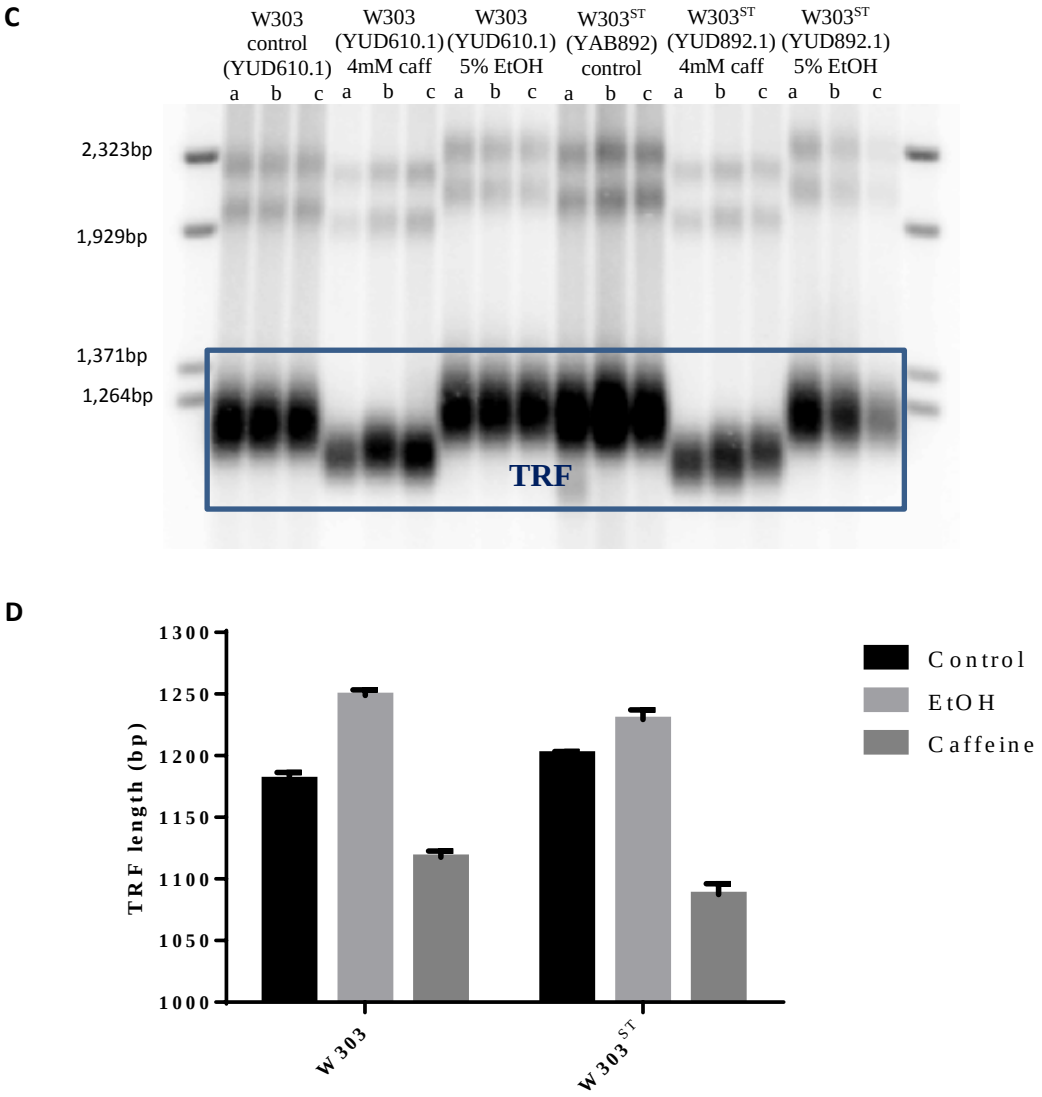

Figure 4-4: Changes in number of population doubling and efficiency of recovery from crisis after telomere lengthening or shortening in telomerase negative strains W303 and W303ST A) Average population doublings (n=3-7, ±SEM) of telomerase negative haploid cells W303 (YUD610.1) and W303ST (YUD892.1) propagated under standard conditions in liquid culture after 5% ethanol pre-treatment (whilst in diploid state), after 4 mM caffeine pre-treatment (whilst in diploid state) or after no pre-treatment (control). Number of population doublings was estimated by converting the relevant OD measurements into approximate cell counts and adding the number of doublings each day until the peak of crisis for each growth curve. **B)** Graph showing cell densities at peak of crisis (n=3-7, ±SEM). This is a measure indicative of efficiency of recovery as the deeper the peak of crisis, the longer the cells remain in crisis without recovery **C)** *XhoI* digested TRFs of three independent replicates of diploid W303 and W303ST cells, heterozygous for telomerase switch, after growth under standard conditions and after growth with exposure to 5% ethanol or 4 mM caffeine stress. Southern blot was probed with pRED571 containing the TG_{1-3} repeats. **D)** TRF length measurements using Image J (n=3, ±SEM). (*p<0.05, **p<0.01)

4.4 Early senescence leads to early rise of survivors in telomerase negative W303ST cell populations

Telomerase negative haploids strains, W303 (YUD610.1 - without construct) and W303ST (YUD892.1- with the TELox33 construct), were grown in liquid media in triplicates and diluted in fresh media every 24 hour as described in section 4.3. The remaining cells in culture after dilution were harvested every day for 8-10 days in order to analyse their TRF for assessing the timing of survivor formation. By examining the changes in TRF of W303ST cell population every day in culture over a period of 10 days and comparing it to that of W303, I was looking to confirm whether survivors arose immediately after early senescence (induced from the short telomere) as suggested by the growth curves or whether the population was merely held at cell arrest synchronously before recovery and without producing survivors in the process.

In haploid W303 cultures, Type II survivors were seen in days 6-7 of the culture. In contrast, survivors were produced in days 2-3 of culture in W303ST strains when the construct was flipped at loxP sites (Figure 4-5A&B). In was in alignment to the timing of senescence of the growth curves observed in Figure 4-3. Furthermore, in the control strain, two out of three cultures produced Type I survivors after crisis and prior to producing Type II survivors. In contrast, strain W303ST produced Type II survivors immediately after crisis in all three cultures. This suggested, early senescence not only led to early production of survivors but also enabled more efficient production of Type II survivors after crisis.

Survivor timing assays were also carried out in telomerase negative W303ST cells after 4mM caffeine pre-treatment. Both caffeine pre-treated W303 control and W303ST cultures underwent early senescence. Similar to W303ST cultures (construct flipped) grown under standard conditions, the caffeine pre-treated W303ST cultures (construct flipped) underwent senescence at day 3 (Figure 4-5C). Two out of the three cultures produced Type II survivors on day 3 immediately after crisis whereas one of the cultures initially produced only Type I survivors at day 3 prior to producing Type II's at day 4. Out of the seven replicates used to generate survivor growth curves, only three were used for survivor time course assay shown in Figure 4-5C as these had relatively faster growth and recovery from crisis compared to other four replicates enabling better DNA extraction. Therefore, the time course assay for caffeine pre-treated W303ST cells

was technically biased towards relatively faster growing cultures and did not fully display the wider spectrum of events such as complete failure of recovery or extreme delay in recovery.

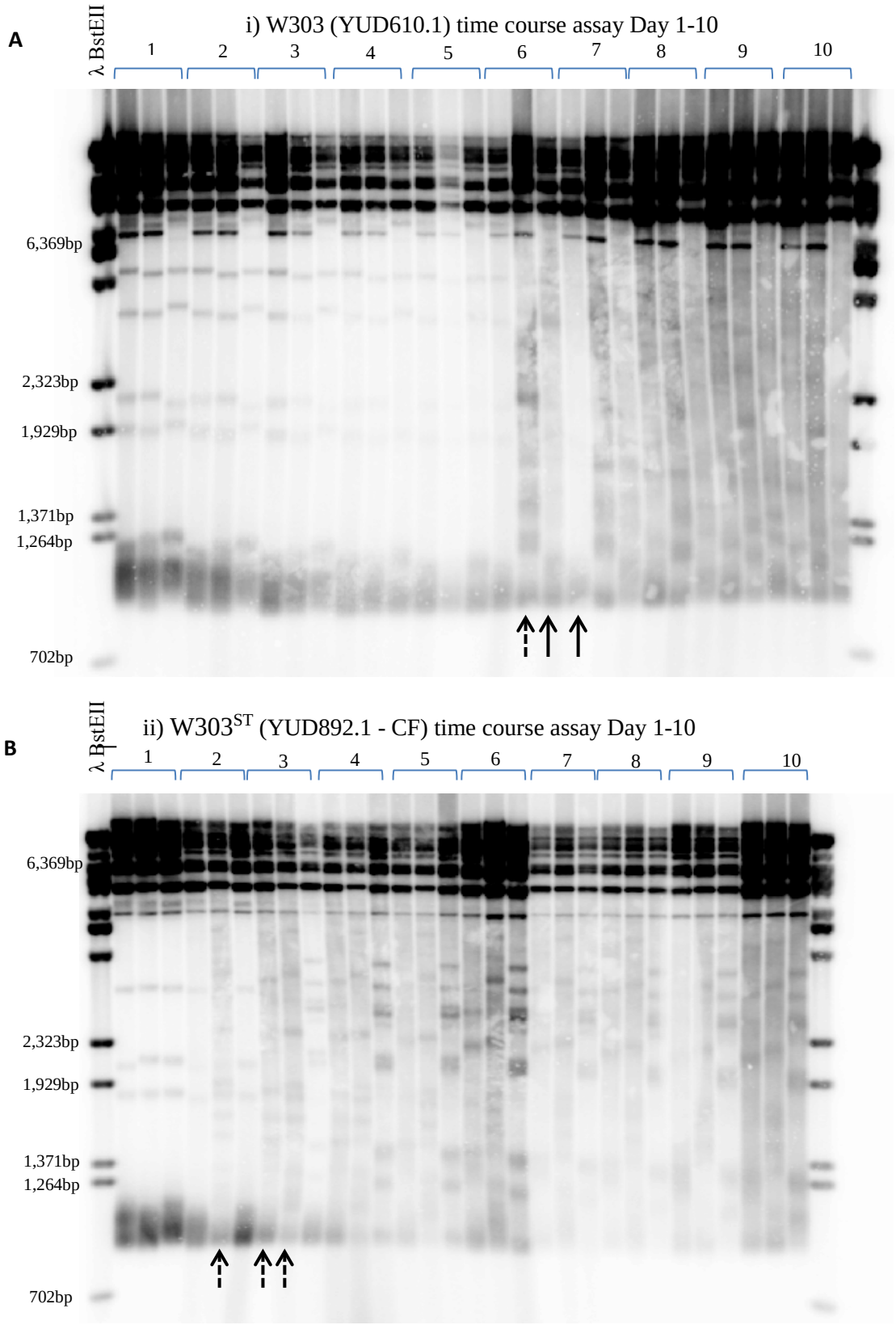

C iii) W303ST (YUD892.1- CF) 4 mM caffeine time course assay Day 1-8

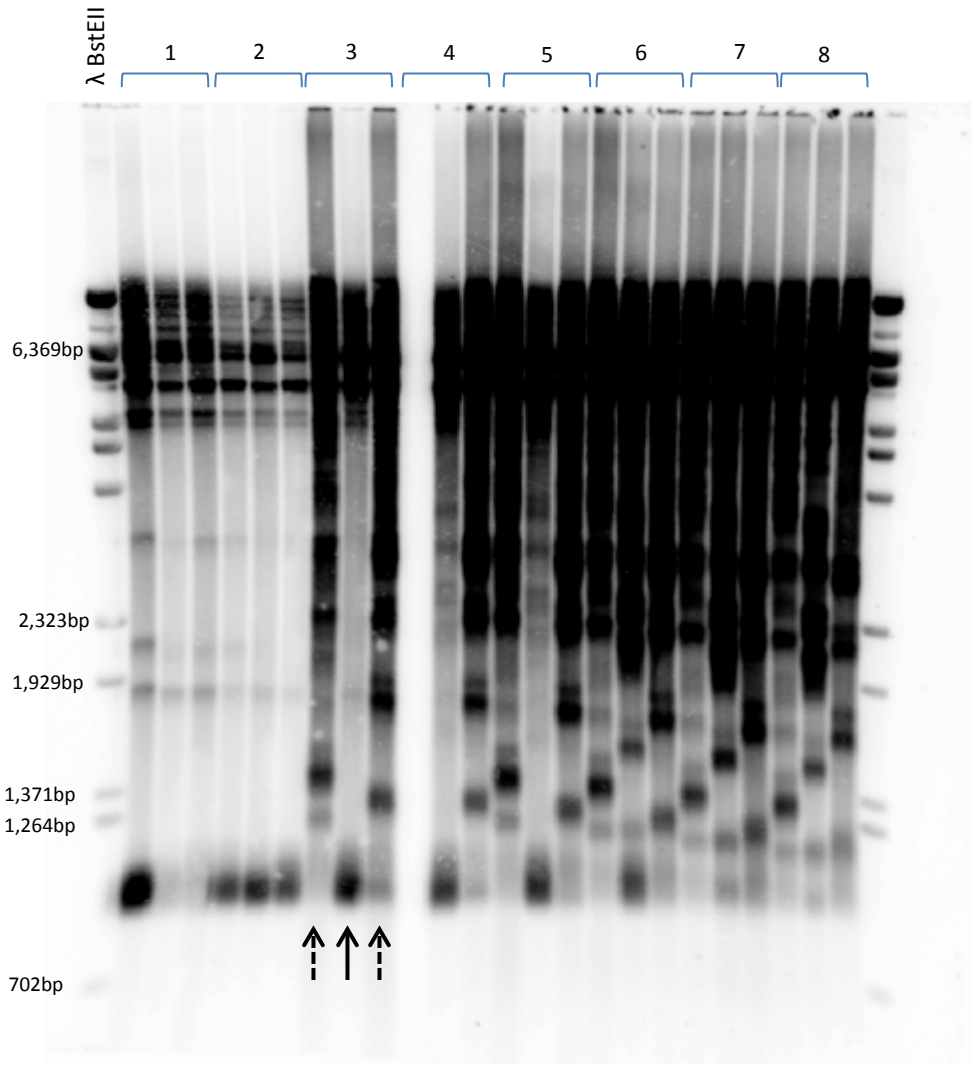

Figure 4-5: Determination of the timing of survivor formation in strains W303 and W303ST. Three independent telomerase negative haploid segregants of strains **A)** control W303 (YUD610.1 - no construct) **B)** W303ST (YUD892.1- containing flipped TELox33 construct - CF) **C)** 4 mM caffeine pre-treated W303ST (CF), were propagated in liquid cultures for 8-10 days and their DNA extracted every 24 hours as their telomeres shortened and survivors were generated. Their DNA was restriction digested with *XhoI* and detected with TG$_{1-3}$ specific probe pRED571. The arrows indicate the point when first survivors are seen. The solid arrows indicate Type I survivors whereas the dotted arrows indicate Type II survivors. A sample is missing in day 4 of figure C as the culture had no growth after overnight incubation until two days later. The time course assay shows survivors arise earlier in W303ST strain when early senescence in induced compared to the otherwise wild-type W303.

4.5 Higher proportion of Type II survivors obtained after inducing early senescence in W303ST strain

After verifying premature senescence induced from a single short telomere end and the early rise of Type II survivors, the proportion of survivor types generated was investigated next. Telomerase negative haploid segregants of the W303ST strain (YUD892.1 - containing TELox33 construct) and control W303 (YUD610.1 - no construct) were streaked into singles on URA drop-out plates and grown until survivor formation via the plate propagation assay. After growth equilibrium of survivors, a single colony from each survivor population was inoculated in liquid media for growth overnight to two days at 30^{o}C shaking incubator and the cells were harvested for DNA extraction. DNA was restriction digested with enzyme *XhoI* and the TRF pattern of individual survivors were examined by Southern-blotting with TG_{1-3} specific probe and survivor proportions examined (Figure 4-6).

In control W303 strain, 7% of the survivors were Type II out of the 41 segregants examined (Table 4-1, Appendix 7.1). In the W303ST strain that undergoes premature senescence and crisis, the proportion of Type II survivors significantly increased to 30% ($p=0.0047$, $n=33$) regardless of whether the construct was intact or flipped at loxP sites (Table 4-1, Appendix 7.1, 7.12-7.13). This suggested, early senescence induced by a single short telomere did in fact lead to increased proportion of Type II survivors. Also, flipping the construct at loxP sites for the removal of Rap1 binding sites and the *LYS2* marker made no difference in the proportion of survivor types seen compared to when the construct was intact. This raised confidence in the observation that early senescence led to an increase in the proportion of Type II survivors rather than the sequences of the construct used for inducing early senescence.

Furthermore, the proportion of survivor types were also analysed after ethanol pre-treatment of W303ST population. Approximately 30% and 35% ($n=20$) of the survivors were Type IIs after artificial telomere lengthening in the W303ST strain when the construct was flipped at loxP site and when it was intact respectively (Table 4-1, Appendix 7.14). This was not different to the proportion of Type II survivor types generated without prior telomere length alteration in W303ST strain. One possibility is that cell arrest leading to senescence from the short telomere was delayed via telomere lengthening at terminal TG_{1-3} end of the construct at CHRVIIL in parallel with other

telomeres, shifting the timing of senescence rather than undergoing early senescence in the presence of elongated telomeres.

The average difference in total population doublings until peak of crisis between ethanol pre-treated W303ST cells and W303 control cells was approximately 20 population doublings (Figure 4-4A). The difference in the number of population doublings until crisis of W303ST and the control, W303, without elongated telomeres was an average of 23 doublings (Figure 4-4A). The fact that the change in number of population doubling between the control strain W303 and the W303ST strain is roughly the same after ethanol pre-treatment and before ethanol pre-treatment suggests that despite artificially induced telomere elongation, their length at the time of senescence is likely to be unchanged. Therefore, the effect of telomere lengthening in combination with early senescence remained inconclusive.

Strains	Description	N	Type I (%)	Type II (%)
W303	WT	41	93	7
W303 (EtOH)	WT	30	100	0
W303ST (CF)	Construct Flipped	33	70	30
W303ST (CI)	Construct Intact	33	70	30
W303ST EtOH (CF)	Construct Flipped	20	70	30
W303ST EtOH (CI)	Construct Intact	20	65	35

Strains	Fishers Exact P value (vs W303)	Fishers Exact P value (vs W303ST)
W303	n/a	n/a
W303 (EtOH)	0.2575	n/a
W303ST (CF)	0.0137*	n/a
W303ST (CI)	0.0137*	n/a
W303ST EtOH (CF)	0.048*	1
W303ST EtOH (CI)	0.0104*	0.7678

Table 4-1: Changes in the proportion of survivor types produced by strains W303 (YUD610.1) and W303ST (YUD892.1) under standard conditions and after 5% ethanol pre-treatment. Survivor types were characterised using Southern blot analysis of *XhoI* digested TRFs as described in Methods 2.7.6 (Southern blots in appendix 7.1-7.2, 7.12 – 7.14). The proportions of survivor types are displayed (rounded to whole numbers) in W303ST both when the construct is intact (CI) and when the construct is flipped at LoxP sites (CF). Changes in proportions of survivor types generated was statistically measured by using Fisher's Exact test and the p-values are displayed. Significant p-values at 95% confidence interval is marked with an asterisk.

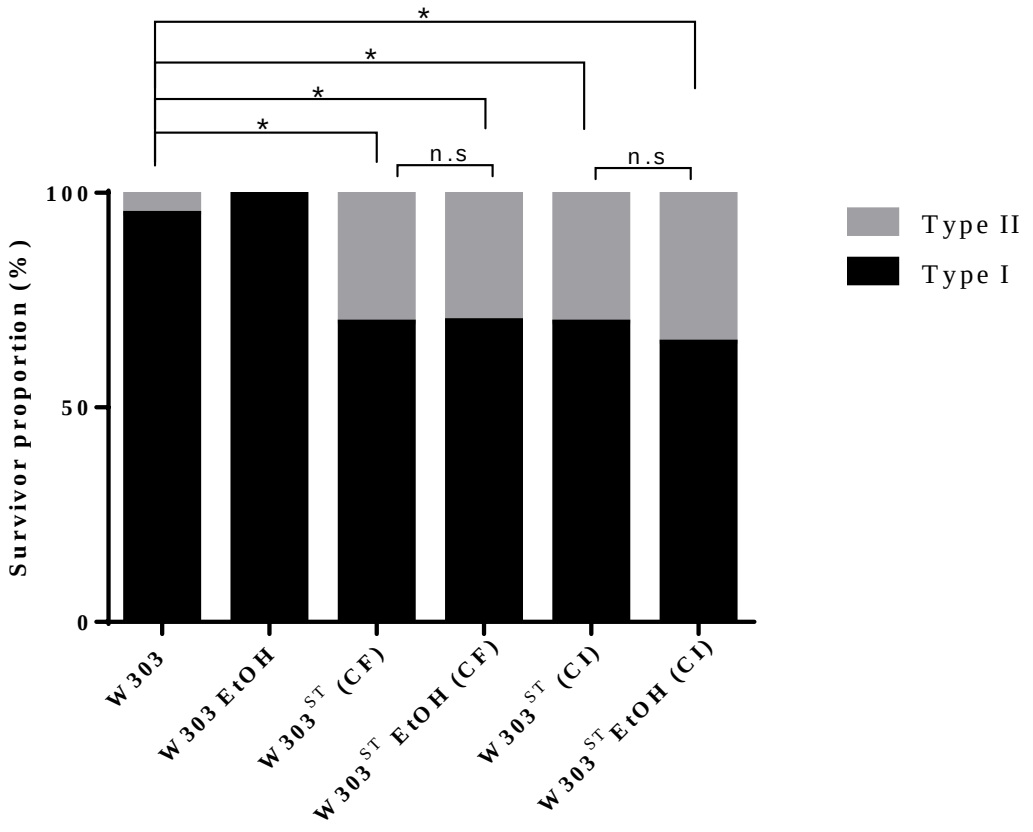

Figure 4-6: Changes in the proportion of survivor types produced by strains W303 (YUD610.1) and W303ST (YUD892.1) under standard conditions and after 5% ethanol pre-treatment. The proportions of Type I and Type II survivors generated in telomerase negative cells W303 and W303ST under standard conditions and after 5% EtOH pre-treatment is displayed as per data in Table 4-1 both when the construct is intact (CI) and when the construct is flipped at LoxP sites (CF). Fisher's exact test was used to calculate the significance of change in proportion of survivor types when compared with control W303. (* $p<0.05$)

4.6 Bulk telomere shortening in combination with early senescence still generates higher proportion of Type II survivors in W303ST strain

As seen above, early senescence arising from a single short telomere at CHRVIIL leads to an increased proportion of Type II survivors. A likely explanation for this could be the presence of longer sister telomeres providing a good substrate for efficient Type II recombination. Next, I addressed whether this increase in Type II survivor proportion occurs only in the presence of long sister telomeres or whether early cell arrest by itself can increase Type II survivor proportions via other independent mechanisms. In order to investigate this, W303ST strain containing the TELox33 construct was subjected to bulk telomere shortening via 4 mM caffeine pre-treatment (Figure 4-4C) and the proportion of survivor types generated was examined via the plate propagation assay (Figure 4-7).

After 6 re-streaks for survivor formation, single colonies from 38 independent segregants were taken for DNA extraction and Southern blot analysis of survivor types. Surprisingly, after caffeine mediated telomere shortening, there was no decrease in the proportion of Type II survivors generated compared to the untreated W303ST cells grown under standard conditions (Table 4-2, Appendix 7.12-7.13, 7.15-7.16). This was the case for both when the construct was flipped and when the construct was intact in the W303ST cells. Hence, in contrast to my proposed hypothesis, it seems unlikely longer initial that telomere length is responsible for increased Type II survivor generation when early senescence is induced from a single short telomere in the cell population.

Strains	Description	N	Type I (%)	Type II (%)
W303ST (CF)	Construct Flipped	33	69.70	30.30
W303ST (CI)	Construct Intact	33	69.70	30.30
W303ST 4 mM caff (CF)	Construct Flipped	38	76.32	23.68
W303ST 4 mM caff (CI)	Construct Intact	38	73.68	26.32

Table 4-2

Strains	Fishers Exact P value (vs W303ST)
W303ST (CF)	n/a
W303ST (CI)	n/a
W303ST 4 mM caff (CF)	0.5969
W303ST 4 mM caff (CI)	0.7941

Table 4-2: Changes in proportion of survivor types in strain W303ST (YUD892.1) under standard conditions and after 4 mM caffeine pre-treatment. Survivor types were characterised using Southern blot analysis of *XhoI* digested TRFs as described in Methods 2.7.6 (Southern blots in appendix 7.12-7.13, 7.15 – 7.16). The proportions of survivor types are displayed (rounded to whole numbers) in W303ST both when the construct is intact (CI) and when the construct is flipped at LoxP sites (CF). Changes in proportions of survivor types generated is statistically measured by using Fishers Exact test and the p-values are displayed. However, the change was found to be statistically non-significant.

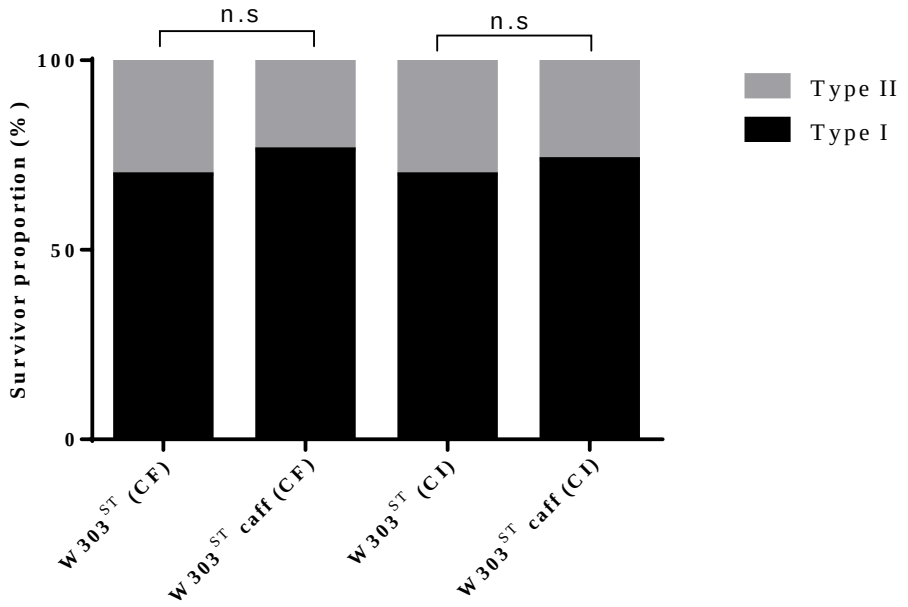

Figure 4-7: Changes in proportion of survivor types in strain W303ST (YUD892.1) under standard conditions and after 4 mM caffeine pre-treatment. The proportions of Type I and Type II survivors generated in telomerase negative cells W303ST under standard conditions and after 4 mM caffeine pre-treatment both when the construct is intact (CI) and when the construct is flipped at LoxP sites (CF) as per data in Table 4-2. Fishers Exact test was used to calculate the significance of change in proportion of survivor types when compared with untreated W303ST, however was found to be statistically non-significant.

4.7 A single long telomere is not sufficient to increase the proportion of Type II survivors

It was established in the previous chapter that longer telomeres lead to an increase in Type II survivor formation and vice-versa. Here, I investigated whether a single artificially lengthened telomere was sufficient to increase the proportion of Type II survivors. A W303 derivate strain of *S. cerevisae*, T131, was created by inserting the construct TELox131 that is able to generate a single long telomere. The construct TELox131 was designed by Bianchi et al (in a manner similar to TELox33) and was inserted at CHRVIIL in the *MluI* restriction site of the *ADH4* gene, removing much of the sub-telomeric elements including the core X. The TELox131 construct consists of 256 bp of $TG_{1\text{-}3}$ repeats upstream of a LYS marker flanked by LoxP sites. Downstream of the LYS marker is a stretch of further $TG_{1\text{-}3}$ repeats inserted at the *BamHI* site. After transformation of the TELox131 into *S. cerevisiae*, the termimal $TG_{1\text{-}3}$ repeat length was regulated to be around 250 bp by telomerase within the cell (Figure 4-8B). Upon expression of Cre recombinase from the GAL promoter, the *LYS2* marker was removed generating a single long telomere of approximately 500 bp length.

The long telomere construct in T131 cells was verified by restriction digestion of genomic DNA with *PacI* or *BamHI* + *PacI* enzymes followed by a Southern blot probed with pRED571 containing the $TG_{1\text{-}3}$ specific sequence both before and after the LYS marker was flipped at LoxP sites. The blot demonstrates generation of a longer TRF fragment in the T131 cells after recombination when compared with TRF of cells prior to recombination (Figure 4-8B).

In order to examine whether a single long telomere had any effect in Type II survivor generation, heterozygous *EST2/est2::URA3* diploid containing the TELox131 construct, $W303^{LT}$ (YUD131.1 – with Long Telomere construct), was first generated by mating haploid T131 to YAB0 followed by transformation of the telomerase switch (*est2::URA3*). The diploids were then sporulated and dissected generating telomerase negative haploids containing the TELox131 long telomere construct and the GAL promoter upstream of Cre recombinase via selection on URA/LYS drop-out plates. 20 independent haploid $W303^{LT}$ segregants were induced to recombine at the LoxP site at approximately 25, 50 or 75 generations in order to generate the long telomere construct. Construct was induced at different time-points to observe whether longer telomeres

nearer crisis would act as more effective substrate for survivor generation as opposed to earlier on. Cells were propagated for survivor formation via the plate-propagation assay and TRFs were analysed via Southern blot. However, data from survivor propagation assay showed no increase in Type II survivors with a single long telomere at any of three time points (Table 4-3, Figure 4-9, Appendix 7.1, 7.18-7.18).

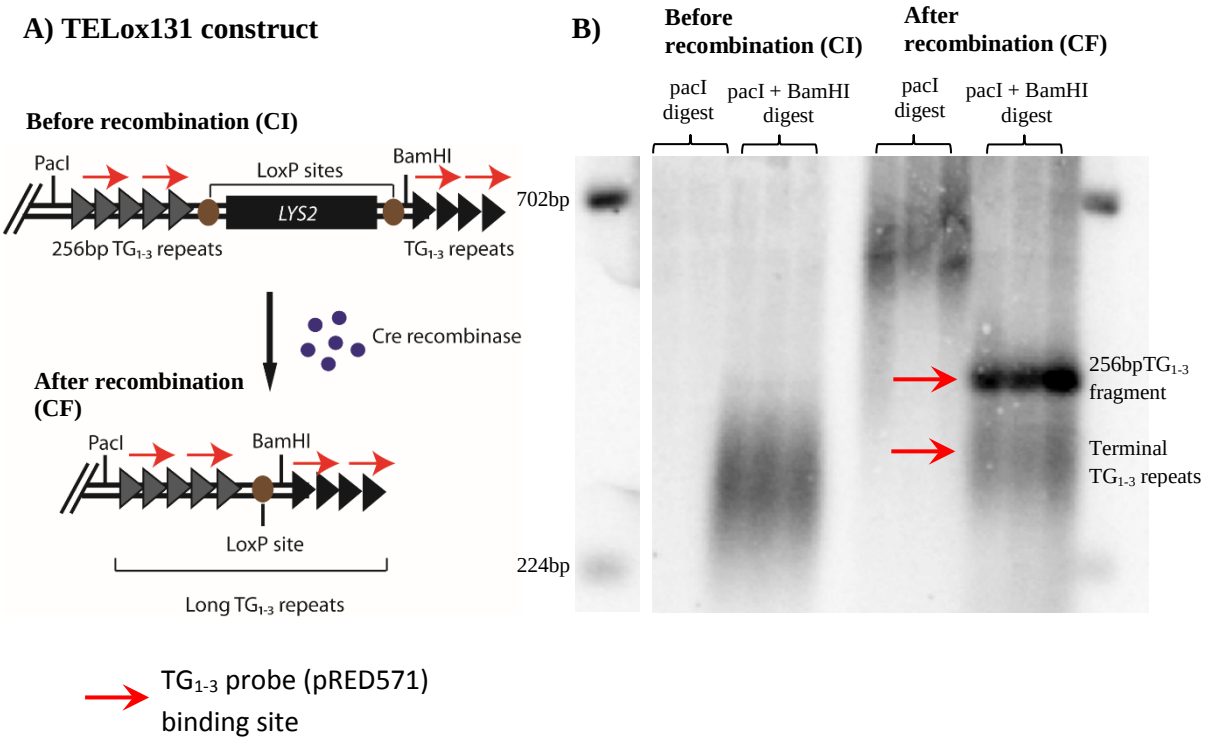

Figure 4-8: Structure of the TELox131 construct and verification of single long telomere generation. A) Diagram showing the TELox131 construct that contains a *LYS2* marker flanked by inducible LoxP sites in between two sets of TG_{1-3} repeats (construct intact – CI). Upon expression of Cre recombinase from the GAL promoter, the *LYS2* marker is excised leading to single long telomere approximately 500 bp long (construct flipped - CF). **B)** Southern blot showing TRFs of T131 cells generated via *PacI* or *BamHI+PacI* restriction digestion before and after recombination in the LoxP sites. Before recombination, short TRFs are generated after *PacI+BamHI* double digest resulting from terminal TG_{1-3} repeats of CHRVIIL and a large fragment bigger than 702 bp (not seen in blot) is obtained after digestion with *PacI* only. However, after recombination, much of the construct is removed and the two stretches of TG_{1-3} repeats come together producing a longer TRF fragment with *PacI* digest (approximately 600 bp). Likewise, digestion with *PacI* and *BamHI* after recombination produces two distinct bands which are the two separate stretches of TG_{1-3} repeats that is separated by the LoxP site. The red arrow displays the binding site for the TG_{1-3} probe within the TELox33 construct.

Strains	Description	N	Type I (%)	Type II (%)	Fishers Exact P value (vs W303)
W303	No construct	41	93	7	n/a
$W303^{LT}$	Construct Flipped (CF) at 25 gen	14	93	7	1
$W303^{LT}$	Construct Flipped (CF) at 50 gen	16	88	12	0.6130
$W303^{LT}$	Construct Flipped (CF) at 75 gen	18	100	0	0.5460

Table 4-3: Changes in proportion of survivor types in telomerase negative haploid strains W303 (YUD610.1) and $W303^{LT}$ (YUD131.1). Survivor types were characterised using Southern blot analysis of *XhoI* digested TRFs as described in Methods 2.7.6 (Southern blots in appendix 7.1, 7.17 – 7.18) and the proportions of survivor types are displayed (rounded to whole numbers). The TELox131 construct in $W303^{LT}$ cells was induced (CF) at three different time-points in senescing haploids generating a single long telomere prior to survivor formation. Changes in proportions of survivor types generated is statistically measured by using Fisher's Exact test and the p-values are displayed.

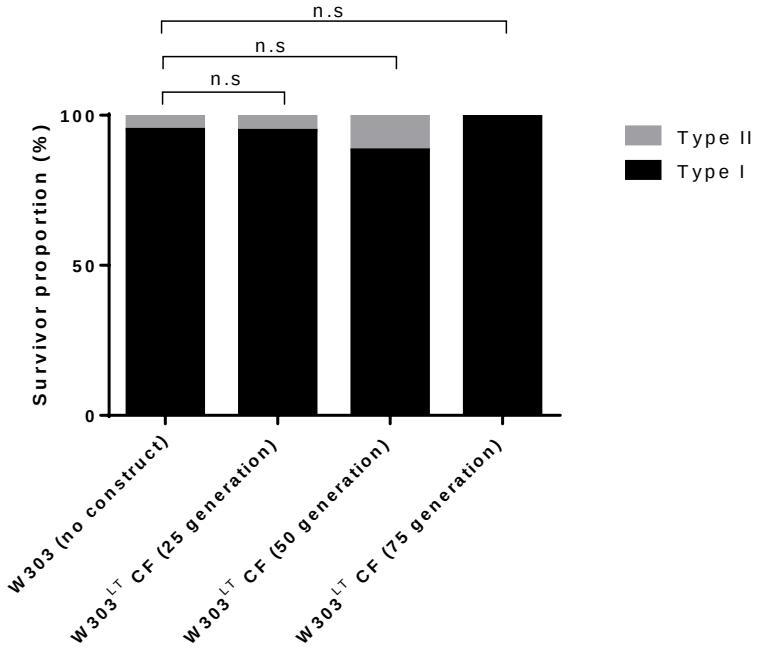

Figure 4-9: Changes in proportion of survivor types in telomerase negative haploid strains W303 (YUD610.1) and $W303^{LT}$ (YUD131.1). Proportions of Type I and Type II survivors generated in telomerase negative cells W303 (w/o construct) and $W303^{LT}$ (containing the long telomere construct TELox131) under standard conditions as per data in Table 4-3. The TELox131 construct in $W303^{LT}$ cells was induced (CF) at three different time-points in senescing haploids generating a single long telomere prior to survivor formation. Fisher's exact test showed no increase in the proportion of Type II survivor types generated when compared with control W303.

4.8 Discussion

This chapter investigates the timing of senescence as a non-genetic factor that influences the formation of survivor types in a telomerase negative cell population. My findings here suggest that timing of senescence is crucial in determining recombinant survivor type formation. Furthermore, I have gathered evidence that indicates telomere length and the timing of senescence of a cell population are separate entities affecting survivor type formation.

Using strain W303ST that harboured a short telomere at a single chromosome end, I initially established that a single short telomere can lead to early senescence of a population in culture as described previously (Abdallah et al., 2009). I also established that early senescence of the cell population leads to early rise of survivors and increased proportion of Type II survivors. In fact, the timing of Type II survivor formation overlapped with that of Type I after early senescence, whereas in control populations Type I survivors are observed prior to Type IIs (Figure 4-5). Taken together, it can be strongly argued that the timing of senescence is an important determinant of survivor type formation.

The experiment to examine the effect of bulk telomere lengthening in conjunction with early senescence on survivor type formation remained inconclusive. This was because the timing of senescence was delayed in a manner proportional to the extent of telomere lengthening itself. Therefore, the length of the telomeres at the point of senescence after artificial lengthening was not different to that of untreated controls. However, a distinction in the role of telomere length and the timing of senescence for survivor formation was established via the bulk telomere shortening experiment. It was expected that if longer telomere lengths at the time of cell arrest or senescence was in fact responsible for generating higher proportions of Type II survivors, shortening of those telomeres would then reduce the proportions of Type II survivors formed. However, inducing early senescence in conjunction with bulk telomere shortening did not lead to a decrease in the proportion of Type II survivors. This was surprising as the ability to generate survivors and recover from crisis of caffeine pre-treated W303ST cells with very short telomeres was greatly diminished when cells underwent early senescence in the liquid culture assay but it did not affect the proportion of Type II survivors

generated. This suggests a decrease in the efficiency of recovery from crisis may not necessarily be correlated with decrease in Type II survivor proportion or vice-versa.

In contrast to my hypothesis and previous suggestion from (Chang et al., 2011), the study also suggests early senescence itself can be responsible for generating higher proportion and early rise of Type II survivors without necessarily requiring the presence of longer telomeres at the point of senescence. It therefore seems the predilection for the Type II survivor pathway is not only dependent on initial telomere length but possibly also on another independent mechanism when premature senescence is induced from a single short telomere. However, the precise mechanism of how early senescence leads to increased proportion of Type II survivors is yet to be elucidated. In addition, it was established in the previous chapter that longer telomeres increase the proportion of Type II survivors generated and the efficiency of recovery from crisis, but whether this pathway overlaps with the senescence pathway is also worth asking in future studies.

A mechanism for Type II survivor generation as discussed previously is the pairing of critically short telomeres with relatively longer telomeres on other chromosomes allowing BIR mediated telomere elongation (McEachern and Haber, 2006). However, considering Type II survivors have heterogeneous telomere lengthening up to 12 kb (Teng and Zakian, 1999), it is unlikely that elongation from a linear telomere end of about 300 bp is sufficient to generate such long telomeres. Therefore, it has been suggested that the presence of t-circles, occasionally arising from recombination event of telomeres in senescing cells to be the substrate for rolling circle based BIR leading to the extraordinary telomere lengthening in survivors (Natarajan and McEachern, 2002, McEachern et al., 2002). The study investigating telomere circles was conducted in *K. lactis* and it was shown that t-circles, even as small as 100 bp, can be a potential source of Type II like telomeric amplification (McEachern et al., 2002). Therefore, an area of future work can be determining whether the proportion of Type II survivors generated correlates with the levels of t-circles present within those cells and whether the molecular pathway involved in early senescence from a single short telomere promotes the production of such t-circles. One technique for observing this is a 2D-gel analysis that can separate DNA fragments based on structure (circular or linear) (Friedman and Brewer, 1995) in strains of interest. Although technically challenging, it has been

successfully used in the past to observe t-circles in telomerase negative survivors in *S. cerevisiae* (Larrivee and Wellinger, 2006).

Proteins of the non-homology based recombination processes have been shown to contribute to the maintenance of t-circles in human ALT positive cells (Li et al., 2011). In the study by Li et al (2011), it was shown that knock-down of yKu70/80 heterodimer results in a significant decrease in the levels of t-circles. Additionally, it is known that yKu70/80 is a NHEJ protein that binds to telomere ends, tethers telomeres to the nuclear periphery in clusters and protects telomeres from recombination (Laroche et al., 1998, Polotnianka et al., 1998). However, as telomeres progressively shorten, yKu70/80 association to telomeres is lost in many chromosomes and it is known that loss of yKu70/80 leads to scattering of telomeres from the nuclear periphery into the nucleoplasm (Laroche et al., 1998). Hence it can be speculated that the rise in Type II survivor formation upon early senescence induced from a single critically short telomere might be due to localisation of telomeres at the nuclear periphery followed by recruitment of recombination proteins to the critically short telomere (and by default to the telomere cluster it is contained in), promoting telomere-telomere recombination or even t-circles formation.

Furthermore, it was observed in time-course assays that early senescence leads to TG_{1-3} amplification at all chromosome ends rather than just in the single telomere that induces cell arrest leading to senescence (Figure 4-5). This could again be due to telomere clustering at the nuclear periphery that enables localization of recombination factors. A recent study by Churikov et al, have in fact demonstrated that proteins bound to eroded telomeres such as replication protein A (RPA) undergo SUMOylation (Small ubiquitin like modifier protein addition) that promotes the binding of Slx5-Slx8 STUbL (proteins involved in the SUMOylation pathway), targeting telomeres to nuclear pore complexes and promoting Type II recombination (Churikov et al., 2016). This reiterates the model whereby telomere clustering to the nuclear periphery is an essential component of Type II survivor pathway and potentially the mechanism for increase in Type II survivor proportion seen when early senescence is induced from a single telomere.

In addition to the timing of senescence, recent studies have also explored various other factors such as the role of non-coding telomeric RNA, also known as TERRA (Telomeric Repeat containing RNA) in relation to telomere and survivor formation

(Pfeiffer and Lingner, 2012, Luke et al., 2008). TERRA is thought to be a regulator of telomere length and therefore also considered to be involved in determining survivor type formation. In fact a study suggests accumulation of TERRA, capable of forming DNA-RNA hybrids, enable bypass of senescence via the Type II recombination pathway (Yu et al., 2014). In addition, a study by Cusanelli et al has showed an increase in the levels of TERRA when a single telomere end is abruptly shortened (Cusanelli et al., 2013). Therefore, it is likely that early senescence occurring from the construct in $W303^{ST}$ cells may lead to increased TERRA levels, enabling efficient bypass of senescence via the Type II survivor pathway and would be worth measuring via qPCR in future work. Likewise, examining the frequency of Type II survivors alongside overexpression of RNAseH could be another way of investigating the role of TERRA in Type II survivor formation.

The second aspect of study in this chapter was to examine the effect of a single long telomere in determining survivor proportions. It was previously established in chapter 3 that longer telomeres lead to higher frequency of Type II survivors. One possible mechanism among others is the presence of longer substrate for telomere-telomere recombination provided by the long $TG_{1\text{-}3}$ repeats. It was therefore investigated whether one long telomere generated from an inducible construct in the $W303^{LT}$ cells was sufficient to cause an increase in Type II survivor proportions. My findings however showed no such increase in the proportion of Type II survivors from a single long telomere. This suggested a single long telomere might not be sufficient to favour the Type II pathway. However, the observed result could likely be due to several caveats in the construct. For instance, the presence of the loxP site after the LYS marker was flipped out could hinder telomere-telomere recombination in generating Type II survivors. Likewise, the removal of much of the sub-telomeric region could also be prohibitive for efficient Type II recombination. However, the latter is unlikely as the loss of sub-telomeric region in the $W303^{ST}$ cells whilst inducing early senescence did not prevent the increase of Type II survivors. Taken together, the data suggests that while long telomeres are able to generate higher proportions of Type II survivors, a single long telomere is not sufficient to bias survivors towards Type II.

In conclusion, I propose that whilst initial telomere length is a prominent factor in determining survivor pathway taken by a cell at crisis, it is one of the many factors that determine survivor types. Another such factor is the timing of senescence. Early

senescence induced from a single critically short telomere leads to higher proportion of Type II survivors independently of the telomere length at the time of senescence. Although the exact mechanism responsible is not clear, some likely avenues for further research include examining levels of t-circle and levels of TERRA expression upon early senescence from a single short telomere and its effect on survivor type formation.

Chapter 5 Quantitative trait analysis of genetic variants regulating telomere length in wild-type populations of *S. cerevisiae*

5.1 Introduction

Telomere length is a complex trait regulated by a large number of genes and gene interactions (Askree et al., 2004, Ungar et al., 2009). Identifying variants responsible for a complex trait using traditional QTL mapping has been a challenging task due to low resolution of the map, requirement of a large sample size and high labour costs. In this chapter, I aim to identify variants, including those in essential genes, affecting telomere length maintenance (TLM) via a novel intercross-Quantitative Trait Loci analysis (i-QTL) method in *Saccharomyces cerevisiae* that overcomes the difficulties of a traditional QTL mapping approach (Liti and Louis, 2012).

S. cerevisiae is a great tool for studying quantitative genetics due to its small genome size (12Mb) and high recombination rate. As a model organism it has helped in the dissection of various complex traits from telomere length to heat resistance and drug resistance (Liti et al., 2009b, Parts et al., 2011). However, a lot of complex trait studies in yeast have been limited to crosses between laboratory strains that do not fully represent natural populations and have fewer genetic variations (Warringer et al., 2011). Likewise, standard knock-out studies of non-essential genes conducted on laboratory strains of *S. cerevisiae* have elucidated hundreds of genes that affect telomere length regulation (Ungar et al., 2009, Askree et al., 2004). However, many variants in essential genes that regulate telomere length and exist in wild populations of *S. cerevisiae* have eluded identification using the traditional knock-out approach.

In this study, two wild-type inbred populations within the *S. cerevisiae* sensu-stricto complex, North American (NA) and Wine European (WE), with varying telomere lengths (the North American strain having shorter telomeres than the Wine European) were used as parental strains to identify natural variations that affect telomere length using i-QTL analysis. The NA and WE strains were obtained from different geographical locations, have the same phylogenetic relationship across their entire genome and are referred to as ‘clean’ non-mosaic lineages (Liti et al., 2009a). Each clean lineage is monomorphic for the major segregating sites meaning there is a large pool of unique SNP’s in each parental strain that can be examined (Figure 5-1).

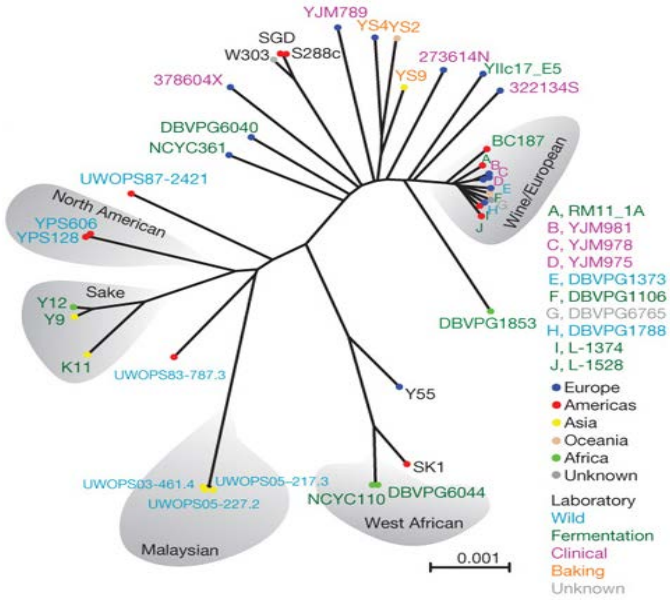

Figure 5-1: Phylogenetic tree based on SNP data of *S. cerevisiae* sensu stricto strains, adapted from (Liti et al., 2009a). The scale bar represents the frequency of base pair differences in each strain with the non-mosaic 'clean' lineages derived from various locations highlighted in grey. (NA = YPS128, WE = DBVPG6765, Sake = Y12, West African = DBVPG6044)

In order to conduct i-QTL analysis, NA and WE parental strains were subjected to 12 rounds of random mating such that their F12 progeny contained shuffled genomes with breakage of linkage groups and a continuum of variation with regards to telomere length. The benefit of i-QTL analysis over traditional QTL analysis is the high resolution mapping of candidate genes (sometimes down to two genes or fewer) (Parts et al., 2011). NA and WE were chosen as parental strains as these strains had the largest difference in their wild-type telomere lengths compared to other *S. cerevisiae* clean lineage strain backgrounds (Muston 2012), generated viable progeny upon mating and had high sporulation efficiency. Unlike in *S. paradoxus* where telomere length variation between strains can be three fold (150 bp to 450 bp) (Liti et al., 2009b), telomere length variation within NA and WE strains of *S. cerevisiae* is less prominent. Nonetheless, it is expected that after sufficient shuffling of the genome through repeated rounds of mating, some segregants will accumulate higher than average number of positive alleles at various loci responsible for telomere elongation or vice-versa (Figure 5-2). Hence, the telomere length variation in progeny from NA and WE cross was expected to be

larger than that of the parents as is seen for virtually every trait studied (Cubillos et al., 2011).

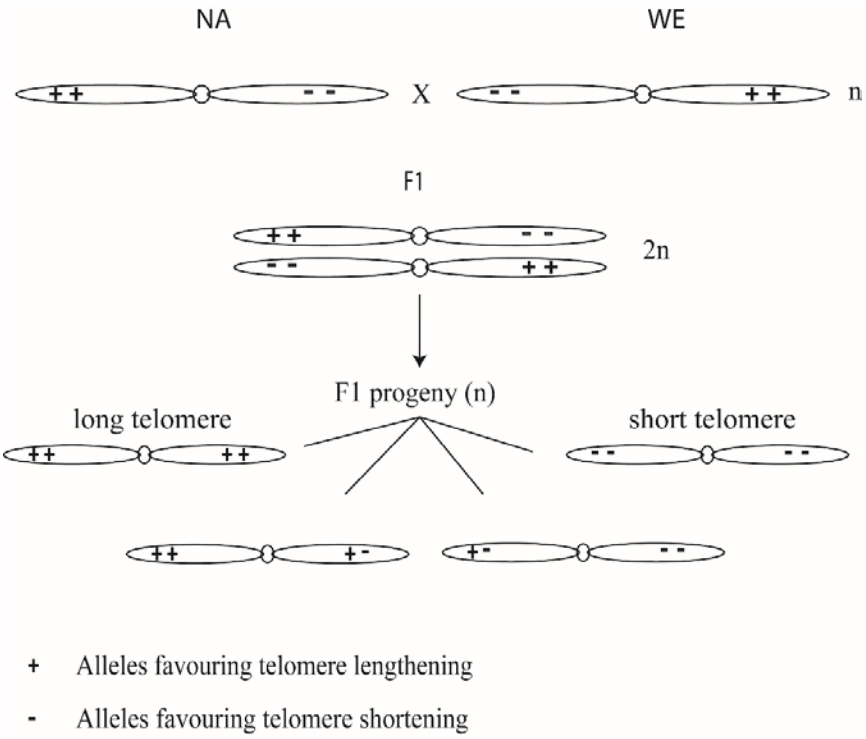

Figure 5-2: Pictorial representation of various positive and negative alleles distribution within parental strains (NA and WE) that regulate telomere length, adapted from (Liti and Louis, 2012). '+' represents alleles that favour telomere lengthening whilst '-' represents alleles that favour telomere shortening. F1 diploids contain all parental alleles whereas the F1 progeny can have a mix of '+' and '-' alleles due to genome shuffling during meiosis. Depending on the load of '+' or '-' alleles present, there will be variation in the overall telomere length.

There are several possible methods of analysing differences in allele frequencies of gene variants for the trait of interest once the trait has been phenotyped. One method is pooling of DNA samples of selected progeny with extreme phenotypes (in both directions) and comparing the variation in allele frequency between the two pools, known as 'bulk segregants analysis' (Michelmore et al., 1991) which can be analysed by 'Multipool' (Edwards and Gifford, 2012). A similar approach of using pooled data to determine variants has been successfully demonstrated in a previous study (Ehrenreich et al., 2010) where resistance to chemical agents was investigated. According to the study, comparing allele frequencies in two pools containing extreme

phenotypes generated several hits with two peaks in the same region but facing the opposite direction (bi-polar peaks). This makes the likelihood of a peak containing a causal variant more robust.

The likely candidates determined from variant calling will be verified by the method of reciprocal hemizygosity, described first by (Steinmetz et al., 2002) in a yeast QTL study examining high temperature growth. In this method, one parental allele of the candidate gene is knocked-out in the original hybrid parental diploid while the other is intact and vice-versa to generate hemizygotes. The telomere length is then measured in the hemizygotes and compared to that containing both parental alleles. If there is a difference in telomere length, the gene is considered to have an effect on the telomere maintenance mechanism (Figure 5-3). Due to the i-QTL method of obtaining F12 segregants whereby large haplotypes are broken down into smaller ones via recombination, the number of genes in the area of interest should be relatively small making the process of pinpointing and identifying the candidate gene simpler. Hence, with the i-QTL approach it is expected that novel gene variants that exists in natural populations will be identified and verified providing better insight into telomere length regulation.

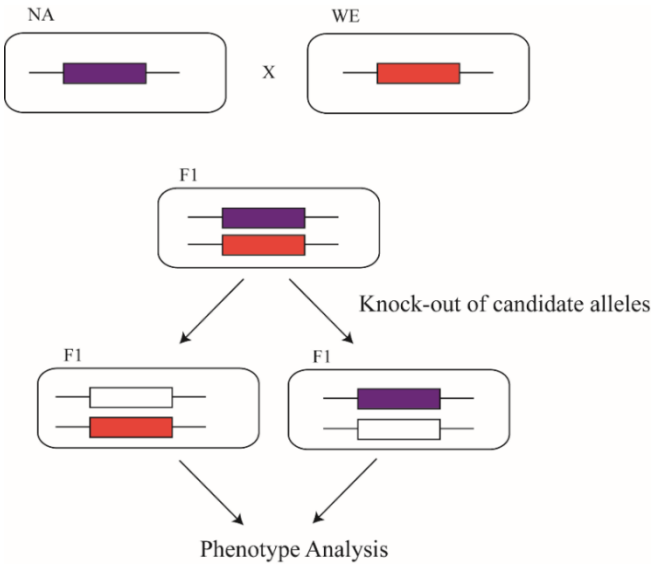

Figure 5-3: Method of reciprocal hemizygosity for candidate gene verification, adapted from (Liti and Louis, 2012). Both alleles (one from each parent) of the candidate gene to be verified are alternatively knocked-out in F1 diploids producing hemizygotes. The phenotype of the hemizygotes are subsequently analysed for the trait of interest. If the loss of an allele leads to a change in the phenotype, they are confirmed to be a causal variant for the trait of interest.

5.2 Inserting a *SpeI* containing tag at telomere CHRXI

In order to phenotype telomere length in parental strains North American (NA), Wine European (WE) and subsequent F12 progeny, a unique 35 bp tag containing a *SpeI* restriction site was inserted at chromosome XIL. The 35 bp tag was initially cloned into plasmid pFEP24 (containing sequences homologous to CHRXIL, a *URA3* marker upstream of core X sequences and $TG_{1\text{-}3}$ repeats), 60 bp upstream of the $TG_{1\text{-}3}$ repeats using appropriate primers via long-template PCR method. The primers were 58-59 bp long and contained the sequence of the tag to be inserted. The resultant linear sequence, containing 35 bp or 36 bp of added nucleotides on both ends with the *SpeI* site on each terminus, was named pUA01. Linear pUA01 was then digested with *SpeI* to create sticky ends, ligated using T4 ligase, transformed into competent JM109 cells and sequenced to verify correct insertion of the final 35 bp tag containing *SpeI* site (Figure 5-4). Plasmid pUA01 with the correct sequence (verified by Sanger sequencing, appendix 7.22) was eventually transformed into haploid *S. cerevisiae* strains NA (OS104) and WE (OS3).

OS104 and OS3 colonies growing on URA drop-out plates were selected as successful pUA01 transformants, subjected to pulse-field gel electrophoresis to separate the chromosomes and transferred to a nylon membrane for Southern blot analysis. The membrane was hybridized with a *URA3* specific probe pRED513 to assess insertion of pUA01 plasmid at CHRXI and to ensure the transformation was unique to one telomere (Figure 5-5). In the WE**a** strain, a single colony out of 8 sampled had successfully inserted the pUA01 plasmid at CHRXI and was referred to as OS3.11. In the NA**a** strain, the pUA01 plasmid inserted at CHRIX as opposed to CHRXIL, most likely due to high levels of sequence conservation in the sub-telomeric region. Nevertheless, it was still incorporated to a unique end allowing telomere lengths to be measured and was referred to as strain OS104.11.

Subsequently, DNA was extracted from successful transformants OS3.11 (WE) and OS104.11 (NA) and restriction digested with *SpeI* to generate Terminal Restriction Fragment (TRF) from a single telomere. The length of the TRF for each parents were later verified by doing a Southern blot (Figure 5-6). Strain OS3.11 showed an average telomere length of 357 bp at CHRXIL whereas strain OS104.11 showed an average telomere length of 316 bp at CHRIX. Furthermore, OS3 and OS104 strains without the

pUA01 transformation produced no TRF bands confirming the bands produced from OS3.11 and OS104.11 colonies (post-transformation) had to be from the *SpeI* containing telomere.

After successfully verifying the insertion of the *SpeI* containing tag at a unique telomere end in OS3.11 (WE**a)**, the *URA3* marker upstream of the *SpeI* restriction site was replaced with a NAT marker generating strain OS3.12 and once again making it auxotrophic for the *URA3* gene. On the other hand, OS104 (Na**α)** without the *SpeI* containing tag was transformed with the *lys2::URA3* construct producing strain OS104.23 that was auxotrophic for *LYS2* but not *URA3*. Knock-out of *LYS2* was further verified via diagnostic PCR in addition to drop-out selection for the auxotrophy. Finally, strains OS3.12 and OS104.23 were mated whereby each parent strain complemented the auxotrophy of the other enabling easy selection of F1 diploids (named UOS1) on minimal media (MIN) for downstream studies.

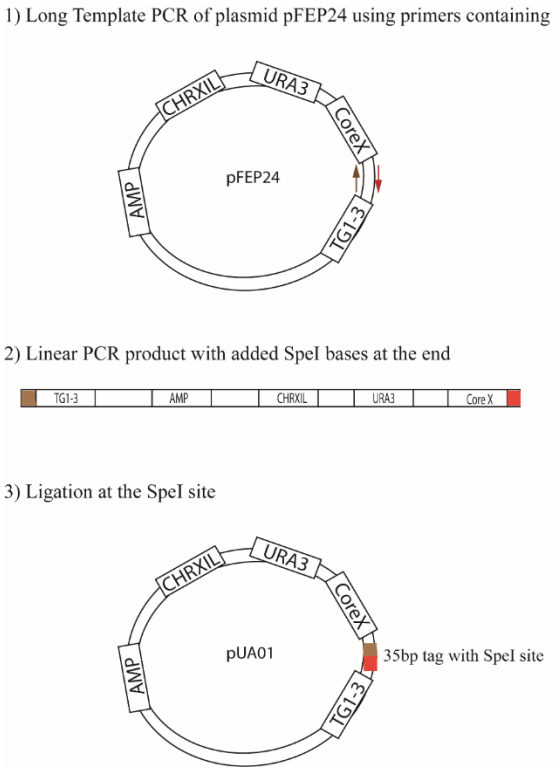

Figure 5-4: Insertion of a 35 bp *SpeI* containing tag in the pFEP24 plasmid. pFEP24 contains sub-telomeric sequences of CHRXIL, a *URA3* marker, CoreX and the $TG_{1\text{-}3}$ repeats and the *SpeI* containing tag is inserted using long template PCR. The PCR product is restriction digested with *SpeI* creating sticky ends at both terminus and eventually ligated generating of plasmid pUA01. The *SpeI* containing tag is inserted approximately 60 bp upstream of the $TG_{1\text{-}3}$ repeats.

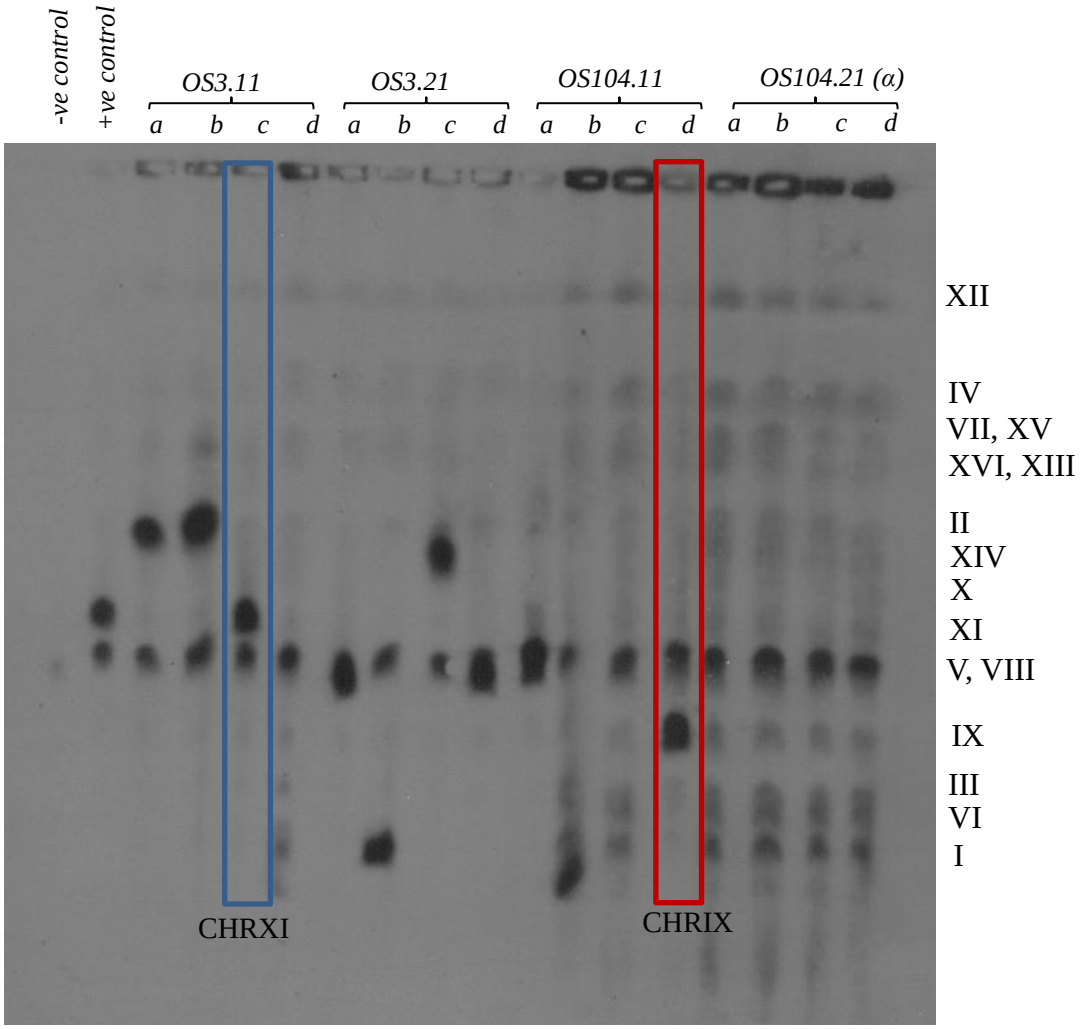

Figure 5-5: Verification of insertion of plasmid pUA01 at CHRXI in WE and NA parental strains of *S. cerevisiae*. The site of plasmid pUA01 integration in the Mat**a** and MAT**α** versions of strains WE strain OS3 (OS3.11 and OS3.21 respectively) and NA strain OS104 (OS104.11 and OS104.21 respectively) is verified by using *URA3* specific probe pRED513. The chromosome of each individual transformant was initially separated using pulse field gel electrophoresis as described in the methods section and transferred to a nylon membrane for southern blotting. +ve control (containing pFEP24 at CHRXIL) and –ve control (without construct) were used to determine the expected site of insertion. A band is produced across all transformants specific to CHRV where the endogenous *URA3* gene is present. Lane highlighted in blue shows OS3.11 transformant with pUA01 incorporated at CHRXI. Although none of the OS104 transformants had pUA01 insertion in CHRXI, one transformant (highlighted in red) contained pUA01 at CHRIX instead.

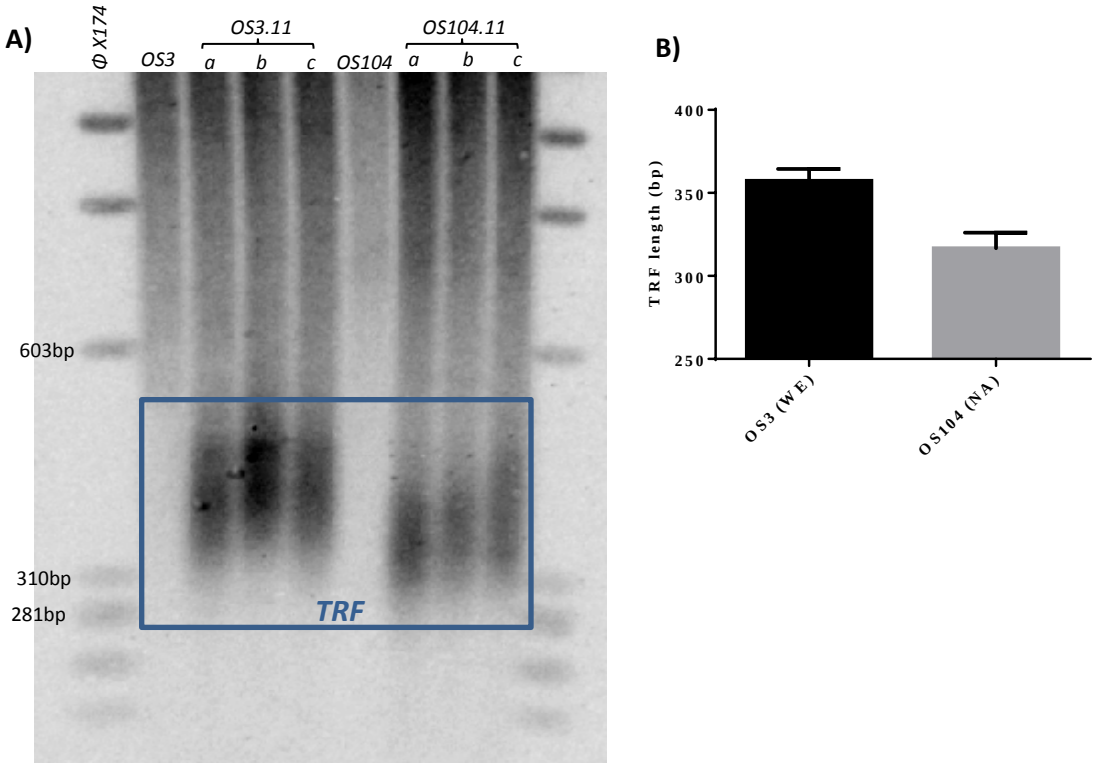

Figure 5-6: TRF length measurement at CHRXI in parental strains WE (OS3.11) and NA (OS104.11) after transformation with plasmid pUA01. (**A)** Southern blot showing TRF fragment from a single chromosome end after *SpeI* restriction digest in strains OS3.11 and OS104.11. The blot is probed with pRED571 specific to TG_{1-3} repeats. Strains OS3 and OS104 that were not transformed with pUA01 did not produce any TRF whereas strains OS3.11 and OS14.11 containing *SpeI* restriction site tagged telomere at CHRXI and CHRIX respectively generated TRF's. **B)** The length of the TRFs were measured using Image J. Strain OS3.11 produces relatively longer average TRF's (357 bp) compared to that of OS104.11 (316 bp).

5.3 Multigenerational cross and phenotypic variation in telomere length of F12 segregants

UOS1 F1 diploids (WE X NA) were subjected to sporulation on KAc media. By day 4 more than 80% of the diploids had sporulated and formed tetrads; of this, $>10^7$ spores were taken and treated with diethyl ether to kill any remaining unsporulated diploids. Outer ascus wall of the tetrads was digested using zymolase and spores mated with each other randomly on NAT media (selecting for segregants with *SpeI* containing tagged telomere at CHRXI) producing F2 diploids. This process of mating and sporulation was repeated 11 more times until F12 progeny were generated as described in previous studies (Parts et al., 2011). The F12 progeny were then dissected and tetrads that displayed 2:2 segregation of the *lys2::URA3* marker were selected for downstream telomere length analysis.

386 F12 segregants were arrayed in 96 well plates and grown on YPD plates for approximately 50 generations prior to DNA extraction. DNA was extracted for all 386 segregants and the *SpeI* digested TRF length was determined in 379 segregants via Southern blotting. As expected the segregants displayed a wide variation in their TRF lengths. Variation in telomere lengths existed not just among segregants of different tetrads but also among segregants of the same tetrad demonstrating well shuffled genome. TRF of 30 segregants were examined per blot in the first round of TRF analysis (Appendix 7.19). The longest and the shortest segregants in each blot, based on relative comparison, were shortlisted for second round of TRF analysis. Approximately 25 segregants with the longest telomeres and 33 segregants with the shortest telomeres were narrowed down in second round of TRF analysis and their lengths were quantitatively measured using the ImageJ software (Appendix 7.20 – 7.21). After telomere length measurements, DNA of the top 20 segregants with the longest telomeres was extracted and pooled together in equal amounts in the 'Long pool.' Likewise, DNA of the bottom 20 segregants with the shortest telomeres was extracted and pooled together in equal amounts in the 'Short pool.' The difference in average TRF length between the two pools was approximately 126 bp (Figure 5-7B) suggesting the variation in F12 progeny is no doubt much greater than that seen in the parents. The pooled DNA was subsequently sequenced using NextGen sequencing as described in the next section.

Lastly, DNA of the first 94 F12 segregants dissected at random from a total of 379 was also extracted and their telomere lengths measured quantitatively using the ImageJ software to determine overall variation in telomere lengths of the F12 segregants (Figure 5-7A, Appendix 7.19).

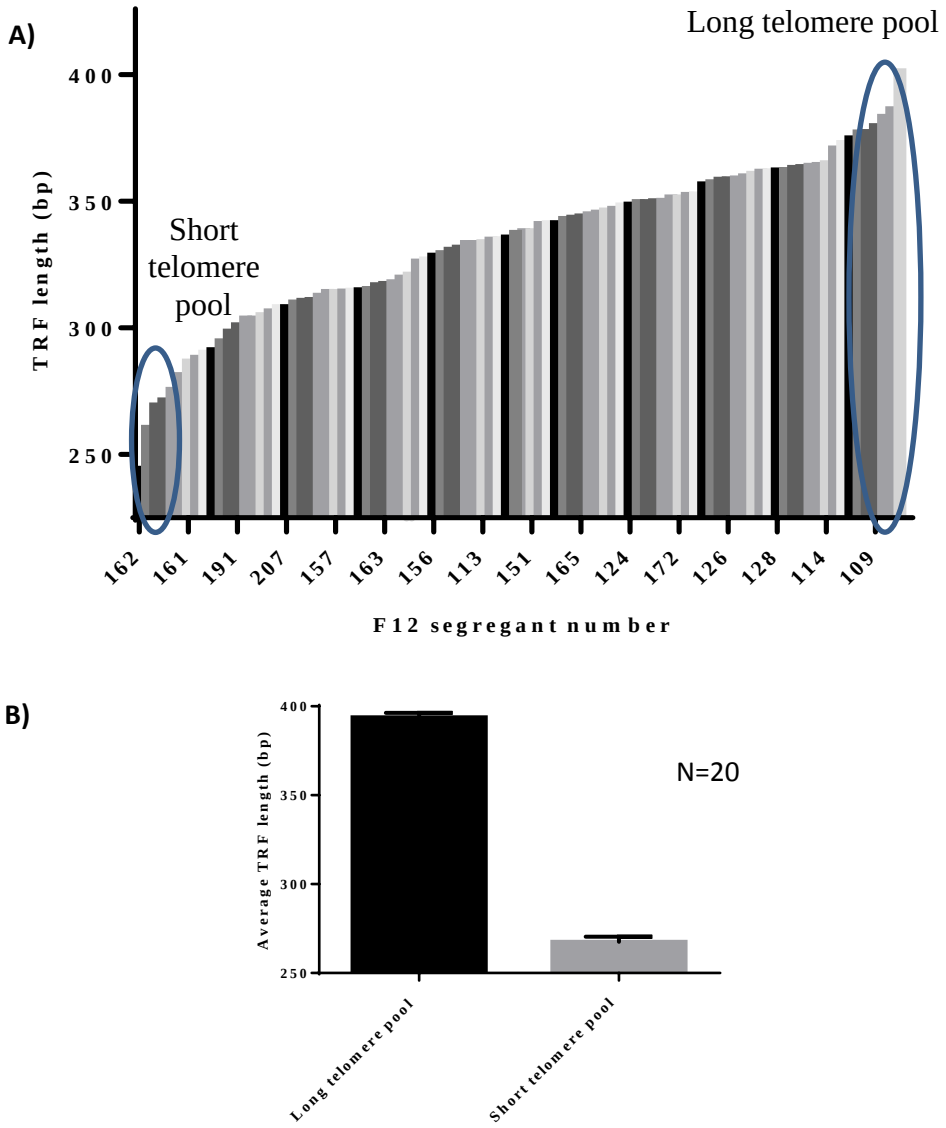

Figure 5-7: TRF length measurement in F12 segregants generated from crossing parental strains WE and NA. **A)** Graph showing a continuum of TRF lengths observed in a random 94 WE X NA F12 segregants out of the 379 examined. TRF's were obtained via southern blotting using $TG_{1\text{-}3}$ specific probes and lengths measured using software Image J. Segregants with TRF's at the extreme ends were picked to be added to a pool containing either the shortest or longest telomeres across all 379 segregants examined and the pools were subsequently analysed to measure allele frequency at all available variant sites. **B)** Graph showing average TRF lengths of segregants with extreme telomere lengths in the 'Long' and 'Short' pools (n=20). The final 20 segregants were picked after two rounds of shortlisting from a starting total of 379 F12 segregants.

5.4 Next Generation sequencing and quality control

In order to identify TLM gene variants, DNA was first extracted from relevant segregants and subjected to whole genome re-sequencing using the Illumina MiSeq platform. The sequencing was conducted by 'NUCLEUS Genomics Core Facility' at the University of Leicester.

DNA was extracted using E.N.Z.A Yeast DNA extraction kit as it produced high yield extraction along with maintaining purity of the samples that is essential for sequencing downstream (described in Methods 2.1.1). MiSeq is a Sequencing-by-Synthesis (SBS) based technology that incorporates a fluorescently labelled reversible terminator dNTP one at a time into a growing oligonucleotide whilst taking images after each addition (McElhoe et al., 2014).

DNA libraries were prepared using the Nextera XT DNA library preparation kit (Illumina, Inc.) which required 1ng of input DNA for each sample. The kit used enzymatic random fragmentation of the genome followed by in vitro ligation of common adapter sequences to both side of the double stranded sequence. Adapter sequences containing the DNA fragments were then hybridized to a flowcell such that each library fragment was bound to a specific tractable channel and denatured. Single fragment of DNA in each flowcell channel was turned into dense clusters via PCR based solid phase bridge-amplification. The clusters were once again denatured allowing the sequencing cycle to begin using fluorescent dNTPs. The base-by-base sequencing produced highly accurate 2x 300 bp paired end reads.

DNA was sequenced at approximately 80x coverage for the two samples of pooled DNA (one containing DNA in equal amounts from 20 segregants with the longest telomeres and other containing DNA in equal amounts from 20 segregants with the shortest telomeres). The sequenced data reads for each sample was then subjected to quality control analysis using the FastQC software (version 0.11.4) from Babraham Bioinformatics by Tom Walsh. FastQC software examines various aspects of raw data reads such as, 'Per base sequence quality,' 'Per tile sequence quality,' ' Per sequence quality score,' 'Per base sequence content,' 'Per sequence GC content,' 'Sequence length distribution,' 'Sequence duplication levels,' 'Over-represented sequence,' 'Adapter Content,' and 'Kmer Content' and gives a summary report on overall quality of sequencing.

Based on the FastQC summary report, both pools had good quality sequenced reads. The average read lengths in both samples were approximately 300 bp which had higher quality score than the threshold of 20 indicating good 'Per base sequence quality.' (Figure 5-8). Another aspect of the sequence reads examined was the percentage of the GC content. *S. cerevisiae* has an average GC content of approximately 40%, however FastQC flagged up an additional smaller peak with approximately 75% GC content in addition to a major peak at 40%, (Figure 5-9A). Upon examination, the high GC content was found to be the result of DNA contamination from *Actinobacter* and was filtered out. Next, the sequence duplication levels were tested by examining the first 100,000 bp of reads as representative for the whole sample. This analysis showed more than 88% of sequences across the sample showed little or no duplication in the long telomere pool and more than 76% of sequences in the short telomere pool. This analysis counted the degree of duplication of every read examined and created a plot showing the relative number of sequences with different degrees of duplication (Figure 5-9B). Overall, the FastQC analysis of sequence reads did not point towards any area of serious concern that would affect this study.

A)

Long Telomere pool

Measure	Value
Filename	Sample95_LongPool_2.trim.fastq
File type	Conventional base calls
Encoding	Sanger / Illumina 1.9
Total Sequences	1581577
Sequences flagged as poor quality	0
Sequence length	50-301
%GC	39

Short Telomere pool

Measure	Value
Filename	Sample96_ShortPool_2.trim.fastq
File type	Conventional base calls
Encoding	Sanger / Illumina 1.9
Total Sequences	1725571
Sequences flagged as poor quality	0
Sequence length	50-301
%GC	45

B)

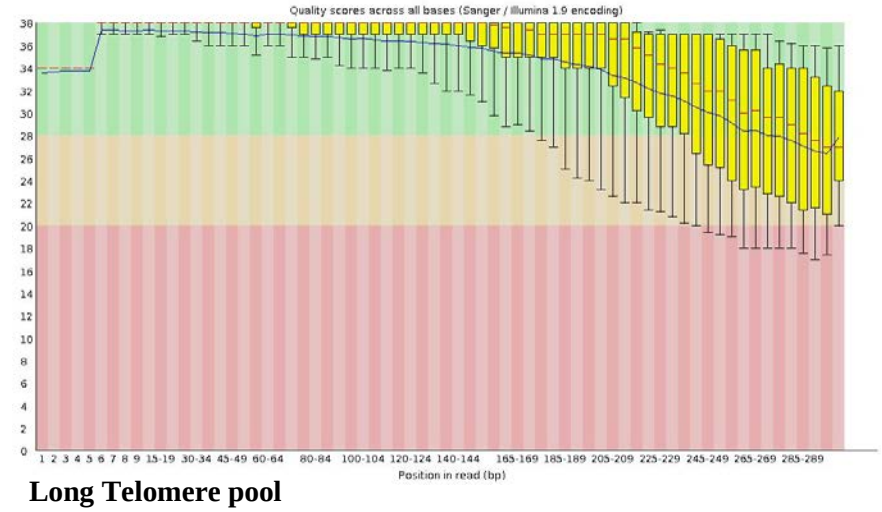

Long Telomere pool

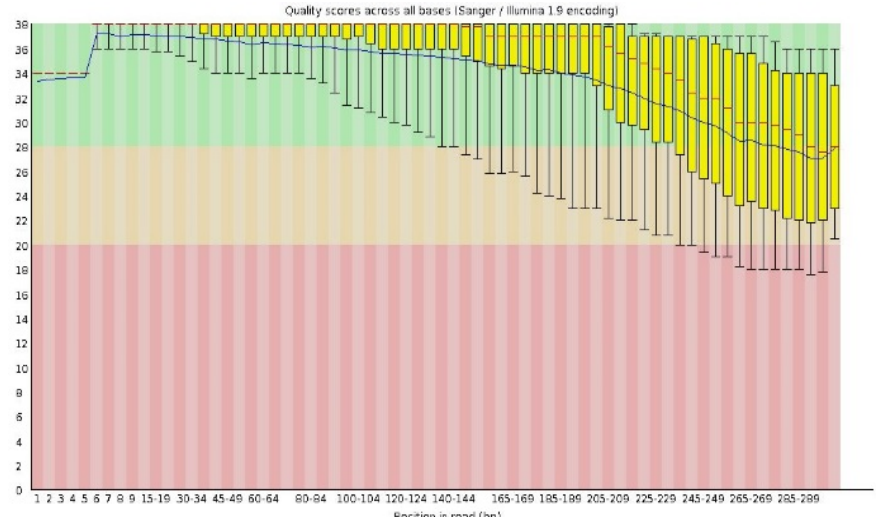

Short Telomere pool

Figure 5-8: FastQC output showing aspects of quality control check of sequenced reads generated from NextGen sequencing (1) A) Quality control summary report of the sequenced reads (produced using FastQC) in the long telomere pool and short telomere pool. The summary shows the total number of sequenced reads in both samples, each of which is 50-301 bp in length, giving an indication of the total sequencing coverage (approximately 80X). **B)** FastQC graph displaying 'Per base sequencing quality'. The x-axis shows the length of the reads whereas the y-axis shows quality score (higher the score, the better the quality). Bases with quality scores less than 20 (red region) is considered to be of poor quality. In the case above, the sequences are of good quality in both pools.

A)

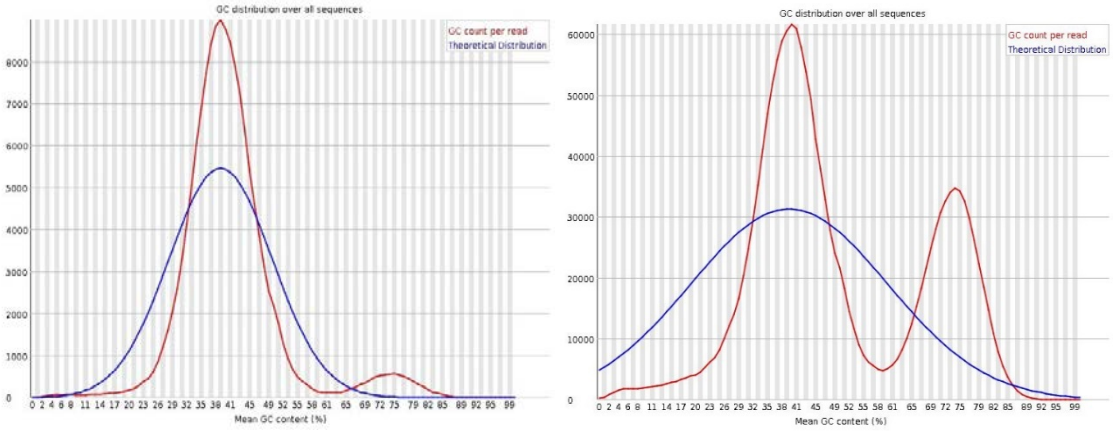

Long Telomere pool **Short Telomere pool**

B)

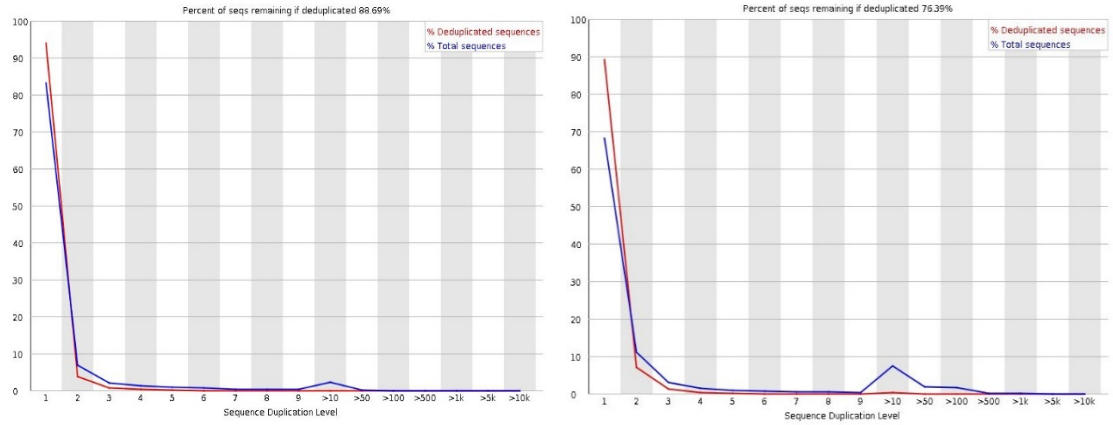

Long Telomere pool **Short Telomere pool**

Figure 5-9: FastQC output showing aspects of quality control check of sequenced reads generated from NextGen sequencing (2) A) FastQC graph showing 'Percentage of GC content' across all sequenced reads. *S. cerevisiae* genome has approximately 40% GC content similar to what is observed in the graph for both pools. However, an additional peak is also observed around 75% which is likely to have resulted from an *Actinobacter* DNA contamination. **B)** Graph showing the 'Sequence duplication levels' across all reads. Approximately 89% of the reads showing 'no duplication' confirming good quality sequencing in the long telomere pool. The short telomere pool has slightly lower percentage of 'no duplication' that is likely to be due to the *Actinobacter* contamination.

5.5 Identification of TLM genes via Multipool analysis

After conducting quality control tests, reads from the two pools were aligned to the S288c reference genome using internal pipeline 'Geno2Pheno' developed by Matthew Blades and Thomas Walsh (University of Leicester). In the long telomere pool 88,725 SNPs were identified initially whereas in the short telomere pool 87,955 SNPs were identified compared to the reference. The overall large SNP pool was subjected to various filters in order to raise quality of variants available without compromising sensitivity. The filters removed SNPs if there were more than 3 SNPs within 10 bp (SNPCluster). It removed SNPs within 10 bp of an indel (SNPGap) with only the most frequent indel being retained. Depth of coverage for each SNP was also taken into account for filtering. For a SNP to be included it had to have a minimum depth of 3X coverage. Maximum depth, calculated using formula described by Heng Li (Fallet et al., 2014) was used to remove SNPs resulting from duplication. A genotyping call rate parameter of 0.8 was also applied. This produced a final SNP count of 57,757 in the long telomere pool and 56,113 in the short telomere pool.

Next, the allele frequency of all variants in the two pools was determined using the Multipool programme (v0.10.2) developed by Matt Edwards (Edwards and Gifford, 2012). Multipool is a great tool for comparing allele frequencies in samples with pooled genomes and has been used in previous studies with yeast (Parts et al., 2011). It functions under the assumption that variants are segregating uniformly across the genome (uniform recombination rate), has equal representation of genome from each sample and sufficient number of input data for calculating allele frequencies. In this study, the pooled samples contained 20 genomes each that were quantified and added in equal amounts to the pool. Also, the 12 rounds of mating ensured sufficient recombination across the genome. The output graph of Multipool run displayed a plot with allele frequency of each variant in the pools in alignment with its position in the chromosome (Figure 5-10). It is worth noting that the frequency of the variant allele displayed in the graph per site is of the WE variants in both pools. A measure of the LOD score is also displayed in the plot however the LOD value is not representative of statistical significance for change in allele frequency between the two pools in this study.

Several intervals with bi-polar peaks were identified across the genome when examining allele frequencies of each variant in the two pools. Intervals where the allele frequency between the two pools differed considerably, such that they faced each other in opposite poles (bi-polar peaks) and had a positive LOD score, were further explored for candidate genes. Although the LOD score is not the best indicator of statistical significance for the presence of candidate regions in this Multipool method due to technical reasons, some peaks with very small LOD scores were nonetheless excluded. This was after further verification the peaks in the intervals of the allele frequency plots were hardly discernible. In total, 12 prominent intervals with bi-polar peaks were identified across the genome (Figure 5-10). The range of each peak was determined and all the genes within the range were examined for possible candidate genes (listed in Table 5-1).

Five of the peaks had obvious candidate genes that are already known to be involved in telomere length regulation, with the most prominent being *EST2* in chromosome XII and *STN1* in chromosome IV. Two of the peaks in chromosome II (452 kbp-480 kbp) and chromosome XII (201 kbp -220 kbp) did not have obvious candidate genes associated with telomere function but contained genes of the RAD family (*RAD16* in chromosome II and *RAD5* in chromosome XII) which are involved in DNA damage repair during replication and possibly even associated with telomere replication. Lastly, five of the remaining peaks, some with very narrow range (example in chromosome XVI with 8000 bp range) contained no known TLM genes. It is likely that one of the genes in this region functions as a telomere length regulator and has not been previously reported. However, there is also a chance that some of these peaks are false positives due to small sample size of the pools (n=20).

In addition to identification of candidate genes, the Multipool output gives a good indication of which parental allele is likely to result in the short telomere or the long telomere phenotype. Whilst it is expected that the WE parent alleles are most likely to result in the long telomere phenotype (as it is the parent strain with relatively longer telomeres), the opposite seems to be the case for some candidate genes. For example, there is a much lower frequency of the WE *RAD16* allele in the long telomere pool compared to the short telomere pool suggesting WE *RAD16* allele leads to comparatively shorter telomeres. Likewise, Multipool suggests, WE allele of *OPI1*,

SBA1 and *EST2* might also lead to shorter telomeres indicating them to be antagonistic variants. However, it could also mean that the WE alleles have no net effect on telomere length and difference in allele frequency is due to the lengthening effect of the NA allele instead. Hence further experimental verification will be required to establish the role of the two parental alleles in determining telomere length.

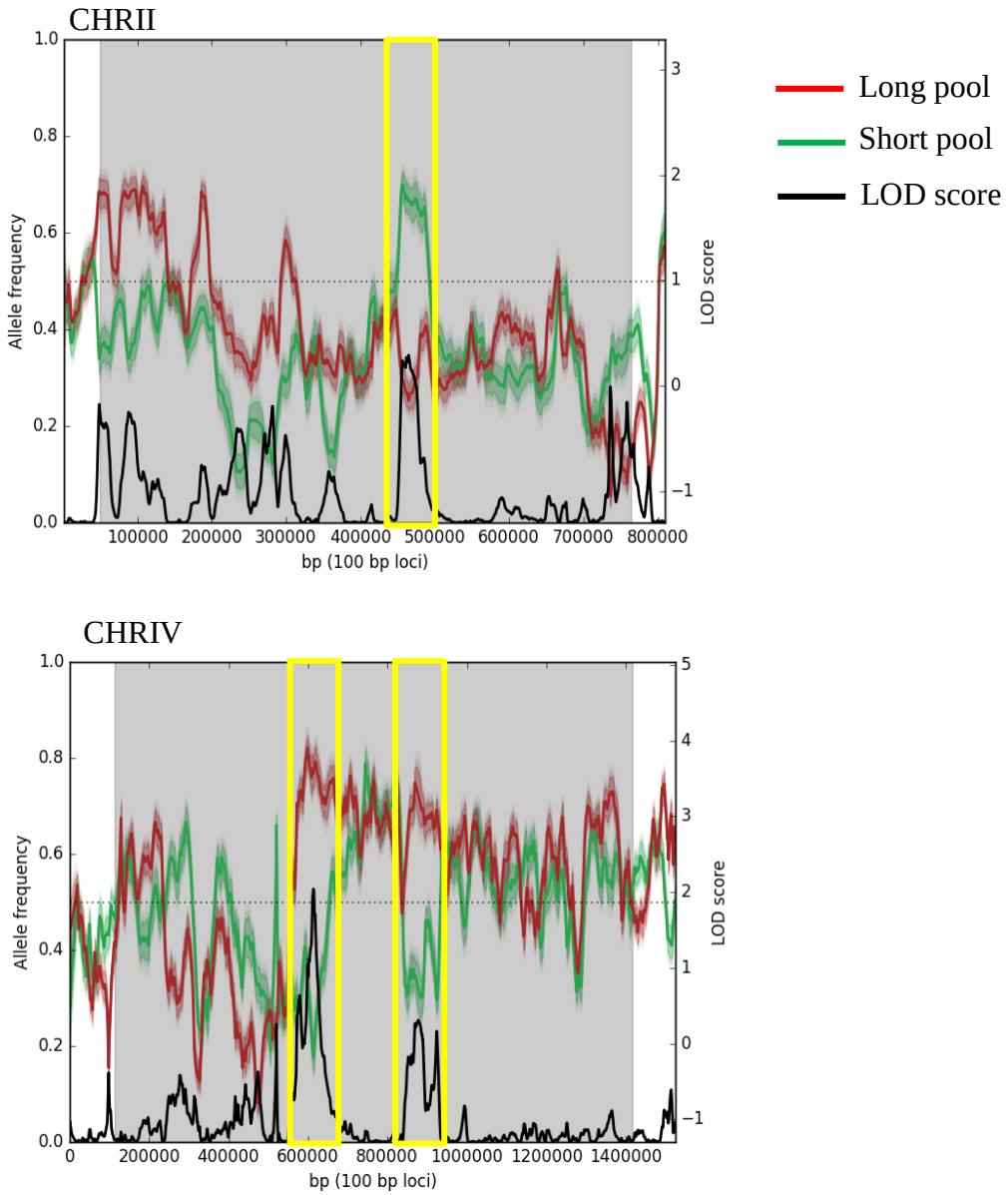

Figure 5-10:

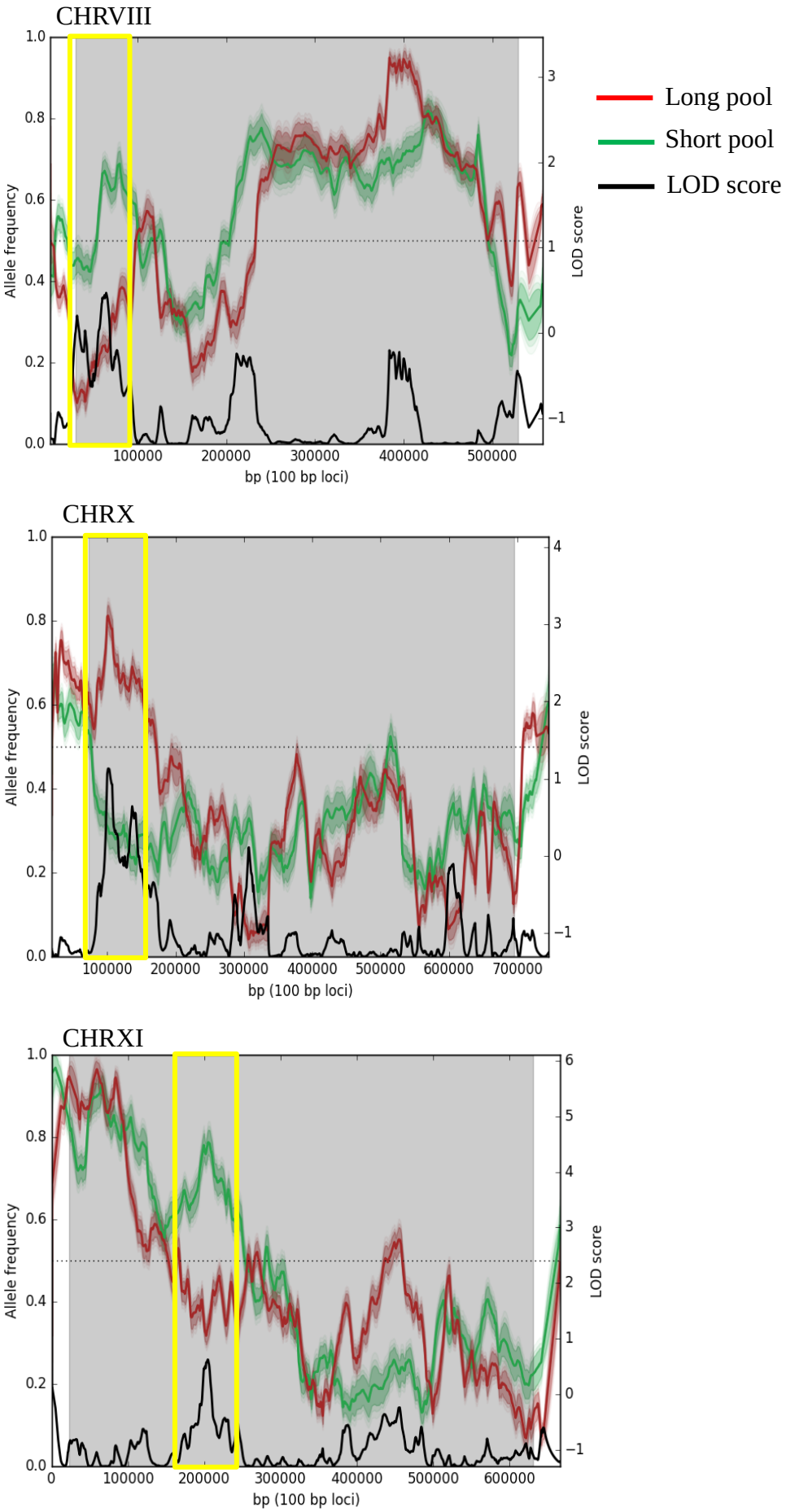
CHRVIII
CHRX
CHRXI
Long pool
Short pool
LOD score
Allele frequency
LOD score
bp (100 bp loci)

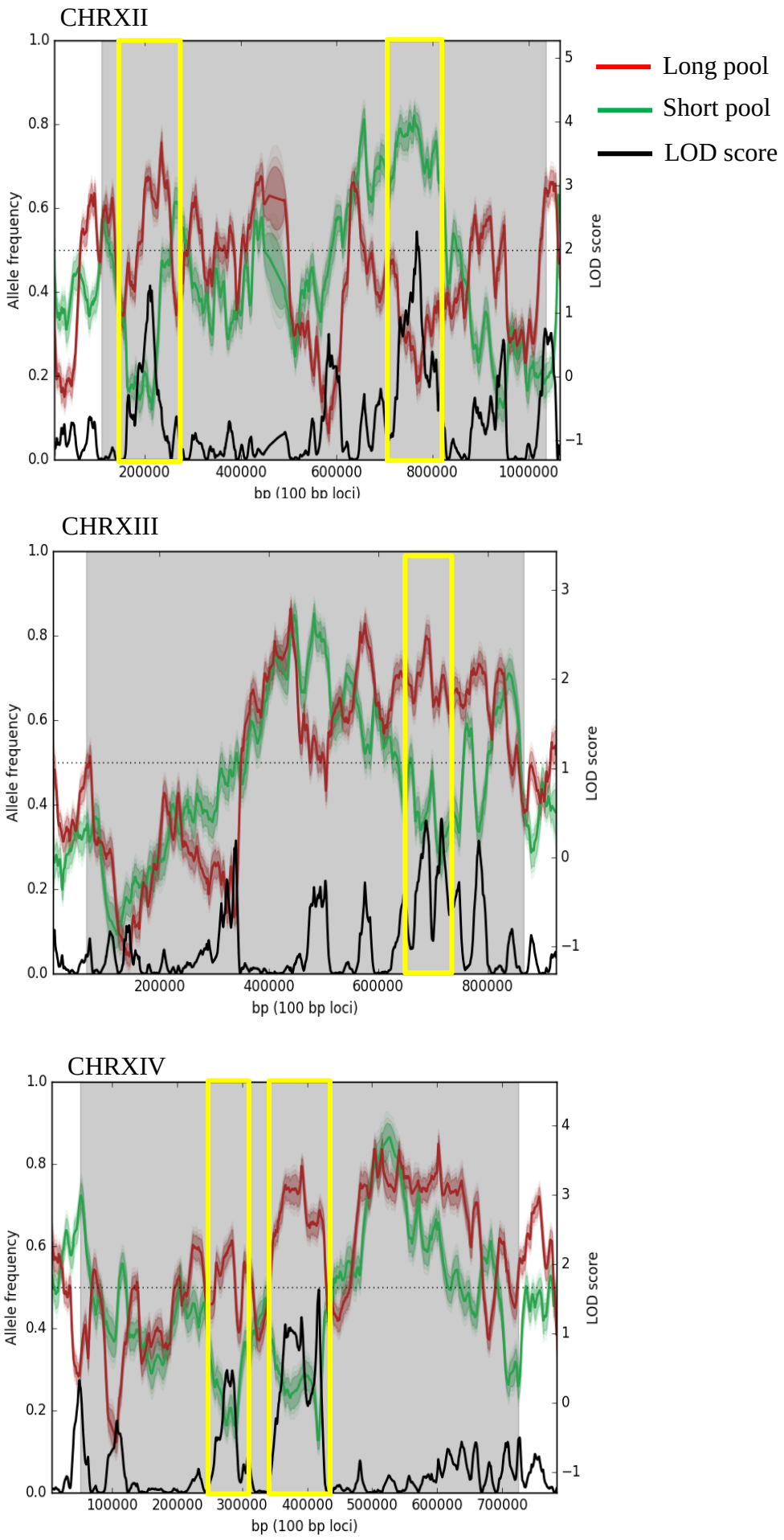
CHRXII
Long pool
Short pool
LOD score
Allele frequency
LOD score
bp (100 bp loci)
CHRXIII
Allele frequency
LOD score
bp (100 bp loci)
CHRXIV
Allele frequency
LOD score
bp (100 bp loci)

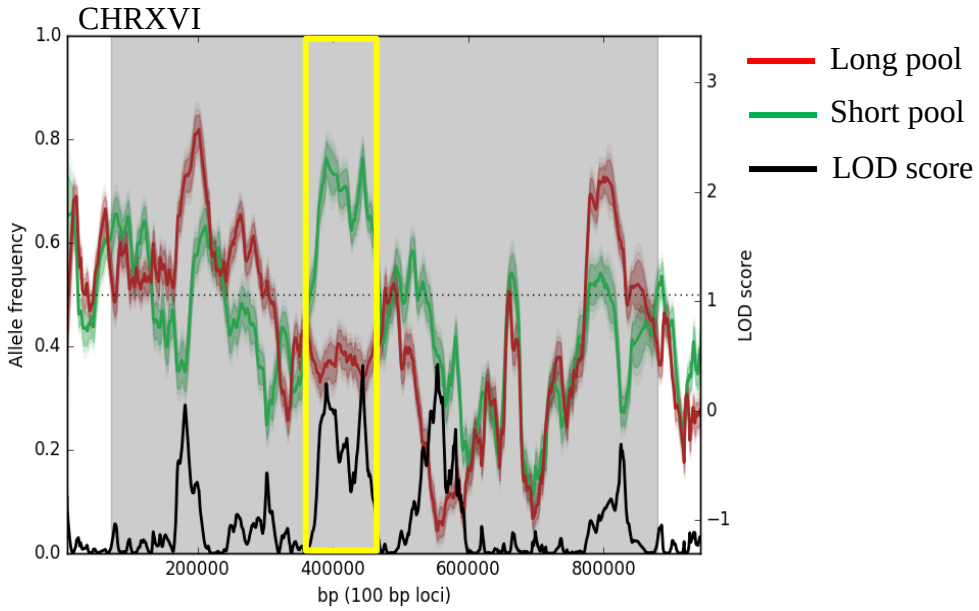

Figure 5-10: **Multipool run output showing bi-polar peaks containing potential QTLs.** The graph displays the allele frequencies of variants on the y-axis and the chromosomal location (bp) on the x-axis. The red line represents the allele frequency of variants in the long telomere pool whereas the green line represents the allele frequency of variants in the short telomere pool. The black line shows the LOD score calculated by the Multipool for each variant. Out of the 16 chromosomes for which Multipool graphs were generated, only those with distinguished bi-polar peaks are shown above. Bi-polar peaks with clear separation of allele frequencies and positive LOD score is highlighted with a yellow box. The grey shaded area shows the confidence intervals for LOD score (very wide in this case as LOD scores are low).

CHR	LOD score	Range (bp)	Interval length (bp)	Peak (bp)	Genes within peak interval range
2	0.34554	452,400 – 480,500	28,100	464,882	*AIM3, ALG1, YSA1, CYC8, SUS1,* ***RAD16****, TLK2, TEF2*
4	2.3828	605,800 – 621,000	15,200	613,474	*PDC2,* ***STN1****, RRP8, TVP23, AFR1, SSS1, RRP1, SLU7*
4	0.37791	846,900 – 893,300	46,400	869,318	*COQ4, MSC2,* ***EBS1,*** *UME6, MSS4*
8	0.41175	49,000 – 81,900	32,900	64,682	*SNF, NPR3, SPO11,* ***OPI1****, RPS20*
10	1.03619	95,900 – 123,400	27,500	103,226	*ASG7, SET2, ERG20, QCR8, HAL5*
11	0.58768	200,000 – 220,500	20,500	210,832	*PGM1, YPK1, RRN3, SSH4,* ***SBA1***
12	2.48515	759,700 – 775,600	15,900	767,280	***EST2***
12	1.43183	200,900 -220,500	19,600	204,832	***RAD5,*** *RSC58, SMF3, MLH2*
13	0.44337	666,100 – 695,600	29,500	687,013	*RAD14, ERG2, TOM40, INP1, PFK2, HFA1, ERG12, YMR209C, YMR210W, DML1*
14	1.58712	412,000 – 420,000	8,000	417,760	*RPC19, DBP2, CYB5 NOP15, YNL108c*
14	1.23092	359,800 – 397,500	37,700	391,350	*TEP1, FAR11, SPC98, ESBP6, NAF1*
16	0.47119	432,300 - 452600	20,300	443,684	*MFM1, PDR12, GRX5, Ty5, TyA*

Table 5-1: **List of genes present within the bi-polar peak range obtained from Multipool graphical output.** Most probable candidate genes are highlighted in bold and were determined based on gene function characterized from previous literature as having TLM function. The LOD score for each peak is displayed as generated by the Multipool programme.

5.6 Variation in primary protein structure of the NA and WE parent alleles of candidate genes

The genomes of the NA and WE parental strains have been sequenced previously by Liti et al (2009a) and Bergstrom et al (2014) independently with deep coverage producing high quality sequence reads. For the seven probable candidate genes that were shortlisted based on gene function (*RAD16, STN1, EBS1, OPI1, SBA1, EST2, RAD5*), the DNA and protein sequences were compared in each parent allele (NA or WE) against the S288c reference genome. The changes in amino acid sequence in each allele of the probable candidates were identified and listed in Table 5-2. It was expected that alleles which affect telomere length maintenance (TLM) would have a few changes in the amino acid sequence leading to changes in protein structure and function. Surprisingly, for majority of the candidate genes examined, both parental alleles had several amino acid variations when compared to the S288c background making it hard to narrow down the causal allele and its function at a molecular level.

Therefore, I next examined whether these variations were conserved across other 'clean lineage' strains namely the 'Sake' and 'West African (WA)' in order to gain better understanding of how essential these variations were to the gene function. For essential gene candidates, the changes in protein sequence are most certainly functional variants as loss of function would render them inviable. However, for non-essential gene candidates, it is more difficult to discern whether the changes in protein sequences causing telomere length alteration is due to complete loss of function or due to functional variation. If the amino acid variations were in fact conserved across multiple other strains from different geographical regions, they were less likely to be loss-of-function mutations. For instance, *STN1* had multiple amino acid substitutions in both WE and NA alleles. However, all of the variations identified were conserved in at least two other *S. cerevisiae* strains suggesting the variations cause changes in protein conformation that alter its telomere capping function.

In the case of WE *RAD16* allele, two amino acid substitutions were identified that were not conserved across the other four strains examined (S288c, NA, Sake and WA). The NA *RAD16* allele on the other hand had complete protein homology with the S288c reference strain. This suggests the WE allele is likely to be the causal variant for telomere length maintenance and more specifically is likely to cause telomere

shortening as the WE *RAD16* allele is enriched in the short telomere pool (Figure 5-10). However, experimental verification is still required for validity. Similarly, the WE allele of *EST2* contained four amino acid substitutions that were not conserved across four other *S. cerevisiae* strains examined. The NA allele of *EST2* also contained 3 amino acid substitutions that were not conserved across other strains. Despite several changes in the protein sequences, it can be established that these variations do not result in loss of *EST2* function as the cells did not undergo telomerase negative senescence when propagated for >100 generations. Amino acid changes in all other candidate genes were also noted and the non-conserved substitutions are highlighted in bold in Table 5-2.

Candidate Genes	Function	DNA Sequence changes compared with S288c		Protein sequence changes compared with S288c	
		WE	**NA**	**WE**	**NA**
RAD16	Nucleotide Excision Repair protein	17 mismatch	7 mismatch	**G41E, N440S**	no change
STN1	Telomere capping protein	4 mismatch	17 mismatch	T206A, I219L	R44W, I93V, K121E, T206A, G218S, I219L, D244E, L281S, S382C, S413L
EBS1	Paralog of *EST1* (subunit of telomerase)	2 mismatch	18 bp insertion, 14 mismatch	I176S, Y833H	N776_A783insASMPPS, I176S, **H190R**, V468I, S597N, Y839H, N884S
OPI1	Transcriptional regulator; TLM gene	In-complete sequence	In-complete sequence	N/A	N/A
SBA1	Homologue of mammalian p23; regulates telomerase activity	7 mismatch	6 mismatch	**V84I, M150T**, Q166K	no change
EST2	Telomerase reverse transcriptase	8 mismatch	3 mismatch	**E219K, I237M, V520A, V597L**	**T240K, Q680H, I757M**
RAD5	DNA helicase; DNA damage tolerance	1 mismatch	32 mismatch	**S553N**	V64L, I124T, I157K, **N383D**, V385A, V388A, L492M, T635N, R898S

Table 5-2: **List of likely TLM candidate genes and the difference in the amino acid sequence in each parent allele of the gene when compared to the S288c reference strain**. Amino acid changes that are highlighted in bold are unique to the specific parent whereas the remaining variations are conserved across other populations of 'clean lineage' strains: NA, WE, S288c, Sake or WA.

5.7 Discussion

In this study, natural genetic variations in two independent populations of *S. cerevisiae* strain, Wine American (WE) and North American (NA), were used as tools to identify novel gene variants that regulate telomere length using the i-QTL approach.

After 12 rounds of mating, transgressive segregation produced F12 progeny whose telomere lengths had much larger variations compared to that of the parental strains. Parental strains WE and NA had telomere length difference of approximately 41 bp whereas the F12 progeny from the same two parents had telomere length variation with a range of 126 bp. This suggested a thorough mixing of the genome with some progeny containing higher than average load of positive alleles for telomere length and some progeny containing higher than average load of negative alleles for telomere length.

Telomere length of 379 progeny were analysed by Southern blotting of which only 40 with extreme phenotypes were used to create the two pools (20 for the long telomere pool and 20 for the short telomere pool). Nevertheless, a small pool size of 20 samples was sufficient to generate several peaks with convincing candidate genes. Moreover, the range of peaks containing the candidate genes were sometimes as narrow as approximately 8,000 bp or 15,900 bp demonstrating the high resolution mapping produced by the i-QTL approach even with a rather obscure phenotype such as mild changes in telomere length. An alternative to southern blot for telomere length analysis could have been telomere PCR using the 35 bp unique marker inserted at CHRXIL as the forward primer. This would allow easier phenotyping of telomere length enabling examination of a larger sample size (>1000 segregants) and subsequently create larger pools with extreme phenotypes for future studies. Furthermore, a larger sample size in the Multipool analysis would produce more reliable allele frequencies for each loci increasing confidence in even the small bi-polar peaks for candidate genes along with reducing the likelihood of false positives. However, telomere PCR would also require a great deal of optimization prior to use which is why Southern blotting was opted for in this study.

Seven promising candidate genes were identified using Multipool, five of which have previously been associated with telomere length regulation (*STN1, EBS1, OPI1, SBA1 and EST2*) and two with DNA repair during replication (*RAD16, RAD5*). Molecular

analysis of variations in protein sequences was carried out to gain insight into the structure of the proteins of the candidate genes.

Among the seven candidate genes identified, *STN1* and *EST2* had the most significant difference in allele frequencies between the two parental alleles (LOD score 2.38 and 2.48 respectively) and the interval peak overlapped directly with the genes themselves. After sequence analysis, it was found that both alleles of the two genes contained several amino acid substitutions compared to S288c (Table 5-2). Stn1 is a crucial telomere capping protein, loss of which is lethal to the cell due to activation of DNA damage response and exonucleolytic resection (Grandin et al., 2001). Two amino acid substitutions were found in the WE *STN1* allele that were conserved with the NA allele. The NA *STN1* allele however contained 8 additional substitutions not conserved with WE or S288c but conserved with the Sake and West African strains. This suggests the NA *STN1* allele is likely to be the causal variant responsible for telomere length alteration possibly due to changes in protein structure and its subsequent TLM function. Furthermore, based on the Multipool output, the NA *STN1* allele frequency is high in the short telomere pool (and vice-versa) suggesting it might be responsible for telomere shortening.

Unlike *STN1*, the *EST2* gene contained unique non-conserved amino acid variations in each parental allele. This will no doubt provide insight into the structure of the *EST2* protein and more interestingly its interaction with other proteins of the telomerase holoenzyme and the telomere itself. A study by Friedman and Cech navigated the N-terminal region of the *EST2* gene containing the reverse transcriptase activity and identified four hypomutable regions that have very low frequency of mutational tolerance for survival or function (Friedman and Cech, 1999). The hypomutable regions included; Region I, amino acids (aa) 31–163; Region II, aa214–265; Region III, aa285–374 and Region IV, aa378–432, interspersed with hypermutable regions. Three of the amino acid substitution identified in my study in the NA (T240K) and WE (E219K, I237M) parent alleles fall within the hypomutable region II, suggesting these are likely to have some effect on the function of the protein and in telomere length regulation. Mutation in region II of the N-terminal domain was also shown to result in loss of *TLC1* binding (Friedman and Cech, 1999, Ji et al., 2005); hence, one possibility can be that the mutations in NA or WE *EST2* leads to decline in *TLC1* binding and thereby shorter telomeres.

Furthermore, the study by Friedman and Cech deleted a large portion of the carboxy-terminal domain of *EST2* (deletion of last 153aa; from aa732) which was found to be non-essential for cell survival and for protein function (Friedman and Cech, 1999). In line with this, it can be suggested that the I757M substitution in NA *EST2* allele is unlikely to be of significance for protein function although might contribute to telomere length regulation via other interactions.

Another study by Ji et al identified several mutations within the *EST2* gene (E76K, N95A) that did not compromise the catalytic activity of telomerase but led to approximately 100 bp increase in telomere length (Ji et al., 2005). A suggested explanation was alteration of a protein subunit that can lead to infidelity in the TG sequences added at the telomeres resulting in disruption of Rap1 binding. Reduced Rap1 binding can consequently lead to telomere elongation. Hence, the amino acid substitutions discovered in the WE and NA strains can elucidate novel mechanism by which it regulates telomere length.

EBS1, homologue of telomerase holoenzyme subunit *EST1* with homology specific to the RNA binding site was also identified as a candidate gene (Zhou et al., 2000). It has previously been shown that loss of *EBS1* leads to shorter telomeres (Zhou et al., 2000). Here, I found that the WE allele of *EBS1* contained two amino acid substitutions when compared to S288c, however these variations were conserved across NA, Sake and West African strains. The NA allele of *EBS1* on the other hand contained 6aa duplication (N776_A783insASMPPS) along with substitutions in 6 other amino acids, one of which was not conserved among the other strains. Furthermore, the short telomere pool had a higher frequency of the NA *EBS1* allele (and vice-versa). Hence, it is likely that the NA allele is causal for telomere shortening either via changes in the protein structure or due to non-functionality. The next candidate gene found in chromosome VIII was *OPI1*. *OPI1* is a transcriptional regulator of numerous genes and was identified by Askree et al as telomere length maintenance gene in a genome wide deletion study, loss of which leads to telomere shortening (Askree et al., 2004). The amino acid sequence could not be analysed in the NA and WE parental alleles due to incomplete sequencing of the *OPI1* gene in both parental strains. However, based on the high allele frequency of the WE *OPI1* allele in the short telomere pool, it is likely to be the causal antagonistic allele responsible for telomere shortening.

The next candidate, *SBA1* is a yeast Hsp90 chaperone that is homologous to vertebrate p23 and has been previously shown to regulate telomerase activity (Fang et al., 1998, Toogun et al., 2007). Sba1 modulates the binding of telomerase to telomeres both positively and negatively. Toogun et al showed Sba1 dissociates stalled complexes of telomerase that are bound to telomeres but not extending and suggested that by default helps the dissociated telomerase bind to other ends for telomere extension (Toogun et al., 2007). Overall, loss of Sba1 was shown to shorten telomeres over five passages of cell cultures by Toogun et al. In this study, I found three amino acid substitutions in the WE allele of *SBA1*, two of which were non-conserved. However, there were no changes in the NA allele. Furthermore, the short telomere pool contained higher frequency of WE *SBA1* allele. Hence, it is likely that the WE allele is contributing to the telomere phenotype, possibly by shortening. This is in contrast to the WE parental strain having relatively longer telomeres at the start meaning the allele is also likely to be an antagonistic variation for the telomere length phenotype.

Finally, other candidate genes included *RAD5* and *RAD16*. *RAD5* is a DNA helicase/ ubiquitin ligase required for post-replication repair of UV damaged DNA (Blastyak et al., 2007, Johnson et al., 1994). Furthermore, *RAD5* has been previously shown to alter length of repetitive sequences (Johnson et al., 1994) and independently also shown to associate with native telomere ends in senescing cells to mediate HR (Fallet et al., 2014). *RAD16* is a nucleotide excision repair protein (Prakash and Prakash, 2000) with no known association with TLM. Several genes affecting DNA metabolism and repair such as *KU* and the *MRX* are known to regulate telomere length making the *RAD* genes reasonable candidates for telomere length regulation, despite no current evidence of direct involvement in TLM.

Identification of telomere associated candidate genes, especially *STN1* and *EST2* demonstrates the success of the experiment in identifying causal variants known to regulate telomere length using the i-QTL and Multipool analysis. More importantly, it builds confidence in the fact that other intervals with bi-polar peaks are also likely to contain genes involved in telomere length regulation despite no prior known associations. In addition to the seven candidate genes described above, there were five other intervals with bi-polar peaks containing genes not associated with telomere function. One way of experimentally identifying and verifying the causal gene or more specifically the causal allele for future investigation is reciprocal hemizygosity

(Steinmetz et al., 2002). Reciprocal hemizygosity can effectively determine which alleles are responsible for the telomere length phenotype and also in what direction it acts, ie shortening or lengthening.

Another aspect leading to greater telomere length variation in F12 progeny when compared to parental strains can be epistatic interaction between TLM alleles of the two parents. In a study conducted by Liti et al in *S. paradoxus* strains CBS and YPS, *yKU* and *TLC1* were identified as major QTLs affecting telomere lengths (Liti et al., 2009b). More interestingly, it was shown that the two parent alleles of yKU (CBS - yKU80 and YPS – yKU70) had negative epistatic interaction resulting in shorter telomeres in the F1 hybrid. Hence, in addition to conducting reciprocal hemizygosity to verify candidate gene variants affecting telomere lengths, it is essential to examine epistatic interaction between parental alleles to gain better insight into regulation of telomere length.

In this study, telomere length regulation variants were identified bioinformatically via the Multipool method using only 20 samples in each of the two pools. 20 segregants per pool out of 379 phenotyped represents approximately top and bottom 5% of the population containing extreme phenotypes which is much lower than the 20% recommended by statistical modelling (Jawaid et al., 2002). Remarkably, even with the small sample size and fairly narrow range of phenotype difference between the two pools, variants of several known TLM genes were identified along with potential novel genes with TLM function. This demonstrates the high level of sensitivity of the i-QTL Multipool method in identifying gene variants which can no doubt be further heightened in future studies by increasing the sample size of the pools. The downside of the approach however is the very low LOD scores generated by Multipool which can be misleading despite the clear association between the gene variant and the phenotype based on differences of allele frequency. A more suitable statistical analysis might be binomial testing. At each location of maximum difference, Fisher's Exact test can be performed. However, it is likely the statistical significance would still be affected by the small sample size.

An alternative method of bioinformatics analysis can also be the use of R-QTL script (Broman et al., 2003) that can identify gene variants in multiple individual segregants that have been phenotyped and potentially generate a plot with more accurate LOD scores. However, the R-QTL method requires a large sample size of individual

segregants and consequently high cost of sequencing. In conclusion, bulk segregants analysis in pools using the i-QTL Multipool analysis is an efficient and cheap method of identifying QTLs with high sensitivity and resolution.

Chapter 6 Concluding Remarks and Future Perspectives

Telomere maintenance is essential for genome integrity and cell viability. In yeast, telomeres are maintained by telomerase and a network of more than 300 telomere length maintenance (TLM) genes (Ungar et al., 2009, Askree et al., 2004). Human somatic cells on the other hand lack telomerase resulting in progressive shortening of telomeres and eventually cell death. However, more than two decades ago, it was demonstrated that telomeres can be maintained by an alternative telomere-telomere recombination mechanism in the absence of telomerase in yeast (Teng and Zakian, 1999, Lundblad and Blackburn, 1993). Likewise in humans, the alternative lengthening of telomere (ALT) mechanism was described by the Reddel group in telomerase negative cancer cells (Bryan et al., 1995, Dunham et al., 2000). However, survival from recombination based telomere maintenance is rare in the absence of telomerase in both yeast and humans and is not a path opted for when telomerase is present. Nonetheless, other organisms such as lower dipterans, for example *Chironomus,* that lack functional telomerase maintain telomeres solely by homologous recombination (Lopez et al., 1996) while drosophila use telomeric retro-transposons to maintain receding chromosome ends (Biessmann and Mason, 1997). Therefore, while there are multiple mechanisms of maintaining telomeres, they are processes that are evolutionarily conserved across species in eukaryotes and important for cell survival and proliferation.

In addition to the TLM genes, environmental factors also regulate telomere length. For instance in humans, it has been found that smoking (Huzen et al., 2014) and heavy alcohol consumption cause telomere shortening (Shin and Baik, 2016). Likewise in yeast, environmental stress factors such as caffeine and heat lead to telomere shortening whereas alcohols and acetic acid lead to telomere lengthening (Romano et al., 2013). Hence, telomere length maintenance is a complex trait regulated by a combination of genetic and environmental determinants.

Past studies have identified numerous genes and mechanisms that have shed light into telomere regulation and maintenance processes, including ALT, in both humans (Cesare and Reddel, 2010) and yeast (Le et al., 1999). In this thesis, I have explored the role of initial telomere length and the timing of senescence in influencing telomere maintenance in the absence of telomerase in budding yeast *S. cerevisiae* along with attempting to identify novel gene variants that regulate telomere length in wild-type populations.

The study described in Chapter 3 demonstrated that initial telomere length greatly influences the frequency of survivors generated with longer initial telomeres leading to higher overall frequency of survivor formation and increased efficiency of recovery from crisis. One explanation would be an increase in the proportion of faster growing Type II survivors when longer telomeres are available. Surprisingly, knocking-out Type II essential genes (*SAE2, SGS1, RAD59* and *MRE11*) still led to significant increase in the frequency of survivor generation and an increase in the efficiency of recovery from crisis after telomere elongation. This suggested that the increase in frequency of survivor formation and efficiency of recovery from crisis after telomere lengthening was not solely dependent on increased frequency of Type II survivor formation. Nonetheless, longer telomeres do favour the Type II pathway as artificially shortening the initial telomere length led to a decline in the proportion of Type II survivors generated. Furthermore, artificial telomere lengthening increased the proportion of transient Type II and Type II-like survivors generated in the absence Type II essential gene *RAD59*. However, a similar increase was not observed in the absence of other Type II essential genes, *SAE2, SGS1 and MRE11*. This suggested that whilst longer telomeres promote the Type II survivor pathway, genes involved in the homologous recombination pathway are still essential for long term maintenance of survivors.

Based on these results, I propose a mechanism whereby longer telomeres favour the overall increase in frequency of survivors generated (both Type I and Type II) by providing a longer template for recombination. Furthermore, this overall increase in the frequency of survivors generated is biased to favour the Type II pathway when telomeres are longer. This could be due to internal cellular processes for telomere length maintenance such as TRD (Bechard et al., 2011) that can potentially generate higher numbers of t-circles in the presence of longer telomeres which may subsequently be used as substrate for Type II rolling circle replication. Finally, although initial telomere length is undoubtedly an important factor for cell survival in the absence of telomerase, particularly in generating Type II survivors, it could not be established they supersede the requirement of homologous recombination proteins for long term maintenance of the Type II survivors.

Chapter 4 examined the timing of senescence in a cell population in relation to survivor type formation. The study showed that early senescence led to an increase in the

proportion of Type II survivors in a cell population. Remarkably, contrary to past assumptions, it was found that the increase in Type II survivors arising from early senescence was independent of the initial telomere length. This raises interest in the potential mechanisms that might be at action. One likely mechanism is that early senescence induced from a single short telomere favours Type II survivor formation via clustering of telomeres that allows localisation of recombination proteins for efficient telomere-telomere recombination.

Formation of telomere clusters at the nuclear periphery has been described previously in yeast with eroding telomeres and has shown to promote Type II survivor formation (Churikov et al., 2016). In fact, is has been well established in mammalian ALT cells that telomeres are present in clusters called APBs (ALT associated PML bodies) along with many homologous recombination proteins (*RAD51, RAD52, RPA, NBS1, SLX4, BLM, MRN, BRCA1* and *BRIT1*) that most likely enables telomere-telomere recombination and lengthening characteristic of ALT cells (Pickett and Reddel, 2015, Cesare and Reddel, 2010). Furthermore, when DSBs are induced at telomeres, there is long range mobility of telomeres themselves in search for donor telomeres for recombination along with increased clustering of telomeres (Cho et al., 2014). Hence, it is likely early senescence leads to efficient telomere-telomere recombination within the existing telomere clusters in yeast whereas in the case of late senescence the telomeres are likely to need re-clustering prior to engaging in recombination making the process of generating survivors comparatively less efficient.

Another possible mechanism that can promote the Type II survivor pathway in case of early senescence can be higher levels of t-circle generation as a by-product of recruitment of recombination proteins to the telomere cluster, enabling rolling circle replication leading to Type II telomere maintenance. Likewise, a third possible mechanism can be increased levels of TERRA (Telomeric Repeat containing RNA) when early senescence is induced (Cusanelli et al., 2013) leading to efficient Type II survivor formation.

Our data here along with increasing evidence from new studies suggest there is more to survivor formation than the known genetic requirements (LeBel et al., 2009, Chang et al., 2011, Grandin and Charbonneau, 2003). Understanding the role of initial telomere length and timing of senescence in telomerase negative telomere maintenance is crucial not just for yeast biology, but also for understanding ALT in human cancer cells. Moreover, if

initial telomere length influences ALT likelihood in human cancer cells as it does in yeast, it could be a potential target for drug therapy. It is known in humans that certain tissues such as those of mesenchymal origin are more prone to ALT positive cancers (Heaphy et al., 2011). One possibility in the origin of such differences between tissues can be the heterogeneity of telomere lengths at senescence. Likewise, it is known that replicative senescence from telomere erosion in mouse (Hemann et al., 2001) and yeast (Abdallah et al., 2009) occurs from the shortest telomere present in the cells. The length of the shortest telomere is likely to vary between individuals and could potentially be a cause for differences in the likelihood and onset of cancer and other disease.

Telomere length regulation in yeast and humans alike is a complex process under genetic and environmental control and regulates various cellular processes such as ageing and genome stability. Furthermore, age-related diseases are increasingly associated with telomere length. Short telomeres have been shown to be associated with diabetes (Tamura et al., 2016), neurodegeneration (Forero et al., 2016) and cardiovascular disease in humans (Chen et al., 2014, Codd et al., 2013) and in predicting early mortality in birds (Barrett et al., 2013). Furthermore, centenarian studies have found longer telomere lengths to be associated with healthy ageing (Terry et al., 2008). Hence, understanding telomere length regulation could potentially work towards finding ways to treat associated diseases, especially in the elderly population with shorter telomeres. Therefore, one of the aims of this study was to explore genetic variants of the TLM pathway in natural populations of *S. cerevisiae* in an attempt to elucidate the complex mechanism of telomere length regulation.

In chapter 5, several major segregating sites associated with the telomere length phenotype were identified after conducting i-QTL Multipool analysis on pooled segregants generated from advanced inter-crossed lines of two *S. cerevisiae* parents. *EST2* and *STN1*, were identified as major QTLs affecting telomere length maintenance whereby each parental allele had multiple substitutions in their amino acid sequence leading to functional variations. In addition to the known TLM candidate genes, several peaks were identified with no known TLM gene within the interval range. This indicated possible identification of novel gene variants with previously unknown TLM function. Future work will include validating the causal gene using reciprocal hemizygosity tests (Steinmetz et al., 2002) and testing for epistatic interactions. In addition, changes in

protein structure of causal genes can be determined to predict possible functional changes. Overall, this study has highlighted the power of i-QTL Multipool method in identifying novel variants even with a small sample size and relatively obscure phenotype.

Having already characterized the telomere lengths of 379 F12 (WE x NA) segregants, future studies can also explore additional factors associated with telomere length regulation, such as environmental stress. In this thesis, I have used ethanol and caffeine as environmental stress factors that artificially alter telomere lengths predominantly via the Rap1/Rif1 pathway (Romano et al., 2013). Other such stress factors include heat, acetic acid and alcohols such as methanol (Romano et al., 2013). A question worth asking is to what extent these environmental stress factors influence telomere lengths based on the genetic background of the F12 segregants. In other words, it can help identify whether certain genetic backgrounds are resistant to environmental influence on telomere shortening or lengthening. Likewise, it can also address whether genetic pre-disposition to short telomeres can be overcome by exposure to certain environmental stress factors. In wider context, this can potentially help find ways to avoid or overcome detrimental telomere shortening with age that increases susceptibility to diseases.

Likewise, another area for future study can be investigation of variability in the timing of senescence with relation to initial telomere length and genetic background. As we have seen in this study, timing of senescence is positively correlated with initial telomere length, more specifically with the shortest telomere available, and is an important factor that influences survivor formation in telomerase negative cells. However, in addition to the initial telomere length, the timing of senescence is also influenced by the genetic background of the cell itself (Enomoto et al., 2002, Joseph et al., 2010). Hence, QTL analysis can be conducted using the F12 segregants to examine genetic variants and subsequently the molecular pathways that lead to early senescence. Furthermore, downstream consequences of early senescence on survivor type proportion can also be examined. Overall, the use of i-QTL analysis using the F12 segregants can help examine the gene-environment interactions that regulate telomere length and its subsequent downstream consequences on timing of senescence and survivor type formation.

Chapter 7 Appendix

All of the southern blots below were developed using TG_{1-3} specific probe pRED571. Telomere restriction fragments (TRFs) of survivors were examined after restriction digestion of their genome with Y' specific *XhoI* enzyme. TRF's of UOS1 strains were obtained after restriction digest with *SpeI*.

7.1 Southern blots examining survivor type proportions in telomerase negative W303 strain (YUD610.1).

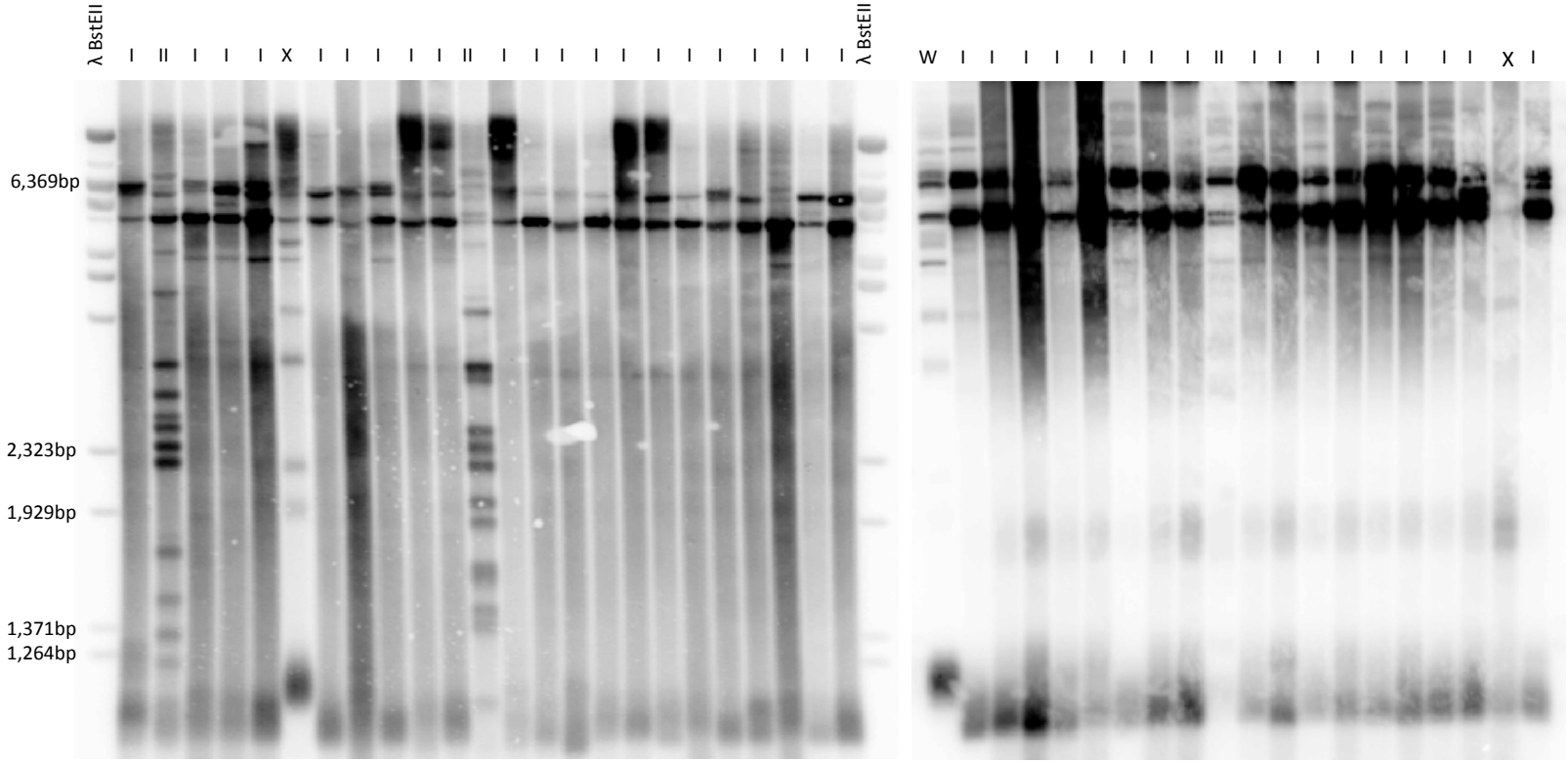

W = Wild-type (telomerase +ve), I = Type I survivors, II = Type II survivors, X = Non-survivor/ambiguous

7.2 Southern blot examining survivor proportions in telomerase negative W303 strain (YUD610.1) after 5% ethanol pre-treatment.

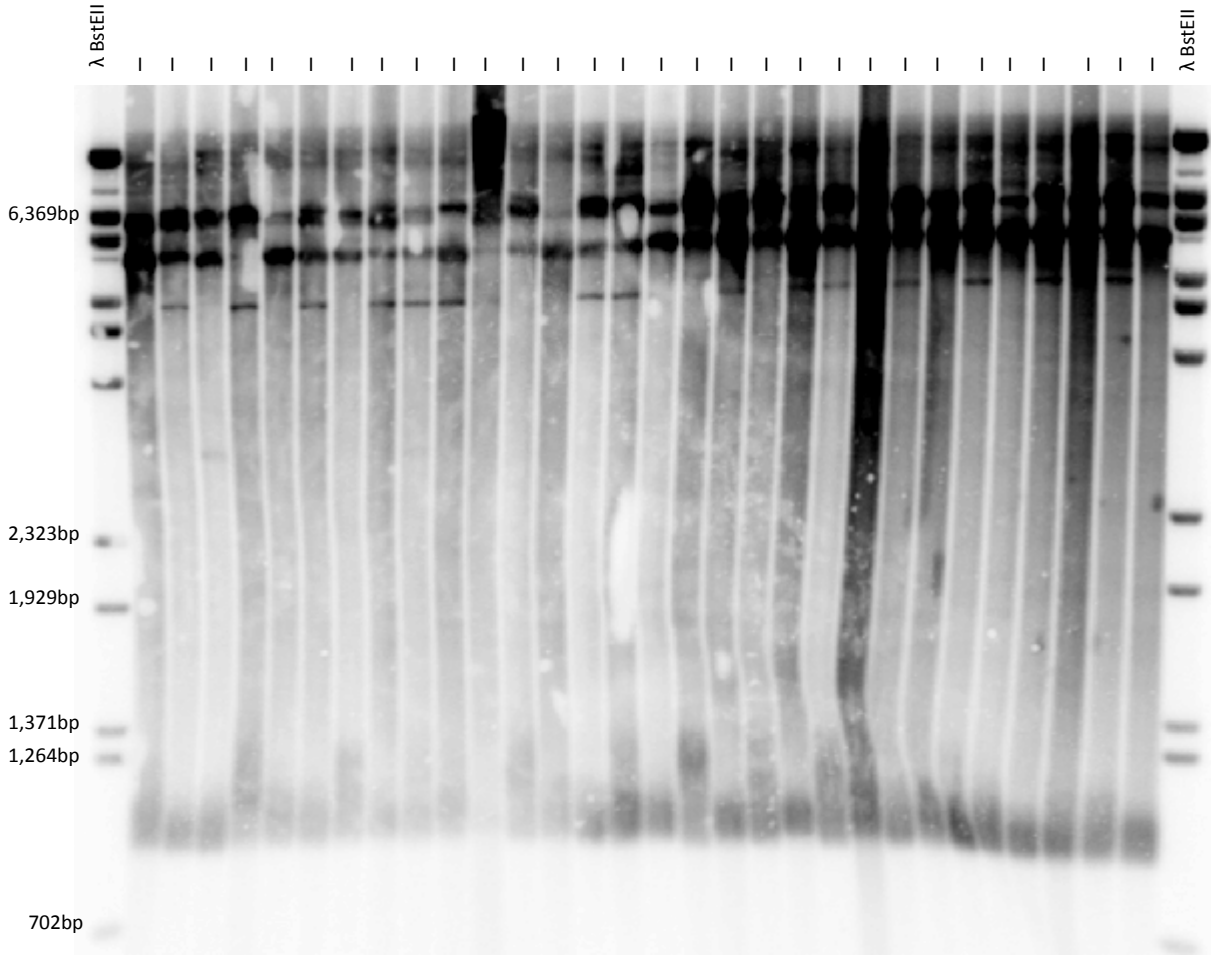

I = Type I survivors

7.3 Southern blots examining survivor proportions in telomerase negative Y55 strain (3466) before and after ethanol pre-treatment.

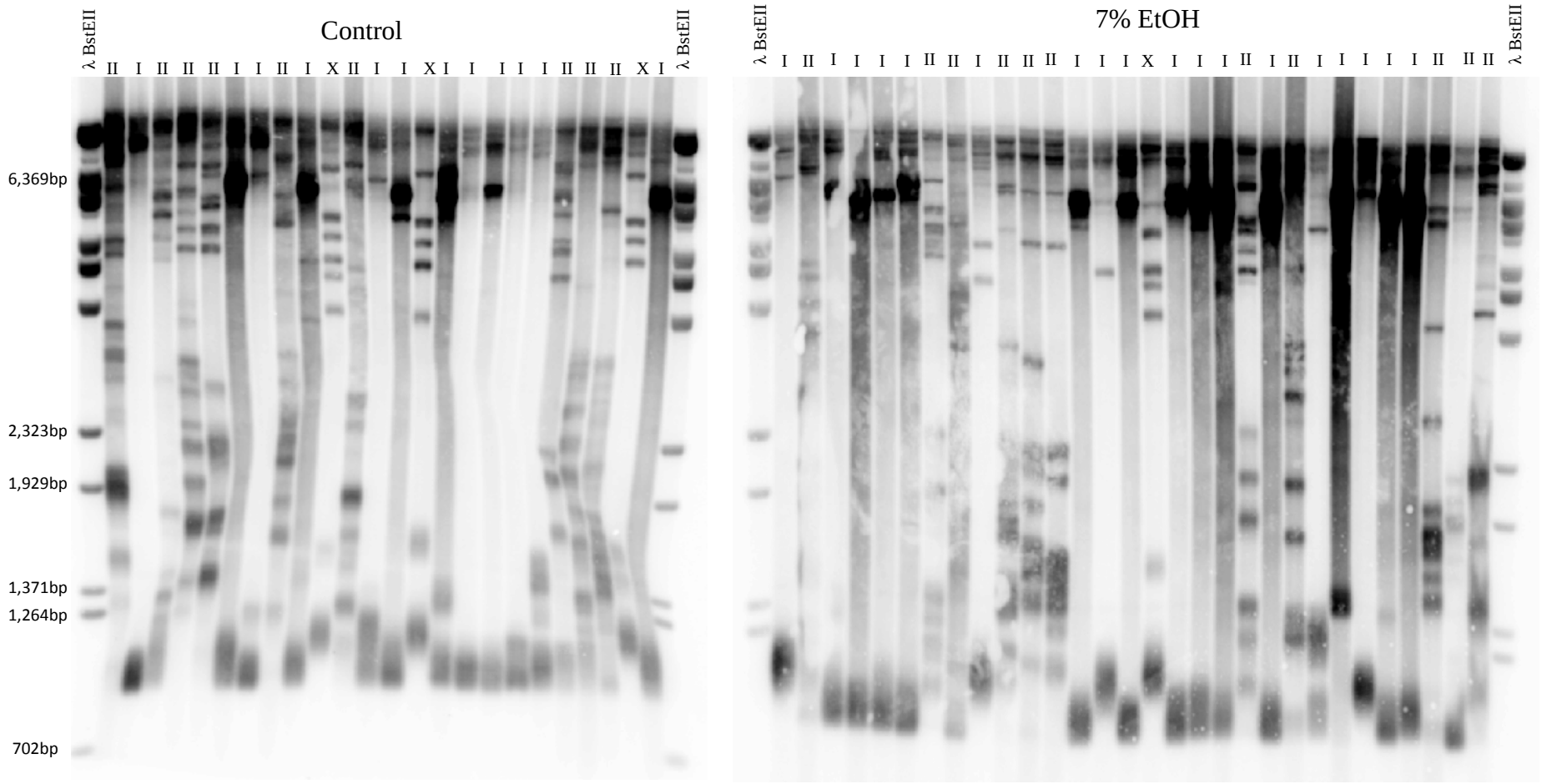

I = Type I survivors, II = Type II survivors, X = Non-survivor

7.4 Southern blots examining survivor proportions in telomerase negative Y55 strain (3466) after 12mM caffeine pre-treatment.

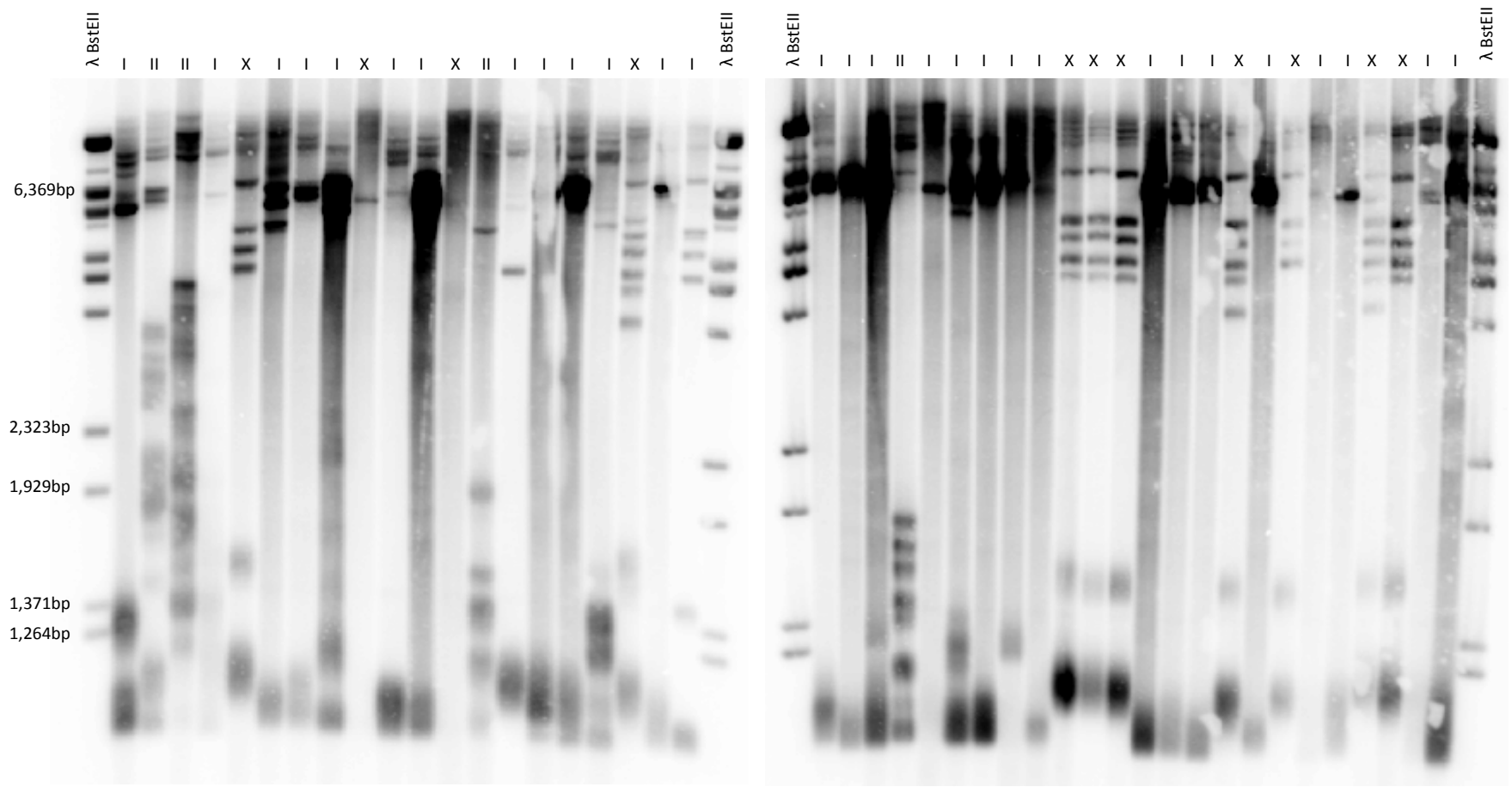

I = Type I survivors, II = Type II survivors, X = Non-survivors/ ambiguous

7.5 Southern blots examining survivor proportions in telomerase negative S288c strain (SUA02).

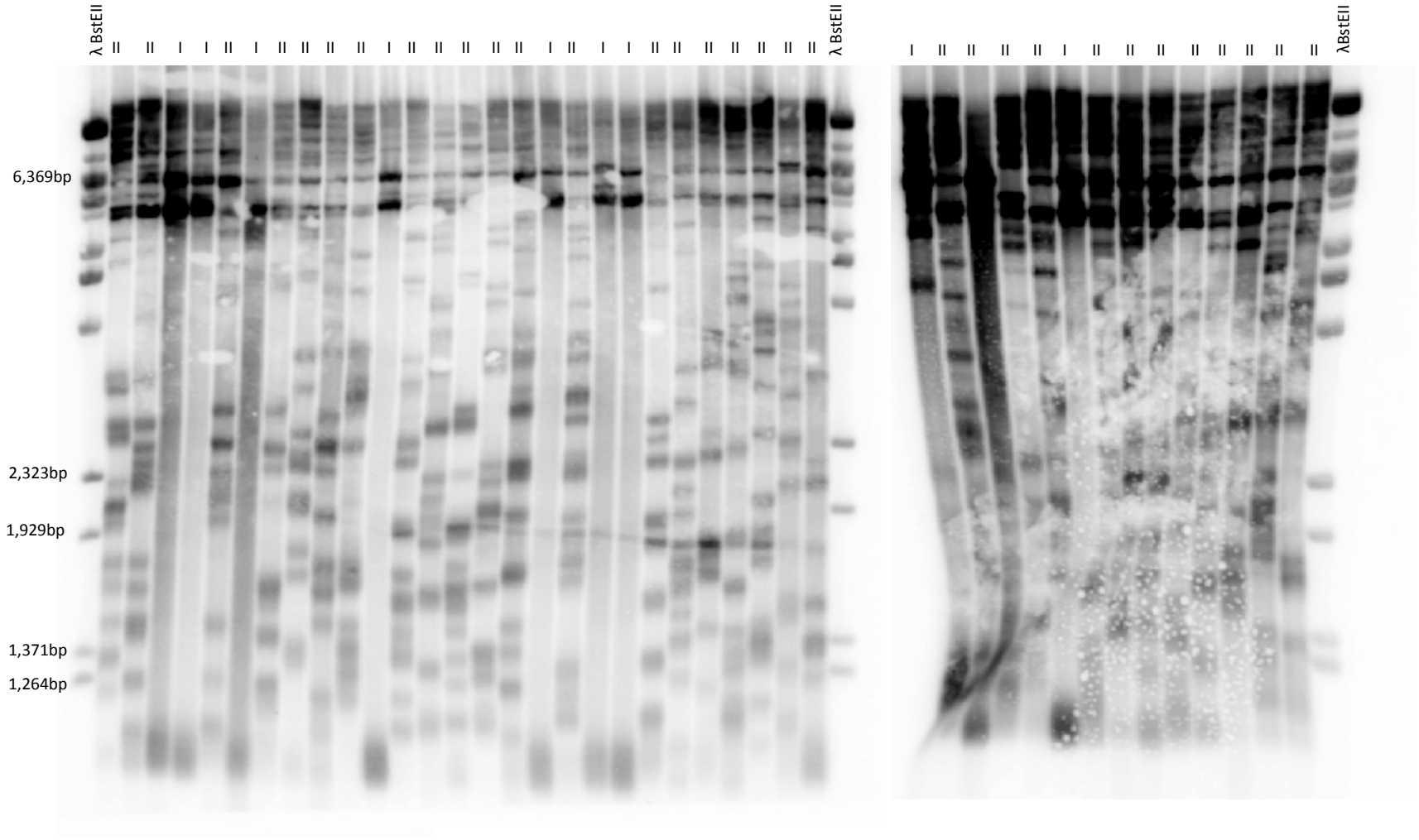

I = Type I survivors, II = Type II survivors

7.6 Southern blot examining survivor proportions in telomerase negative control strain S288c (SUA02) after 12mM caffeine pre-treatment.

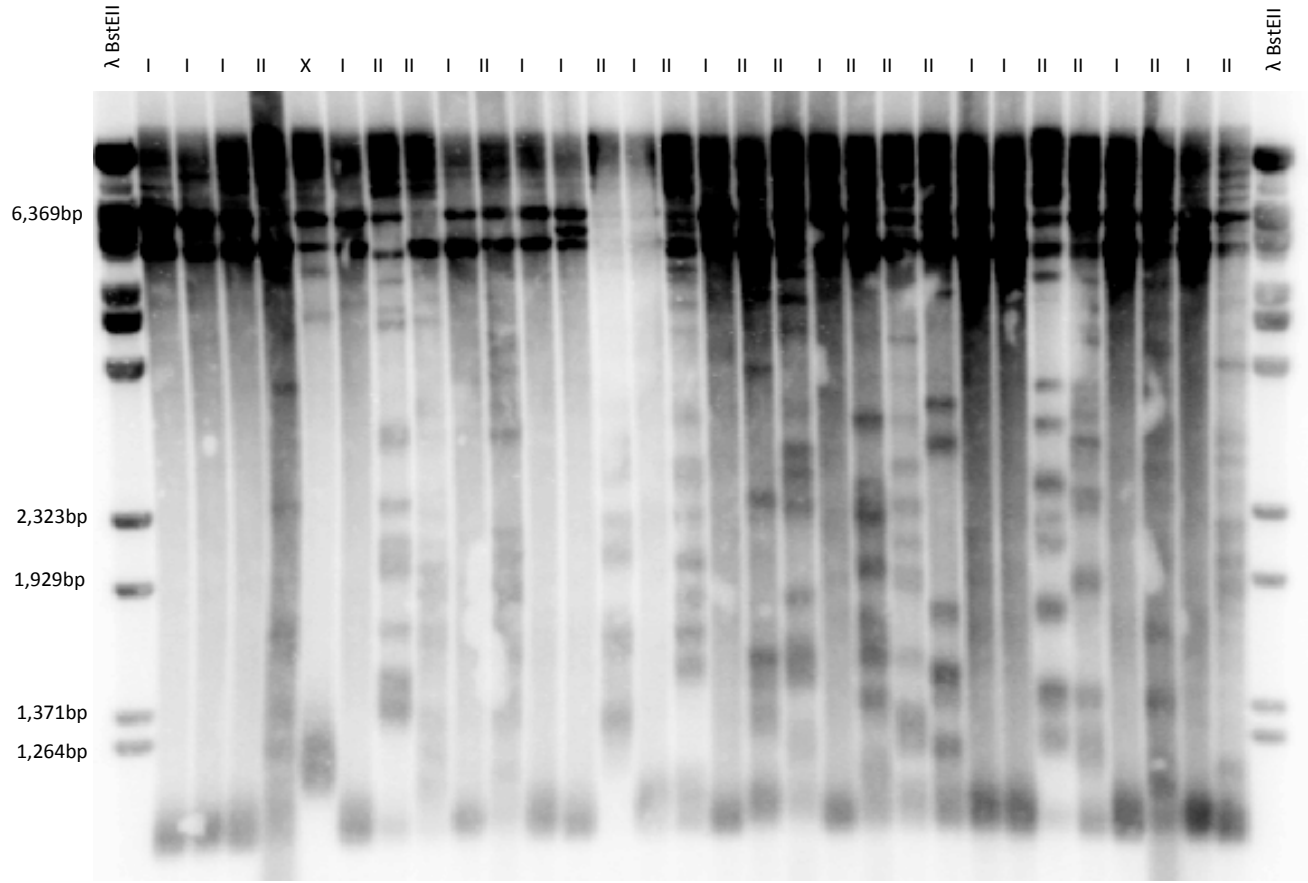

I = Type I survivors, II = Type II survivors, X = Non-survivor

7.7 Southern blot examining survivor proportions in telomerase negative double knockout 3466.1 (*est2Δsae2Δ*) before and after ethanol pre-treatment

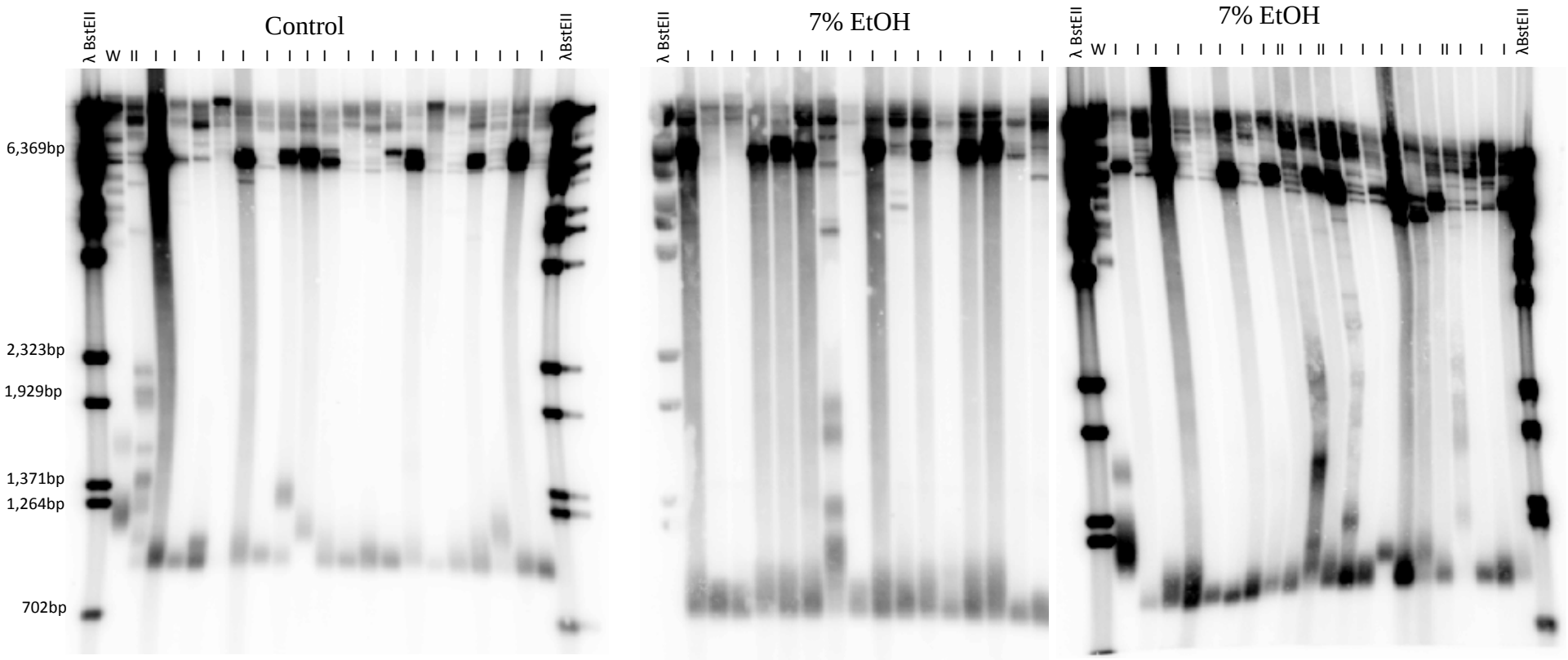

W = Wild-type (telomerase +ve), I = Type I survivors, II = Type II survivors

7.8 Southern blot examining survivor proportions in telomerase negative double knockout 3466.2 (*est2Δsgs1Δ*) before and after ethanol pre-treatment.

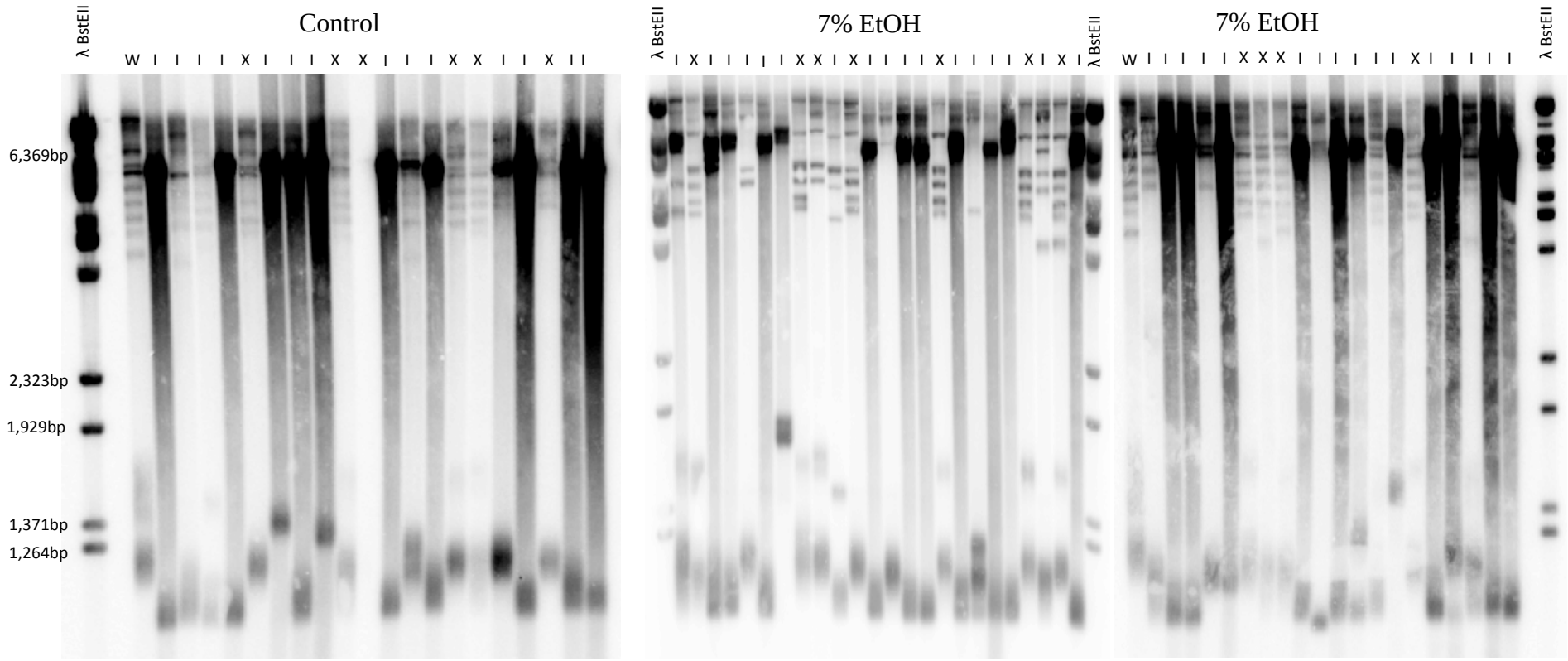

W = Wild-type (telomerase +ve) , I = Type I survivors, II = Type II survivors, X = Non-survivors

7.9 Southern blot examining survivor proportions in telomerase negative double knockout 3466.3 (*est2Δrad59Δ*) control.

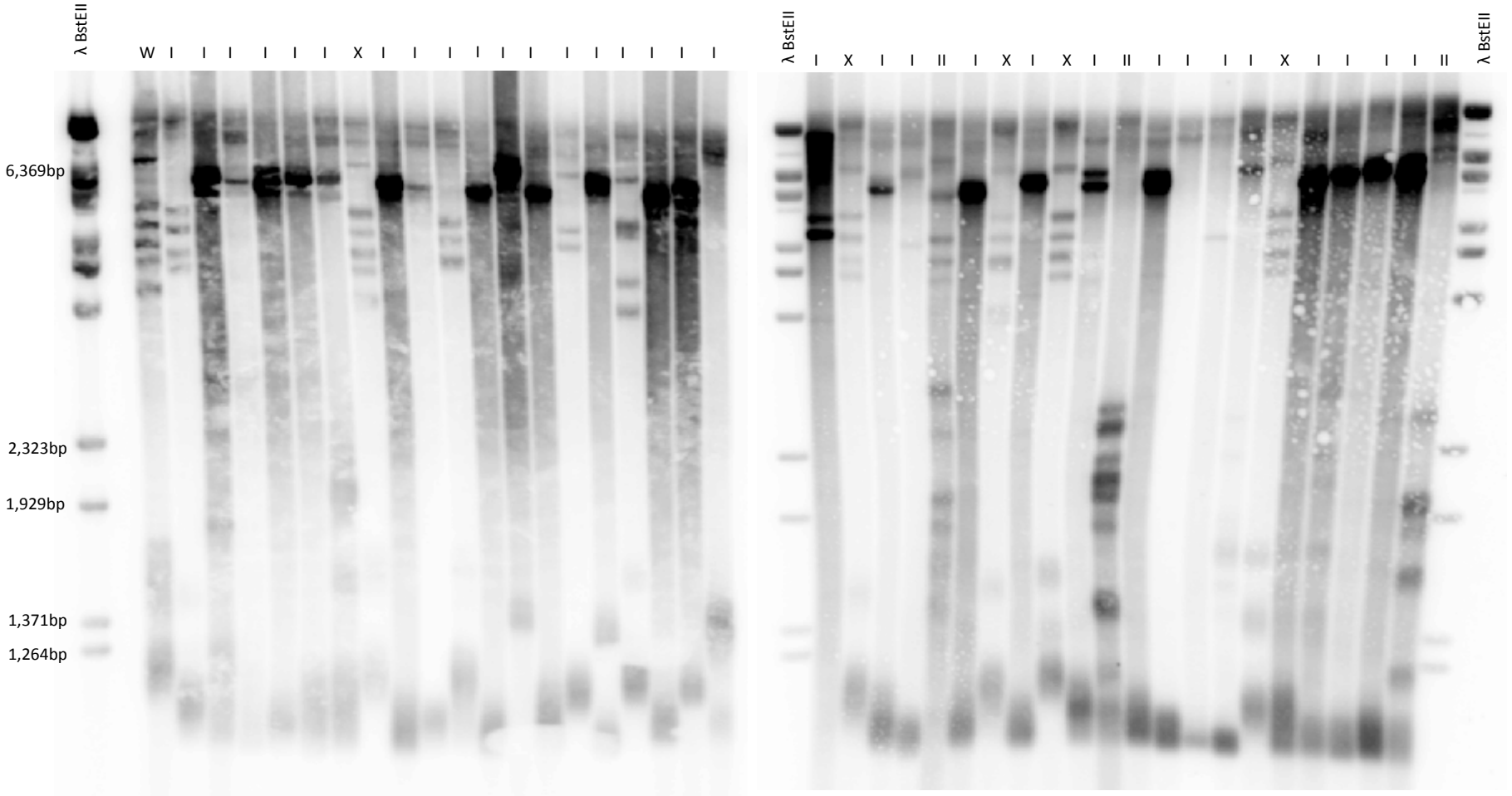

W = Wild-type (telomerase +ve) , I = Type I survivors, II = Type II survivors, X = Non-survivors

7.10 Southern blot examining survivor proportions in telomerase negative double knockout 3466.3 (*est2Δrad59Δ*) after 7% ethanol pre-treatment.

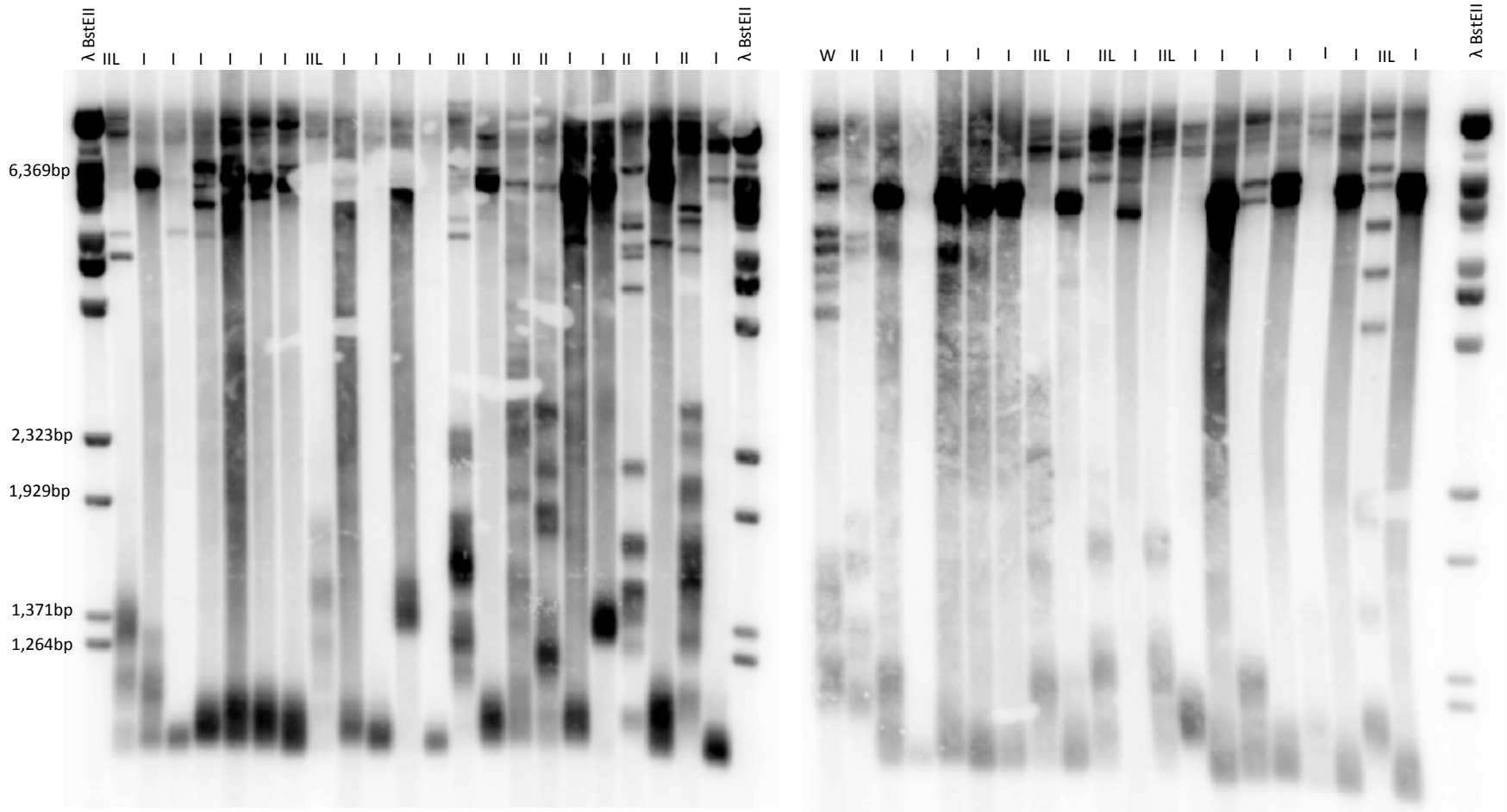

W = Wild-type (telomerase +ve), I = Type I survivors, II = Type II survivors, IIL = Type II like survivors

7.11 Southern blot examining survivor proportions in telomerase negative double knockout 3466.3 (*est2Δmre11Δ*) before and after 7% ethanol pre-treatment.

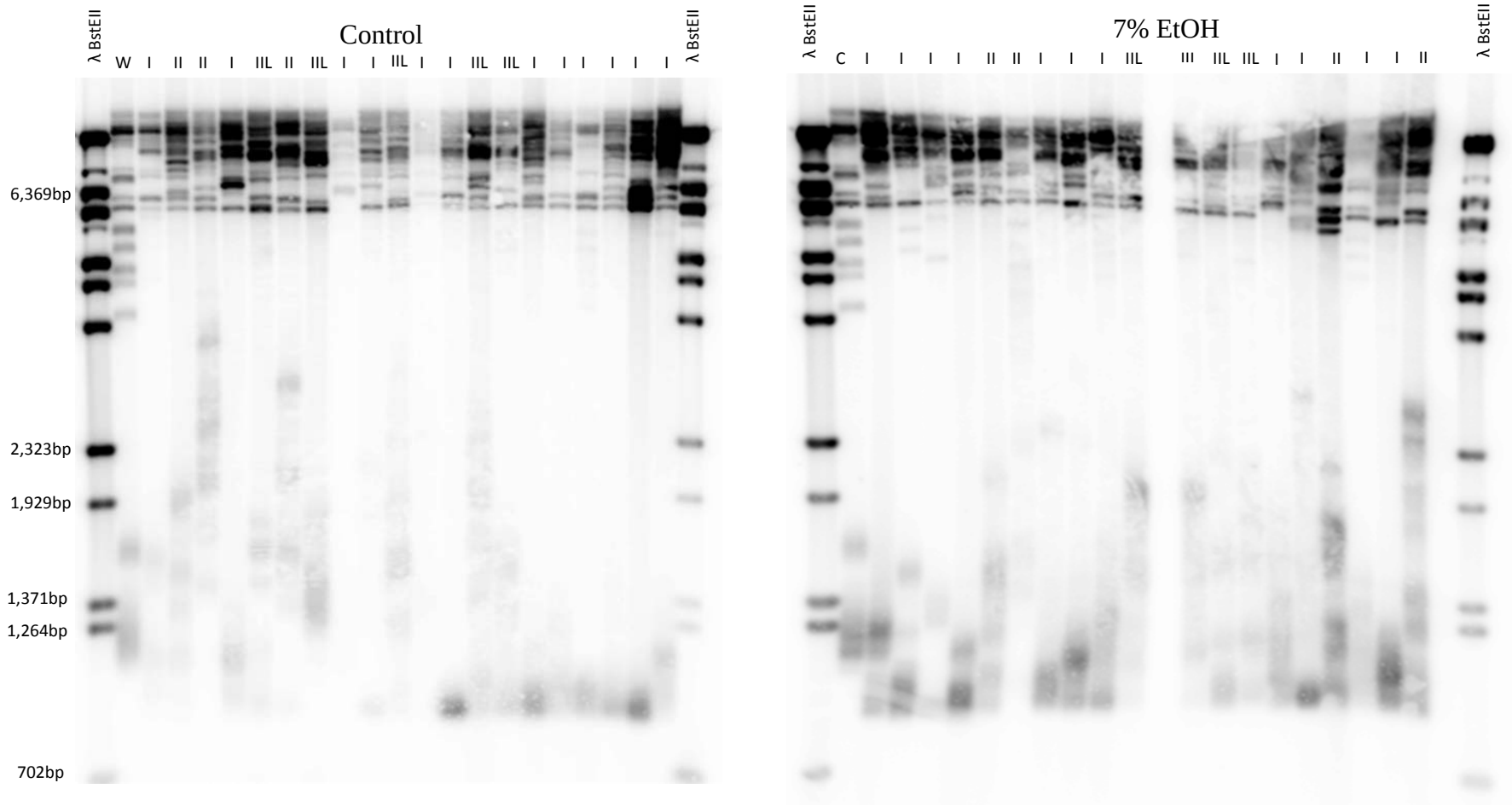

W = Wild-type (telomerase +ve), I = Type I survivors, II = Type II survivors, IIL = Type II-like

7.12 Southern blot examining survivor proportions in telomerase negative YUD892.1 cells (Construct Intact)

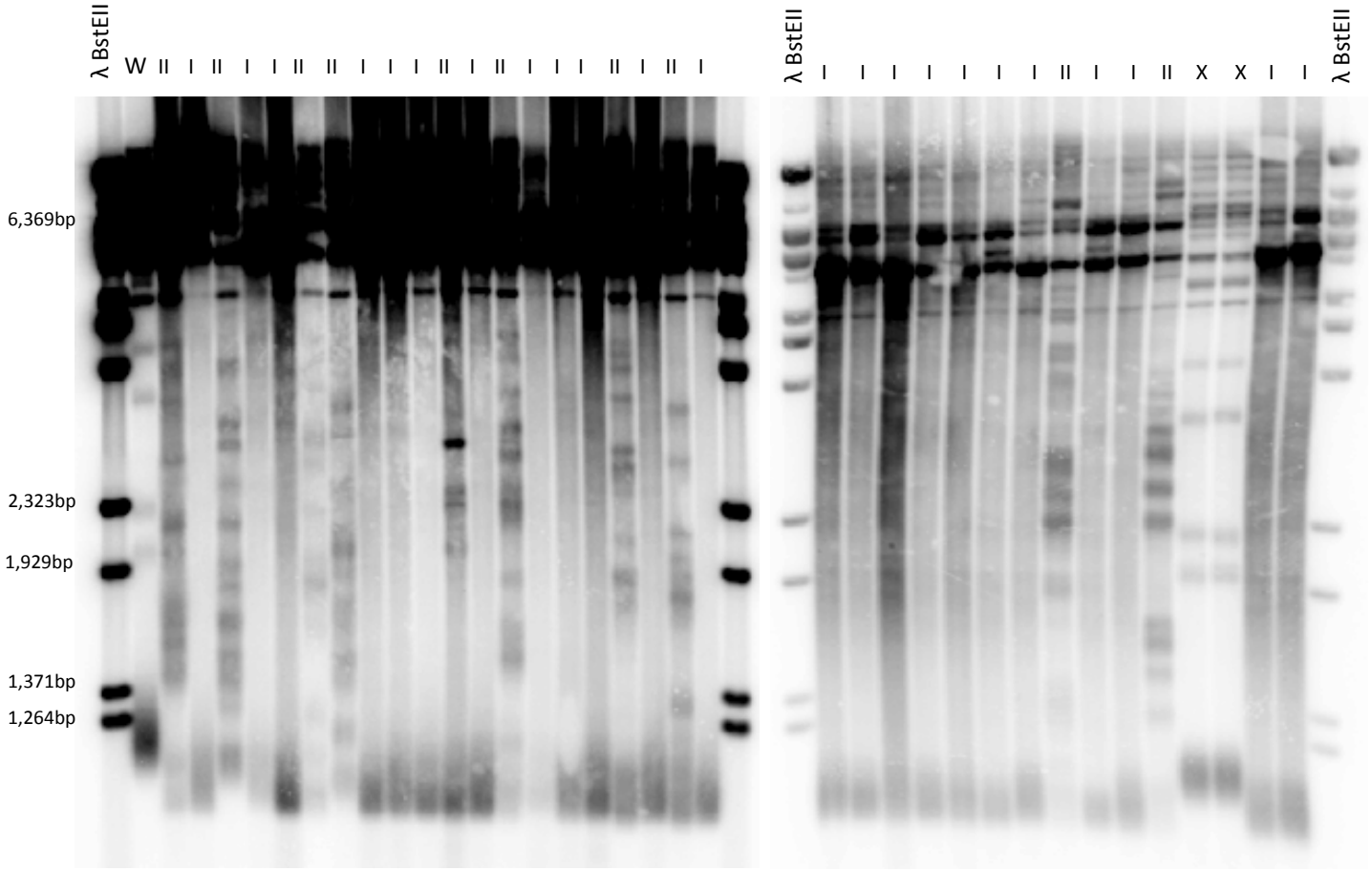

W = Wild-type (telomerase +ve), I = Type I survivors, II = Type II survivors, X = Non-survivors

7.13 Southern blot examining survivor proportions in telomerase negative YUD892.1 cells (Construct Flipped)

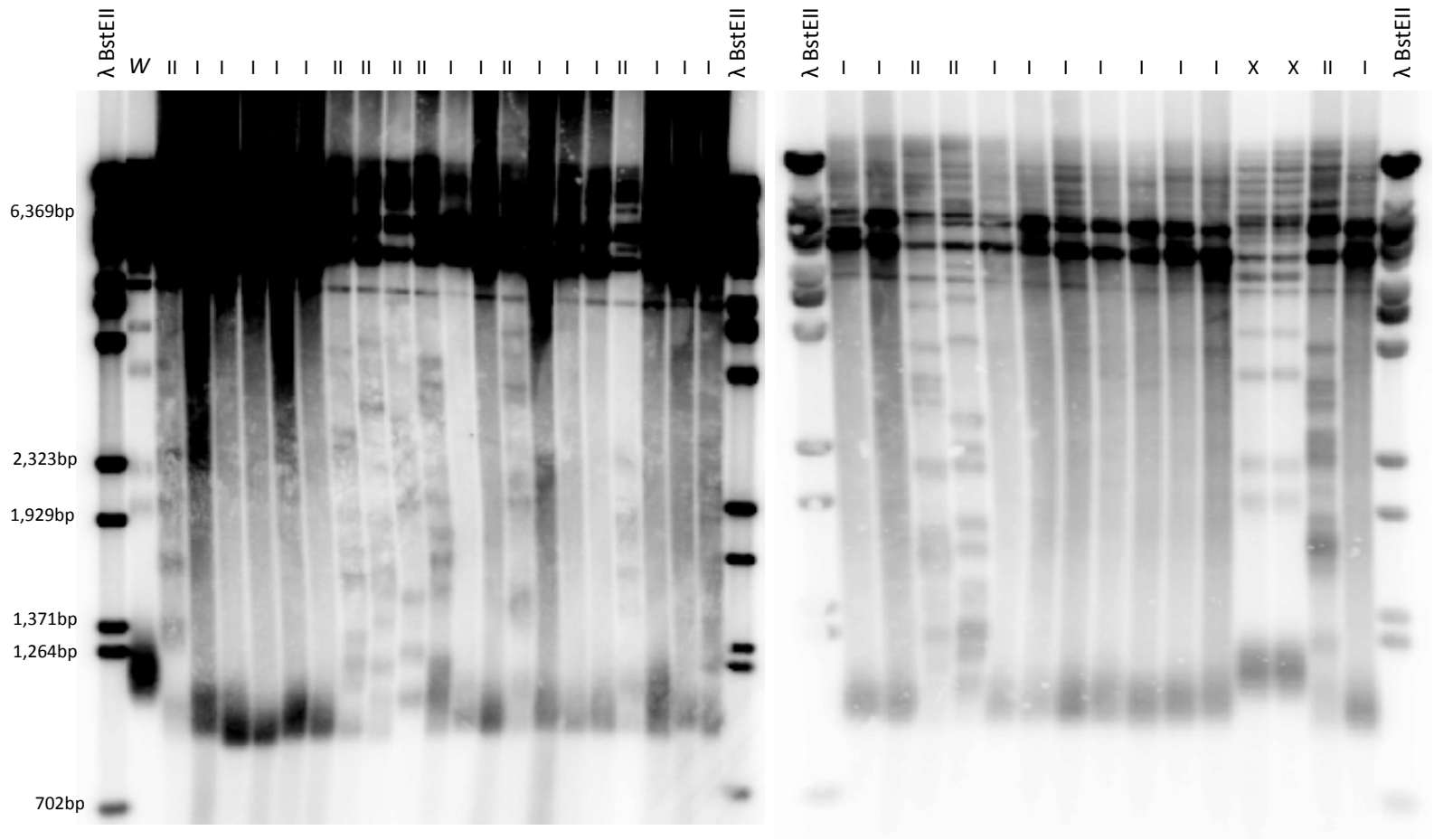

W = Wild-type (telomerase +ve), I = Type I survivors, II = Type II survivors, X = Non-survivors

7.14 Southern blot examining survivor proportions in telomerase negative YUD892.1 cells after 5% ethanol pre-treatment

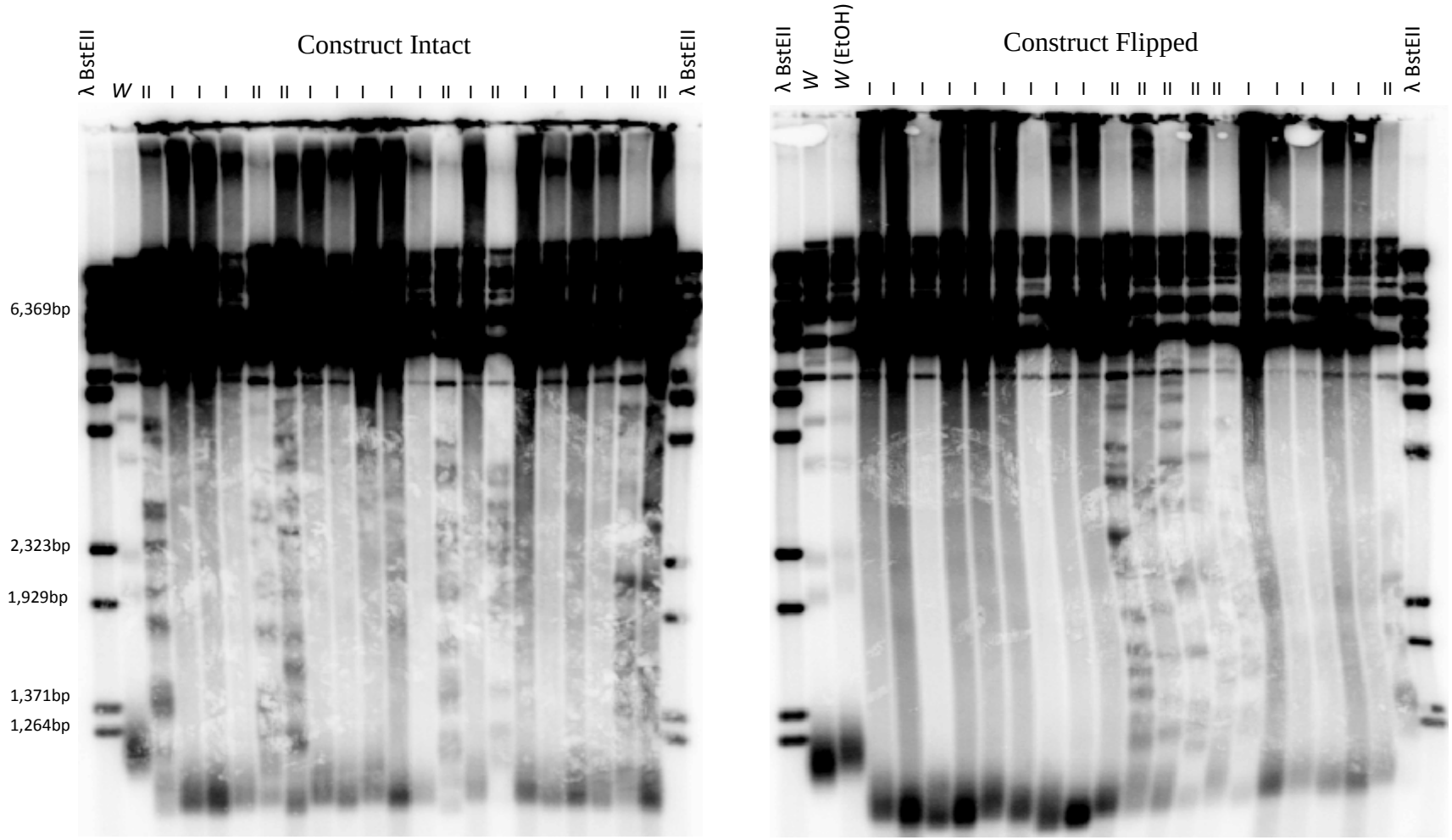

W = Wild-type (telomerase +ve), I = Type I survivors, II = Type II survivors

7.15 Southern blot examining survivor proportions in telomerase negative YUD892.1 cells (Construct Intact) after 4mM caffeine pre-treatment.

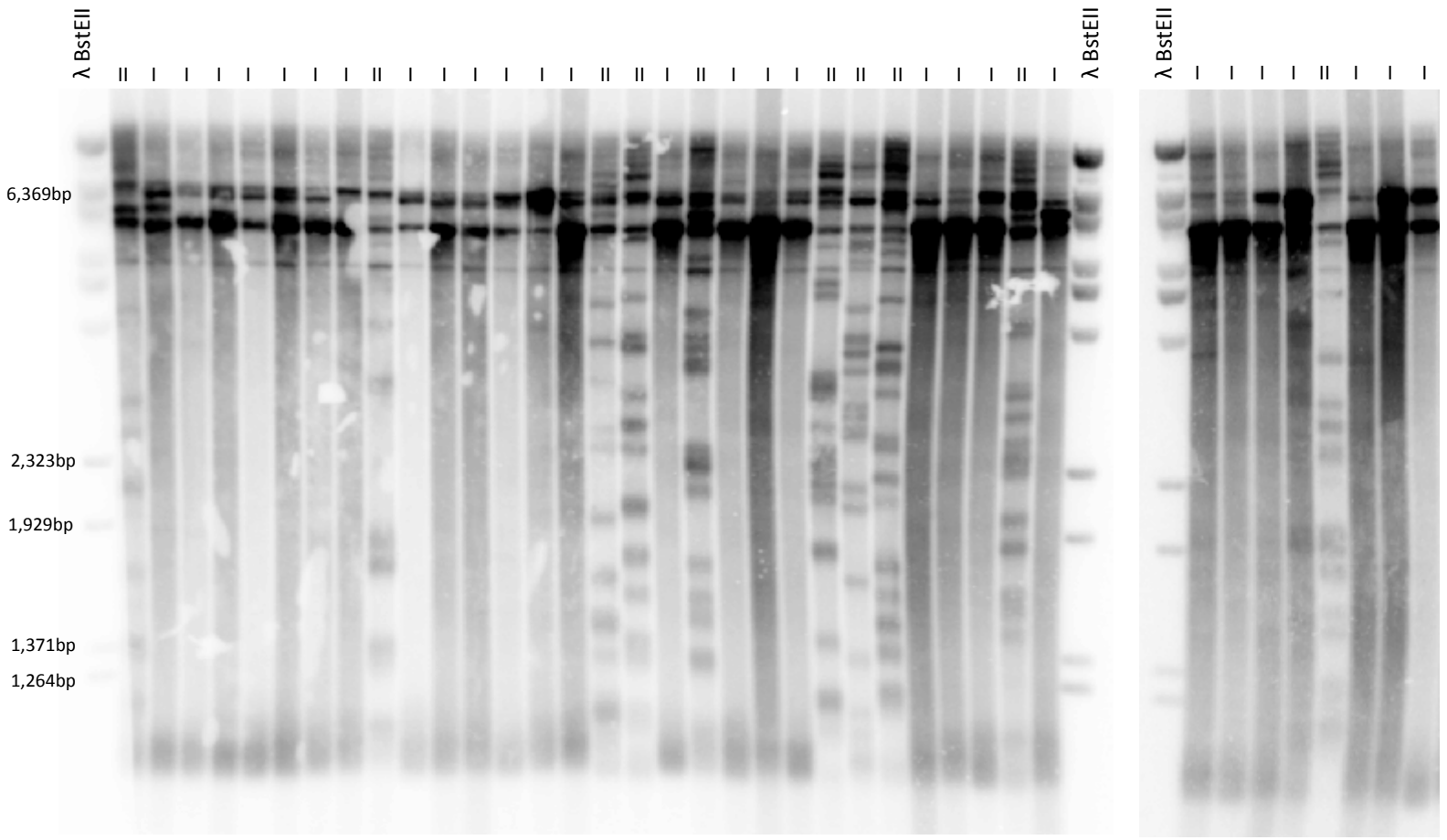

I = Type I survivors, II = Type II survivors

7.16 Southern blot examining survivor proportions in telomerase negative YUD892.1 cells (Construct Flipped) after 4mM caffeine pre-treatment.

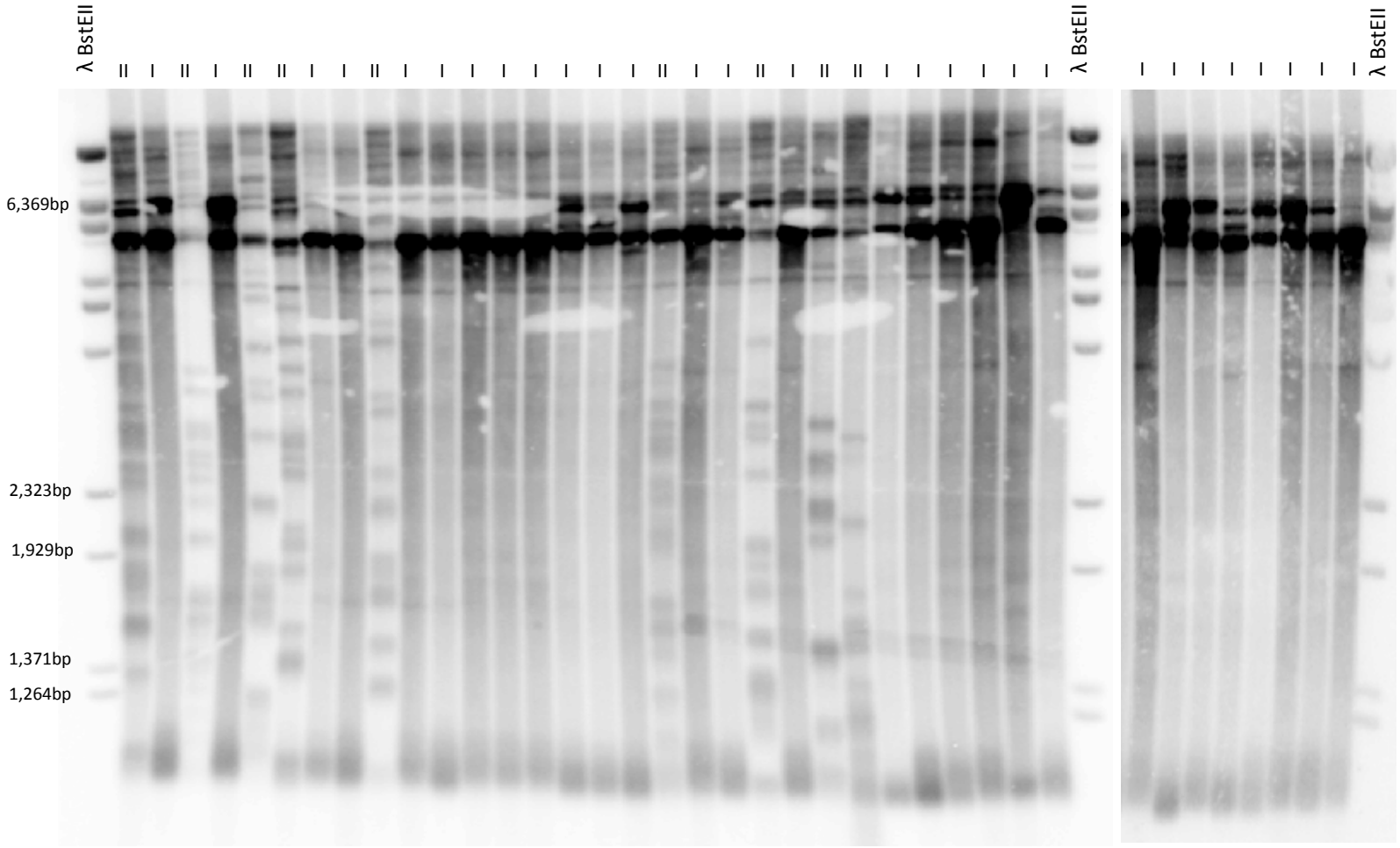

I = Type I survivors, II = Type II survivors

7.17 Southern blot examining survivor proportions in telomerase negative YUD131.1 cells (Construct Flipped after 25 and 50 cell cycles).

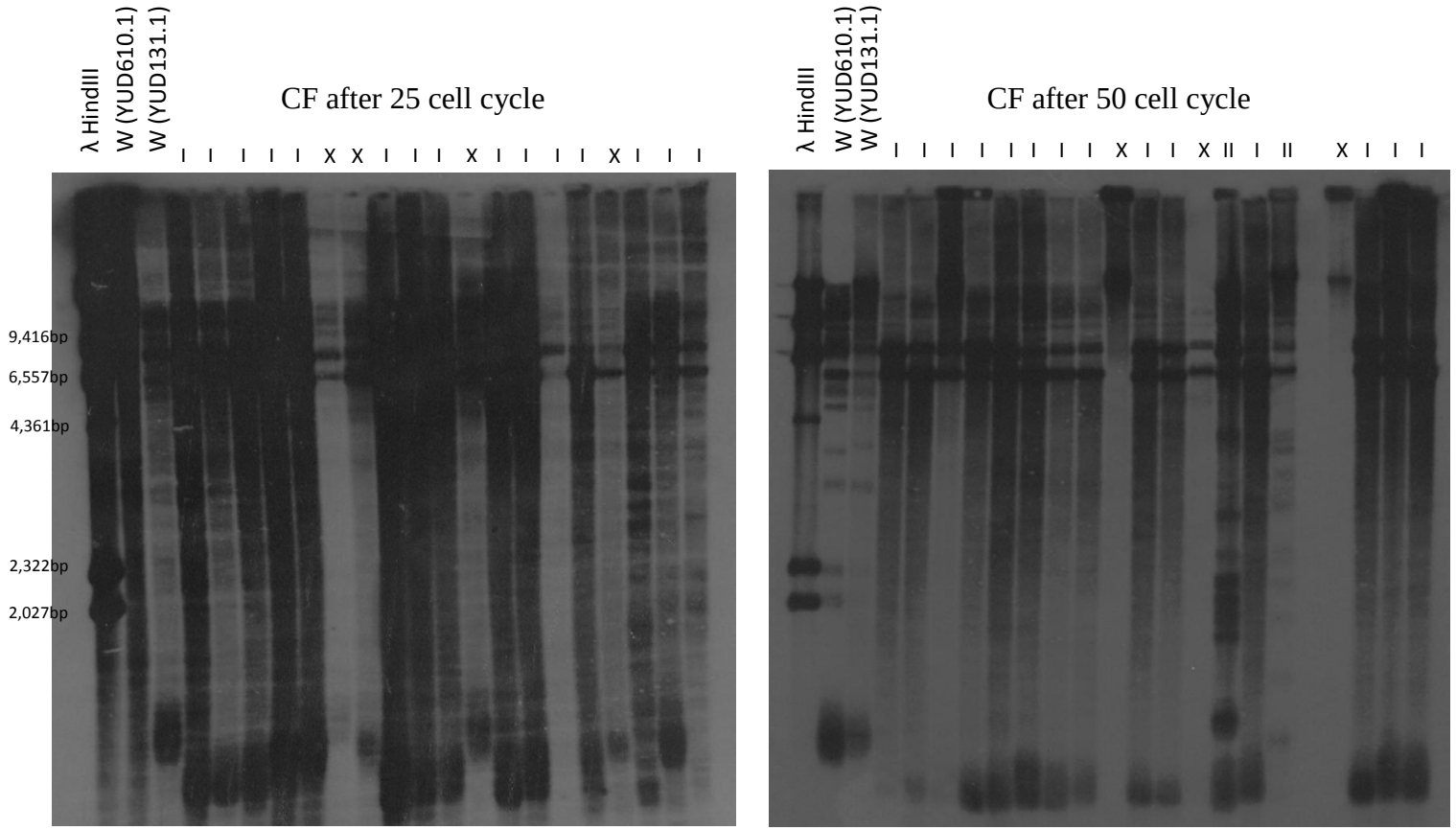

W = Wild-type (telomerase +ve), I = Type I survivors, II = Type II survivors, X = Non-survivors/ ambiguous

7.18 Southern blot examining survivor proportions in telomerase negative YUD131.1 cells (Construct Flipped after 75 cell cycles).

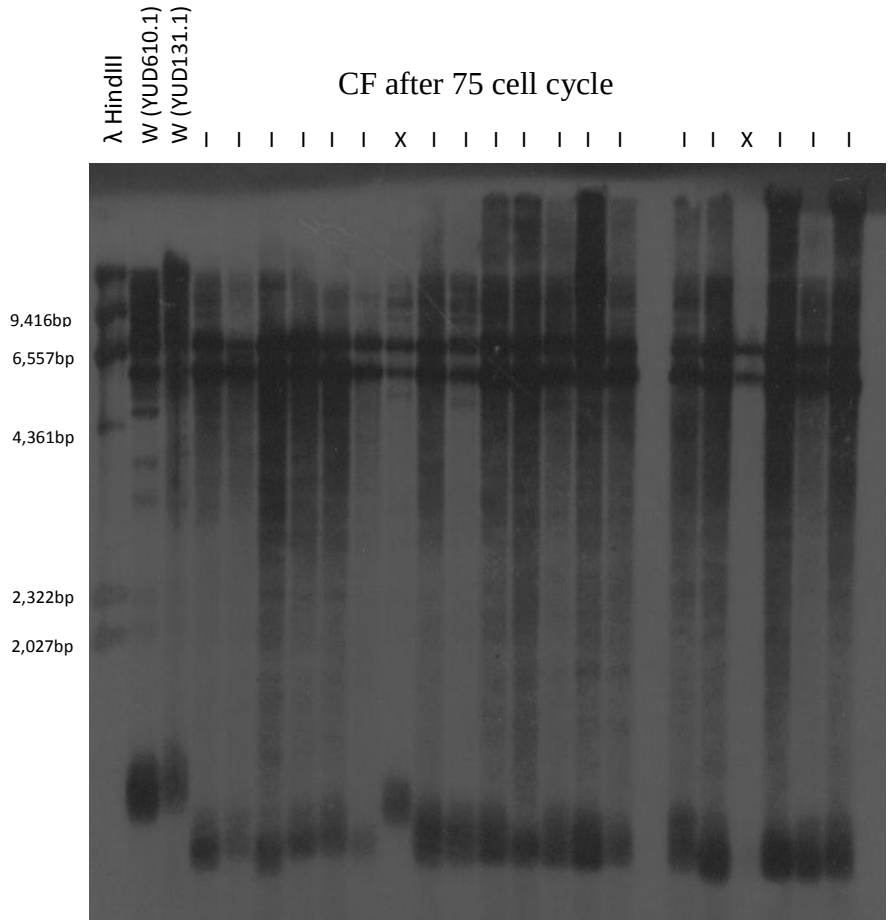

W = Wild-type (telomerase +ve), I = Type I survivors, II = Type II survivors, X = Non-survivors/ambiguous

7.19 Southern blot examining TRF of UOS1 F12 progeny (first 90 segregants: 101-206).

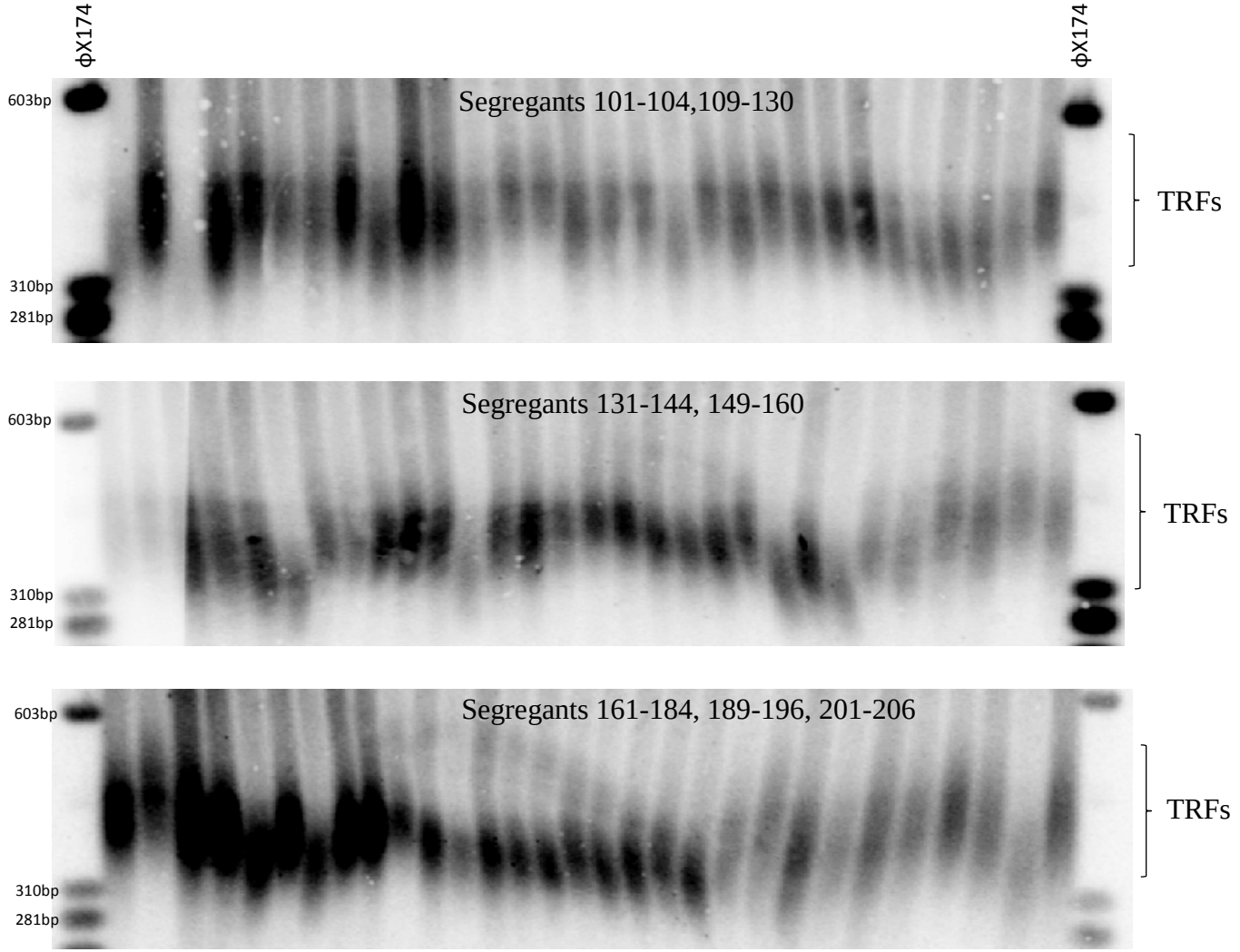

7.20 Southern blot examining TRF of 25 UOS1 F12 progeny shortlisted for the ‘Long’ telomere pool (from 379 segregants).

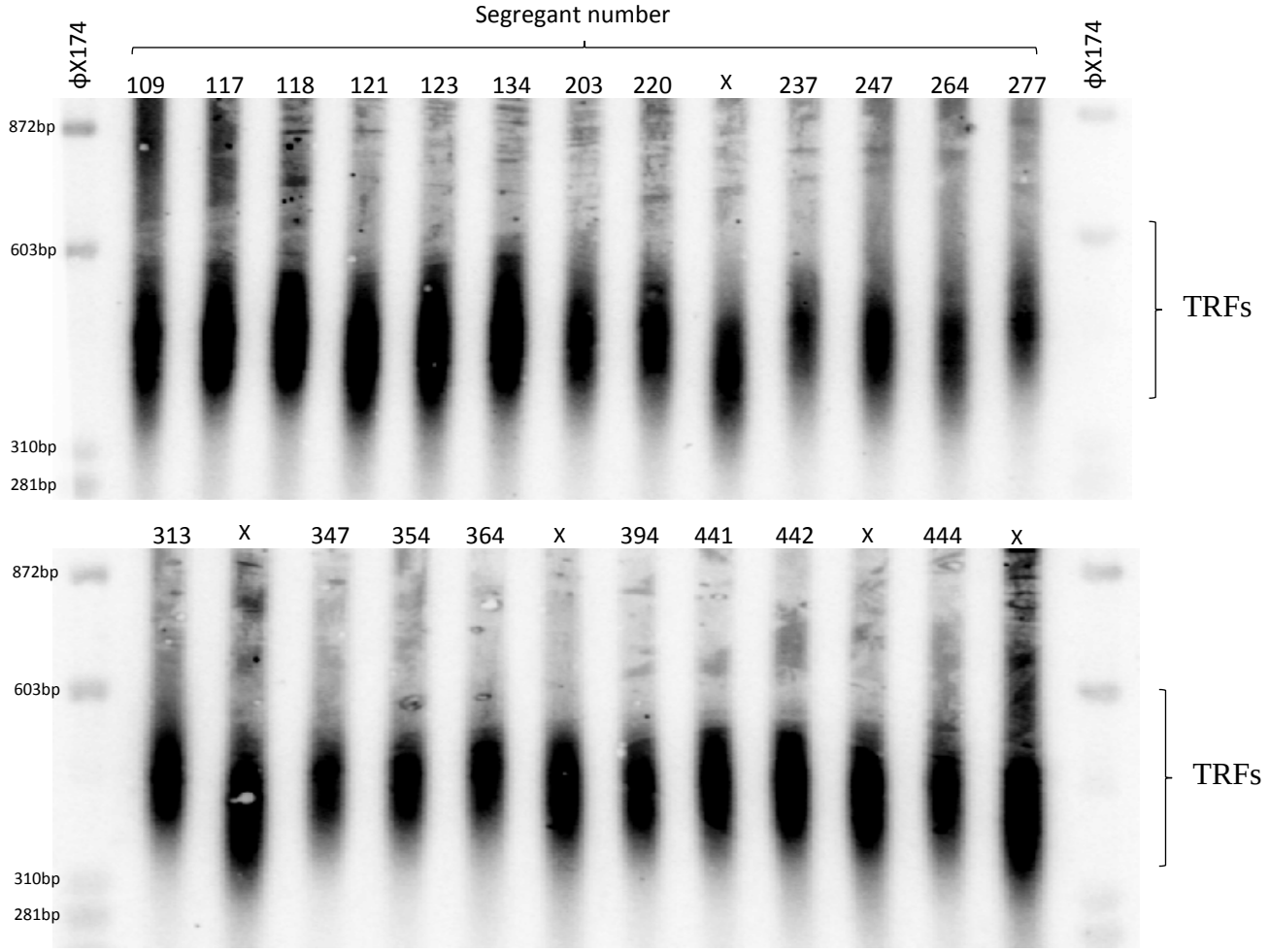

X = segregants not selected for the final long telomere pool

7.21 Southern blot examining TRF of 33 UOS1 F12 progeny shortlisted for the ‘Short’ telomere pool (from 379 segregants).

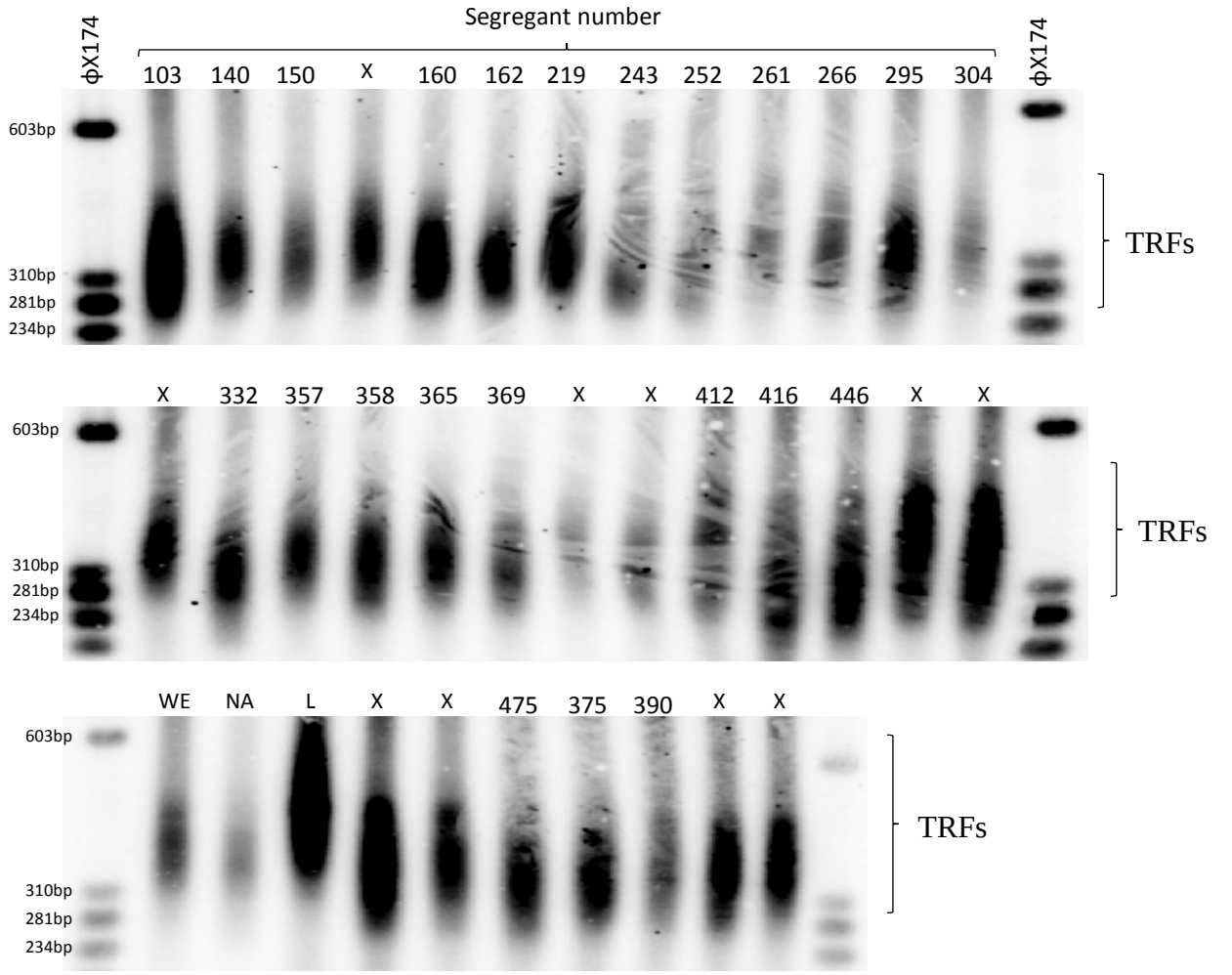

X = segregants not selected for the final short telomere pool

WE = Wine European parent, NA = North American Parent

L = A segregant from the long telomere pool

7.22 Sanger sequencing read of a segment of UOS1 plasmid (derived from pFEP24) containing the *SpeI*-tag

CCTCNATGATGGGTTATATGAGTAATGGGAGGGTAACGGTTTATGGTGGACGGTGGGCTG

GTGACAGTAGAGAGATGGATGGTGGGTGGGAGTGGTATGGTCGAGTGGGGCAGGGTAACN

AGTGGAGAGGTAGGGTAATGTGAGGGTAGGTTTGGCTCTCAGAGTGTGGACTCACTAGTC

CATAACAAGGGAAACAGGTTGATCAGGGTTGGATTAGAATAGGGTTAGAGTAGTGGGTGT

GGTGTGTGGNTGTNGTGTNTGGGTGTGNTGTGTGTGNGGGTGTGGTGTGTNTGTGTGGNG

TGCGTGTNGGTGTGG

Sequences of 35bp *SpeI*-tag insert

Sequences of terminal TG_{1-3}

References

ABDALLAH, P., LUCIANO, P., RUNGE, K. W., LISBY, M., GELI, V., GILSON, E. & TEIXEIRA, M. T. 2009. A two-step model for senescence triggered by a single critically short telomere. *Nature Cell Biology,* 11**,** 988-U174.

ALLSHIRE, R. C., DEMPSTER, M. & HASTIE, N. D. 1989. Human telomeres contain at least three types of G-rich repeat distributed non-randomly. *Nucleic Acids Res,* 17**,** 4611-27.

AS, I. J. & GREIDER, C. W. 2003. Short telomeres induce a DNA damage response in Saccharomyces cerevisiae. *Mol Biol Cell,* 14**,** 987-1001.

ASKREE, S. H., YEHUDA, T., SMOLIKOV, S., GUREVICH, R., HAWK, J., COKER, C., KRAUSKOPF, A., KUPIEC, M. & MCEACHERN, M. J. M. 2004. A genome-wide screen for Saccharomyces cerevisiae deletion mutants that affect telomere length. *Proceedings of the National Academy of Sciences of the United States of America,* 101**,** 8658-8663.

AYLON, Y. & KUPIEC, M. 2003. The checkpoint protein Rad24 of Saccharomyces cerevisiae is involved in processing double-strand break ends and in recombination partner choice. *Mol Cell Biol,* 23**,** 6585-96.

AZZALIN, C. M., REICHENBACH, P., KHORIAULI, L., GIULOTTO, E. & LINGNER, J. 2007. Telomeric repeat containing RNA and RNA surveillance factors at mammalian chromosome ends. *Science,* 318**,** 798-801.

BACHRATI, C. Z. & HICKSON, I. D. 2003. RecQ helicases: suppressors of tumorigenesis and premature aging. *Biochem J,* 374**,** 577-606.

BAI, Y. & SYMINGTON, L. S. 1996. A Rad52 homolog is required for RAD51-independent mitotic recombination in Saccharomyces cerevisiae. *Genes & Development,* 10**,** 2025-2037.

BAILEY, S. M., BRENNEMAN, M. A. & GOODWIN, E. H. 2004. Frequent recombination in telomeric DNA may extend the proliferative life of telomerase-negative cells. *Nucleic Acids Res,* 32**,** 3743-51.

BALK, B., MAICHER, A., DEES, M., KLERMUND, J., LUKE-GLASER, S., BENDER, K. & LUKE, B. 2013. Telomeric RNA-DNA hybrids affect telomere-length dynamics and senescence. *Nat Struct Mol Biol,* 20**,** 1199-205.

BARRETT, E. L. B., BURKE, T. A., HAMMERS, M., KOMDEUR, J. & RICHARDSON, D. S. 2013. Telomere length and dynamics predict mortality in a wild longitudinal study. *Molecular Ecology,* 22**,** 249-259.

BAUMANN, P. & CECH, T. R. 2001. Pot1, the putative telomere end-binding protein in fission yeast and humans. *Science,* 292**,** 1171-1175.

BECHARD, L. H., JAMIESON, N. & MCEACHERN, M. J. 2011. Recombination can cause telomere elongations as well as truncations deep within telomeres in wild-type Kluyveromyces lactis cells. *Eukaryot Cell,* 10**,** 226-36.

BERGSTROM, A., SIMPSON, J. T., SALINAS, F., BARRE, B., PARTS, L., ZIA, A., NGUYEN BA, A. N., MOSES, A. M., LOUIS, E. J., MUSTONEN, V., WARRINGER, J., DURBIN, R. & LITI, G. 2014. A high-definition view of functional genetic variation from natural yeast genomes. *Mol Biol Evol,* 31**,** 872-88.

BERNARDI, R. & PANDOLFI, P. P. 2007. Structure, dynamics and functions of promyelocytic leukaemia nuclear bodies. *Nat Rev Mol Cell Biol,* 8**,** 1006-16.

BERNARDS, A., MICHELS, P. A. M., LINCKE, C. R. & BORST, P. 1983. GROWTH OF CHROMOSOME ENDS IN MULTIPLYING TRYPANOSOMES. *Nature,* 303**,** 592-597.

BIANCHI, A. & SHORE, D. 2007a. Early replication of short telomeres in budding yeast. *Cell,* 128**,** 1051-1062.
BIANCHI, A. & SHORE, D. 2007b. Increased association of telomerase with short telomeres in yeast. *Genes Dev,* 21**,** 1726-30.
BIANCHI, A. & SHORE, D. 2008. How telomerase reaches its end: mechanism of telomerase regulation by the telomeric complex. *Mol Cell,* 31**,** 153-65.
BIESSMANN, H. & MASON, J. M. 1997. Telomere maintenance without telomerase. *Chromosoma,* 106**,** 63-69.
BLACKBURN, E. H. 1992. TELOMERASES. *Annual Review of Biochemistry,* 61**,** 113-129.
BLACKBURN, E. H. & GALL, J. G. 1978. TANDEMLY REPEATED SEQUENCE AT TERMINI OF EXTRACHROMOSOMAL RIBOSOMAL-RNA GENES IN TETRAHYMENA. *Journal of Molecular Biology,* 120**,** 33-53.
BLAGOEV, K. B. & GOODWIN, E. H. 2008. Telomere exchange and asymmetric segregation of chromosomes can account for the unlimited proliferative potential of ALT cell populations. *DNA Repair (Amst),* 7**,** 199-204.
BLASCO, M. A., RIZEN, M., GREIDER, C. W. & HANAHAN, D. 1996. Differential regulation of telomerase activity and telomerase RNA during multi-stage tumorigenesis. *Nature Genetics,* 12**,** 200-204.
BLASTYAK, A., PINTER, L., UNK, I., PRAKASH, L., PRAKASH, S. & HARACSKA, L. 2007. Yeast Rad5 protein required for postreplication repair has a DNA helicase activity specific for replication fork regression. *Molecular Cell,* 28**,** 167-175.
BONETTI, D., CLERICI, M., ANBALAGAN, S., MARTINA, M., LUCCHINI, G. & LONGHESE, M. P. 2010. Shelterin-like proteins and Yku inhibit nucleolytic processing of Saccharomyces cerevisiae telomeres. *PLoS Genet,* 6**,** e1000966.
BONETTI, D., MARTINA, M., CLERICI, M., LUCCHINI, G. & LONGHESE, M. P. 2009. Multiple pathways regulate 3' overhang generation at S. cerevisiae telomeres. *Mol Cell,* 35**,** 70-81.
BOSWELL, R. E., KLOBUTCHER, L. A. & PRESCOTT, D. M. 1982. INVERTED TERMINAL REPEATS ARE ADDED TO GENES DURING MACRONUCLEAR DEVELOPMENT IN OXYTRICHA-NOVA. *Proceedings of the National Academy of Sciences of the United States of America-Biological Sciences,* 79**,** 3255-3259.
BOULE, J. B. & ZAKIAN, V. A. 2006. Roles of Pif1-like helicases in the maintenance of genomic stability. *Nucleic Acids Res,* 34**,** 4147-53.
BROMAN, K. W., WU, H., SEN, S. & CHURCHILL, G. A. 2003. R/qtl: QTL mapping in experimental crosses. *Bioinformatics,* 19**,** 889-90.
BRYAN, T. M., ENGLEZOU, A., GUPTA, J., BACCHETTI, S. & REDDEL, R. R. 1995. Telomere elongation in immortal human cells without detectable telomerase activity. *EMBO J,* 14**,** 4240-8.
BUCHOLC, M., PARK, Y. & LUSTIG, A. J. 2001. Intrachromatid excision of telomeric DNA as a mechanism for telomere size control in Saccharomyces cerevisiae. *Molecular and Cellular Biology,* 21**,** 6559-6573.
CESARE, A. J. & GRIFFITH, J. D. 2004. Telomeric DNA in ALT cells is characterized by free telomeric circles and heterogeneous t-loops. *Molecular and Cellular Biology,* 24**,** 9948-9957.
CESARE, A. J., GROFF-VINDMAN, C., COMPTON, S. A., MCEACHERN, M. J. & GRIFFITH, J. D. 2008. Telomere loops and homologous recombination-dependent telomeric circles in a Kluyveromyces lactis telomere mutant strain. *Mol Cell Biol,* 28**,** 20-9.
CESARE, A. J. & REDDEL, R. R. 2008. Telomere uncapping and alternative lengthening of telomeres. *Mechanisms of Ageing and Development,* 129**,** 99-108.

CESARE, A. J. & REDDEL, R. R. 2010. Alternative lengthening of telomeres: models, mechanisms and implications. *Nat Rev Genet,* 11**,** 319-30.

CHAN, C. S. M. & TYE, B. K. 1983. ORGANIZATION OF DNA-SEQUENCES AND REPLICATION ORIGINS AT YEAST TELOMERES. *Cell,* 33**,** 563-573.

CHANG, M., DITTMAR, J. C. & ROTHSTEIN, R. 2011. Long telomeres are preferentially extended during recombination-mediated telomere maintenance. *Nature Structural & Molecular Biology,* 18**,** 451-U85.

CHEN, Q. J., IJPMA, A. & GREIDER, C. W. 2001. Two survivor pathways that allow growth in the absence of telomerase are generated by distinct telomere recombination events. *Molecular and Cellular Biology,* 21**,** 1819-1827.

CHEN, S., YEH, F., LIN, J., MATSUGUCHI, T., BLACKBURN, E., LEE, E. T., HOWARD, B. V. & ZHAO, J. 2014. Short leukocyte telomere length is associated with obesity in American Indians: the Strong Heart Family study. *Aging (Albany NY),* 6**,** 380-9.

CHEN, Y. H. & SANCHEZ, Y. 2004. Chk1 in the DNA damage response: conserved roles from yeasts to mammals. *DNA Repair,* 3**,** 1025-1032.

CHO, N. W., DILLEY, R. L., LAMPSON, M. A. & GREENBERG, R. A. 2014. Interchromosomal homology searches drive directional ALT telomere movement and synapsis. *Cell,* 159**,** 108-21.

CHONG, L., VAN STEENSEL, B., BROCCOLI, D., ERDJUMENT-BROMAGE, H., HANISH, J., TEMPST, P. & DE LANGE, T. 1995. A human telomeric protein. *Science,* 270**,** 1663-7.

CHURIKOV, D., CHARIFI, F., ECKERT-BOULET, N., SILVA, S., SIMON, M. N., LISBY, M. & GELI, V. 2016. SUMO-Dependent Relocalization of Eroded Telomeres to Nuclear Pore Complexes Controls Telomere Recombination. *Cell Rep,* 15**,** 1242-53.

CHURIKOV, D., CHARIFI, F., SIMON, M. N. & GELI, V. 2014. Rad59-facilitated acquisition of Y' elements by short telomeres delays the onset of senescence. *PLoS Genet,* 10**,** e1004736.

CODD, V., NELSON, C. P., ALBRECHT, E., MANGINO, M., DEELEN, J., BUXTON, J. L., HOTTENGA, J. J., FISCHER, K., ESKO, T., SURAKKA, I., BROER, L., NYHOLT, D. R., MATEO LEACH, I., SALO, P., HAGG, S., MATTHEWS, M. K., PALMEN, J., NORATA, G. D., O'REILLY, P. F., SALEHEEN, D., AMIN, N., BALMFORTH, A. J., BEEKMAN, M., DE BOER, R. A., BOHRINGER, S., BRAUND, P. S., BURTON, P. R., DE CRAEN, A. J., DENNIFF, M., DONG, Y., DOUROUDIS, K., DUBININA, E., ERIKSSON, J. G., GARLASCHELLI, K., GUO, D., HARTIKAINEN, A. L., HENDERS, A. K., HOUWING-DUISTERMAAT, J. J., KANANEN, L., KARSSEN, L. C., KETTUNEN, J., KLOPP, N., LAGOU, V., VAN LEEUWEN, E. M., MADDEN, P. A., MAGI, R., MAGNUSSON, P. K., MANNISTO, S., MCCARTHY, M. I., MEDLAND, S. E., MIHAILOV, E., MONTGOMERY, G. W., OOSTRA, B. A., PALOTIE, A., PETERS, A., POLLARD, H., POUTA, A., PROKOPENKO, I., RIPATTI, S., SALOMAA, V., SUCHIMAN, H. E., VALDES, A. M., VERWEIJ, N., VINUELA, A., WANG, X., WICHMANN, H. E., WIDEN, E., WILLEMSEN, G., WRIGHT, M. J., XIA, K., XIAO, X., VAN VELDHUISEN, D. J., CATAPANO, A. L., TOBIN, M. D., HALL, A. S., BLAKEMORE, A. I., VAN GILST, W. H., ZHU, H., CONSORTIUM, C., ERDMANN, J., REILLY, M. P., KATHIRESAN, S., SCHUNKERT, H., TALMUD, P. J., PEDERSEN, N. L., PEROLA, M., OUWEHAND, W., KAPRIO, J., MARTIN, N. G., VAN DUIJN, C. M., HOVATTA, I., GIEGER, C., METSPALU, A., BOOMSMA, D. I., JARVELIN, M. R., SLAGBOOM, P. E., THOMPSON, J. R., SPECTOR, T. D., VAN DER HARST, P. & SAMANI, N. J. 2013. Identification of seven loci affecting mean telomere length and their association with disease. *Nat Genet,* 45**,** 422-7, 427e1-2.

COMPTON, S. A., CHOI, J. H., CESARE, A. J., OZGUR, S. & GRIFFITH, J. D. 2007. Xrcc3 and Nbs1 are required for the production of extrachromosomal telomeric circles in human alternative lengthening of telomere cells. *Cancer Res,* 67**,** 1513-9.

CUBILLOS, F. A., BILLI, E., ZORGO, E., PARTS, L., FARGIER, P., OMHOLT, S., BLOMBERG, A., WARRINGER, J., LOUIS, E. J. & LITI, G. 2011. Assessing the complex architecture of polygenic traits in diverged yeast populations. *Mol Ecol,* 20**,** 1401-13.

CUSANELLI, E., ROMERO, C. A. P. & CHARTRAND, P. 2013. Telomeric Noncoding RNA TERRA Is Induced by Telomere Shortening to Nucleate Telomerase Molecules at Short Telomeres. *Molecular Cell,* 51**,** 780-791.

DAVIS, A. P. & SYMINGTON, L. S. 2004. RAD51-dependent break-induced replication in yeast. *Molecular and Cellular Biology,* 24**,** 2344-2351.

DELANGE, T., SHIUE, L., MYERS, R. M., COX, D. R., NAYLOR, S. L., KILLERY, A. M. & VARMUS, H. E. 1990. Structure and Variability of Human-Chromosome Ends. *Molecular and Cellular Biology,* 10**,** 518-527.

DI DOMENICO, E. G., ROMANO, E., DEL PORTO, P. & ASCENZIONI, F. 2014. Multifunctional role of ATM/Tel1 kinase in genome stability: from the DNA damage response to telomere maintenance. *Biomed Res Int,* 2014**,** 787404.

DUNHAM, M. A., NEUMANN, A. A., FASCHING, C. L. & REDDEL, R. R. 2000. Telomere maintenance by recombination in human cells. *Nature Genetics,* 26**,** 447-450.

EDWARDS, M. D. & GIFFORD, D. K. 2012. High-resolution genetic mapping with pooled sequencing. *BMC Bioinformatics,* 13 Suppl 6**,** S8.

EHRENREICH, I. M., TORABI, N., JIA, Y., KENT, J., MARTIS, S., SHAPIRO, J. A., GRESHAM, D., CAUDY, A. A. & KRUGLYAK, L. 2010. Dissection of genetically complex traits with extremely large pools of yeast segregants. *Nature,* 464**,** 1039-42.

ENOMOTO, S., GLOWCZEWSKI, L. & BERMAN, J. 2002. MEC3, MEC1, and DDC2 are essential components of a telomere checkpoint pathway required for cell cycle arrest during senescence in Saccharomyces cerevisiae. *Mol Biol Cell,* 13**,** 2626-38.

EPEL, E. S., BLACKBURN, E. H., LIN, J., DHABHAR, F. S., ADLER, N. E., MORROW, J. D. & CAWTHON, R. M. 2004. Accelerated telomere shortening in response to life stress. *Proc Natl Acad Sci U S A,* 101**,** 17312-5.

ESPOSITO, M. S., ESPOSITO, R. E., ARNAUD, M. & HALVORSON, H. O. 1969. Acetate utilization and macromolecular synthesis during sporulation of yeast. *J Bacteriol,* 100**,** 180-6.

EVANS, S. K. & LUNDBLAD, V. 1999. Est1 and Cdc13 as comediators of telomerase access. *Science,* 286**,** 117-120.

FALLET, E., JOLIVET, P., SOUDET, J., LISBY, M., GILSON, E. & TEIXEIRA, M. T. 2014. Length-dependent processing of telomeres in the absence of telomerase. *Nucleic Acids Res,* 42**,** 3648-65.

FANG, Y. F., FLISS, A. E., RAO, J. & CAPLAN, A. J. 1998. SBA1 encodes a yeast Hsp90 cochaperone that is homologous to vertebrate p23 proteins. *Molecular and Cellular Biology,* 18**,** 3727-3734.

FENG, J. L., FUNK, W. D., WANG, S. S., WEINRICH, S. L., AVILION, A. A., CHIU, C. P., ADAMS, R. R., CHANG, E., ALLSOPP, R. C., YU, J. H., LE, S. Y., WEST, M. D., HARLEY, C. B., ANDREWS, W. H., GREIDER, C. W. & VILLEPONTEAU, B. 1995. THE RNA COMPONENT OF HUMAN TELOMERASE. *Science,* 269**,** 1236-1241.

FORERO, D. A., GONZALEZ-GIRALDO, Y., LOPEZ-QUINTERO, C., CASTRO-VEGA, L. J., BARRETO, G. E. & PERRY, G. 2016. Meta-analysis of Telomere Length in Alzheimer's Disease. *J Gerontol A Biol Sci Med Sci*.

FOSTER, S. S., ZUBKO, M. K., GUILLARD, S. & LYDALL, D. 2006. MRX protects telomeric DNA at uncapped telomeres of budding yeast cdc13-1 mutants. *DNA Repair (Amst),* 5**,** 840-51.

FREESE, E. B., CHU, M. I. & FREESE, E. 1982. Initiation of yeast sporulation of partial carbon, nitrogen, or phosphate deprivation. *J Bacteriol,* 149**,** 840-51.

FRIEDMAN, K. L. & BREWER, B. J. 1995. Analysis of replication intermediates by two-dimensional agarose gel electrophoresis. *Methods Enzymol,* 262**,** 613-27.

FRIEDMAN, K. L. & CECH, T. R. 1999. Essential functions of amino-terminal domains in the yeast telomerase catalytic subunit revealed by selection for viable mutants. *Genes Dev,* 13**,** 2863-74.

FU, X. H., DUAN, Y. M., LIU, Y. T., CAI, C., MENG, F. L. & ZHOU, J. Q. 2014. Telomere Recombination Preferentially Occurs at Short Telomeres in Telomerase-Null Type II Survivors. *Plos One,* 9.

GALLARDO, F., OLIVIER, C., DANDJINOU, A. T., WELLINGER, R. J. & CHARTRAND, P. 2008. TLC1 RNA nucleo-cytoplasmic trafficking links telomerase biogenesis to its recruitment to telomeres. *Embo Journal,* 27**,** 748-757.

GANGLOFF, S., MCDONALD, J. P., BENDIXEN, C., ARTHUR, L. & ROTHSTEIN, R. 1994. The yeast type I topoisomerase Top3 interacts with Sgs1, a DNA helicase homolog: a potential eukaryotic reverse gyrase. *Mol Cell Biol,* 14**,** 8391-8.

GARVIK, B., CARSON, M. & HARTWELL, L. 1995. Single-stranded DNA arising at telomeres in cdc13 mutants may constitute a specific signal for the RAD9 checkpoint. *Mol Cell Biol,* 15**,** 6128-38.

GILSON, E., ROBERGE, M., GIRALDO, R., RHODES, D. & GASSER, S. M. 1993. DISTORTION OF THE DNA DOUBLE HELIX BY RAP1 AT SILENCERS AND MULTIPLE TELOMERIC BINDING-SITES. *Journal of Molecular Biology,* 231**,** 293-310.

GLASEL, J. A. 1995. Validity of nucleic acid purities monitored by 260nm/280nm absorbance ratios. *Biotechniques,* 18**,** 62-3.

GOUDSOUZIAN, L. K., TUZON, C. T. & ZAKIAN, V. A. 2006. S. cerevisiae Tel1p and Mre11p are required for normal levels of Est1p and Est2p telomere association. *Mol Cell,* 24**,** 603-10.

GRANDIN, N., BAILLY, A. & CHARBONNEAU, M. 2005. Activation of Mrc1, a mediator of the replication checkpoint, by telomere erosion. *Biol Cell,* 97**,** 799-814.

GRANDIN, N. & CHARBONNEAU, M. 2003. The rad51 pathway of telomerase-independent maintenance of telomeres can amplify TG(1-3) sequences in yku and cdc13 mutants of Saccharomyces cerevisiae. *Molecular and Cellular Biology,* 23**,** 3721-3734.

GRANDIN, N. & CHARBONNEAU, M. 2009. Telomerase- and Rad52-Independent Immortalization of Budding Yeast by an Inherited-Long-Telomere Pathway of Telomeric Repeat Amplification. *Molecular and Cellular Biology,* 29**,** 965-985.

GRANDIN, N., DAMON, C. & CHARBONNEAU, M. 2001. Ten1 functions in telomere end protection and length regulation in association with Stn1 and Cdc13. *EMBO J,* 20**,** 1173-83.

GRAVEL, S., CHAPMAN, J. R., MAGILL, C. & JACKSON, S. P. 2008. DNA helicases Sgs1 and BLM promote DNA double-strand break resection. *Genes Dev,* 22**,** 2767-72.

GREIDER, C. W. 2016. Regulating telomere length from the inside out: the replication fork model. *Genes Dev,* 30**,** 1483-91.

GREIDER, C. W. & BLACKBURN, E. H. 1985. IDENTIFICATION OF A SPECIFIC TELOMERE TERMINAL TRANSFERASE-ACTIVITY IN TETRAHYMENA EXTRACTS. *Cell,* 43**,** 405-413.

GRENON, M., GILBERT, C. & LOWNDES, N. F. 2001. Checkpoint activation in response to double-strand breaks requires the Mre11/Rad50/Xrs2 complex. *Nature Cell Biology,* 3**,** 844-847.

GROBELNY, J. V., GODWIN, A. K. & BROCCOLI, D. 2000. ALT-associated PML bodies are present in viable cells and are enriched in cells in the G(2)/M phase of the cell cycle. *J Cell Sci,* 113 Pt 24**,** 4577-85.

GROFF-VINDMAN, C., CESARE, A. J., NATARAJAN, S., GRIFFITH, J. D. & MCEACHERN, M. J. 2005. Recombination at long mutant telomeres produces tiny single- and double-stranded telomeric circles. *Molecular and Cellular Biology,* 25**,** 4406-4412.

HARDY, C. F. J., SUSSEL, L. & SHORE, D. 1992. A Rap1-Interacting Protein Involved in Transcriptional Silencing and Telomere Length Regulation. *Genes & Development,* 6**,** 801-814.

HARDY, J., CHURIKOV, D., GELI, V. & SIMON, M. N. 2014. Sgs1 and Sae2 promote telomere replication by limiting accumulation of ssDNA. *Nat Commun,* 5**,** 5004.

HAYFLICK, L. & MOORHEAD, P. S. 1961. SERIAL CULTIVATION OF HUMAN DIPLOID CELL STRAINS. *Experimental Cell Research,* 25**,** 585-&.

HAYS, S. L., FIRMENICH, A. A. & BERG, P. 1995. COMPLEX-FORMATION IN YEAST DOUBLE-STRAND BREAK REPAIR - PARTICIPATION OF RAD51, RAD52, RAD55, AND RAD57 PROTEINS. *Proceedings of the National Academy of Sciences of the United States of America,* 92**,** 6925-6929.

HEAPHY, C. M., SUBHAWONG, A. P., HONG, S. M., GOGGINS, M. G., MONTGOMERY, E. A., GABRIELSON, E., NETTO, G. J., EPSTEIN, J. I., LOTAN, T. L., WESTRA, W. H., SHIH IE, M., IACOBUZIO-DONAHUE, C. A., MAITRA, A., LI, Q. K., EBERHART, C. G., TAUBE, J. M., RAKHEJA, D., KURMAN, R. J., WU, T. C., RODEN, R. B., ARGANI, P., DE MARZO, A. M., TERRACCIANO, L., TORBENSON, M. & MEEKER, A. K. 2011. Prevalence of the alternative lengthening of telomeres telomere maintenance mechanism in human cancer subtypes. *Am J Pathol,* 179**,** 1608-15.

HECTOR, R. E., SHTOFMAN, R. L., RAY, A., CHEN, B. R., NYUN, T., BERKNER, K. L. & RUNGE, K. W. 2007. Tel1p preferentially associates with short telomeres to stimulate their elongation. *Molecular Cell,* 27**,** 851-858.

HEMANN, M. T., STRONG, M. A., HAO, L. Y. & GREIDER, C. W. 2001. The shortest telomere, not average telomere length, is critical for cell viability and chromosome stability. *Cell,* 107**,** 67-77.

HENSON, J. D., CAO, Y., HUSCHTSCHA, L. I., CHANG, A. C., AU, A. Y., PICKETT, H. A. & REDDEL, R. R. 2009. DNA C-circles are specific and quantifiable markers of alternative-lengthening-of-telomeres activity. *Nat Biotechnol,* 27**,** 1181-5.

HENSON, J. D., HANNAY, J. A., MCCARTHY, S. W., ROYDS, J. A., YEAGER, T. R., ROBINSON, R. A., WHARTON, S. B., JELLINEK, D. A., ARBUCKLE, S. M., YOO, J. Y., ROBINSON, B. G., LEAROYD, D. L., STALLEY, P. D., BONAR, S. F., YU, D. H., POLLOCK, R. E. & REDDEL, R. R. 2005. A robust assay for alternative lengthening of telomeres in tumors shows the significance of alternative lengthening of telomeres in sarcomas and astrocytomas. *Clinical Cancer Research,* 11**,** 217-225.

HENSON, J. D., NEUMANN, A. A., YEAGER, T. R. & REDDEL, R. R. 2002. Alternative lengthening of telomeres in mammalian cells. *Oncogene,* 21**,** 598-610.

HIRANO, Y., FUKUNAGA, K. & SUGIMOTO, K. 2009. Rif1 and Rif2 Inhibit Localization of Tel1 to DNA Ends. *Molecular Cell,* 33**,** 312-322.

HOROWITZ, H. & HABER, J. E. 1985. IDENTIFICATION OF AUTONOMOUSLY REPLICATING CIRCULAR SUBTELOMERIC-Y' ELEMENTS IN SACCHAROMYCES-CEREVISIAE. *Molecular and Cellular Biology,* 5**,** 2369-2380.

HUANG, P. H., PRYDE, F. E., LESTER, D., MADDISON, R. L., BORTS, R. H., HICKSON, I. D. & LOUIS, E. J. 2001. SGS1 is required for telomere elongation in the absence of telomerase. *Current Biology,* 11**,** 125-129.

HUGHES, T. R., EVANS, S. K., WEILBAECHER, R. G. & LUNDBLAD, V. 2000. The Est3 protein is a subunit of yeast telomerase. *Current Biology,* 10**,** 809-812.

HUZEN, J., WONG, L. S. M., VAN VELDHUISEN, D. J., SAMANI, N. J., ZWINDERMAN, A. H., CODD, V., CAWTHON, R. M., BENUS, G. F. J. D., VAN DER HORST, I. C. C., NAVIS, G., BAKKER, S. J. L., GANSEVOORT, R. T., DE JONG, P. E., HILLEGE, H. L., VAN GILST, W. H., DE BOER, R. A. & VAN DER HARST, P. 2014. Telomere length loss due to smoking and metabolic traits. *Journal of Internal Medicine,* 275**,** 155-163.

IGLESIAS, N., REDON, S., PFEIFFER, V., DEES, M., LINGNER, J. & LUKE, B. 2011. Subtelomeric repetitive elements determine TERRA regulation by Rap1/Rif and Rap1/Sir complexes in yeast. *EMBO Rep,* 12**,** 587-93.

IMAI, S., ARMSTRONG, C. M., KAEBERLEIN, M. & GUARENTE, L. 2000. Transcriptional silencing and longevity protein Sir2 is an NAD-dependent histone deacetylase. *Nature,* 403**,** 795-800.

IRA, G. & HABER, J. E. 2002. Characterization of RAD51-independent break-induced replication that acts preferentially with short homologous sequences. *Molecular and Cellular Biology,* 22**,** 6384-6392.

IYER, S., CHADHA, A. D. & MCEACHERN, M. J. 2005. A mutation in the STN1 gene triggers an alternative lengthening of telomere-like runaway recombinational telomere elongation and rapid deletion in yeast. *Mol Cell Biol,* 25**,** 8064-73.

JAWAID, A., BADER, J. S., PURCELL, S., CHERNY, S. S. & SHAM, P. 2002. Optimal selection strategies for QTL mapping using pooled DNA samples. *European Journal of Human Genetics,* 10**,** 125-132.

JI, H., PLATTS, M. H., DHARAMSI, L. M. & FRIEDMAN, K. L. 2005. Regulation of telomere length by an N-terminal region of the yeast telomerase reverse transcriptase. *Mol Cell Biol,* 25**,** 9103-14.

JOHNSON, E. M. 1980. A FAMILY OF INVERTED REPEAT SEQUENCES AND SPECIFIC SINGLE-STRAND GAPS AT THE TERMINI OF THE PHYSARUM RDNA PALINDROME. *Cell,* 22**,** 875-886.

JOHNSON, R. E., PRAKASH, S. & PRAKASH, L. 1994. Yeast DNA repair protein RAD5 that promotes instability of simple repetitive sequences is a DNA-dependent ATPase. *J Biol Chem,* 269**,** 28259-62.

JOSEPH, I. S., KUMARI, A., BHATTACHARYYA, M. K., GAO, H. H., LI, B. B. & LUSTIG, A. J. 2010. An mre11 Mutation That Promotes Telomere Recombination and an Efficient Bypass of Senescence. *Genetics,* 185**,** 761-770.

KAMMORI, M., KANAUCHI, H., NAKAMURA, K., KAWAHARA, M., WEBER, T. K., MAFUNE, K., KAMINISHI, M. & TAKUBO, K. 2002. Demonstration of human telomerase reverse transcriptase in human colorectal carcinomas by in situ hybridization. *Int J Oncol,* 20**,** 15-21.

KEARSEY, M. J. 1998. The principles of QTL analysis (a minimal mathematics approach). *Journal of Experimental Botany,* 49**,** 1619-1623.

KHADAROO, B., TEIXEIRA, M. T., LUCIANO, P., ECKERT-BOULET, N., GERMANN, S. M., SIMON, M. N., GALLINA, I., ABDALLAH, P., GILSON, E., GELI, V. &

LISBY, M. 2009. The DNA damage response at eroded telomeres and tethering to the nuclear pore complex. *Nature Cell Biology,* 11**,** 980-U161.
KIM, N. W., PIATYSZEK, M. A., PROWSE, K. R., HARLEY, C. B., WEST, M. D., HO, P. L., COVIELLO, G. M., WRIGHT, W. E., WEINRICH, S. L. & SHAY, J. W. 1994. Specific association of human telomerase activity with immortal cells and cancer. *Science,* 266**,** 2011-5.
KIM, S. H., KAMINKER, P. & CAMPISI, J. 1999. TIN2, a new regulator of telomere length in human cells. *Nat Genet,* 23**,** 405-12.
KITAMURA, K., KANEKO, T. & YAMAMOTO, Y. 1971. Lysis of viable yeast cells by enzymes of Arthrobacter luteus. *Arch Biochem Biophys,* 145**,** 402-4.
KROGH, B. O. & SYMINGTON, L. S. 2004. Recombination proteins in yeast. *Annual Review of Genetics,* 38**,** 233-271.
KUPIEC, M. 2014. Biology of telomeres: lessons from budding yeast. *FEMS Microbiol Rev,* 38**,** 144-71.
LANDER, E. S. & SCHORK, N. J. 1994. Genetic dissection of complex traits. *Science,* 265**,** 2037-48.
LAROCHE, T., MARTIN, S. G., GOTTA, M., GORHAM, H. C., PRYDE, F. E., LOUIS, E. J. & GASSER, S. M. 1998. Mutation of yeast Ku genes disrupts the subnuclear organization of telomeres. *Curr Biol,* 8**,** 653-6.
LARRIVEE, M. & WELLINGER, R. J. 2006. Telomerase- and capping-independent yeast survivors with alternate telomere states. *Nat Cell Biol,* 8**,** 741-7.
LE, S., MOORE, J. K., HABER, J. E. & GREIDER, C. W. 1999. RAD50 and RAD51 define two pathways that collaborate to maintain telomeres in the absence of telomerase. *Genetics,* 152**,** 143-152.
LEBEL, C., ROSONINA, E., SEALEY, D. C. F., PRYDE, F., LYDALL, D., MARINGELE, L. & HARRINGTON, L. A. 2009. Telomere Maintenance and Survival in Saccharomyces cerevisiae in the Absence of Telomerase and RAD52. *Genetics,* 182**,** 671-684.
LEVY, D. L. & BLACKBURN, E. H. 2004. Counting of Rif1p and Rif2p on Saccharomyces cerevisiae telomeres regulates telomere length. *Mol Cell Biol,* 24**,** 10857-67.
LI, B. & LUSTIG, A. J. 1996. A novel mechanism for telomere size control in Saccharomyces cerevisiae. *Genes Dev,* 10**,** 1310-26.
LI, B., REDDY, S. & COMAI, L. 2011. Depletion of Ku70/80 reduces the levels of extrachromosomal telomeric circles and inhibits proliferation of ALT cells. *Aging (Albany NY),* 3**,** 395-406.
LI, H. 2014. Toward better understanding of artifacts in variant calling from high-coverage samples. *Bioinformatics,* 30**,** 2843-51.
LI, H. & DURBIN, R. 2009. Fast and accurate short read alignment with Burrows-Wheeler transform. *Bioinformatics,* 25**,** 1754-60.
LIEB, J. D., LIU, X., BOTSTEIN, D. & BROWN, P. O. 2001. Promoter-specific binding of Rap1 revealed by genome-wide maps of protein-DNA association (vol 28, pg 327, 2001). *Nature Genetics,* 29**,** 100-100.
LITI, G., CARTER, D. M., MOSES, A. M., WARRINGER, J., PARTS, L., JAMES, S. A., DAVEY, R. P., ROBERTS, I. N., BURT, A., KOUFOPANOU, V., TSAI, I. J., BERGMAN, C. M., BENSASSON, D., O'KELLY, M. J. T., VAN OUDENAARDEN, A., BARTON, D. B. H., BAILES, E., BA, A. N. N., JONES, M., QUAIL, M. A., GOODHEAD, I., SIMS, S., SMITH, F., BLOMBERG, A., DURBIN, R. & LOUIS, E. J. 2009a. Population genomics of domestic and wild yeasts. *Nature,* 458**,** 337-341.
LITI, G., HARICHARAN, S., CUBILLOS, F. A., TIERNEY, A. L., SHARP, S., BERTUCH, A. A., PARTS, L., BAILES, E. & LOUIS, E. J. 2009b. Segregating YKU80 and TLC1

alleles underlying natural variation in telomere properties in wild yeast. *PLoS Genet,* 5**,** e1000659.
LITI, G. & LOUIS, E. J. 2003. NEJ1 prevents NHEJ-dependent telornere fusions in yeast without telornerase. *Molecular Cell,* 11**,** 1373-1378.
LITI, G. & LOUIS, E. J. 2012. Advances in quantitative trait analysis in yeast. *PLoS Genet,* 8**,** e1002912.
LOPEZ, C. C., NIELSEN, L. & EDSTROM, J. E. 1996. Terminal long tandem repeats in chromosomes form Chironomus pallidivittatus. *Mol Cell Biol,* 16**,** 3285-90.
LOUIS, E. J. 1995. The chromosome ends of Saccharomyces cerevisiae. *Yeast,* 11**,** 1553-1573.
LOUIS, E. J. & HABER, J. E. 1990. The subtelomeric Y' repeat family in Saccharomyces cerevisiae: an experimental system for repeated sequence evolution. *Genetics,* 124**,** 533-45.
LOUIS, E. J. & HABER, J. E. 1992. THE STRUCTURE AND EVOLUTION OF SUBTELOMERIC-Y REPEATS IN SACCHAROMYCES-CEREVISIAE. *Genetics,* 131**,** 559-574.
LUKE, B., PANZA, A., REDON, S., IGLESIAS, N., LI, Z. & LINGNER, J. 2008. The Rat1p 5' to 3' exonuclease degrades telomeric repeat-containing RNA and promotes telomere elongation in Saccharomyces cerevisiae. *Mol Cell,* 32**,** 465-77.
LUNDBLAD, V. & BLACKBURN, E. H. 1993. AN ALTERNATIVE PATHWAY FOR YEAST TELOMERE MAINTENANCE RESCUES EST1- SENESCENCE. *Cell,* 73**,** 347-360.
LUNDBLAD, V. & SZOSTAK, J. W. 1989. A MUTANT WITH A DEFECT IN TELOMERE ELONGATION LEADS TO SENESCENCE IN YEAST. *Cell,* 57**,** 633-643.
LYDALL, D. 2003. Hiding at the ends of yeast chromosomes: telomeres, nucleases and checkpoint pathways. Journal of Cell Science, 116, 4057-4065.
MACKAY, T. F., STONE, E. A. & AYROLES, J. F. 2009. The genetics of quantitative traits: challenges and prospects. *Nat Rev Genet,* 10**,** 565-77.
MAICHER, A., KASTNER, L., DEES, M. & LUKE, B. 2012. Deregulated telomere transcription causes replication-dependent telomere shortening and promotes cellular senescence. *Nucleic Acids Res,* 40**,** 6649-59.
MARCAND, S., PARDO, B., GRATIAS, A., CAHUN, S. & CALLEBAUT, I. 2008. Multiple pathways inhibit NHEJ at telomeres. *Genes & Development,* 22**,** 1153-1158.
MARCAND, S., WOTTON, D., GILSON, E. & SHORE, D. 1997. Rap1p and telomere length regulation in yeast. *Ciba Foundation symposium,* 211**,** 76-93; discussion 93-103.
MARINGELE, L. & LYDALL, D. 2002. EXO1-dependent single-stranded DNA at telomeres activates subsets of DNA damage and spindle checkpoint pathways in budding yeast yku70Delta mutants. *Genes Dev,* 16**,** 1919-33.
MARINGELE, L. & LYDALL, D. 2004. Telomerase- and recombination-independent immortalization of budding yeast. *Genes Dev,* 18**,** 2663-75.
MARTENS, U. M., BRASS, V., ENGELHARDT, M., GLASER, S., WALLER, C. F., LANGE, W., SCHMOOR, C., POON, S. S. S. & LANSDORP, P. M. 2000. Measurement of telomere length in haematopoietic cells using in situ hybridization techniques. *Biochemical Society Transactions,* 28**,** 245-250.
MARTIN, S. G., LAROCHE, T., SUKA, N., GRUNSTEIN, M. & GASSER, S. M. 1999. Relocalization of telomeric Ku and SIR proteins in response to DNA strand breaks in yeast. *Cell,* 97**,** 621-633.
MAZIN, A. V., ALEXEEV, A. A. & KOWALCZYKOWSKI, S. C. 2003. A novel function of Rad54 protein. Stabilization of the Rad51 nucleoprotein filament. *J Biol Chem,* 278**,** 14029-36.

MAZON, G., MIMITOU, E. P. & SYMINGTON, L. S. 2010. SnapShot: Homologous recombination in DNA double-strand break repair. *Cell,* 142**,** 646, 646 e1.
MCCLINTOCK, B. 1939. The behavior in successive nuclear divisions of a chromosome broken at meiosis. *Proceedings of the National Academy of Sciences of the United States of America,* 25**,** 405-416.
MCEACHERN, M. J. & HABER, J. E. 2006. Break-induced replication and recombinational telomere elongation in yeast. *Annual Review of Biochemistry.* Palo Alto: Annual Reviews.
MCEACHERN, M. J., UNDERWOOD, D. H. & BLACKBURN, E. H. 2002. Dynamics of telomeric DNA turnover in yeast. *Genetics,* 160**,** 63-73.
MCELHOE, J. A., HOLLAND, M. M., MAKOVA, K. D., SU, M. S. W., PAUL, I. M., BAKER, C. H., FAITH, S. A. & YOUNG, B. 2014. Development and assessment of an optimized next-generation DNA sequencing approach for the mtgenome using the Illumina MiSeq. *Forensic Science International-Genetics,* 13**,** 20-29.
MCKENNA, A., HANNA, M., BANKS, E., SIVACHENKO, A., CIBULSKIS, K., KERNYTSKY, A., GARIMELLA, K., ALTSHULER, D., GABRIEL, S., DALY, M. & DEPRISTO, M. A. 2010. The Genome Analysis Toolkit: a MapReduce framework for analyzing next-generation DNA sequencing data. *Genome Res,* 20**,** 1297-303.
MICHELMORE, R. W., PARAN, I. & KESSELI, R. V. 1991. Identification of Markers Linked to Disease-Resistance Genes by Bulked Segregant Analysis - a Rapid Method to Detect Markers in Specific Genomic Regions by Using Segregating Populations. *Proceedings of the National Academy of Sciences of the United States of America,* 88**,** 9828-9832.
MIMITOU, E. P. & SYMINGTON, L. S. 2008. Sae2, Exo1 and Sgs1 collaborate in DNA double-strand break processing. *Nature,* 455**,** 770-4.
MITCHELL, J. R., WOOD, E. & COLLINS, K. 1999. A telomerase component is defective in the human disease dyskeratosis congenita. *Nature,* 402**,** 551-555.
MUNTONI, A., NEUMANN, A. A., HILLS, M. & REDDEL, R. R. 2009. Telomere elongation involves intra-molecular DNA replication in cells utilizing alternative lengthening of telomeres. *Hum Mol Genet,* 18**,** 1017-27.
MUNTONI, A. & REDDEL, R. R. 2005. The first molecular details of ALT in human tumor cells. *Hum Mol Genet,* 14 Spec No. 2**,** R191-6.
MURNANE, J. P., SABATIER, L., MARDER, B. A. & MORGAN, W. F. 1994. Telomere dynamics in an immortal human cell line. *EMBO J,* 13**,** 4953-62.
MUSTON, P. 2012. *Genome instability in yeast without telomerase.* PhD, University of Nottingham.
NAIKI, T., WAKAYAMA, T., NAKADA, D., MATSUMOTO, K. & SUGIMOTO, K. 2004. Association of Rad9 with double-strand breaks through a Mec1-dependent mechanism. *Molecular and Cellular Biology,* 24**,** 3277-3285.
NATARAJAN, S. & MCEACHERN, M. J. 2002. Recombinational telomere elongation promoted by DNA circles. *Molecular and Cellular Biology,* 22**,** 4512-4521.
O'SULLIVAN, R. J. & KARLSEDER, J. 2010. Telomeres: protecting chromosomes against genome instability. *Nature Reviews Molecular Cell Biology,* 11**,** 171-181.
OPITZ, O. G., SULIMAN, Y., HAHN, W. C., HARADA, H., BLUM, H. E. & RUSTGI, A. K. 2001. Cyclin D1 overexpression and p53 inactivation immortalize primary oral keratinocytes by a telomerase-independent mechanism. *J Clin Invest,* 108**,** 725-32.
OSTERHAGE, J. L., TALLEY, J. M. & FRIEDMAN, K. L. 2006. Proteasome-dependent degradation of Est1p regulates the cell cycle-restricted assembly of telomerase in Saccharomyces cerevisiae. *Nature Structural & Molecular Biology,* 13**,** 720-728.
PARTS, L., CUBILLOS, F. A., WARRINGER, J., JAIN, K., SALINAS, F., BUMPSTEAD, S. J., MOLIN, M., ZIA, A., SIMPSON, J. T., QUAIL, M. A., MOSES, A., LOUIS, E.

J., DURBIN, R. & LITI, G. 2011. Revealing the genetic structure of a trait by sequencing a population under selection. *Genome Res,* 21**,** 1131-8.
PETERSON, S. E., STELLWAGEN, A. E., DIEDE, S. J., SINGER, M. S., HAIMBERGER, Z. W., JOHNSON, C. O., TZONEVA, M. & GOTTSCHLING, D. E. 2001. The function of a stem-loop in telomerase RNA is linked to the DNA repair protein Ku. *Nature Genetics,* 27**,** 64-67.
PETREACA, R. C., CHIU, H.-C., ECKELHOEFER, H. A., CHUANG, C., XU, L. & NUGENT, C. I. 2006. Chromosome end protection plasticity revealed by Stn1p and Ten1p bypass of Cdc13p. *Nature Cell Biology,* 8**,** 748-U202.
PFEIFFER, V. & LINGNER, J. 2012. TERRA Promotes Telomere Shortening through Exonuclease 1-Mediated Resection of Chromosome Ends. *Plos Genetics,* 8.
PICKETT, H. A., CESARE, A. J., JOHNSTON, R. L., NEUMANN, A. A. & REDDEL, R. R. 2009. Control of telomere length by a trimming mechanism that involves generation of t-circles. *EMBO J,* 28**,** 799-809.
PICKETT, H. A. & REDDEL, R. R. 2015. Molecular mechanisms of activity and derepression of alternative lengthening of telomeres. *Nat Struct Mol Biol,* 22**,** 875-80.
POLOTNIANKA, R. M., LI, J. & LUSTIG, A. J. 1998. The yeast Ku heterodimer is essential for protection of the telomere against nucleolytic and recombinational activities. *Current Biology,* 8**,** 831-834.
PRAKASH, S. & PRAKASH, L. 2000. Nucleotide excision repair in yeast. *Mutat Res,* 451**,** 13-24.
PRYDE, F. E., HUCKLE, T. C. & LOUIS, E. J. 1995. SEQUENCE-ANALYSIS OF THE RIGHT END OF CHROMOSOME-XV IN SACCHAROMYCES-CEREVISIAE - AN INSIGHT INTO THE STRUCTURAL AND FUNCTIONAL-SIGNIFICANCE OF SUB-TELOMERIC REPEAT SEQUENCES. *Yeast,* 11**,** 371-382.
PRYDE, F. E. & LOUIS, E. J. 1999. Limitations of silencing at native yeast telomeres. *Embo Journal,* 18**,** 2538-2550.
QI, H. Y. & ZAKIAN, V. A. 2000. The Saccharomyces telomere-binding protein Cdc13p interacts with both the catalytic subunit of DNA polymerase alpha and the telomerase-associated Est1 protein. *Genes & Development,* 14**,** 1777-1788.
REED, K. C. & MANN, D. A. 1985. Rapid transfer of DNA from agarose gels to nylon membranes. *Nucleic Acids Res,* 13**,** 7207-21.
ROMANO, G. H., HARARI, Y., YEHUDA, T., PODHORZER, A., RUBINSTEIN, L., SHAMIR, R., GOTTLIEB, A., SILBERBERG, Y., PE'ER, D., RUPPIN, E., SHARAN, R. & KUPIEC, M. 2013. Environmental Stresses Disrupt Telomere Length Homeostasis. *Plos Genetics,* 9.
ROSONINA, E., KANEKO, S. & MANLEY, J. L. 2006. Terminating the transcript: breaking up is hard to do. *Genes Dev,* 20**,** 1050-6.
ROYLE, N. J., FOXON, J., JEYAPALAN, J. N., MENDEZ-BERMUDEZ, A., NOVO, C. L., WILLIAMS, J. & COTTON, V. E. 2008. Telomere length maintenance--an ALTernative mechanism. *Cytogenet Genome Res,* 122**,** 281-91.
SABOURIN, M., TUZON, C. T. & ZAKIAN, V. A. 2007. Telomerase and Tel1p preferentially associate with short telomeres in S. cerevisiae. *Mol Cell,* 27**,** 550-61.
SANDELL, L. L. & ZAKIAN, V. A. 1993. Loss of a Yeast Telomere - Arrest, Recovery, and Chromosome Loss. *Cell,* 75**,** 729-739.
SHAMPAY, J., SZOSTAK, J. W. & BLACKBURN, E. H. 1984. DNA-SEQUENCES OF TELOMERES MAINTAINED IN YEAST. *Nature,* 310**,** 154-157.
SHIN, C. & BAIK, I. 2016. Associations Between Alcohol Consumption and Leukocyte Telomere Length Modified by a Common Polymorphism of ALDH2. *Alcoholism-Clinical and Experimental Research,* 40**,** 765-771.

SHORE, D. & NASMYTH, K. 1987. PURIFICATION AND CLONING OF A DNA-BINDING PROTEIN FROM YEAST THAT BINDS TO BOTH SILENCER AND ACTIVATOR ELEMENTS. *Cell,* 51**,** 721-732.

SINGER, M. S. & GOTTSCHLING, D. E. 1994. TLC1 - TEMPLATE RNA COMPONENT OF SACCHAROMYCES-CEREVISIAE TELOMERASE. *Science,* 266**,** 404-409.

SMOGORZEWSKA, A., KARLSEDER, J., HOLTGREVE-GREZ, H., JAUCH, A. & DE LANGE, T. 2002. DNA ligase IV-dependent NHEJ of deprotected mammalian telomeres in G1 and G2. *Curr Biol,* 12**,** 1635-44.

SONG, B. W. & SUNG, P. 2000. Functional interactions among yeast Rad51 recombinase, Rad52 mediator, and replication protein A in DNA strand exchange. *Journal of Biological Chemistry,* 275**,** 15895-15904.

SOUTHERN, E. M. 1975. Detection of Specific Sequences among DNA Fragments Separated by Gel-Electrophoresis. *Journal of Molecular Biology,* 98**,** 503-&.

STANSEL, R. M., DE LANGE, T. & GRIFFITH, J. D. 2001. T-loop assembly in vitro involves binding of TRF2 near the 3' telomeric overhang. *EMBO J,* 20**,** 5532-40.

STEINMETZ, L. M., SINHA, H., RICHARDS, D. R., SPIEGELMAN, J. I., OEFNER, P. J., MCCUSKER, J. H. & DAVIS, R. W. 2002. Dissecting the architecture of a quantitative trait locus in yeast. *Nature,* 416**,** 326-30.

SUGAWARA, N., IRA, G. & HABER, J. E. 2000. DNA length dependence of the single-strand annealing pathway and the role of Saccharomyces cerevisiae RAD59 in double-strand break repair. *Molecular and Cellular Biology,* 20**,** 5300-5309.

SUGIYAMA, T. & KOWALCZYKOWSKI, S. C. 2002. Rad52 protein associates with replication protein A (RPA)-single-stranded DNA to accelerate Rad51-mediated displacement of RPA and presynaptic complex formation. *J Biol Chem,* 277**,** 31663-72.

SYMINGTON, L. S. & GAUTIER, J. 2011. Double-strand break end resection and repair pathway choice. *Annu Rev Genet,* 45**,** 247-71.

SZOSTAK, J. W. & BLACKBURN, E. H. 1982. CLONING YEAST TELOMERES ON LINEAR PLASMID VECTORS. *Cell,* 29**,** 245-255.

TAMURA, Y., TAKUBO, K., AIDA, J., ARAKI, A. & ITO, H. 2016. Telomere attrition and diabetes mellitus. *Geriatr Gerontol Int,* 16 Suppl 1**,** 66-74.

TEIXEIRA, M. T., ARNERIC, M., SPERISEN, P. & LINGNER, J. 2004. Telomere length homeostasis is achieved via a switch between telomerase- extendible and -nonextendible states. *Cell,* 117**,** 323-35.

TENG, S. C., CHANG, J., MCCOWAN, B. & ZAKIAN, V. A. 2000. Telomerase-independent lengthening of yeast telomeres occurs by an abrupt Rad50p-dependent, Rif-inhibited recombinational process. *Molecular Cell,* 6**,** 947-952.

TENG, S. C. & ZAKIAN, V. A. 1999. Telomere-telomere recombination is an efficient bypass pathway for telomere maintenance in Saccharomyces cerevisiae. *Molecular and Cellular Biology,* 19**,** 8083-8093.

TERRY, D. F., NOLAN, V. G., ANDERSEN, S. L., PERLS, T. T. & CAWTHON, R. 2008. Association of longer telomeres with better health in centenarians. *Journals of Gerontology Series a-Biological Sciences and Medical Sciences,* 63**,** 809-812.

TOH, G. W. L. & LOWNDES, N. F. 2003. Role of the Saccharomyces in sensing and responding cerevisiae Rad9 protein to DNA damage. *Biochemical Society Transactions,* 31**,** 242-246.

TOOGUN, O. A., ZEIGER, W. & FREEMAN, B. C. 2007. The p23 molecular chaperone promotes functional telomerase complexes through DNA dissociation. *Proceedings of the National Academy of Sciences of the United States of America,* 104**,** 5765-5770.

TRAN, P. T., ERDENIZ, N., DUDLEY, S. & LISKAY, R. M. 2002. Characterization of nuclease-dependent functions of Exo1p in Saccharomyces cerevisiae. *DNA Repair (Amst),* 1**,** 895-912.

TRUJILLO, K. M., ROH, D. H., CHEN, L., VAN KOMEN, S., TOMKINSON, A. & SUNG, P. 2003. Yeast xrs2 binds DNA and helps target rad50 and mre11 to DNA ends. *J Biol Chem,* 278**,** 48957-64.

TRUJILLO, K. M. & SUNG, P. 2001. DNA structure-specific nuclease activities in the Saccharomyces cerevisiae Rad50*Mre11 complex. *J Biol Chem,* 276**,** 35458-64.

TSUBOUCHI, H. & OGAWA, H. 2000. Exo1 roles for repair of DNA double-strand breaks and meiotic crossing over in Saccharomyces cerevisiae. *Mol Biol Cell,* 11**,** 2221-33.

UNGAR, L., YOSEF, N., SELA, Y., SHARAN, R., RUPPIN, E. & KUPIEC, M. 2009. A genome-wide screen for essential yeast genes that affect telomere length maintenance. *Nucleic Acids Res,* 37**,** 3840-9.

WANG, R. C., SMOGORZEWSKA, A. & DE LANGE, T. 2004. Homologous recombination generates T-loop-sized deletions at human telomeres. *Cell,* 119**,** 355-68.

WANG, S. S. & ZAKIAN, V. A. 1990. SEQUENCING OF SACCHAROMYCES TELOMERES CLONED USING T4-DNA POLYMERASE REVEALS 2 DOMAINS. *Molecular and Cellular Biology,* 10**,** 4415-4419.

WARRINGER, J., ZORGO, E., CUBILLOS, F. A., ZIA, A., GJUVSLAND, A., SIMPSON, J. T., FORSMARK, A., DURBIN, R., OMHOLT, S. W., LOUIS, E. J., LITI, G., MOSES, A. & BLOMBERG, A. 2011. Trait Variation in Yeast Is Defined by Population History. *Plos Genetics,* 7.

WEINERT, T. A. & HARTWELL, L. H. 1993. Cell cycle arrest of cdc mutants and specificity of the RAD9 checkpoint. *Genetics,* 134**,** 63-80.

WELLINGER, R. J. & ZAKIAN, V. A. 2012. Everything You Ever Wanted to Know About Saccharomyces cerevisiae Telomeres: Beginning to End. *Genetics,* 191**,** 1073-1105.

WOLNER, B., VAN KOMEN, S., SUNG, P. & PETERSON, C. L. 2003. Recruitment of the recombinational repair machinery to a DNA double-strand break in yeast. *Mol Cell,* 12**,** 221-32.

WOTTON, D. & SHORE, D. 1997. Novel Rap1p-interacting factor, Rif2p, cooperates with Rif1p to regulate telomere length in Saccharomyces cerevisiae. *Genes & Development,* 11**,** 748-760.

XU, Z., FALLET, E., PAOLETTI, C., FEHRMANN, S., CHARVIN, G. & TEIXEIRA, M. T. 2015. Two routes to senescence revealed by real-time analysis of telomerase-negative single lineages. *Nature Communications,* 6.

YAMADA, M., HAYATSU, N., MATSUURA, A. & ISHIKAWA, F. 1998. Y '-Help1, a DNA helicase encoded by the yeast subtelomeric Y ' element, is induced in survivors defective for telomerase. *Journal of Biological Chemistry,* 273**,** 33360-33366.

YEAGER, T. R., NEUMANN, A. A., ENGLEZOU, A., HUSCHTSCHA, L. I., NOBLE, J. R. & REDDEL, R. R. 1999. Telomerase-negative immortalized human cells contain a novel type of promyelocytic leukemia (PML) body. *Cancer Res,* 59**,** 4175-9.

YU, T. Y., KAO, Y. W. & LIN, J. J. 2014. Telomeric transcripts stimulate telomere recombination to suppress senescence in cells lacking telomerase. *Proc Natl Acad Sci U S A,* 111**,** 3377-82.

ZHOU, J., HIDAKA, K. & FUTCHER, B. 2000. The Est1 subunit of yeast telomerase binds the Tlc1 telomerase RNA. *Mol Cell Biol,* 20**,** 1947-55.

ZHU, X. & GUSTAFSSON, C. M. 2009. Distinct Differences in Chromatin Structure at Subtelomeric X and Y ' Elements in Budding Yeast. *Plos One,* 4.

ZHU, Z., CHUNG, W. H., SHIM, E. Y., LEE, S. E. & IRA, G. 2008. Sgs1 helicase and two nucleases Dna2 and Exo1 resect DNA double-strand break ends. *Cell,* 134**,** 981-94.